New developments in stormwater characterization and remediation for water reuse

By **Dinushika Shyamali Senavirathne Ekanayake**

Thesis submitted in fulfilment of the requirements for the degree of

Doctor of Philosophy

Under the supervision of Prof. Saravanamuthu Vigneswaran
A/ Prof. Jaya Kandasamy

University of Technology Sydney
Faculty of engineering and information technology (FEIT)

June 2020

Certificate of authorship/ originality

I, *Dinushika Ekanayake* declare that this thesis, is submitted in fulfilment of the requirements for the award of *doctor of philosophy* , in the *School of Civil and Environmental Engineering, Faculty of Engineering and Information Technology* at the University of Technology Sydney.

This thesis is wholly my own work unless otherwise referenced or acknowledged. In addition, I certify that all information sources and literature used are indicated in the thesis.

This document has not been submitted for qualifications at any other academic institution.

This research is supported by the Australian Government Research Training Program.

Signature:

Production Note:
Signature removed prior to publication.

Date: 30/06/2020

Acknowledgement

It would not have been possible to achieve this thesis without the help and support of all the people around me. I am highly appreciative to everyone for their help and support during my research. Firstly, I would like to express my deep appreciation and gratitude to my principal supervisor, Professor Saravanamuth Vigneswaran, for his patient guidance and unwearying mentorship, from when I commenced on the PhD degree through to completion of this work. I am sure that this dissertation would not have been possible without his support, understanding and encouragement. Secondly, my deepest thanks go to my co-supervisor, Prof. Paripurnanda Loganathan for his great help and support through my entire PhD study. I would also like to thank my co- supervisor A. Prof. Jaya Kandasamy for his assistance as well.

I'm also thankful for the help offered by Dr. Rupak Aryal, M. Kalaruban, Roobavanan, Sharaniya, Alex, Seongchul, Niren and all my other colleagues and lab mates at CTWW for their help and support. I had a wonderful time working with them. Special thanks to senior technical officer of environmental engineering laboratories, Md Abu Hasan Johir who had always been supportive in sharing his valuable time and ideas. Further I acknowledge Craig Bush of Blacktown City Council, Blacktown, NSW for the support of my research. I am grateful to University of Technology Sydney and GRS for their support of my candidature.

I am extremely thankful to my dear husband, Bhanushka Ekanayake, who gave me all his support to complete this PhD successfully. I would never have been able to achieve this project without his backing, and he made me believe in myself and encouraged me through the whole process of research and always stayed beside me during my periods of struggle. I will always be grateful for your selfless support in sharing our household burdens and for loving me the way you do. Furthermore, I would like to use this opportunity to express my deepest gratitude for my late father E.M. Senavirathne, mother Lalitha Kumari Ranathunga and my brothers for providing me with great opportunities in life, for their blessings, love, care and support not only for my PhD study but for my whole life. Last but not least, I would

also like to show my gratitude to the rest of my family and friends who have also offered great support during my candidature.

DEDICATION OF THIS THESIS
TO MY LOVING PARENTS AND HUSBAND

Research outcome summary

Publications arising from this work

Eeshwarasinghe, D., Loganathan, P., Kalaruban, M. *et al.* 2018, Removing polycyclic aromatic hydrocarbons from water using granular activated carbon: kinetic and equilibrium adsorption studies. *Environ Sci Pollut Res* **25,** 13511–13524.

Eeshwarasinghe, D., Loganathan, P. & Vigneswaran, S. 2019, 'Simultaneous removal of polycyclic aromatic hydrocarbons and heavy metals from water using granular activated carbon', *Chemosphere*, vol. 223, pp. 616-27.

Ekanayake, D., Aryal, R., Johir, M.A.H., Loganathan, P., Bush, C., Kandasamy, J. & Vigneswaran, S. 2019, 'Interrelationship among the pollutants in stormwater in an urban catchment and first flush identification using UV spectroscopy', *Chemosphere*, vol. 233, pp. 245-51.

Ekanayake, D., Loganathan, P., Johir, M.A.H. *et al.* Enhanced Removal of Nutrients, Heavy Metals, and PAH from Synthetic Stormwater by Incorporating Different Adsorbents into a Filter Media. *Water Air Soil Pollut* **232,** 96 (2021).

Conference papers

D. Eeshwarasinghe[1], C. Bush[2], P. Loganathan[1], J. Kandasamy[1], S. Vigneswaran[1] 2017, The importance of determining pollutant loads from varying rainfall events for stormwater harvesting and reuse schemes, NSW Stormwater Conference September 2017

Eeshwarasinghe, D., Loganathan. P., Kalaruban. M., Southararajah. D.P., Kandasamy, J., Vigneswaran, S. 2017, Polycyclic aromatic hydrocarbons in water: simple analytical method and removal technique. International Conference in Waste Water and Waste Management for Extractive Industries. October 23-24, 2017, Nusa Dua, Bali, Indonesia, Book of Abstract page 68.

Conferences

Presented at International Conference in Waste Water and Waste Management for Extractive Industries, October 23-24, 2017, Nusa Dua, Bali, Indonesia.

Presented at Stormwater NSW Conference which was held at the Newcastle Exhibition & Convention Centre on Wednesday, 6th and Thursday, 7th September, 2017

Presented at 11TH CESE conference, Sukosol, 4-8 November 2018, Bangkok, Thailand

Table of Contents

Contents

List of Figures

List of Tables

List of Abbreviations

AC= Activated Carbons

$(NH4)_2NO_3$ = ammonium sulphate

AET = apparent effects threshold

Barrett-Joyner-Hanlenda (BJH)

Brunauer = Emmett-Teller (BET)

$Ca(OH)_2$ = Calcium hydroxide

Ca^{2+} = Calcium

Ce = equilibrium concentration of adsorbate (mg/L)

Co = initial concentration of adsorbate (mg/L)

Cs = the concentration on the external surface (mg/L)

Ct = concentration of adsorbate at time t (mg/L)

DOC = dissolved organic carbon

Dw = dry weight

FTIR = Fourier transform infrared spectroscopy

G = gram

g/L = gram per litre

GAC = Granular activated carbon

GSMS =Gas chromatography–mass spectrometry

HA = humic acid

HCl = hydrochloric acid

HCO3 = bicarbonates

HPLC =High-performance liquid chromatography

hr = hours

hr/h = hours

k1 = equilibrium rate constant of pseudo-first-order sorption (1/min)

k2 = equilibrium rate constant of pseudo-second-order (1/min)

k_{AB} = kinetic constant, (L/mg.min)

KCl = Potassium chloride

KF = Freundlich constants (mg/g)

kf = the external mass transfer coefficient (m/s)

KH_2PO_4 = Monopotassium phosphate

KL = Langmuir constant related to the energy of adsorption (L/mg)

KNO_3 = Potassium nitrate

K_{ow} = Octanol-water partition coefficient

L = litre

M = mass of dry adsorbent (g)

m/h = meter per hour

mg/L = miligram per litre

$MgCl2.6H_2O$ = Magnesium Chloride Hexahydrate

µg/L = Micrograms per litter

min = minutes

mL/min = millilitre per minute

MQ = Milli-Q water MW = Molecular weight

n = Freundlich constant

Na_2CO_3 = sodium carbonate

NaCl = sodium chloride

$NaHCO_3$ = sodium bicarbonate

$NaNO_3$ = sodium nitrate

NaOH = Sodium hydroxide

PAH = Polynuclear aromatic hydrocarbon

PCB = Polychlorinated biphenyl

Q = Flow rate (cm3/s)

Qe = amount of adsorbate adsorbed per unit mass of adsorbent (mg/g)

qmax = maximum amount of adsorbate adsorbed per unit mass of adsorbent (mg/g)

qo= equilibrium adsorbate uptake per g of adsorbent (mg/g)

rpm = revolutions per minute

SEM = Scanning Electron Microscopy

SS = suspended solids

t = filtration time (min).

TEF = Toxic equivalency factor

TEQ = toxicity equivalent quotient

TOC = total organic carbon

UV /VIS spectrum= Ultraviolet–visible spectroscopy

V = the interstitial velocity (m/s)

WHO = World Health Organization

USEPA = United States Environmental Protection Agency

WUSD = Water Sensitive Urban Design

Abstract

Water scarcity due to persistent drought is forcing many countries around the world to explore alternative freshwater resources. Australia is the world's driest inhabited continent, and has one of the most variable rainfall intensities. This has encouraged the harvesting of stormwater and reuse of water in order to reduce the demand placed on municipal water supplies. Urban and industrial stormwater runoff has high potential as a reusable water resource for agricultural irrigation, irrigation of parks and sportsgrounds, and toilet flushing. However, stormwater contains many pollutants which can have dire effect on plants, animals, aquatic organisms and humans and for this reason they should be removed before the water is used for these beneficial purposes.

Assessing urban stormwater quality by investigation and characterisation of pollutants is a prerequisite for its effective management, for reuse and safe discharge. The stochastic nature of rainfall, dry weather periods, topology, human activities and climatic conditions generate and wash-off pollutants differently from event to event. Therefore, a study was commenced to investigate the major physico-chemical pollutants in stormwater runoff collected from an urban catchment system after several rainfall events over a period of three years. Correlation analysis and principal component analysis (PCA) were done to identify the possible relationships among measured pollutants. Although correlation analysis revealed some relationships between pollutants, PCA biplots suggested a few group-related pollutants and revealed that a two-component model could explain nearly 72% of the variability between pollutants. Pollutants in the group that included dissolved organic carbon (DOC) behaved in a similar manner. Most of the pollutants were washed off during an early stage of an event giving rise to the first flush phenomenon. UV spectroscopy was applied to identify the first flush by comparing the recorded spectrum of consecutive samples that were collected in an event. Analysis of the spectra was able to isolate the point when first flush ends for DOC and pollutants that behaved similar to it.

The second part of the thesis dealt with remediation of stormwater by removing important organic and inorganic pollutants. Organic pollutants and heavy metal concentrations in stormwater are expected to increase and reach toxic levels in the near future because of rapid urbanisation leading to increasing density of motor

vehicles. Polycyclic aromatic hydrocarbons are a group of highly persistent, toxic and widespread environmental micropollutants that are increasingly found in water. A study was conducted in removing five PAHs, namely naphthalene, acenaphthylene, acenaphthene, fluorene and phenanthrene from water by adsorption onto granular activated carbon (GAC). The pseudo-first order (PFO) model satisfactorily described the kinetics of adsorption of the PAHs. Batch equilibrium adsorption data fitted well to Langmuir, Freundlich and Dubinin-Radushkevich models with the Freundlich model having the best fit. The Langmuir adsorption capacities for naphthalene, acenaphthylene, acenaphthene, fluorene and phenanthrene were 33.7, 76.6, 40.8,45.7 and 47 (mg/g), respectively. The adsorption affinities were related to the hydrophobicity of the PAHs as determined by the log k_{ow} values. Overall the results showed that GAC can be effectively used to remove PAHs from stormwater.

Polycyclic aromatic hydrocarbons and heavy metals are dangerous pollutants that commonly co-occur in water. Therefore, it is important to determine their adsorption capacities when they are present together, because there could be competition for adsorption between the two groups of pollutants and this would reduce their removal efficiency. Most previous adsorption studies were conducted either on PAHs or heavy metals separately and not when they occur together. An adsorption study conducted on the simultaneous removal of PAHs (acenaphthylene, phenanthrene) and heavy metals (Cd, Cu, Zn) by GAC showed that, when these pollutants are present together, their adsorption capacities were less than when they were present individually due to competition for adsorption. Between the two classes of pollutants, PAHs had higher adsorption capacities than heavy metals. The reduction in adsorption of PAHs by heavy metals followed the orders of heavy metals' adsorption capacity and reduction in the negative zeta potential of GAC (Cu > Zn > Cd).

Bio-retention beds constitute a widespread treatment measure used in sustainable stormwater management particularly by the local councils in Sydney, Australia. However, most of the bio-retention treatment systems are not efficient in removing pollutants from stormwater. Final part of the research was on evaluating the efficiency in removing pollutants using a bio-retention medium (R165, natural

soil with a texture sandy loam) and enhancing the pollutant removal capacity by mixing with GAC (0.3%) and zeolite (10%). Column experiments were carried out at the flow velocity of 100 mm/hr and 300 mm/hr in down-flow mode. The soil-based filter without additions removed substantial amounts of PO_4-P and NH_4-N for up to 8 h at a flow velocity of 100 mm/h which is a one-year time-equivalent of rainfall at a locality in Sydney, Australia. An addition of 10% zeolite to the soil-based filter extended the column saturation period to 24 h. The breakthrough data for PO_4-P and NH_4-N were satisfactorily described by the Thomas model. The majority of the nine heavy metals tested were removed by more than 50% for upto 4 h in the soil-based filter. This level of removal increased to 16 h when 10% zeolite was added to the filter. The column with the soil-based filter + 10% zeolite had higher affinity for Pb, Cu, Zn and As than Ni, with Pb having the highest percentage removal. Soil-based filter + 10% zeolite removed considerable amounts of 3 PAHs (30-50%), while Soil-based filter + 10% zeolite + 0.3% GAC removed 65 to > 99% of the PAHs at 24 h operation. Phenanthrene and pyrene were almost 100% removed. This application will greatly facilitate the reduction of pollutant concentration in biofilter-treated stormwater in many stormwater harvesting projects which are currently experiencing difficulties in achieving clean reusable water.

Chapter 1

Introduction

Chapter One

1.0 Introduction

Stormwater harvesting is the collection, storage and treatment of stormwater from urban areas for re-use as recycled water. Notably, stormwater is collected from drains or creeks rather than roofs. Stormwater harvesting offers major benefits. Firstly, there are reductions in the demand for town (potable) water and irrigation use through use of harvested stormwater for potable water substitution, supplementing urban irrigation and industrial uses. Secondly, stormwater pollution loads to downstream waterways and estuaries decrease. Stormwater contributes 94% of sediments and 50-60% of nutrients to Sydney Harbour (Premiers 1997). Thirdly, stormwater volumes and discharges are better managed (Birch et al. 2004). Improving the harvesting of stormwater will contribute to Australia's water security and this issue is becoming increasingly important now that the world's water resources are under threat.

Australians live on the driest inhabited continent and over the last 20 years the five largest Australian cities, and now its regional centres, have all experienced severe water shortages resulting in water restrictions (e.g. Sydney 2000-2009, 2017-2020). The Australian Bureau of Statistics predicts that Australia's current population could grow up to 35.9 million by 2050, requiring almost an additional three times of current water demand (Cahill & Lund 2013). Complicating this is the danger of climate change, which will increase the variability of both rainfall and runoff. Managing scarce and unpredictable water resources will therefore be a major challenge. A key strategy is to shift from natural water resources to alternative water supplies such as recycled wastewater, desalinated water and stormwater harvesting and to build a diversified water supply portfolio that will survive well into the future.

Stormwater that is not harvested for beneficial use, if allowed to freely runoff, may pollute the natural waterways and simply ends up as a wasted resource. Therefore, identifying and quantifying the available contaminants in stormwater which flows through a particular catchment are highly recommended when it comes to stormwater harvesting and reuse. Comprehensive water quality data from different landforms at different rainfall events is essential for stormwater management because the concentration of contaminants varies according to the site, and intensity and duration of rainfall events. Relationships between rainfall and contaminants concentrations at different stages during a rainfall event can give information on suitable times after a rainfall event, and stormwater needs to be harvested and the type of treatments necessary. With each rainfall event, the first flush of stormwater is the most important stage for investigating pollutant concentrations as this stage carries most of the pollutants from the land. Such information is not widely available, particularly in Australia.

Design and implementation of well-functioning treatment system must take into account the nature of stormwater entering the system. Stormwater contains a wide range of pollutants that can be physical (suspended solids), chemical (nutrients, metals, metalloids, chemicals of concern such as pesticides/herbicides, alkyl phenols, pharmaceutical and personal care products (PPCP), surfactants, polycyclic aromatic hydrocarbons (PAHs)) and biological organic matter. Pollutants currently thought to be present in generally small concentrations in stormwater in Australia can potentially accumulate in future causing toxic effect to aquatic and terrestrial environments. Such pollutants include heavy metal/metalloids, PAHs and PPCPs. Notably, heavy metal concentrations in stormwater are expected to increase above current values due to rapid urbanisation leading to increasing density of motor vehicles. However, even now, some heavy metals in Australian stormwater, such as Cd and Zn, are higher than the global values. Extensive research has been done on macro pollutants but research on removal of micro pollutants is limited (Sounthararajah et al. 2015a).

PAHs, which are priority micro pollutants due to their carcinogenic, mutagenic, and toxic properties (Manoli & Samara 1999), are present in stormwater in low concentrations in Australia. However, they pose the danger of accumulating with toxic characteristics, due to the current rapid urbanisation of communities (Nguyen et al. 2014). Even though PAH concentrations in stormwater are low in most stormwaters in Australia, the sediments in some areas have been reported as having very high concentrations of PAHs (Aryal et al. 2013). As in other countries, the continued urbanisation in Australia, especially the widespread practice of 'urban in-fill', is expected to increase the levels of PAHs in the environment and this would lead to rising concentrations in stormwater. Therefore, it is necessary to develop suitable remediation measures for the removal of PAHs from water and have this technology in place to treat PAHs whenever they are found to have high concentrations in stormwater. PAHs are often resistant to biological degradation and are not efficiently removed by conventional physico-chemical and biological methods such as coagulation, flocculation, sedimentation, filtration or ozonation (Persson et al. 1994). However, adsorption is effective in the removal of persistent organic pollutants and, in particular, activated carbon is widely used as an adsorbent for their removal (Cooney et al. 1999a; Crisafully et al. 2008). A few static batch studies have been reported on the adsorptive removal of PAHs, adsorption data on fixed-bed columns, so studies are scarce on this topic. Generating experimental data on dynamic column adsorption system is highly desirable when designing practical treatment systems for removing PAHs.

Heavy metals are also key pollutants in stormwater which can be persistent and toxic. Exposure to different heavy metals can cause severe health problems to mankind. PAHs and heavy metals generally co-exist in stormwater. Both kinds of pollutants have high affinity towards suspended particles and easily bind to them in stormwater and are transported together to natural water bodies. Not only PAHs and heavy metals, but also many other organic and inorganic ions/compounds are present in stormwater. When they are removed using adsorbents there can be interactive effects such as competitive and synergistic adsorption behaviour between the ions/compounds. Therefore, absorbents' efficiency in removing pollutants must be studied in the presence of multi-component pollutants/contaminants. This would offer the information necessary to support the application of adsorbents in field-scale treatment systems.

There are a number of pollutants such as nutrients, TSS and metals which have an immediate impact on end use scenarios as well as to affecting the life span of the treatment system. Not many studies have been done on improving bio-retention media by mixing with more economically viable and readily available adsorbents, which can be directly beneficial to water treatment professionals and their work. The adsorption of pollutants from stormwater using different adsorbents including a bio-retention media was studied in this thesis. There are a few issues and drawbacks that will not be addressed in this research.

1.1 Research questions and scope

There are plenty of stormwater harvesting and reuse systems in practice and research has also been done on their application to real world situations. However, most of these systems have failed to meet the expected water quality requirements. An important challenge of stormwater harvesting is to evaluate the nature of stormwater runoff of particular catchments. Stormwater characterisation will support our ability to understand the complexity of stormwater quality changes with respect to different storm events. Further data generated through monitoring will facilitate several models to predict stormwater trends and patterns. Secondarily, monitoring of existing treatment systems is also important to evaluate the performance of different treatment systems and propose better systems. This research presents the relevant information in designing an affordable on-site treatment system for stormwater to improve its water quality to meet the standards for outdoor use. Before designing such systems, it is important to conduct some fundamental analyses in the laboratory. This thesis presents new information on this subject using both laboratory and field experiments.

1.1.1 Objectives of the research

1. To establish relationships between the concentrations of a number of critical stormwater pollutants and rainfall. Here, the effect of rainfall intensity, duration and duration of dry period prior to the rainfall need to be studied to decide on when the stormwater should be harvested and the appropriate treatment necessary to remove pollutants.

2. First flush is another important phenomenon which greatly influences stormwater harvesting as it carries a large number of pollutants. Here the aim was to detect the first flush using a simple spectroscopic technique.
3. The PAHs are important pollutants in stormwater and are difficult to remove using current treatment methods. One of the objectives was to investigate the efficiency of removal selected PAHs from water by adsorption onto granular activated carbon (GAC), which is a very abundant and cost-effective material.
4. To analyse the interactions of pollutants during adsorption on to GAC. Heavy metals and PAHs are important pollutants in stormwater and they co-occur. There consequently be interactions between them during adsorption.
5. To develop and test a simple on-line treatment system for selected pollutants based on adsorption to meet Australian standards for outdoor use. This objective mainly addresses possible enhancements of current existing field applications of stormwater treatment systems.

1.2. Organisation of the thesis

In order to meet the above objectives, the experimental work and results are organised into 7 chapters. A summary of each chapter is provided here.

Chapter 1 introduces the topic of this research, describing the context, the nature of the problem and objectives to be achieved. Specific details with results and discussions are given in Chapters 3 to 7.

Chapter 2 presents existing research backgrounds on stormwater characterisation, current practices of stormwater technologies of stormwater harvesting and reuse. It also discusses the impacts of the main micro and macro pollutants in stormwater and the removal technologies used for them. In Chapter 3, the characterisation of stormwater in Angus Creek catchment, Blacktown, Sydney, Australia is described. Most importantly, relationships were established between the concentrations of a number of critical stormwater pollutants, and rainfall.

Referring to the second half of the thesis, Chapter 4 discusses the removal of PAHs from stormwater using GAC in batch and fixed-bed columns. Then in Chapter 5 the focus is on the adsorptive removal efficiencies of three selected PAHs onto GAC individually and in combination with heavy metals (Cd,Cu,Zn). Chapter 6 looks at a new method of permeable barriers/ filtration system to remove a wide range of pollutants from urban stormwater. This system uses a bio-retention medium (mixed with a small proportion of zeolite and GAC to remove specific pollutants). Finally, Chapter 7 presents the main conclusions of this research, and suggested recommendations for future analyses on this topic to consider.

Introduction to the topic

New developments in stormwater characterisation and remediation for water reuse

Identified research gaps and importance of the research

Chapter 2 presents a literature review on studies that investigated stormwater characterisation, current stormwater technologies/practices of stormwater harvesting and reuse. It also examines impacts of main micro and macro pollutants in stormwater

Chapter 3 presents a characterisation of stormwater at the Angus Creek catchment, Blacktown, Sydney, Australia. Relationship between the rainfall and pollutants is explained.

Chapter 4 presents more information about micro pollutants (PAHs) in stormwater and removal techniques (using GAC).

Chapter 5 describes and explains the competitive behaviour of pollutants in the stormwater and removal techniques (PAHs and heavy metals on to GAC).

Chapter 6 discusses the removal of a wide range of pollutants from urban stormwater.

Chapter 7 presents the key findings of this study and recommendations for future research to take up.

Chapter 2

Literature Review

Chapter Two

2.1 Stormwater

Stormwater originates from precipitation such as rain, hail, and snow. Stormwater quantity and quality can vary widely depending on the landscape of the area and amount and intensity of precipitation. When precipitation occurs through natural landscapes, most precipitation is absorbed into the soil, whereas in an urban landscapes, stormwater falls mostly onto impervious surfaces such as roads, sidewalks, rooftops, or parking lots and is not soaked up by the ground. Because of this, the falling water is swept across these surfaces as runoff to nearby water bodies. As a result, stormwater transports large quantities of pollutants and nutrients from the land to the surface water bodies in neighbouring surroundings. When stormwater drains too much water at once, it can cause landslides and localised flooding or flash flooding (especially on dried-out impermeable land surfaces subjected to sustained heat during summer) due to erosion and sedimentation.

Stormwater has now become an important water-reuse resource as the demand for water grows with the increase of the world's population and industries, particularly in arid and drought-prone climates. The runoff in Australian cities generally exceeds the volume of water that the cities draw from their catchments and groundwater sources, which is estimated to be an annual total of 2100 gigalitres; annually, Australia's urban areas produce around 3000 gigalitres of average annual runoff (Stormwater Management in Australia 2015). Fig. 2.1 shows that each city can potentially save a lot of potable water by investing in stormwater harvesting so that it is not wasted. Stormwater harvesting techniques and purification could potentially make some urban environments self-sustaining in terms of water requirement.

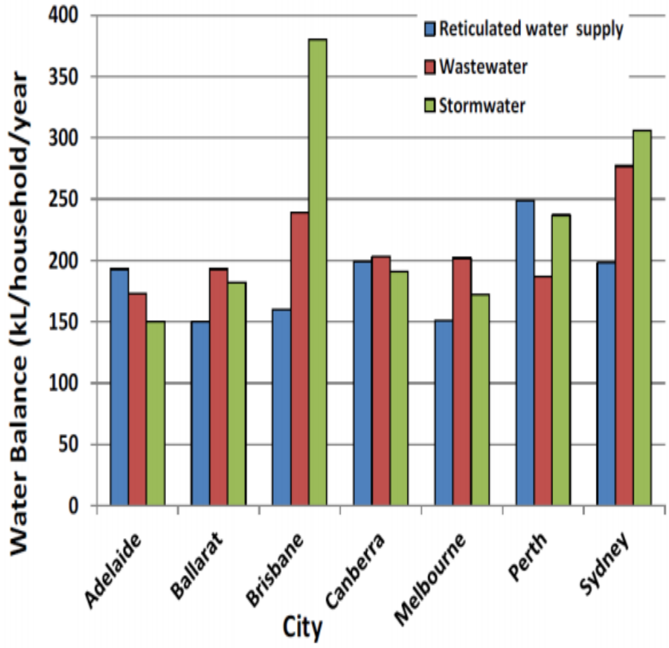

Figure 2.1 Average annual water balances from households, various cities (Stormwater Management in Australia 2015)

Australian per capita domestic water use (320 litre per person per day) is the world's second highest after the USA (Price 2002). Australia has historically received very small amounts of rainfall each year, given the nature of its climate and especially south of the tropic zone. The millennium drought (2000–2009) led to policies promoting and implementing desalination and water recycling guidelines for recycled water, including stormwater (Radcliffe & Page 2020). In Australia's cities only about 4% of rainwater and stormwater was recycled, while less than 1% of reclaimed wastewater was reused (Dillon & Ellis 2004). However, total recycled water supply during 2016-2017 rose in major cities as follows: Adelaide (25%) 25

$564*10^3$ m^3; Melbourne (30%) 42 085 $*10^3$ m^3; and Sydney (12%) 42 833 $*10^3$ m^3 (Bureau of Meteorology Annual Performance Report 2017–18).

The average annual volume of urban stormwater runoff in Australian cities is almost equal to the average annual urban water usage, of which at least 50% is for non-potable use (Mitchell, McMahon & Mein 1999). Stormwater is the best source for reuse when compared to grey water and industrial wastewater (Mitchell, Mein & McMahon 2002). In Australia most recycled urban stormwater is used for field irrigation such as watering of public parks, gardens, and ovals. Although the recycling of stormwater is still not fully in place throughout Australia, several investigations suggested that recycled stormwater is a feasible and economical option for potable water and this would also successfully help to reduce damage to the environment caused by stormwater (Strategy 2001). Hence, there is a demand for techniques that collect, treat and store stormwater. Existing stormwater recycling practices are not efficient, and novel compared to wastewater recycling. Currently, the general stormwater pollution control and recycling processes are managed mainly by Australia's state government agencies or departments, but they are not scientifically evaluated (Hatt, Deletic & Fletcher 2006).

2.1.1. Uses of stormwater

Stormwater is a good source of water which can reduce the rising demands on portable water supply. Treated stormwater can also be employed for non-potable uses which account more than 40% of household domestic water demand (Loh & Coghlan 2003). Stormwater treatment can be less expensive and more acceptable to the public compared with wastewater recycling (Kus et al. 2012). Treated stormwater can be used for agricultural irrigation, toilet flushing, gardening, car washing, and for residential purposes. It can also be used to irrigate public places such as golf courses and gardens and for aesthetic purposes. Stormwater harvesting and reuse is somewhat a novel technique but popular among local governments. However, there are potential limitations of stormwater harvesting because the process totally relies on climatic changes and rainfall patterns, and relative cost of stormwater treatment, although these do not hamper the multiple benefits of stormwater (DEC 2006).

2.2 Characterisation of stormwater

Stormwater runoff transport pollutants to nearby water surfaces and the receiving water bodies are becoming increasingly polluted from non-point and point sources. Point sources are easy to detect and control such as illegal spilling from industries and mining. Non-point sources are identified as one of the major causes of stormwater deterioration (Brown & Peake 2006; Davis & Birch 2009). Due to the complex nature of non-point sources such as atmospheric deposition, road dust and soil erosion, stormwater is difficult to characterise and quantify. Increased industrialisation and rapid urbanisation create more impervious areas contributing to nonpoint sources (Davis & Birch 2009; Lee & Bang 2000; Wang et al. 2001). Pollution load of stormwater depends on land use pattern, geography, and atmospheric depositions in the catchment area.

There are many organic and inorganic pollutants found in urban stormwater (Hvitved-Jacobsen, Vollertsen & Nielsen 2010). The major categories of these pollutants are: (i) total suspended solids (TSS), (ii) heavy metals, (iii) micro pollutants such as polycyclic aromatic hydrocarbons (PAHs), (iv) nutrients, and (v) oxygen-demanding substances and pathogens. These contaminants go through various physico-chemical processes before they impact on the aquatic community (Aryal et al. 2010). Characterisation of stormwater is also important for developing mathematical models for predicting pollutant loads in runoff and discharge into water bodies, as well as to validate existing models (Adams 2000). The unpredictable nature of stormwater is a key challenge for field practitioners of environmental agencies. Characterisation of stormwater over a long period of time at different rainfall regimes is necessary prior to developing predictive models and successful design/implementation of stormwater management plans.

2.2.1. Stormwater monitoring

For determining the proper use of stormwater, stormwater needs to be characterised by monitoring it in the field at different places and times after many rainfall events. A few years ago, Li et al. (2015) conducted a stormwater characterisation study in Tongsha reservoir watershed of the city of Dongguan, China, a typical, rapidly industrialised metropolis. This study showed that the pollutant wash-off process of runoff during rainfall events has significant temporal and spatial variations. Of the monitoring program the sampling and characterising the first flush after the rain is most important. First flush is known as the initial period of stormwater runoff which carries large amounts of pollutants than other stages of the stormwater flow. A catchment's pollution accumulation mostly occurs during the dry period, and this gets washed off at high concentrations mainly during the initial part of the rain event (Hoffman et al. 1984). First flush is more polluted than the rest; when more rain follows this first flush, the runoff from the catchment becomes more diluted and stormwater is comparatively less polluted than at the initial flush, because most pollutants accumulated during the dry period had been washed off during the first flush. A more increased impervious area results in higher discharge peaks and runoff volume (Barbosa, Fernandes & David 2012).

Usually, stormwater is characterised by flow measurements and chemical/physical analysis of the water by taking significant number of samples in a given location and pollutants are characterised periodically after each rain event. This information can generate hydrographs and pollutographs for each event, and eventually help to ascertain the pollutant loads with respect to different storm events.

2.2.2 Correlation between pollutant concentrations

Appropriate data on stormwater characteristics are vital for mitigation. Also, knowledge on correlation among stormwater pollutants is vital to understand the behaviour and management of pollutants in stormwater. This can reduce the cost of monitoring a large number of pollutants, because some pollutants' concentrations can be predicted from the others. Over a decade ago, (Han et al. 2006) conducted a correlation study on highway stormwater runoff characteristics in California, and they reported strong correlation among dissolved and total metals; DOC, COD, TKN and oil and grease; conductivity and Cl, total metals.

2.2.3. Photometric applications in stormwater monitoring

Dissolved organic matter (DOM) is one of the key parameters determining stormwater quality. It can be used as an indicator parameter for other pollutants such as nutrients, heavy metals and other organic micro pollutants from the catchment (Davis 1984; Mostofa et al. 2011; Zafiriou et al. 1984). Optical spectroscopic techniques such as UV and fluorescence spectroscopies can provide useful information on the characteristics of a wide range of DOM in stormwater (Aryal, Grinham & Beecham 2014). These techniques are rapid to perform and also can be applied to continued changes in DOM characteristics when exposed to chemical, biological and physical variations. Information on certain types of DOM present in the water samples can be taken from measurements made at specific wavelength in the spectrum (GHOSH & Schnitzer 1979; Korshin, Li & Benjamin 1997; Roig & Thomas 2003). Applications of these techniques are becoming more popular among researchers and the water professionals due to their high sensitivity, simplicity and economics. Similar to the online pH sensors, online UV sensors can also be used to monitor DOM in incoming water.

2.3 Specific pollutants in stormwater

2.3.1. Polycyclic aromatic hydrocarbons

Polycyclic aromatic hydrocarbons are a large class of organic compounds with two or more fused aromatic rings (Douben 2003; Johnsen & Karlson 2005). PAHs are mainly composed of carbon and hydrogen atoms with no substituent atoms or groups, whereas the general term, Polycyclic Aromatic Compounds (PACs) refers to those carrying substituent functional derivative. PAHs are dangerous pollutants due to their low biodegradability which can be accumulated through the food chain in an ecosystem and endanger the health of animals and people. They are an ubiquitous class of organic compounds which have been identified in a variety of waters and wastewaters (Walters & Luthy 1984). PAHs in the environment originate from either anthropogenic activities or natural sources, with emissions from anthropogenic sources accounting for the largest percentage in terms of annual global input (Gachanja 2005a). Their production is typically associated with the processing of coal and crude oil, power generation plants, incinerating plants, various industrial processes, domestic and residential heating (especially by wood and coal), motor vehicle exhaust, fires (either forest, or agricultural) and tobacco smoking (Menichini & Bocca 2003). Volcanoes and hydrocarbon deposits also represent a natural source of PAHs. As a result of these numerous and widespread sources, PAHs are widely spread pollutants which can be detected in all environmental matrices - air, water, soil and food. They enter surface water through wet and dry atmospheric deposition, hydrocarbon spillages, rainwater runoff into water bodies, and industrial effluent discharge, especially from hydrocarbon processing (Awoyemi 2011). PAHs are always present as a group and not as individual compounds (Menichini & Bocca 2003).

2.3.1.1. Health effects of PAHs

Human exposure to PAHs has been associated with an increased risk of developing cancer in a variety of tissues, such as the lungs, bladder, stomach, and skin (including the scrotum), depending on the mode of exposure and form of PAH (Jiminez 2014). The International Agency for Research on Cancer (IARC) evaluated the carcinogenic evidence for 43 PAHs using evidence reported for experimental animals (Menichini & Bocca 2003). Also, based on an overall evaluation of available data, the IARC classified three PAHs as ‘probably’ carcinogenic to humans and nine as ‘possibly’ carcinogenic (Menichini & Bocca 2003). There are more than one hundred known PAHs, of which seventeen are actively monitored by the US EPA (Awoyemi 2011). Table 2.1 shows the carcinogenic potency and the Toxicity Equivalency Factor (TEF) of some PAHs as determined by USEPA and IARC.

Table 2.1 Carcinogenicity and some properties of selected PAHs adopted from Nguyen (2016)

PAH	Cycles	Vaporisation	Solubility	TEF values (*)
Naphthalene	2	Very	High	0.001
Acenaphthylene	2	Very	High	0.001
Acenaphthene	3	Very	Medium	0.001
Fluorene	3	Very	Medium	0.001
Phenanthrene	3	Very	Medium	0.001
Anthracene	4	Insignificant	Low	0.01
Fluoranthene	4	Insignificant	Low	0.001
Pyrene	4	Insignificant	Low	0.01
Benzo(a)anthracene	4	Insignificant	Low	1
Chrysene	5	Insignificant	Low	0.01
Benzo(b+k)fluoranthene	5	Insignificant	Low	1
Benzo(a)pyrene Indeno(1,2,3-cd)pyrene	5	Insignificant	Low	0.1
Dibenzo(a,h)anthracene	6	Insignificant	Low	5
Benzo(g,h,i)perylene	6	Insignificant	Low	0.01

2.3.1.2. Characteristics of PAHs

The water solubility of PAHs declines when the number of rings/molecular weight of PAH increases, whereas hydrophobicity rises with the number of rings/molecular weight of PAH (Table 2.2). PAHs with higher molecular weights tend to have higher hydrophobicity as measured by the octanol-water coefficient

(K_{ow}). It is generally believed that toxicity is also dependent on the number of aromatic rings/molecular weight, with the heavier PAHs being the more toxic. They, however, have very low water solubility but are soluble in organic solvents, and are highly lipophilic.

Table 2.2. Properties of some major PAHs adopted from (Awoyemi 2011)

PAH	Molecular formula	Molecular structure	Mol.Weight (g/mol)	Aqueous solubility at 25^0C (mg/l)	Henry's law constant (atm.m^3. mol^{-1})	Log K_{ow}
Naphthalene	$C_{10}H_8$		128	31.7	$4.4E^{-4}$	3.3
Acenaphthene	$C_{12}H_{10}$		154	3.9	$1.84E^{-4}$	3.92
Acenaphthylene	$C_{12}H_8$		152	16.1	$1.14E^{-5}$	3.94
Fluorene	$C_{13}H_{10}$	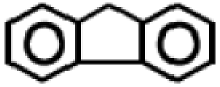	166	1.9	$9.62E^{-5}$	4.18
Anthracene	$C_{14}H_{10}$		178	0.0434	$5.56E^{-5}$	445

Phenanthrene	$C_{14}H_{10}$	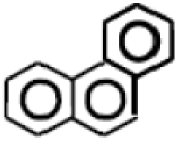	178	1.15	4.23E^{-5}	4.46
Fluoranthene	$C_{16}H_{10}$	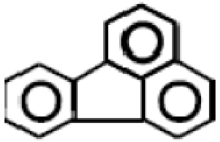	202	0.26	8.8E^{-6}	5.16
Pyrene	$C_{16}H_{10}$	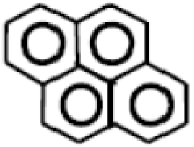	202	0.135	1.19E^{-5}	4.88
Benz[a]anthracene	$C_{18}H_{12}$	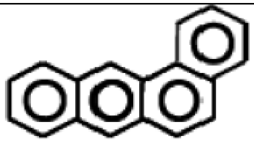	228	0.0094	1.2E^{-5}	5.76
Chrysene	$C_{18}H_{12}$	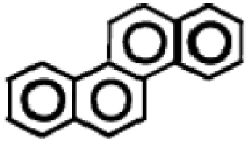	228	0.002	5.23E^{-6}	5.81

Benzo[b]fluoranthene	$C_{20}H_{12}$	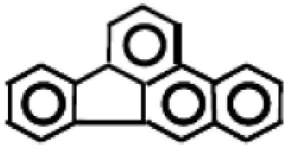	252	0.0015	$6.57E^{-7}$	5.78
Benzo[j]fluoranthene	$C_{20}H_{12}$	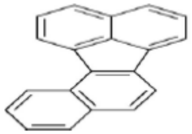	252	0.0025	$2.03E^{-7}$	6.11

2.3.1.3. Measuring techniques of PAHs

Gas (Awoyemi 2011; Crisafully et al. 2008; Lesage, Sperandio & Tiruta-Barna 2010) and liquid chromatographic (Walters & Luthy 1984) techniques are complementary methods that are commonly used to characterise PAHs in various types of environmental samples. For high molecular mass and non-volatile PAHs, liquid chromatography is superior to gas chromatography which saves time and cost. Furthermore, UV photometry can also be used to measure PAHs. PAH molecules are naturally strongly fluorescent, and give sensitised luminescence under peroxyoxalate chemiluminescence (PO-CL) conditions (Gachanja 2005b). Therefore UV absorption and fluorescence detection are increasingly being used in the analysis of PAHs in studies where only single PAHs are being considered (Ania et al. 2007). Each PAH has a specific wavelength where its absorbance is highest. Spectrophotometry is a popular technique used to measure PAHs, because it is a simple and a cost-effective technique (Ania et al. 2007; Awoyemi 2011; Valderrama et al. 2007).

2.3.1.4. PAH removal techniques

Due to high concerns about the hazardousness of PAHs it is important to eradicate as much of them as possible from the environment. In the literature the following treatment methodologies are cited for removing PAH from water: (i) biodegradation (Holman et al. 2002); (ii) high-energy electron beam irradiation (Cooper et al. 2002); (iii) ozonation (Gottschalk, Libra & Saupe 2009); (iv) catalytic combustion (Shie et al. 2005); and (v) adsorption (Chang et al. 2004). It should be noted that the first four methods may or may not completely remediate certain PAHs from the environment. The last one, adsorption, is considered to be one of the most viable options available due to its high removal efficiency, simplicity, and cost-effectiveness. Most PAHs with more aromatic rings show evidence of low biodegradability, hence they cannot be easily destroyed by biological treatment. A major advantage of adsorption is that the persistent PAHs can also be easily removed, rather than being broken down to potentially dangerous metabolites such as those produced by oxidation or reductive remediation processes (Valderrama et al. 2007). Activated carbon is widely adjudged to be the most effective and widely used adsorbent in the treatment of wastewater containing PAHs, because of its very high surface area, porous structure and hydrophobicity (Awoyemi 2011).

2.3.1.5. PAHs in sediments and stormwater

PAHs are one of the major pollutants in stormwater as have been reported in many countries (Aryal, Furumai, et al. 2006a). A detailed study on 16 PAHs in Kogarah, Sydney conducted by Nguyen et al. (2014) showed that the total PAH concentrations (mg/kg) in natural soils, road-deposited sediments and water sediments ranged from 0.40 to 7.49 (mean 2.80), 1.65 to 4.00 (mean 2.91), and 0.49 to 5.19 (mean 1.76), respectively. An earlier study on the distribution of PAHs in surficial sediments of Sydney Harbour, Australia showed that the spatial distribution of PAHs was predominantly originated from urban run-off (McCready et al. 2000). Aryal et al. (2013) conducted research in Sydney Harbour and discovered that the PAHs concentrations in the sediment existed in the 54–23,440 ng/g range. The result suggests that the harbour is contaminated with PAHs from low and to very high concentrations. Among the total PAHs found in the sediments, approximately 75% were medium to higher molecular weight 4- and 5-ring member PAHs. The TEF was found to be between 22 and 8,277 ng TEQ/g. The TEQ value indicated potential adverse ecological and human health effects in many locations. Aryal et al. (2006) reported that PAHs concentration in the first flush in highway runoff in Winterthur, Switzerland to be high with a concentration range of 1.3 - 13.1 μg/L.

2.3.2. Heavy metals

Heavy metals are deemed to be critical pollutants in stormwater because they are persistent and are toxic. Long-term exposure to heavy metals will result in adverse health outcomes for flora, fauna and humanity (Ahmaruzzaman 2011). Heavy metals are defined as block metals having a specific gravity greater than 5 g/cm^3 (Nies 1999). Metalloids are defined as the elements having properties of both metals and non-metals. In this report metalloids are grouped under heavy metals. Heavy metals such as lead (Pb), mercury (Hg), cadmium (Cd) and metalloids such as arsenic (As) are in the top six hazardous chemicals listed by the US Agency for Toxic Substances and Disease Registry (ATSDR 2014).

2.3.2.1. Health effects of heavy metals

Health outcomes or side effects can vary depending on the magnitude of exposure. Usually humans are exposed to various heavy metals by contaminated food and water in their work at contaminated sites and especially when heavy metals are involved (Martin & Griswold 2009). Other than anthropogenic activities, geological sources such as deposition of minerals with certain heavy metals can contribute to heavy metal contamination that is threatening the natural environment. A number of heavy metals found in wastewater include arsenic, cadmium, chromium, copper, lead, nickel, and zinc, all of which cause serious risks for human health and the environment (Lambert, Leven & Green 2000). Heavy metal toxicity can lower energy levels and damage the functioning of the brain, lungs, kidneys, liver, blood composition and other important organs. Long-term exposure can lead to gradually progressing physical, muscular, and neurological degeneration that imitate diseases such as multiple sclerosis, Parkinson's disease, Alzheimer's disease and muscular dystrophy. Repeated long-term exposure of some metals and their compounds may even cause cancer (Jaishankar et al. 2014; Järup 2003).

Cadmium is one type of heavy metal which is used in many industries such as welding, electroplating, pesticides, fertiliser, cadmium and nickel batteries, and nuclear fission plant. Depending on the level of exposure, Cd toxicity can cause renal dysfunction, lung disease, lung cancer, bone defects, increased blood pressure, kidney damage, bronchitis, gastrointestinal disorder, and various kinds of cancer (Singh et al. 2011). Zn is heavily applied in refineries, brass manufacture, zinc metal plating, plumping and it is a substance that can cause damage to the nervous system. Copper can be released to the environment from human activities such as mining, pesticide production, chemical industry and metal piping. Accumulation of Cu inside the body can lead to illnesses like anaemia, liver and kidney damage, stomach and intestinal irritation (Singh et al. 2011).

Lead is a heavy metal widely utilised in many industries like mining, manufacturing and fossil fuel burning batteries, cosmetics, metal products such as ammunition, paints, gasoline and pipes. This substance increases the risk of exposure to people and other living organisms (Martin & Griswold 2009). The US Environmental Protection Agency (EPA), designated lead as a carcinogen. Lead poisoning affects different parts of the body and is deposited in various tissues in the form of insoluble phosphate in skeletal bones (Papanikolaou et al. 2005). Lead is an extremely toxic heavy metal that disturbs various plant physiological processes and unlike other metals micro elements, it can be accumulated through food chains.

Arsenic is a toxic and carcinogenic element, and is extensively available in the form of oxides or sulfides or as a salt of iron, sodium, calcium, copper, etc. (Singh, Kumar & Sahu 2007). Vietnam is an example of a country battling problems with its drinking water, the result of decades of being contaminated by heavy use of arsenical pesticides, natural mineral deposits or inappropriate disposal of arsenical chemicals. Chronic exposure can cause cancer, bronchitis, dermatitis and acute poisoning, which can all be lethal.

2.3.2.2. Heavy metals removal techniques

Treatments such as precipitation as metal hydroxides, coagulation, ion exchange, electrochemical removal, and adsorption are some of the popular techniques that have been used to remove metals from stormwater. Of these, liquid phase adsorption has attracted much attention due to its efficiency, simplicity and minimum waste generation. Furthermore, adsorption is an inexpensive technique which can be handled easily with simple design (Chen et al. 2013). However the adsorption of metals onto an adsorbent relies on many factors, namely, pH, ionic strength, initial metal ion concentrations, temperature, adsorbent type and dosage, and presence of competitive pollutants, complexing agent and co-ions (Chen 2012). Furthermore pH can influence changes in the charge of the adsorbent surface and the properties of metals. The ionic strength of the medium can change the surface charges of the adsorbent and chemical species of the metals leading to changes in adsorption capacity (Loganathan et al. 2018).

The concentration and type of heavy metal influences the adsorption of each heavy metal generally by competition for adsorption sites. In natural conditions there are more pollutants co-existing in stormwater. When selecting the treatment system, the method must be able to remove a number of pollutants for it to be considered an effective system. Similarly, it is very important to understand the interaction of pollutants as well as to study the competitive adsorption behaviour in the presence of different metals and other pollutants such as suspended solids and organic pollutants (Ahmaruzzaman 2011; Chen 2012). Many studies have addressed the interactions between macro pollutants in stormwater but rarely have they tackled interactions involving organic micropollutants and trace metals. Different types of adsorbents have been trialled to remove heavy metals from stormwater such as plant-based agricultural and industrial by products, GAC and metal oxides (Ahmaruzzaman 2011; Hang et al. 2014; Nguyen et al. 2015; Nguyen et al. 2014).

2.3.2.3. Heavy metals in the environment

Usually most heavy metals are essential micro elements for plant growth. However, the ecological balance of the environment is greatly altered when they accumulate above a certain level. Heavy metals do not degrade through biological processes. Excessive uptake of heavy metals by plants occurs through plant tissues but this disrupts plant physiology. At the same time these elements can be passed on to other organisms through the food chain and accumulate in body tissues, subsequently causing various diseases and mutational problems. Heavy metal contamination in the soil, water and air is a huge concern because once these metals are in the environment they are very difficult to eradicate. Polluted stormwater transports heavy metals to nearby water bodies along with other pollutants which are deposited at the bottom of rivers, but also penetrate through the soil to contaminate groundwater. Heavy metals can be found as particle bounded pollutant similar to

PAHs. Remediation processes are challenging due to the co-existence of different pollutants in the environment.

2.3.3. Nutrients

Nitrogen and phosphorus are essential nutrients for plants and are the main nutrients found in runoff. They exist in various forms. Nitrate (NO_3), nitrite (NO_2) and ammonium (NH_4^+) are the inorganic fractions of nitrogen. Ammonium nitrogen is a form of nitrogen that is usually the most readily toxic to aquatic life. The sum of organic and ammonia nitrogen forms is known as the total Kjeldahl nitrogen (TKN). The organic component of N can be determined by subtracting the inorganic forms from the total N. Total phosphorus measures the total amount of phosphorus in both the organic and inorganic forms. Most of the soluble phosphorus in stormwater is usually present in the ortho-phosphate form (Strassler, Pritts & Strellec 1999).

2.3.3.1 Health effects of Nutrients

Forms of N compounds such as nitrate, nitrite and nitroso amine can contaminate ground and surface water sources simultaneously (Lerner 1986). An increase of these compounds in drinking water sources is harmful to human health. High levels of nitrate can cause what is called ‘blue baby syndrome’ in which babies have much elevated levels of nitrates which are carcinogenic (Majumdar & Gupta 2000). Ammonia is a toxic compound that can adversely affect fish and other aquatic fauna and flora. Normally excessive accumulation of phosphate is due to it being a very convenient and popular fertiliser that is extracted from rock depositions. Many heavy metals can be found along with the phosphate as by-products of the fertiliser manufacturing processes. Hence phosphate contamination simultaneously enhances the health hazardous as well. Recovery of phosphates from the environment is another important aspect that must be better managed to preserve the world's available phosphate deposits. Phosphate exploitation can be lead to future food scarcity as it is one of the major nutrients for plant growth.

2.3.3.2 Nutrients removal techniques

Nitrate ions in water are highly soluble and difficult to remove by precipitation and adsorption (Bhatnagar & Sillanpää 2011), so the application of conventional water treatment methods is not feasible (Islam & Patel 2010). Alternatively, there are some physico-chemical and biological processes that can remove dissolved phosphate in water and wastewater. Adsorption is a successful method for phosphate removal from water and it is very popular among water treatment professionals due to its efficiency, convenience, simplicity of design and minimal waste production (Gupta et al. 2009; Loganathan et al. 2014).

Other possible techniques for removing phosphates are biological methods, constructed wetlands, reverse osmosis, nano filtration and electrodialysis (De-Bashan & Bashan 2004). Biological methods have been well established and in this process, biological phosphate removal is achieved in the activated sludge with the support of anaerobic or anoxic zone ahead of an aerobic stage (Nur 2014). Chemical precipitation is another feasible strategy which seems to be as reliable and efficient as most other methods. In this method usually divalent or trivalent metal salts are added to wastewater to precipitate insoluble metal phosphate, which is allowed to settle, and later is removed via sedimentation. Since phosphorus is known to be a rapidly depleting resource, the precipitated phosphorous as a metal salt through physico-chemical processes may have a potential agricultural value as a fertiliser (Yeoman et al. 1988).

2.3.3.3. Stormwater pollution by nutrients

Generally, nitrogen is more abundant than P in stormwater (Howarth 1988; Nixon et al. 1996). Due to the high accumulation of these nutrients in aquatic water bodies the growth of aquatic plants and algae occurs at alarming rates; this is known as eutrophication (RANGES 2017). When eutrophication occurs, the natural balance of the ecosystem will be disturbed and it collapses. Massive growth of aquatic plants and algae can cause the depletion of available oxygen levels in a body of water and harm fish and other aquatic life. Eutrophication is considered one of the most harmful problems due to its impact on the aquatic ecosystem. Eutrophication promotes excessive plant growth, and when the plant mass starts decaying, huge oxygen depletion occurs which favours the growth of some toxic-producing algae such as cyanobacteria *Microsystis* sp., phytoplankton and dinoflagellates. Toxic algae can cause health problems for mankind and animals. The water body can become cloudy and coloured with a shade of green, yellow, brown, or red colours due to the presence of excessive algae. Eutrophication destroys the recreational and aesthetic attraction of surface water bodies and people's access to them has to be restricted.

2.3.4. Total Suspended solids

Fine particles are often carried as suspended materials by stormwater runoff. The total load of these suspended materials is called total suspended solids (TSS) (Shammaa & Zhu 2001). There are many sources of TSS in stormwater such as soil erosion, siltation, sewer outflow systems, dust particles, asphalt, etc. (Shammaa & Zhu 2001). As a result of increased impervious areas, TSS load in the stormwater can be increased and receiving waters become more turbid and poor in quality (Pope & Bevans 1984). Excessive TSS levels present in the water bodies can hinder the growth of aquatic plants and animals. On the other hand, other pollutants such as metals and organic pollutants are bonded to these particles and get transported along with the runoff and settle along the river bottoms which is a serious environmental problem (Nguyen et al. 2014). Hence reducing the contents of particles in stormwater is an important part of stormwater management. Controlling the sediments load which enters surface runoff is another important approach. Catchments and creeks must be monitored and maintained well to reduce the TSS load in the stormwater runoff (Novotny 1995). TSS in stormwater can be reduced by infiltration, filtration and detention facilities. Most of these structural techniques are effective in removing TSS from stormwater (Smirnova 2011).

2.4. Water Treatment technologies

As discussed in earlier sections (2.1-2.4) stormwater treatment and reuse has become an important issue for water treatment professionals because they have to manage the increasing stresses on water resources throughout the world including Australia. However, due to the presence of large amounts of pollutants, both organic and inorganic, in their dissolved and colloidal forms it is still a challenging process. The major difficulty for any kind of treatment method is its inability to comply 100% with the expected stormwater quality standards. Most treatment systems target low-cost simple designs due to the shortage of funds, government reluctance to pursue such ideas, and not fully developed technical facilities which make the process more difficult to remediate all pollutants in the water.

2.4.1 Removing pollutants from stormwater

2.4.1.1. Adsorption process

Adsorption is becoming a more popular technique due to its low cost, simplicity and minimal waster generation (Loganathan, Vigneswaran & Kandasamy 2013). Performance of the adsorption process relies on the adsorbent dosage, adsorbate concentration, pH, temperature and co-ions concentration. Adsorption can be classified into two groups: (i) chemical adsorption and (ii) physical adsorption (McKay 1996). Physical adsorption mainly occurs through the attraction of ions to the adsorbent surface by Van der Waal's and electrostatic force where no activation energy is required. These processes are reversible whereas the chemical adsorption occurs at low or high temperature where the heat of adsorption is high. This type of adsorption is not reversible, highly specific to the adsorbate, and activation energy is required.

Granular activated Carbon

Granular activated carbon (GAC) is a common and widely used adsorbent in water treatment because it can remove a range of contaminants such as organic carbon, turbidity, and nutrients. GAC was also found to be effective in removing many heavy metals (Sounthararajah et al. 2015a), and polycyclic aromatic hydrocarbons (Valderrama et al. 2008). GAC is widely known for its large surface area which can vary from 700 and 1,200 m^2/g (Loganathan et al. 2014) and higher degree of surface reactivity. Powdered AC is used in waste and potable water treatment, air emissions cleaning, chemical processes such as solvent recovery and decolourising, and general domestic applications such as odour removal (Kavitha & Namasivayam 2008). Nevertheless, its application fields are restricted due to its high cost (Baccar et al. 2009). Low cost wastes and agricultural by-products are also now being used to produce activated carbon which provides an economical solution to the high cost of the treatment process (Cimino et al. 2005). According to the literature, there is limited information available on PAH adsorption onto GAC, especially in the presence of other co-existing pollutants such as heavy metals.

Zeolite

Natural zeolite is a popular adsorbent which can be used to remove heavy metals (Nguyen et al. 2015; Sounthararajah 2016) and ammonia and phosphates (Karapınar 2009; Mažeikiene et al. 2008). Zeolite is locally available and relatively cheap and can be found in large quantities. The adsorption capacity is not too high under natural conditions. Hence chemical modification of this adsorbent is needed. Zeolites are crystalline hydrated aluminium silicates with a framework structure containing pores that are occupied by water and by alkali and alkaline earth cations. Due to their high cation-exchange ability as well as molecular sieve properties, it has special importance in water and gas purification, adsorption and catalytic activities (Inglezakis 2005). Zeolites also have an advantage over other filter materials because of their significant permeability and therefore they are widely used for water purification by the filtration process (Brannvall, Mažeikienė & Valentukevičienė 2006).

2.4.1.2. Dynamic adsorption column experiments

Column adsorption is a dynamic process and it is normally used with large amounts of water to be treated. This type of experiment mimics the water treatment process used in actual treatment plants, unlike in the batch type of experiments which are conducted in static conditions for a short time. In the column, the adsorbents are fixed at a desired bed height and it is operated with a desired flow rate of wastewater/stormwater in the up-flow mode or down-flow mode. The effluent solution is collected at different time intervals for adsorbate concentration analysis. If the effluent water concentration of adsorbate from the column reaches the influent adsorbate concentration the adsorbent is said to be saturated and full breakthrough of adsorbate has occurred. The exhausted adsorbent can be regenerated by a suitable solution which can desorb the adsorbate from the adsorbent and the adsorbent can be reused to remove further amounts of adsorbate (Nur, Loganathan, et al. 2014). The continued reuse of the adsorbent reduces the treatment costs.

In the column adsorption, the top layer of the adsorbent starts to adsorb the solute first until it reaches the saturation level and then the next layer, which is known as the mass transfer zone, which adsorbs the solute. Gradually the mass transfer zone moves down to the bottom and the column become fully saturated, and this time is called breakthrough time. Then the concentration of the effluent starts to increase and reaches the same concentrate as influent. The graph of C_t/C_0 vs time (C_t- concentration of effluent at time t, C_0 –influent concentration) generally gives a S shape curve for this process and the curve is called the breakthrough curve. The shape of the curve depends on the influent flow rate, concentration of adsorbate and the volume capacity of the adsorbent.

2.4.1.3. Designing a stormwater treatment system

As discussed earlier in this chapter (sections 2.1-2.3) stormwater treatment and reuse has become an important approach among water treatment professionals to reduce the increasing stress on water resources throughout the world and Australia. However due to the presence of an extensive amount of pollutants, both organic and inorganic, both in their dissolved and colloidal forms it is still a challenging process. The major challenge for any kind of treatment method is lack of 100% compliance with official stormwater quality standards.

2.4.1.4. Guidelines, and standards applied to stormwater

The water quality of treated stormwater for public use should meet certain health and safety criteria and it should have a high level of uniformity and certainty to meet end-use requirements. It is important to be fully aware of stormwater quality standards before designing the treatment process. Elevated levels of some pollutants such as nutrients, heavy metals, suspended particles, and organic pollutants can lead to socio-economic and environmental problems, which means that in effect the desired treatment process is a failure.

2.4.1.5. ANZECC guidelines for fresh and marine water quality (2000)

These guidelines were formulated to protect environmental values of water resources in line with the community needs. The guidelines mainly consider five priority environmental values. The first concerns ecosystem protection (both freshwater and marine) including protection of waters used for shellfish and fish production and wildlife, while the second is the recreation and aesthetics values. Thirdly, raw water for drinking water supply is important, and fourthly and finally, agricultural and industrial water uses are considered. Tables 2.3, 2.4 and 2.5 summarise the permissible limits for major pollutants recommended for marine ecosystem, irrigation, drinking water and harvested stormwater quality.

Table 2.3. Australian guidelines on permissible levels of target pollutants for different end uses and environmental protection (Anzecc 2000)

Pollutants	**Unit**	**Marine ecosystems**	**Freshwater ecosystems**	**Irrigation**		**Drinking water**	**Aesthetic**
				Long-term	**Short-term**		
DO							
TP	mg/L	0.02-0.1	0.01-0.025				
TN							
pH				6.5-8.5	6.5-8.5	6.5-8	
TSS	mg/L					500	
Turbidity	NTU					5	
Al	mg/L		0.08	5	20		
As	mg/L		0.042	0.1	2	0.01	
Cd	mg/L	0.0014	0.0004	0.01	0.05	0.002	
Cr	mg/L		0.00001	0.1	1	0.05	
Cu	mg/L	0.003	0.0018	0.5	5	2	

Fe	mg/L			0.2	10		0.3
Pb	mg/L	0.0066	0.0056	2	5	0.01	
Hg	mg/L	0.0007	0.0019	0.002	0.002	0.001	
Ni	mg/L	0.2	0.013	0.2	2	0.02	3
Zn	mg/L	0.023	0.015	2	5		
Faecal Coliforms	CFU/100 mL					0	

1 (Anzecc 2000); 2 (NHMRC 2011) ; a Values are reported for 90% of species protection

Table 2.4. Australian and New Zealand guidelines for fresh and marine water quality limits for Na and SAR factor (RWCC 1993)

Sodium (mg/L)	**Risk level**	**SAR**	**Risk level**
115	Sensitive crops	2-8	Very sensitive crops
115-230	Moderately sensitive crops	8-18	Sensitive crops
230–460	Moderately tolerant	18–146	Moderately tolerant
>460	Tolerant crops	46–102	Tolerant crops

Specific guidelines for water recycling and reuse can be found in Australian guidelines for water recycling and managing health and environmental risks (Stormwater harvesting and reuse July 2009)

Table 2.5. Criteria for public health risk management associated with various end uses of harvested stormwater edian for E. coli, 24-hour (Anzecc 2000; NSW 2006; RWCC 1993) [1] Values are median for E. coli, 24-hour median for turbidity and 90th percentile for pH, [2] Maximum is 5 NTU

Level	Criteria[1]	Applications
Level 1	E. coli[1] <1 cfu/100 mL	Reticulated non-potable residential uses, for instance garden watering, toilet flushing, car washing
	Turbidity ≤ 2 NTU[2]	
	pH 6.5–8.5	
	1 mg/L Cl_2 residual after 30min or equivalent level of pathogen reduction	
Level 2	E. coli <10 cfu/100 mL	Spray or drip irrigation of open spaces, parks and sportsgrounds (no access controls)
	Turbidity ≤ 2 NTU[2]	Industrial use, dust suppression, construction site use (human exposure possible)
	pH 6.5–8.5	Ornamental water bodies (no access controls)
	1 mg/L Cl_2 residual after 30 min or equivalent level of pathogen reduction	Fire fighting
Level 3	E. coli <1,000 cfu/100 mL	Spray or drip irrigation (controlled access) or subsurface irrigation of open spaces, parks and sportsgrounds
	pH 6.5–8.5	Industrial use, dust suppression, construction site use, process water (no human exposure)
		Ornamental waterbodies (access controls)

2.5. Current stormwater treatment practices in Australia

Fig. 2.2 presents the typically used treatment methods in stormwater pollution control throughout Australia. Of these techniques, advanced treatments (23%) are the most popular with litter and sediments traps (21%) and infiltration systems (20%) taking the second and third places, respectively. Usually litter and sediments traps are installed at the beginning of the treatment train and advanced treatments are at the end of the treatment train.

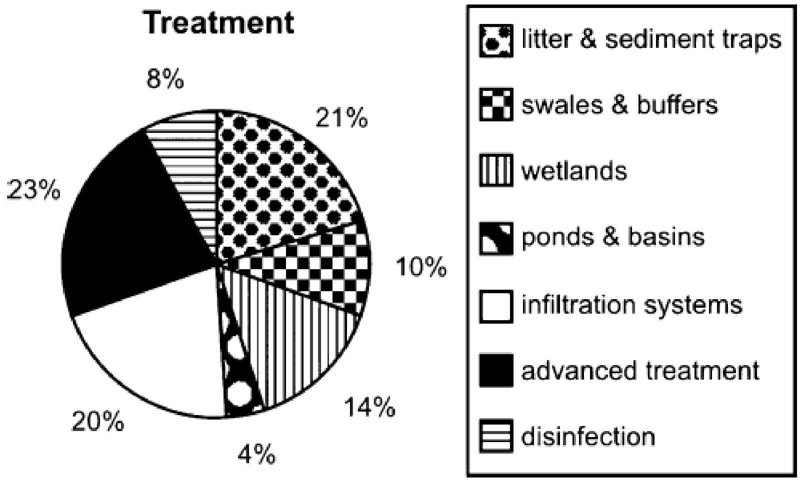

Figure 2.2 Distribution of stormwater treatment methods used in Australia ; adopted from (Hatt, Deletic & Fletcher 2006)

2.5.1 Infiltration methods

Infiltration systems can include porous and permeable pavements, infiltration basins and trenches, sand filters and biologically engineered soils which can be accompanied by certain types of plant species. In this method, stormwater infiltrates through the pavement surface and there is a temporary storage of water in the pavement structure before it is followed by further infiltration methods to underlying soils or is removed by a subsurface drain. In this process, pollutants get trapped and filtered in the structure and runoff volume is reduced. Streets runoff and runoff from parking areas can be infiltrated and penetrated through the soil to accumulate into groundwater recharge. Sand filtration is another popular method and effective in removing suspended solids, nutrients, pathogens, oil and grease from urban runoff (Kandasamy, Beecham & Dunphy 2008).

2.5.1.1 Biofilters

Biofilters are normally composed of vegetated soil filter medium and contain a porous collection pipe to transport treated water for end use (Philp et al. 2008). The best example of a biofilter is a wetland which utilises physical and biological processes simultaneously. This method is very popular in Australia and many researchers have worked on evaluating the adoptability, functionality and the enhancement of this particular process (Bratieres et al. 2008; Hatt, Deletic & Fletcher 2007; Read et al. 2008). They have used different types of biofilter for their experiments. According to their findings, TP, suspended solids and heavy metals were removed effectively by gravel biofilters but not TN. Elsewhere, (Hatt, Deletic & Fletcher 2007) and Read et al. (2008) reported that certain plant species can be used to enhance the performance and significantly improve the removal of TN and TP. A column study conducted by Bratieres et al. (2008) in Melbourne, Australia, showed that up to 70% nitrogen, 85% phosphorus, and >95% suspended solids were removed from stormwater by biofilters.

Constructed wetlands are widely used to recover urban stormwater runoffs and as a tertiary treatment for industrial wastewater (Deletic et al. 2014). Wetlands are more attractive due their passive operation and creating more habitat by enhancing the ecological balance and aesthetic values in the urban landscape. However, wetlands for stormwater remediation require large open spaces which are now extremely limited in urban areas and threatened by building ‘in-fill’. Also, continuous base flow or a high water table to support vegetation is difficult to achieve in dry seasons (Headley & Tanner 2012).

Wetland systems with horizontal subsurface flow (Headley & Tanner 2012) are commonly used for wastewater treatments. Applications of wetlands are limited for stormwater treatment whenever there are high flow velocities which causes hydraulic limitations of the substrate. Another limitation is that the vegetation in the constructed wetlands can tolerate only relatively shallow water depths of 30-50 cm and are susceptible to chronic die-back if inundated beyond these depths too frequently or for extensive periods (Davies & Bavor 2000; Greenway et al. 2007; Jenkins & Greenway 2007).

2.5.1.2. Bio-retention system

A bio-retention system is generally composed of several layers of filter media, certain types of plants in the top layers, and an over-flow outlet (Hunt et al. 2008). Bio-retention systems are designed based on the natural hydrologic cycle by retaining runoff to decrease flow rates and volumes. Bio-retention systems help to enhance the aesthetic value of a given area by preserving the habitat, preventing soil erosion and supporting groundwater recharge by enhancing the quality of surface water flows (Dietz 2007; Shafique & Kim 2015). Vegetation planted in the top layer of the bio-retention system uptake water and nutrients from the media. Once the media is saturated mainly by particles of incoming water the performance of the system will be greatly affected. When this happens the incoming water will overflow from the system.

The major constituents of bio-retention media are sand, soil, and organic mixture. Water treatment professionals prefer to add gravel or mulch to the top layer, grow various species of vegetation which are easy to maintain and can take up some nutrients from the incoming water. Vegetation layer helps to slow down the infiltration velocity of water which in turn, allows sufficient time for the chemical, biological, and physical processes in the water to take place and withdraw pollutants from the influent water (Davis & Birch 2009; Lucas 2009). Because of a bio-retention system, peak flows of the urban stormwater runoff, as well as the volume, and pollutant loads, are reduced (Brown & Hunt 2011; Hunt et al. 2006; Li & Davis 2008b, 2009; Li et al. 2009). Media depth is an important parameter of a bio-retention system which determines how well it functions hydrologically.

2.5.1.3. Pollutant removal by Bio-retention system

Removal of nitrogen species in bio-retention system includes several processes such as ammonification, volatilisation, nitrification, denitrification, and vegetative uptake (Liu et al. 2014). Breaking up organic N compounds into ammonium is known as ammonification and ammonia can be released from the ammonium as a gas which is known as volatilisation (Liu et al. 2014). Certain bacteria are capable of oxidising ammonium to nitrate and nitrite species (NO_2^- and NO_3^-) through a process called nitrification (Hunt et al. 2008). These nitrogen species are removed from the system by plant uptake (Hunt et al. 2008). Hunt et al. (2015) in North Carolina, conducted a field investigation and discovered high annual

NO_3^- mass removal rates varying between 13% and 75%. However, nutrient removal via bio-retention media by itself is very insignificant (Hunt et al. 2006).

As found in the case of N species, there are several processes that can remove P species from the bio-retention system such as precipitation, adsorption, filtration, and vegetation uptake. P ions can be adsorbed readily by many soils through the process of ion exchange or ligand exchange (Goldberg et al. 2005). Using the adsorption method to remove P is one of the important processes of bio-retention media. Most of the soluble P forms can be removed by plant uptake. Soil temperature and soil pH are important and influential factors in this process (Barber 1995). Metals comprise a pollutant which draws much attention due to its persistence and toxicity to people, animals and landscapes. It has been stressed in one study (Li & Davis 2008a) that the surface vegetative layer is a major contributor to the removal of metals from the incoming waters. Field- and laboratory-scale experiments have proved that bio-retention media are able to remove certain types of metals from stormwater by the adsorption process (Hatt, Deletic & Fletcher 2006).

Solid particles in stormwater are important pollutants as they can contribute to the shelf life of the bio-retention system. Clogging of the media can greatly reduce the infiltration velocity and finally the system can become inefficient or even inoperative due to reduced hydraulic flow through the system. However, total suspended solids can be easily trapped by the top vegetation as well as the media. A study conducted in the state of Maryland, USA, reported 54-59% mass removals of TSS in a bio-retention system (Davis 2007). Aged bio-retention can hold more particles hence filtration and sedimentation of TSS results in improved TSS removal efficacy (Liu et al. 2014). Previous research conducted on bio-retention media and pollutant removal efficiencies are presented in Table 2.6. According to the table performance results on pollutant removal conducted by bio-retention systems from both laboratory and field studies, suggest that bio-retention systems have greater potential for removing pollutants from stormwater (Davis & Birch 2009). References to pollutant removals are referred to as mass load reduction as a percentage.

Table 2.6. Water quality improvement through the bio-retention system , adopted from (Liu et al. 2014)

Source	Media composition	TSS	TN	TP	Zn	Cu	Pb
(Brown & Hunt 2009)	98% sand, 2% fines	92	80	70	*	*	*
(Brown & Hunt 2011)	Sandy clay loam, 96% sand, 4% fines	58	58	-10	*	*	*
(Brown & Hunt 2012)	87% sand, 13% fines	71	12	53	*	*	*
(Chen et al. 2013)	Sand with hardwood mulch and sandy loam planting soil, 20% OM	*	56	*	*	*	*
(DeBusk & Wynn 2011)	Washed sand with fines and leaf compost, 88% sand, 8%	99	99	99	*	*	*

	fines, 4% OM						
(Hathaway et al. 2011)	Bay mead fine sand, 87%–88% sand, 12%–13% fines	100	*	*	*	*	*
(Hunt et al. 2006)	Organic sand	*	68	*	*	*	*
(Hunt et al. 2008)	Loamy sand, 6% fines	60	32	31	71	60	77
(Li & Davis 2008b)	50% sand, 30% topsoil, 20% mulch	55-59	*	*	*	*	
(Li & Davis 2009) College Park, MD	Sandy loam, 80% sand, 20% fines, 6% OM	96	-3	-36	92	65	83
(Li & Davis 2009) Silver Spring, MD	Sandy clay loam, 54% sand, 46% fines, 12% OM	99	97	100	100	99	96

2.6 Conclusions

Stormwater originates from precipitation such as rain, hail, and snow. Stormwater quantity and quality can vary widely depending on the landscape of the area and amount and intensity of precipitation. Untreated stormwater runoff can cause environmental pollution from the many pollutants it carries from the land surfaces. Australia is one such continent and despite its variation in geography, geology, landscapes, etc., it generally and consistently suffers from water scarcity. According to the current urban water demand, alternative sources of water are required to reduce the pressure on existing potable water sources. As stormwater harvesting in urban environments is a relatively new strategy for supplying water, treatment techniques have so far been based on either stormwater treatment for environmental protection, or on treatments designed for conventional water supply or industrial applications. Quantification of pollutants is necessary for stormwater harvesting and reuse as well as to design treatment systems.

In wet weather events, most pollutants are washed off during an early stage (of runoff) giving rise to the first flush phenomenon. Being high in pollutants concentrations, this stage often carries a large proportion of pollutants load for that event. Identifying the first flush and characterising pollutants in it is a key priority in terms of pollution control and management. A number of pollutants exist in the first flush due to its association with human and environmental health-related risks. The most commonly queried pollutants are suspended solids, heavy metals, sodium, polycyclic aromatic hydrocarbons, nitrate, and phosphate, which have varying conductivity and turbidity characteristics. Because pollutants co-exist in nature, they may play a synergistic or antagonistic role on the health of humans and aquatic organisms. These interactions may also exert a direct impact on remediation strategies. Our limited knowledge and understanding of the pollutants is due to their complexity and dynamic relationships during wash-off phases. Understanding the relationships between concentrations of pollutants and developing onsite testing are vital for the management of stormwater runoff.

Dissolved organic matter (DOM) is one of the key parameters determining stormwater quality. It can also be used as an indicator parameter for other pollutants such as nutrients, heavy metals and organic micro pollutants from the catchment (Davis 1984; Mostofa et al. 2011). Optical techniques such as UV and fluorescence spectroscopies can provide useful information on the characteristics of a wide range of DOM in stormwater.

The literature review in this chapter has shown that elevated concentrations of nutrients, heavy metals, organic matter, and some micro organic pollutants such as PAHs in stormwater can damage the environment and human health. There are many methodologies and technologies to remove these macro and micro pollutants from stormwater runoffs. Adsorptive removal of pollutants especially PAHs from stormwater using different adsorbents has been extensively studied. However, only a few studies have used the dynamic fixed-column arrangement to treat stormwater which is more practical than the commonly used static batch mode of adsorption used in other studies. Very often stormwater carries more than one pollutant and there can be competition for adsorption between metals and other micro pollutants such as PAHs. However, most studies conducted adsorption of a single pollutant and not with mixtures of metals and PAHs. Information on the adsorption of organic pollutants in the presence of heavy metals is limited. Therefore, the suitability of an adsorbent which is readily available and economical to remove multi-component pollutants needs to be examined. This would provide information on the application of adsorption for treating stormwater in field-scale applications.

Wetlands, bio-retention, and permeable pavements are widely used in stormwater management. Current bio-retention systems in Australia for stormwater pollution control seldom provide the quality of water necessary for recycling due to their varied removal efficiencies for a range of inflow conditions and pollutants. Stormwater discharge in certain periods is relatively large, and for this reason, it needs to be treated intensively at high rates. The current paucity in research data means that water treatment specialists must improve their management of bio-retention media for effective stormwater treatment. Incorporating adsorbents with contrasting properties into the bio-retention media to target pollutants with different chemical characteristics is an attractive option.

Chapter 3

Interelationships between stormwater pollutants at Angus Creek Catchment, Blacktown and first flush identification using UV spectroscopy

The major part of this chapter is published in ‘Chemosphere’. Publication details are given below:

Ekanayake, D., Aryal, R., Johir, M.A.H., Loganathan, P., Bush, C., Kandasamy, J. & Vigneswaran, S. 2019, 'Interrelationship among the pollutants in stormwater in an urban catchment and first flush identification using UV spectroscopy', *Chemosphere*, vol. 233, pp. 245-51

Chapter Three

3.1. Introduction

The last chapter reported that during a rainfall event most pollutants are washed off in the early stages of the event giving rise to the first flush phenomenon. Identification of the duration of the first flush and factors affecting the quality and amount of pollutants in stormwater, especially in the first flush, are key components required for effective stormwater management. This requires a comprehensive set of water quality data from different rainfall events. The quantification of pollutants in terms of concentration is necessary for stormwater harvesting and reuse as well as to design a suitable treatment system before discharging the stormwater to natural water bodies for the purposes of ecological protection. Many urban non-point source pollution models utilise pollutant build-up and wash-off functions to simulate storm runoff quality of urban catchments (Aryal et al. 2005; Furumai 2008). Rain events wash off pollutants that build up during intervening dry weather periods. The dissolved and particle-bound pollutants deteriorate the runoff water quality (Aryal, Furumai, et al. 2006b; Aryal & Lee 2009; Larsen, Broch & Andersen 1998; Lee et al. 2002). Investigating the changes in concentrations of key pollutants in stormwater during rain events like turbidity, suspended solids, conductivity, nitrate, phosphate, hydrocarbons, metals, organic matter, and pathogens are of interest for effective stormwater management (He et al. 2010; Miguntanna et al. 2010).

Several methods and mechanisms have been proposed to estimate the first flush but all are empirical, based on data specific to particular locations (Bach, McCarthy & Deletic 2010; Gil & Kim 2012; Massoudieh, Abrishamchi & Kayhanian 2008; Sharifi, Massoudieh & Kayhanian 2011). The stochastic nature of rainfall and its runoff is transmitted to the concentration of pollutants in the runoff, especially the first flush. The variation in pollutants concentration in runoff differs from event to event even within the same catchment (Aryal et al. 2005). Overestimation of the first flush runoff volume potentially increases the treatment cost whereas underestimation can pose a serious risk to human and ecological health (Weiss, Gulliver & Erickson 2007).

In terms of best management practices (BMP), it is important to estimate the volume of stormwater that needs to be treated as precisely as possible (Lee et al. 2010) in real time. Given the current methods of estimating the first flush are not satisfactory, and laboratory methods to quantify the nature of pollutants and their concentrations in the first flush are expensive and time-consuming, newer and more precise methods are required. This can happen if water quality is continuously monitored in an event, and results can be compared and analysed to identify the point that indicates the end of first flush.

UV spectroscopy has been used to monitor water quality (Kim & Yu 2005; Zhang & He 2015). However, this practice is often limited to a few wave lengths. For example, UV 254 has been widely used to monitor hydrophorbic organic matter in water and wastewater (Awad et al. 2018; Fabris et al. 2015; Vaillant, Pouet & Thomas 2002; Watson et al. 2018). Kalbitz et al. (2000) used UV absorbance at 285 nm to measure fulvic acid. The UV spectrum arises when a sample absorbs electromagnetic radiation in the UV range. The ultra-violet region (200-400 nm) comprises photon energies of 1433-72 K cal/mole. This energy is enough to excite a molecular electron to a higher energy orbital of many organic substances, i.e. those having a lone pair of electrons, double bond, aromatic (conjugated double bond), functional group such as carboxylic, amino, ketone, etc. Since stormwater comprises a number of organic pollutants, and different organic molecules absorb radiation at varying wavelengths, the spectral information recorded within the UV range over time could reveal the nature and possible changes in the composition of pollutant (mainly organic) in the stormwater runoff over time.

In this study, stormwater sampling was carried out for 16 rainfall events during 2016-2018 at the Blacktown International Sportspark, Sydney, as part of the Angus Creek Stormwater harvesting and reuse scheme with the support of Blacktown City Council. The objective was to assess the effect of rainfall on stormwater quality. The specific objectives of this study were as follows. The first was to determine the pollutant concentrations in the stormwater runoff in several rainfall events and determine the relationships between stormwater quality parameters. For the second, this referred to establishing the effect of rainfall on stormwater quality and to compare the pollutants' concentrations in the stormwater with those in the Australian water quality standards recommended for irrigation. Regarding the third objective, UV spectroscopy served to identify the first flush. In this study, the variation of pollutants during the passage of a rain event and the relationships among the measured pollutants was analysed to help broaden the application of UV spectroscopy beyond the detection of organic matter and first flush based on organic matter.

3.2. Background

3.2.1. Catchment description

Stormwater monitoring was conducted from June 2016 to November 2018 at Angus Creek catchment, Blacktown city Council, Sydney, Australia. Angus Creek catchment is considered to be the second highest polluting catchment out of a total of 22 catchments which are the responsibility of Blacktown Council. A catchment composed of a larger impervious area which can cause larger pollutant load levels in the creek. The catchment's land composition is displayed in Fig. 3.1 and Fig. 3.2. Hot-spot areas for litter, oils and metals are the commercial areas, and shaded in blue in Figure 3.1.

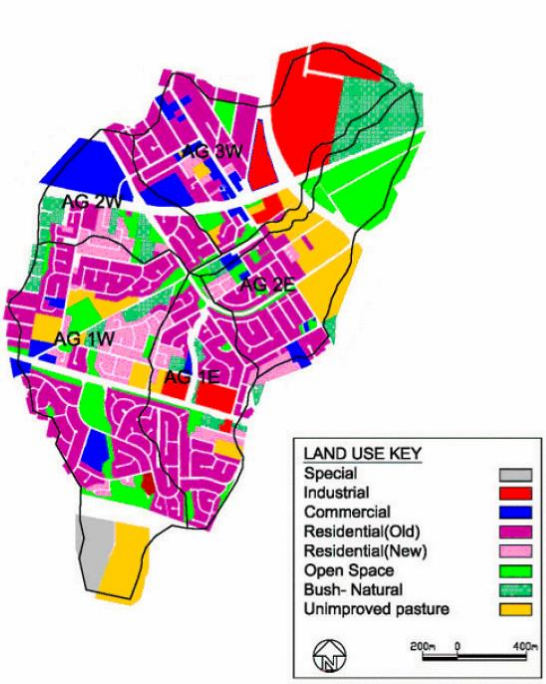

Figure 3.1 Angus Creek Catchment and land use distribution (State of the water ways, published by Blacktown City Council, Sydney)

Total area of land covers 445 ha. Figure 3.2 shows that the catchment is composed of mainly residential lands, industrial areas, commercial lands, roads and rail corridors, improved pastures, open spaces and smaller percentage of bushlands. Since the catchment contains more than 90% of impervious areas, it is expected to wield a greater impact on downstream environments. Based on the catchment composition, high amounts of nutrients, sediments and other micro pollutant loads are expected to end up in the creek when storms occur. However, the catchment does not contain farmlands. Hence the higher variations among nutrient loads are uncertain.

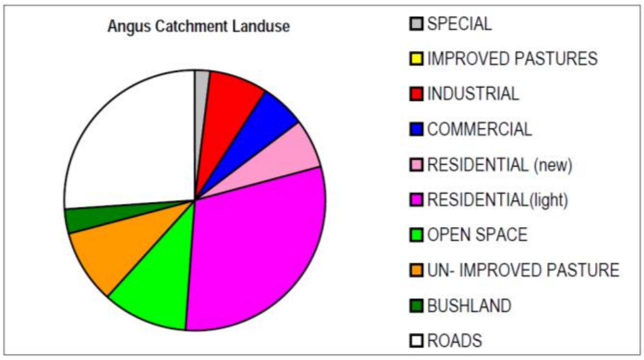

Figure 3.2 Land use composition as a percentage of the catchment (State of the water ways, published by Blacktown Council, Sydney)

3.3. Stormwater sampling

Stormwater sampling was scheduled and carried out based on two things: weather forecast and the expected rainfall duration and amount. Typically, rainfall events occur after at least 5 preceding dry days were monitored. Stormwater quality monitoring of runoff was carried out using an auto-sampler (ISCO Avalanche Portable Refrigerated Sampler; Teledyne Isco, Inc. USA) installed at Blacktown International Sportspark, Sydney (Fig. 3.3 a & b). Eight sampling bottles labelled 1-8 were placed inside the sampler to collect up to 750 mL of stormwater at specific time intervals.

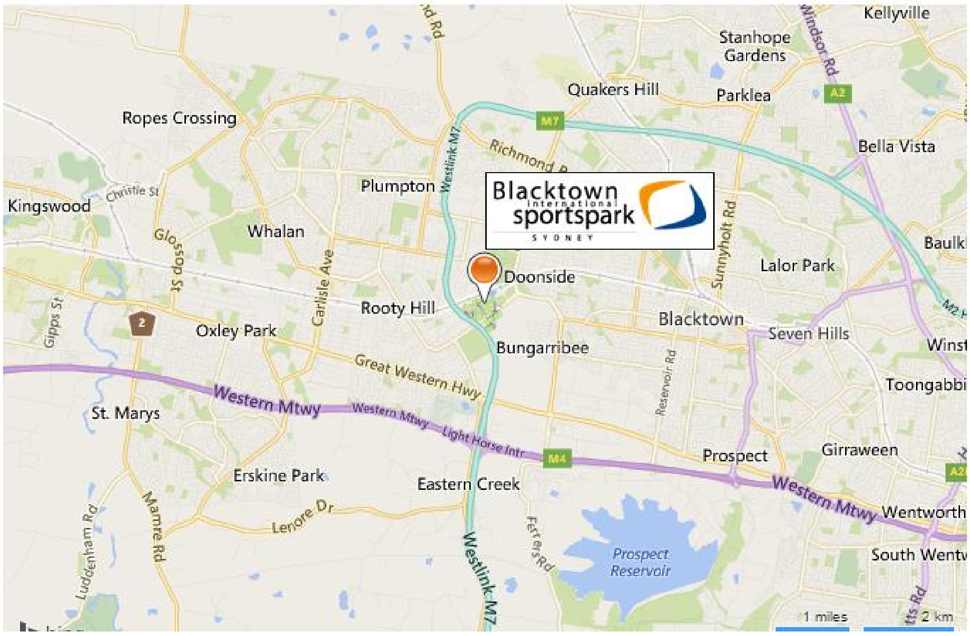

(a) Sampling location map

(source: http://www.blacktownsportspark.com.au/About_Us/Location)

(b) Auto Sampler at Angus Creek

Figure 3.3 Location of the sampling point ;(a) Sampling location map; (b) Auto Sampler at Angus Creek

Sampling dates and the times are reported in Table 3.1. The samples collected were immediately placed in a light-proof insulated box containing icepacks to ensure rapid cooling. Within two hours of collection, the samples were transported to the laboratory and stored in a laboratory fridge at 4 ^{0}C. Samples were filtered using 1.2 µm glass fibre filters and filtrate analysed within 48 hours. The parameters analysed were total suspended solids (TSS), nutrients (total dissolved nitrogen (TDN), NO_3-N & NO_2-N, total Kjeldahl-N, NH_3-N, total dissolved phosphates (TDP)), turbidity, total dissolved solids (TDS), conductivity, pH, dissolved organic carbon (DOC), polycyclic aromatic hydrocarbons (PAHs), and pharmaceutical and personal care products (PPCPs), sodium, sodium adsorption ratio, and microbial components (*Escherichia coli* and total coliforms). pH, conductivity and TDS, were measured using pH/Conductivity meter (HACH HQ40d meter, pH probe (PHC301), conductivity probe (CDC40101) and TDS probe (CDC40101, Romania), respectively. The instruments were calibrated before measurement according to the standard procedures described in the manual of the corresponding measurement. TSS was measured by filtering 100 mL stormwater through a glass fibre 1.2 µm (micron) Whatman GF/C filter (EPA Method 160.2) within the 7 days of sample collection. The filtrates plus solids were dried at 104°C for 24 h, cooled, and weighed using a digital balance (ADAM, PW 254, with an accuracy of 0.0001 g, MA USA).

Duplicate samples were used to ensure the result was accurate. The relative % difference [(sample 1-sample2)/(sample1+sample)/2] was less than 5% of their average value. A blank correction was also carried out and subtracted from the sample measurement. DOC was measured using a total organic carbon analyser (Multi N/C 3100, Analytik Jena, Germany) after filtering the sample through a 0.45 µm filter (APHA 5310B- high-temperature combustion method). Photometric method using HACH DR3900 was used to measure phosphate, nitrate and ammonia using respective calibrants supplied by HACH, UK. Heavy metals were analysed using 4100 MP-AES (microwave plasma-atomic emission spectrometry) (APHA 3120) and quantified against 7 standards of different concentrations (0.1, 0.5, 1, 10, 100, 1000, 10000 ppm) using environmental calibration standard (Agilent Technologies, Australia).

Parameter values were compared with those of Australian standards for irrigation and stormwater management (see Chapter 2). XPRAFTS 2016 software model was employed to calculate the discharge hydrograph for each rainfall event. The flow discharge served to calculate the load of each pollutant during the events. The XPRAFTS model data was supplied by Blacktown City Council. The analytical methods used to measure the concentrations of pollutants in the stormwater samples are summarised in Table 3.1. Further sampling dates and the rainfall intensities are tabulated in Table 3.2.

Table 3.1 Analytical methods used for stormwater parameter analysis

Parameter	**Unit**	**Test method**	**Detection limit**
Na	mg/L	APHA 3120 using 4100 MP-AES (microwave plasma - atomic emission spectrometry)	0.65
Ca	mg/L		0.05
Mg	mg/L		0.12
Sodium Adsorption Ratio		Calculated using following formula $SAR = [Na^+]/\sqrt{((Ca^{2+}/2) + (Mg^{2+}/2))}$	
DOC	mg/L	APHA 5310B-High temperature combustion method (using a Multi N/C 3100 analyser (Analytik Jena, AG))	0.05
Metals	mg/L	APHA 3120 using 4100 MP-AES (microwave plasma - atomic emission spectrometry)	0.01-0.05
Total Dissolved N	mg/L	Photometric method using test kit and HACH DR3900 spectrophotometer	0-16
Total Dissolved P	mg/L	Photometric method using test kit and HACH DR3900 spectrophotometer	0.05-1.5
Ammonium	mg/L	Photometric method using test kit and HACH DR3900 spectrophotometer	0.015-2
Turbidity	NTU	Turbidity meter (HACH 2100P)	1000
pH		HACH HQ40d meter and PHC301 pH probe	0-14
TDS	mg/L	HACH HQ40d meter and CDC40101 probe	0-50,000
Conductivity	ms/cm	HACH HQ40d meter and CDC40101 probe	0.01-200
TSS	mg/L	Known volume of sample was filtered	

		using 1.2 µm glass fibre filter and the residue oven-dried (104 ^{0}C), and weighed	
UV absorbance		UV–VIS Spectrophotometry (UV-1700, Shimadzu)	
Escherichia coli	CFU/100 mL	Membrane filtration method	1
Faecal coliforms	CFU/100 mL	Membrane filtration method	1

Table 3.2 Sampling dates, time and rainfall

Event number/date	**Sampling time**	**Rainfall interval (mm)**	**Event number /date**	**Sampling time**	**Rainfall interval (mm)**
E1 (19/06/16)	12.30	1.5	E10 (31/7/17)	13:17	0.3
	13:00	1		14:17	6.3
	13:30	1		15:17	0
	14:00	2.6		16:17	0
	16:00	11.4		17:17	0
E 2 (20/7/16)	8.55	1.7		18:17	0
	9.15	0		19:17	0
	9.35	0		20:17	0
	9.55	0	E11 (19/10/17)	8.30	3.3
	10.15	0		9.30	0.3
	10.35	0		10.30	0.2
	10.55	0		11.30	0.8
	11.15	0		12.30	0.5
E 3(20/7/16)	9.34	29.5		13.30	0.7

	10:04	3.8		14.30	3.6
	10:34	3.1		15.30	5.8
	11:04	0.2	E12 (20/3/18)	10.04	9.6
	11:34	0.3		12.04	2.4
	12:04	1.2		14.02	2.7
	12:34	0.3		16.04	0
	13:04	0		18.04	0
E4 (24/8/16)	10.00	1.7		20.04	0
	10:30	0.8		22.04	0
	11:00	0.5		0.04	0
	11:30	0.3	E 13 (26/9/18)	8.30	12.9
	12:00	0		9.00	0.8
	12:30	0.2		9.30	0
	13:00	1.3		10.00	1.2
	13:30	0.5		10.30	0.5
E5(7/2/17)	10.22	0		11.00	0
	11.07	0.3		11.30	0
	11.52	0.5		12.00	0
	12.37	3.5	E 14 (4/10/18)	7.38	0
	13.22	5.1		8.38	2
	14.07	2.3		9.38	2.3
	14.52	1.8		10.38	0
	15.37	0		11.38	0
E6 (8/2/17)	8.58	0		12.38	0
	9.43	0		13.38	1
	10.28	0.3		14.38	2.8
	11.13	0.8		15.54	1.8
	11.58	0		17.24	0.7
	12.43	0		18.54	1

	13.28	0		20.24	0
	14.13	5		21.54	2.1
E 7 (21/3/17)	15.11	0		23.24	24.4
	15.56	0		00.54	14.7
	16.41	0		2.24	5.6
	17.26	0.3	E15 (7/11/18)	11.45	1
	18.11	10.1		12.45	1.2
	18.56	1.8		13.45	2.3
	19.41	2.3		14.45	1.3
	20.26	0.5		15.45	0.5
E 8(22/3/17)	15.34	13.5		16.45	0
	16.00	5.5		17.45	0
	16.34	4.2		18.45	0
	17.00	0	E 16 (28/11/18)	7.45	17.5
	17.34	0		9.15	6.6
	18.00	0		10.45	12.7
	18.34	0		12.15	9.6
	19.00	0		13.45	23.2
E 9 (30/3/17)	8.57	0		15.15	5.3
	9.57	0		16.45	6.6
	10.57	3.6		18.15	1.5
	11.57	1.7			
	12.57	1.6			
	13.57	3			
	14.57	0.5			
	15.57	0.3			

3.3.1 UV absorbance calculations

The filtered samples (0.45 μm) for 4 events (events 13, 14, 15 and 16 which captured the first flush) were used for UV spectra recording. The UV spectra were recorded in the range of 200-500 nm at a medium scanning speed using 1 cm quartz cuvette cell (UV1700, Shimadzu, Japan). A blank correction was carried out each time before measuring the sample using Milli-Q water to avoid interference.

$$\boldsymbol{Area} = \sum_{\boldsymbol{\lambda}=\mathbf{200}}^{\mathbf{500}} \boldsymbol{A(\lambda)} \tag{3.1}$$

where, A(λ) is the absorbance and λ is the wavelength.

The normalised absorbance Abs(λ_N) was calculated by dividing the absorbance occurring at i wavelength by the total area (eqn 1). The value was multiplied by the norm N (N=80) to adjust the scale. The normalised absorbance Abs(λ_N) is calculated as:

$$Abs(\boldsymbol{\lambda_N}) = \boldsymbol{Abs(\lambda)} \frac{\boldsymbol{N}}{\boldsymbol{Area}} \tag{3.2}$$

This normalisation made it possible to identify a change in chemical composition irrespective of chemical concentration. The plotting of normalised spectra of samples from an event either shows overlap in spectra if only concentration changes or intersect (at one or more points, called isosbestic point) when chemical composition changes between samples.

3.3.1.1 Statistical Analysis

Linear relationships among water quality variables were determined using Pearson's correlation coefficients (*r*) using a standard statistical software package

(IBM SPSS Statistics version 25). Principal Component Analysis (PCA), a variable reduction technique, was carried out using SPSS (Version 25) so that the measured variables could be categorised into two principal components. The extraction method used included Kaiser-Meyer-Olkin (KMO) and Bartlett tests, and rotation-varimax. The KMO measured sampling adequacy was 0.561 (>0.5 is considered satisfactory). The Bartlett's test was used for the null hypothesis test, with varimax type rotation having a significance of 0.000 (should be less than 0.001). The ratio of the case to variable was 0.3 between the variables.

3.3.2. Urban pollutant build-up

The build-up of pollutants and wash-off govern stormwater quality (Aryal et al. 2015). It is assumed there is a constant build-up of pollutants on the surface during the dry weather period (Murphy, Cochrane & O'Sullivan 2015). Pollutant accumulation on the surface of any catchment during dry weather periods is usually expressed mathematically as a linear or non-linear such as power, exponential, or Michaelise-Menten function (Huber et al. 1988). The exponential function is the most widely surface of the catchment follows an exponential growth curve that approaches a maximum limit asymptotically (Shaheen 1975; Wang et al. 2011):

$$\frac{dB}{dt} = K_o - K_2 B \qquad \boxed{3.3}$$

where B is the pollutant amount per unit area on the catchment surface (mg/m^2); K_O is the pollutant deposition rate (mg/m^2 d); K_2 is the pollutant removal rate (1/d); t is the time (d).

The parameter K2 accounts for pollutant losses by resuspending the particles in the atmosphere by wind and/or vehicles as well as the biological and chemical decay of pollutant (Alley 1981; Alley & Smith 1981). Integration of Equation (3.3) yields:

$$B = K_1[(1 - \exp(-K_2T)] + B_O \exp(-K_2T) \qquad \boxed{3.4}$$

where K1 = K0/K2 is the maximum pollutant amount per unit area that can accumulate on the catchment surface (mg/m^2); T is the antecedent dry days (day); B0 is the residual pollutant amount per unit area after the previous storm runoff event (mg/m^2). If we assume there is no residual pollutant left on the surface after the previous storm event, then the above Equation (3.4) will be written as:

$$B = K_1[(1 - \exp(-K_2T)] \qquad \boxed{3.5}$$

3.4. Results and discussion

3.4.1. Pollutants concentrations and suitability of stormwater for field irrigation applications

Figures 3.4-3.8 present the trends observed for the various stormwater quality parameters and the rainfall distribution during the 16 rainfall events. The concentrations of the parameters had no relationship to the amount of rainfall (Table 3.4). However, regardless of the rainfall, many parameters (TDS, conductivity, DOC, and SAR) had the highest concentrations at the beginning of the rainfall event. This indicates that the first flush after a dry period carried the dissolved constituents, which have accumulated during the dry period, with the stormwater. It is interesting to note that in some events when the rainfall long after the first flush was highest the parameter concentrations were low (events 7, 9, 14). This is due to two reasons. Firstly, most of the constituents which accumulated during the dry period would have been removed with the stormwater in the first flush. Secondly, the high rainfall would have diluted the concentration of the constituents.

The pH varied between 6.4 and 8.5, which are within the safety limits for irrigation (Chapter 2), although, turf specialists would prefer to use a pH that is lower than 7.5 for irrigation, when feasible. However, continuous irrigation with stormwater with a pH level ranging from 6.5-8.5 will reduce/nullify the effect of the high pH waters which occurred at some stages. Alternatively, the pH of the water can be checked with a field pH kit before irrigation to avoid waters with extremely high pH for use in irrigation.

The TDS and conductivity were substantially lower than the ANZECC guidelines levels as the sporting surfaces in Blacktown International Sportspark, Sydney, are high profile and receive a large amount of irrigation (Fig. 3.4). However, during some of the first flush, these parameters were relatively high and much above the safety limit reported for salt sensitive/moderately sensitive crops due to the accumulation of salts during dry periods. Large amounts of irrigation water that are high in salts can lead to poor turf performance due to gradual salt accumulation. It is therefore important to only harvest stormwater during storm events above 5 mm as this should dilute the salt content and avoid first flush waters that are high in salts.

The SAR values were also below the permissible guideline levels of 8-18 for SAR-sensitive crops at most events except during the first flush periods in some instances (Fig. 3.8). However, at most periods of some events they were higher than the level of 2 which indicates that the water may not be suitable for very sensitive crops. Also, the turf specialists would prefer the water used for irrigation to have a SAR value of less than 4 (at its highest level). It is therefore important to only harvest stormwater avoiding first flush waters. The sodium concentration was also high in some events especially at the first flush, thus indicating that the water is not suitable for irrigating crops which are highly sensitive to sodium (safe limit 115 mg/L). In some samples of events 14 and 15 the sodium concentrations were much higher than 115-230 mg/L - the safety limit for crops that are moderately sensitive to sodium. Samples from E 12 to E16 were tested for 22 polycyclic hydrocarbons (PAHs) and the results are presented in Table A.1 (Appendix A). All tested PAHs were below the detection limit of <1 μg/L. Concentrations of pharmaceutical and personnel care products (PPCPs) were also very low and in most cases below the quantifiable concentrations of 5-50 ng/L (Table A.2).

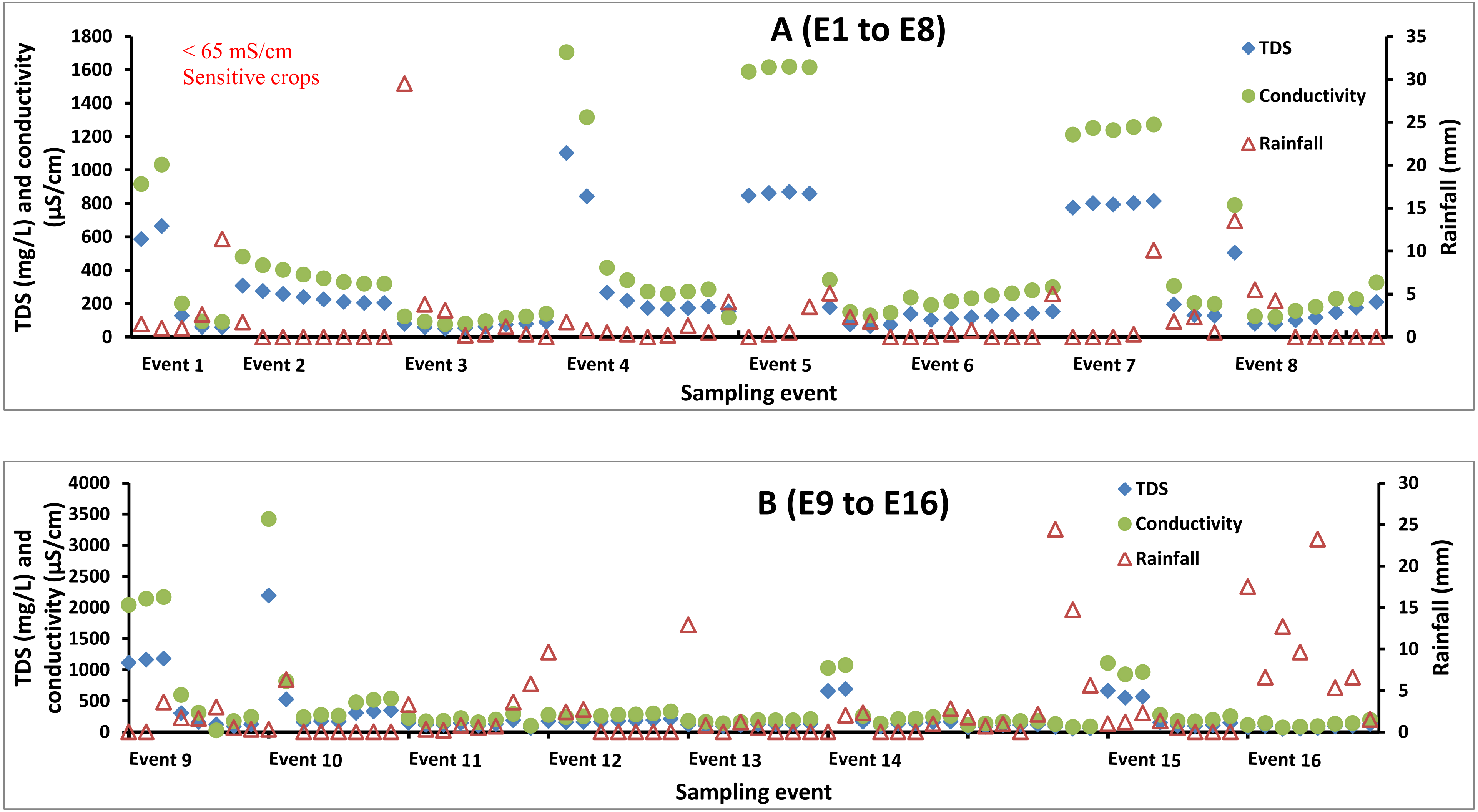

Figure 3.4 A & B. Variation of TDS and conductivity

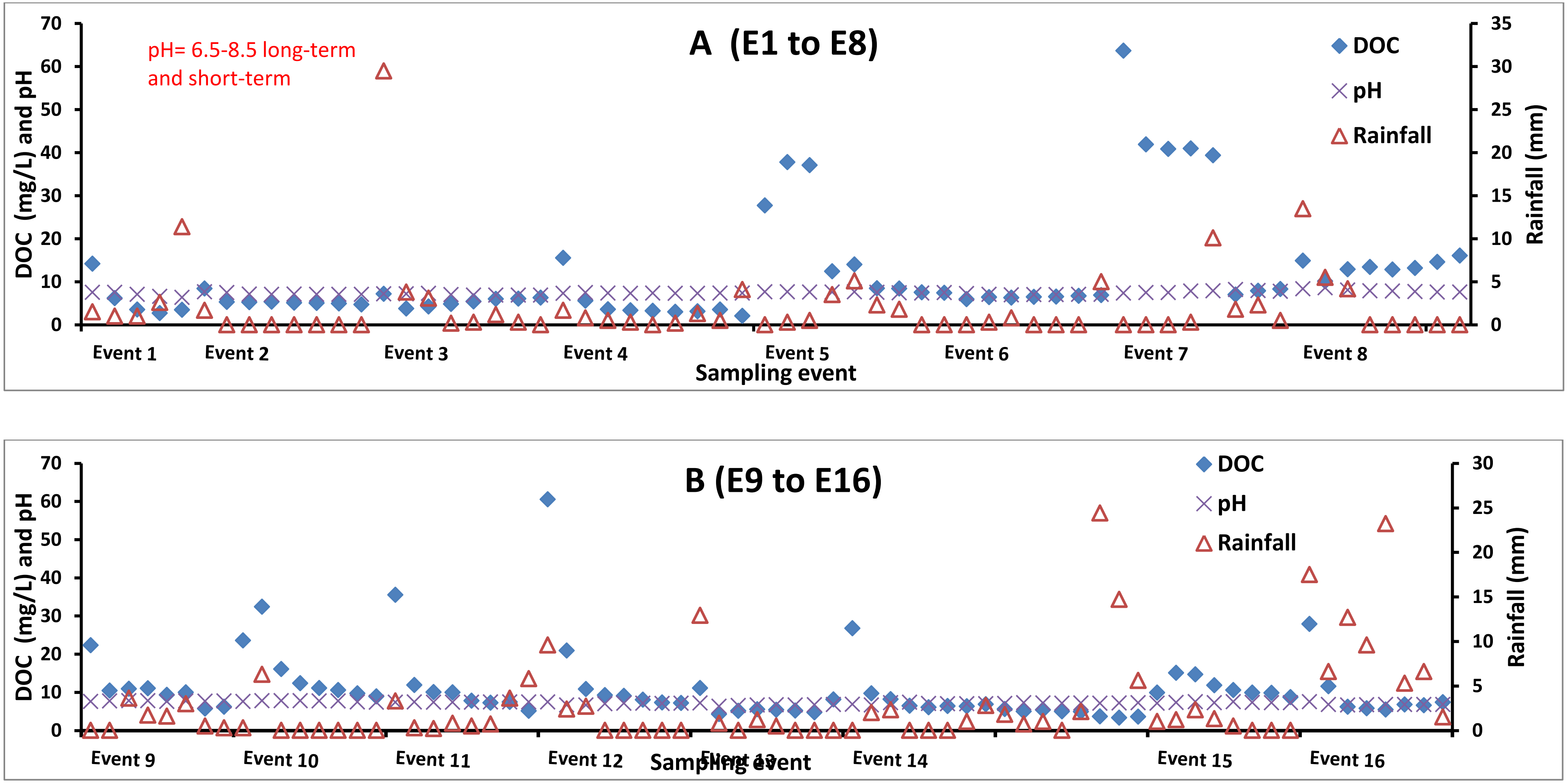

Figure 3.5 A& B Variation of DOC and pH

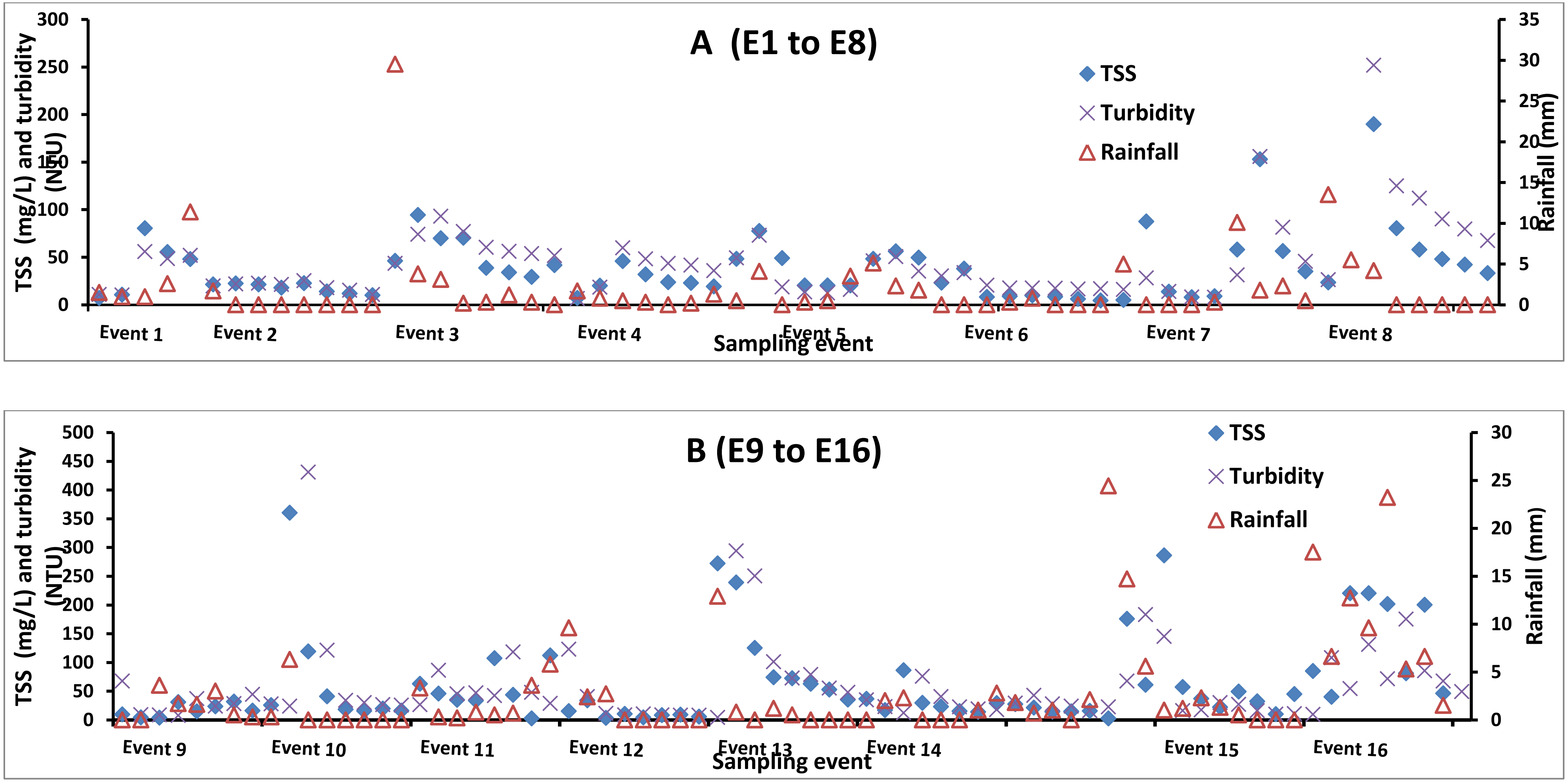

Figure 3.6 A & B Variation of TSS and turbidity

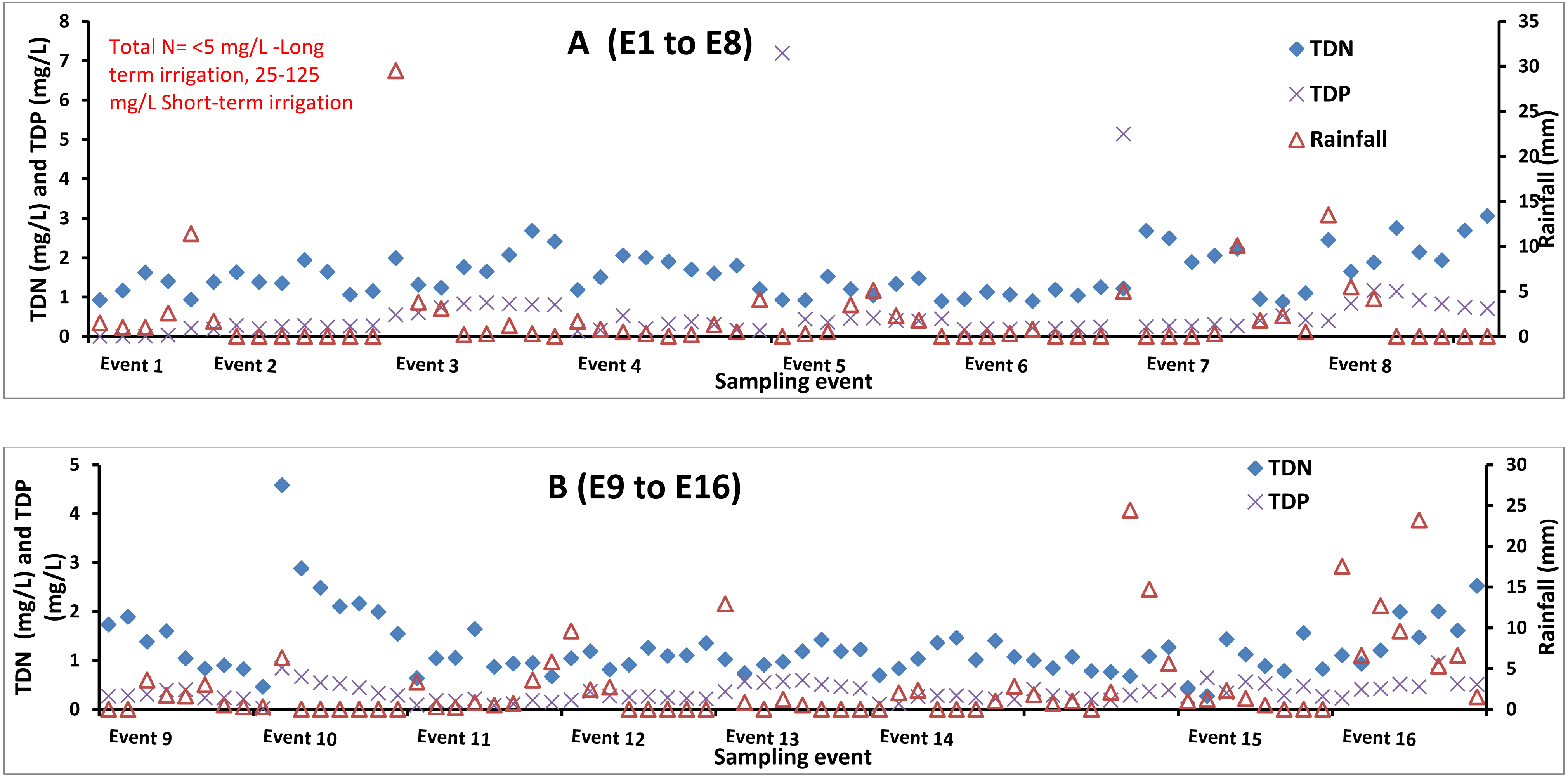

Figure 3.7 A & B Variation of TDN and TDP

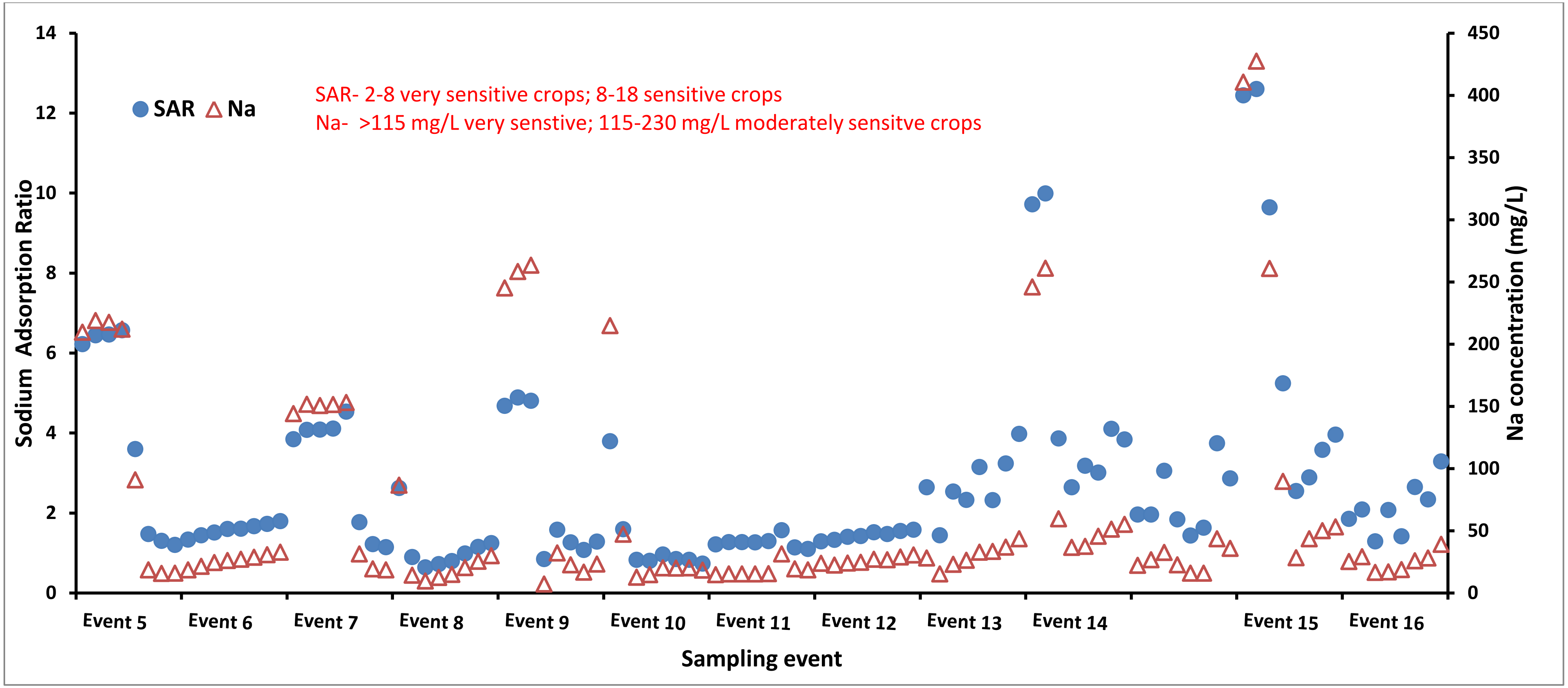

Figure 3.8 Variation of Sodium Adsorption Ratio (SAR) and Na

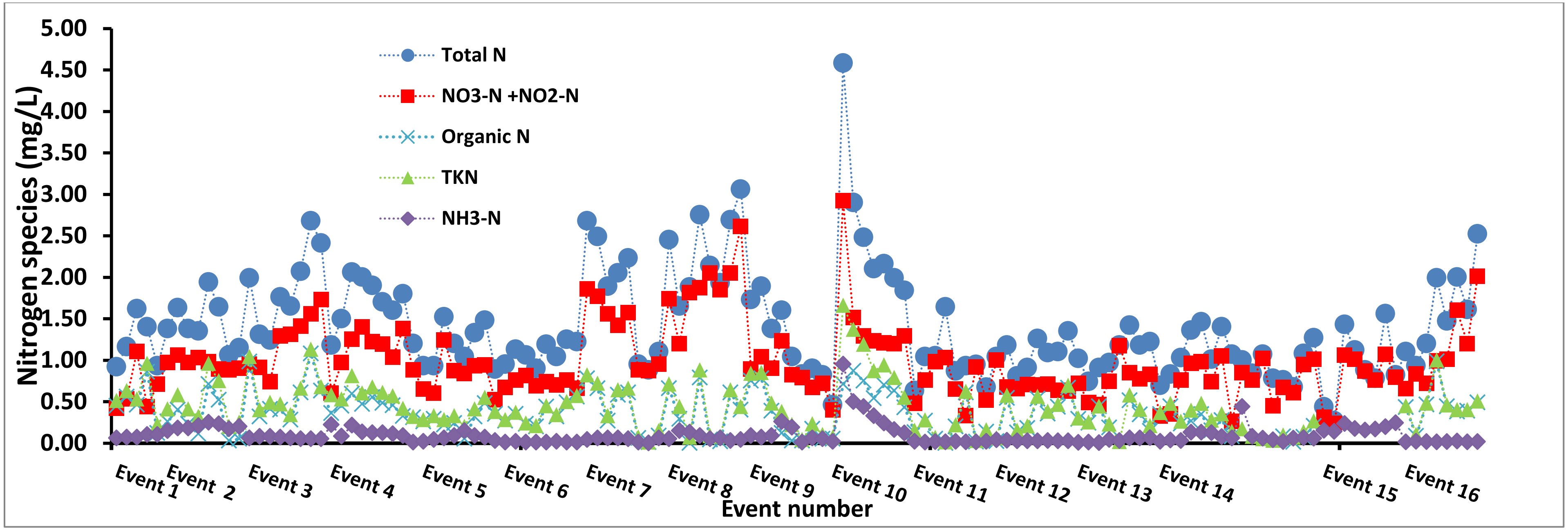

Figure 3.9 Nitrogen speciation variation over the time

3.4.1.1. Characterisation of N species in stormwater

At present, the standard limit of nitrogen in stormwater is based on total-N. The organic or dissolved forms of nitrogen are bio-available and there are no distinct standards for the different forms of nitrogen such as nitrate, nitrite, and ammonium. The traditional treatment techniques remove mainly the particulate form of nitrogen. A policy on treating dissolved forms of nitrogen will help in designing remediation methods for removing more harmful forms of nitrogen. Thus, in this study, initially, different forms of nitrogen in stormwater were measured so that appropriate techniques could be developed to remove different forms of N. Figure 3.9 shows that the major fraction of N composed of inorganic forms of N which can have direct effect on eutrophication. Organic components remained much lower in tested stormwater samples. Further, recorded concentrations for ammonia were also much lower.

3.4.1.2. Heavy metals

Figure 3.10 shows the range of heavy metal concentrations in the runoff samples. The measured metal concentrations were in the range (all in μg/L): Fe 639.93 - 965.32; Al 10.06-148.14; Mn 8.73-93.32; Cr 13.41-14.90; Co 11.91–12.59; Ni 15.41-20.58; Cu 21.40-77.44; Zn 4.64-44.76; Cd 8.45-8.97; Pb 23.49-23.91 and As 18.19-30.31. All heavy metals, except Fe, had concentrations below the respective safety levels for both short – and long-term irrigation (Chapter 2). Fe concentrations were higher than the safety limit for the latter at many sites but much lower than the safety limit for the former. This is not a problem because the water will not be used for irrigation on the same crop for a long period (100 years - for which the safety limit was considered). Furthermore, Fe added to irrigation water gets adsorbed/precipitated in the soils and becomes mostly unavailable to crops. It was observed that a wide range of variation in the heavy metals concentrations in the sample became evident. Heavy metals concentrations measured in the runoff samples were within the range of reported literature values, indicating that runoff from peri-urban contexts is not a serious concern from runoff discharge. However, attention is required if stormwater is recycled and reused and also to minimise the pollutants long-term risk to the environment (Becouze-Lareure et al. 2019; Graves, Wan & Fike 2004; Lau et al. 2009). Within the heavy metals concentrations data, Zn, Pb and Mn had a number of outliers and of these, Pb had the largest number. These stochastic data suggest the metals may have different sources of origin and the contribution from each source is irregular.

Many studies have reported that Cu and Zn have similar sources of origin in urban commercial or industrial land use (Aryal, Murakami, et al. 2006; Budai & Clement 2011). Vehicles are another potential source of Cu and Zn (Davis, Shokouhian & Ni 2001; Loganathan, Vigneswaran & Kandasamy 2013). The release of Zn from vehicle use includes tyre wear, and Cu from brake wear, and both Cu and Zn from road surface wear and leaking petroleum products. The relationship between dissolved Cu and Zn in stormwater runoff when assessed led to a positive correlation being observed. This outcome suggested that metals are generated from a mixture of land use and share common features with other peri-urban catchments.

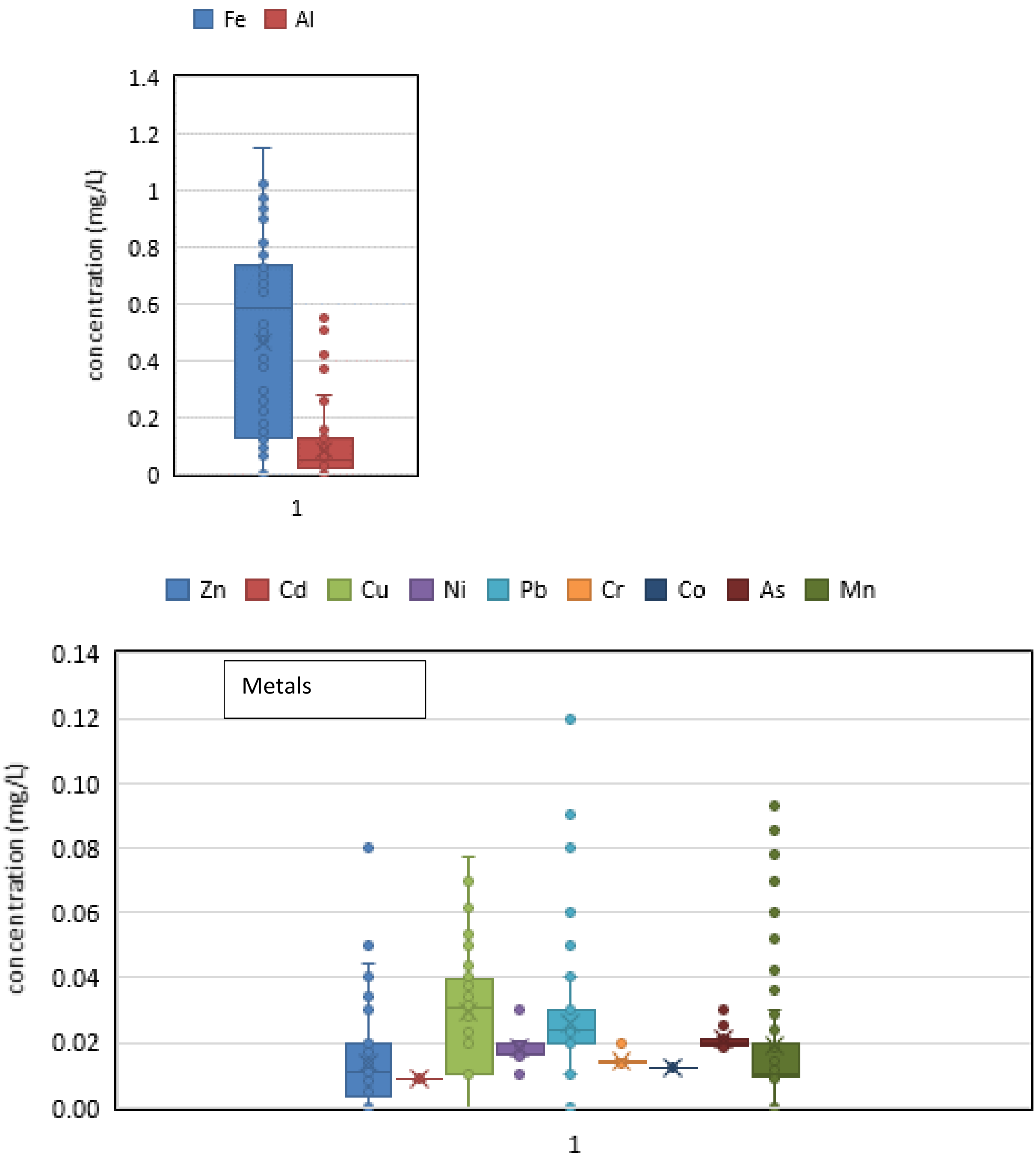

Figure 3.10 Boxplot for the concentrations of the analysed heavy metals. Risk level for long-term irrigation (mg/L): Fe (0.2), Zn (2), Cd (0.01), Cu (0.5), Ni (0.2), Pb (2), Cr (0.1, Mn (0.2), Co (0.05); Fe short-term (20 years) irrigation 10 mg/L

3.4.1.3 Microbiology analysis

Table 3.3 tabulates the figures concerning microbial analysis for few events. E. coli and faecal coliforms concentrations were very high and much above the safety limits for irrigation of food crops and spray/drip irrigation of open spaces, parks and sports grounds. Therefore, the water needs to be either disinfected or used in secured applications. However, it can be used for pasture and fodder, for example grazing animals except pigs and dairy animals, i.e. cattle, sheep and goats (ARMCANZ, ANZECC & NHMRC 2000). It can also be used for silviculture, turf, cotton, etc. (with restricted public access).

Table 3.3 Microbiological results for the stormwater analyses

Sampling Date	**Analysis**	**Unit**	**Result**
7 Feb 2017	Faecal Coliforms	CFU/ 100 mL	30000
	Escherichia coli	CFU/ 100 mL	30000
8 Feb 2017	Faecal Coliforms	CFU/ 100 mL	5200
	Escherichia coli	CFU/ 100 mL	5200
19 Oct 2017	Faecal Coliforms	CFU/ 100 mL	23000
	Escherichia coli	CFU/ 100 mL	23000
4 Oct 2018	Faecal Coliforms	CFU/ 100 mL	5000
5 Oct 2018	Faecal Coliforms	CFU/ 100 mL	16000

7 November 2018	Faecal Coliforms	CFU/ 100 mL	49*
	Faecal Coliforms	CFU/ 100 mL	49*

*Results not reliable because samples were kept too long before analysis was done

3.4.2. Rainfall characteristics

Figure 3.11 shows flow hydrographs and pollutographs of DOC for four events. These four events were selected out of the 16 events to represent four different rainfall characteristics. The remainder is given in the supplementary information (Fig. A.1-16,Appendix A). The event on 26th September 2018 had very high rainfall at the beginning of the event. The event on 4th October 2018 was moderate and rainfall stopped for almost 5.5 hours. The minimum inter-event time between the two consecutive events was assumed 8 hours (Aryal et al. 2007). The halt in rainfall in this event was less than the assumed minimum inter-event time and so it was considered a single event. The event on 7 November 2018 was a weak one but was continuous and peaked in the middle of the event. The event on 28 November 2018 was more intense and runoff peaked during the later stage of monitoring. Figure 3.11 shows that for all monitored events the DOC concentration was high at the beginning of runoff and receded over time. During the 4-5th October 2018 period, a small peak appeared in the middle of the event caused by the halt in rainfall during the middle of the event. Despite this, DOC concentration was highest at the beginning of the event.

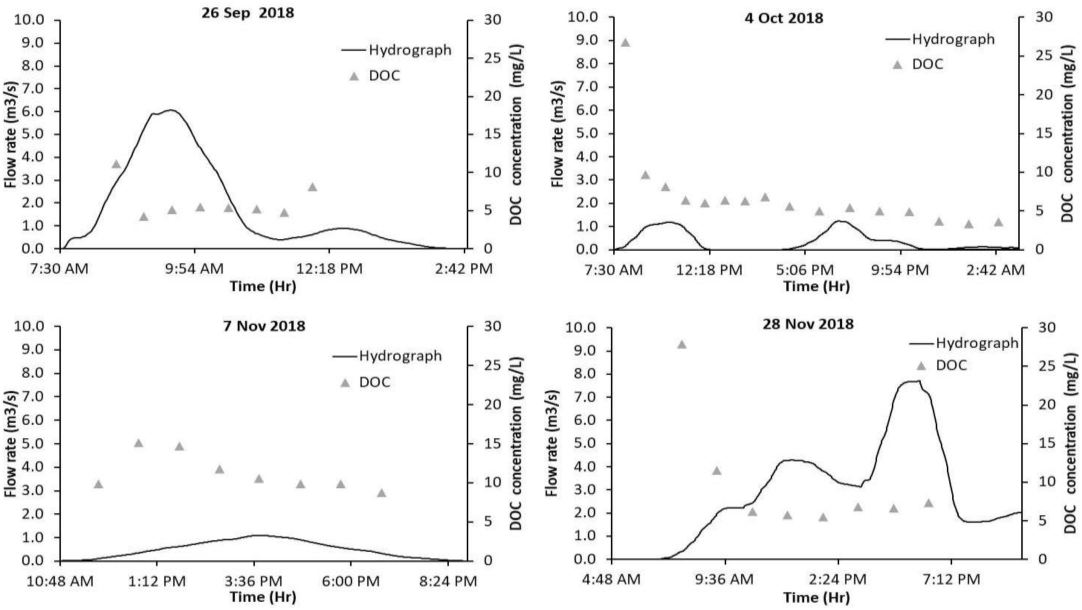

Figure 3.11 Hydrograph and DOC pollutograph during 26th September 2018, 4th October

3.4.3. Correlation among pollutants

The pollutants concentration ranges were found to be within the reported literature values (Huang et al. 2007). Table 3.4 shows the correlation between the dissolved pollutants (metals not included) in all the measured stormwater samples (number of samples =134). Although the flow rate is the impetus for the transport of pollutants, we observed high pollutants concentration at the beginning of the runoff and there was no good correlation between the flow rate and pollutants concentrations.

There was a strong correlation between conductivity and TDS (*r* = 0.99). Among other pollutants, there was a positive correlation between DOC and conductivity (*r* = 0.55), and between DOC and TDS (*r* = 0.52). The strong relationship between TSS and turbidity *(r* = 0.91) shows that turbidity arises in stormwater mainly due to TSS. The significant relationship between DOC and conductivity is probably due to the presence of organic anions in DOC which caused increased conductivity (Monteiro et al. 2014). Monteiro *et al.* (2014) reported strong positive relationships between DOC and conductivity in a stream during wet and dry seasons in Amazonian blackwater catchment by analysing over 10,000 water samples. The statistically significant relationship observed between some parameters indicates that they may have a dependency on mobilisation and also the possibility of a similar source of release. This claim has support in literature (Ghane et al. 2016). Although the correlation analysis revealed some relationships between pollutants, in general, they were not strong and were not helpful in revealing pollutants that could be expected to behave similarly.

Figure 3.12 shows the outcome of principal component analysis (PCA) analysis. The distributions of principal loadings bi-plots for pollutants are presented in Figure 3.12. Even though there were rainfall 16 events in total, only 13 events were considered for the PCA analysis. Rainfall events with very low rainfall which was less than 2 mm were omitted. The pollutants that produced communalities of more than 0.5 (as required for PCA analysis) were used for in the plots. Bi-plots show loadings that are situated closely together and represent parameters that are highly correlated. The bi-plot suggests that most of the data variance is contained in the first two components, namely C1 and C2. According to the graph total dissolved solids (TDS), conductivity (Cond) and dissolved organic-carbon (DOC) have a close relationship . As seen previously (Table 3.4), these parameters have high correlation coefficients and have similar behaviour. TKN, Total N, NO_3N and Total P have a close relationship and is explained by component 1. The two components C1 and C2 explains 72% of the variability between parameters. Heavy metals were not used for the PCA analysis because of their relative scarcity in the sampled data.

Table 3. 4 Correlation among dissolved pollutants in stormwater runoff

	DOC	TN	NO_3N	TKN	NH_3N	TP	Turb	pH	Cond	TDS	TSS	Flow
DOC	1.00	0.05	0.02	0.32	0.29	0.05	0.23	0.24	0.55**	0.52**	-0.04	0.02
TN		1.00	0.88**	0.56**	0.17	0.37*	0.07	0.26	0.38*	0.38	0.03	0.19
NO_3N			1.00	0.22	0.02	0.42*	0.01	0.08	0.53**	0.53**	-0.12	0.24
TKN				1.00	0.46**	0.08	0.26	0.53**	-0.16	0.14	0.32*	0.06
NH_3N					1.00	0.08	0.40*	0.61**	0.11	0.08	-0.30	-0.11
TP						1.00	0.31	0.24	0.28	0.3	0.29	0.25
Turb							1.00	-0.58*	0.33*	-0.32*	0.91***	0.15
pH								1.00	0.30	0.27	0.44**	0.23

Cond	1.00	0.99**	0.01	0.09
TDS		1.00	-0.02	0.09
TSS			1.00	0.25
Flow				1.00

n-1 =134; Highlights marked with yellow, blue, and green colours represent statistical significance at probability levels of 0.05, 0.01, and 0.001, respectively. Numbers in the table are correlation coefficients

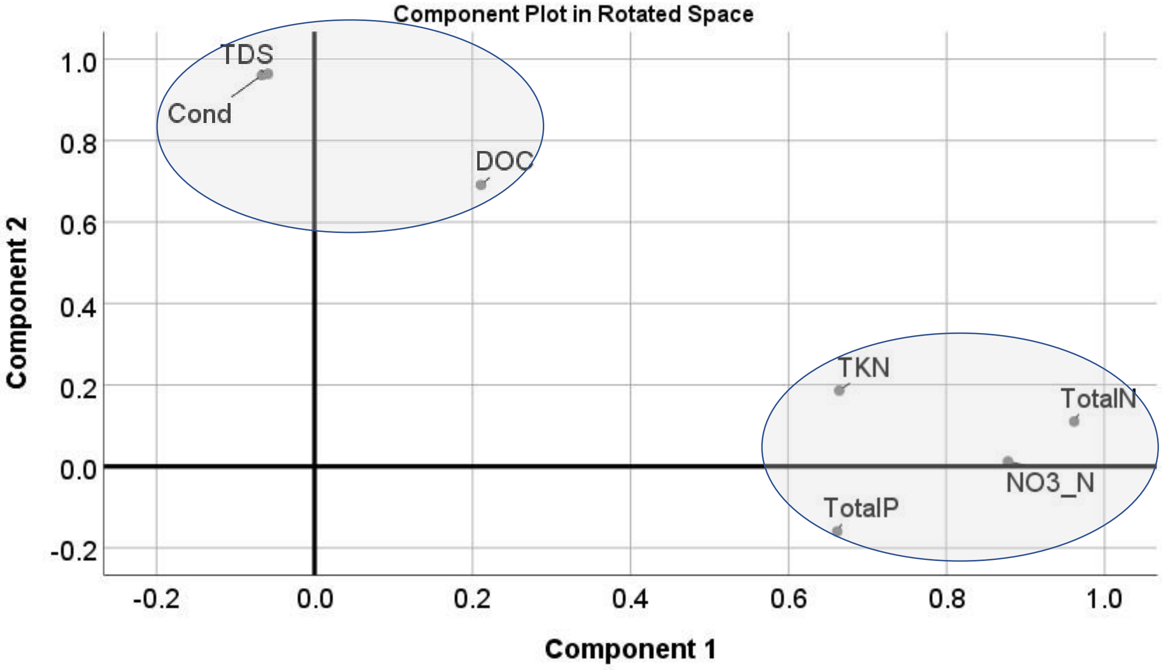

Figure 3.12 PCA plot of the water quality parameters from 13 stormwater runoff events

3.4.4. first flush identification using UV

UV measurement at 254nm has been widely used as an indicator for DOC and aromatic compounds in water and wastewater (Altmann et al. 2016; Madzivhandila & Chirwa 2017; Musikavong & Wattanachira 2007). The UV spectra arise when an organic molecule having a double bond or lone pair of electron gets excited by UV irradiation. Different pollutants have different chemical structure, and the absorbance occurs in different regions of the UV spectrum (Aryal, Vigneswaran & Kandasamy 2011). By definition, the first flush occurs during the early phase of runoff and where most of the pollutants are washed off. Since the nature and concentration of pollutants vary with time of runoff in an event, capturing the UV spectrum of samples provide a chemical fingerprint of runoff at that time.

When the recorded UV fingerprints are compared, it would help to locate the time where the fingerprint changes. Figure 3.13 (a-d) shows the UV spectra plot for the 4 rain events (26th September 2018, 4th October 2018, 7th November 2018, 28th November 2018). The UV spectra show subtle variations in the UV spectrum among the samples collected consecutively during an event.

To investigate further, we normalised the spectra shown in Figure 3.13 a-d and replotted (Figure 3.13 e-h). The normalisation allowed the spectrum to display any differences in chemical fingerprint irrespective of chemical concentration. In each event, the UV spectrum produced two sets of spectral groups that intersect each other at wavelengths between 225-230 nm. The intersect is also called the isosbestic point which is a sign of a change in chemical composition in the sample. UV spectrum shape is obviously dependent on the pollutant nature and concentration available in the tested water sample (Thomas et al. 2017). When the chemical composition of a sample was changed, the UV spectrum also shifted to the different zone. Clearly indicated that the UV spectra of all samples intersect at one point known as the isobestic point.

In Figure 3.13 e-h, two groups of curves were observed in each event and are for samples at the beginning of the event and for samples at the later stage of run-off. The result implies that the first set of samples have different chemical composition than those samples from the later stage. We ascribe the isosbestic point as a first flush indicator point. Since the quality of runoff depends on a number of catchment characteristics such as topography, geology, traffic, vegetation, etc., the isosbestic point may appear in a different region(s) from the samples measured in another catchments. Aryal et al. (2017) identified the isosbestic point between 218-225 nm when measured in road runoff.

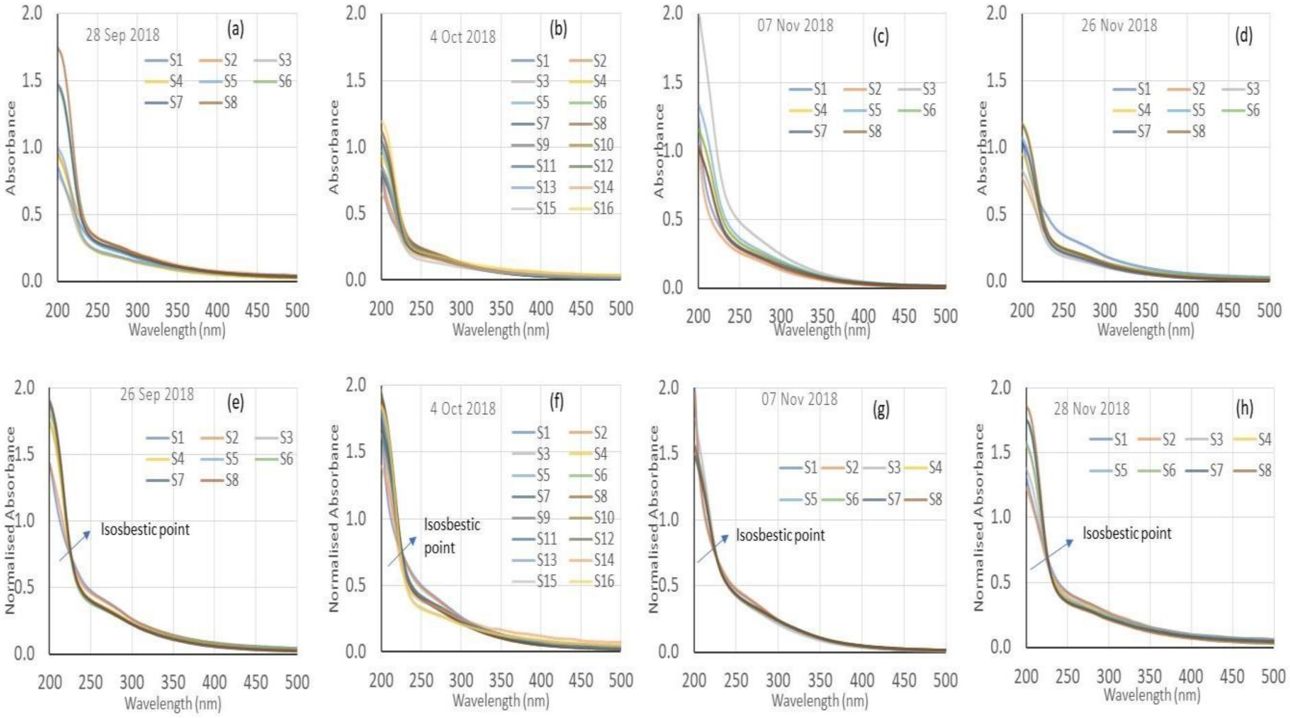

Figure 3. 13 UV absorbance record in runoff events

3.4.4.1. Relationship between measured parameters in the first flush

Figure 3.14 is the correlation plots between parameters that PCA had revealed as behaving similarly to DOC (TDS vs DOC, Conductivity vs DOC, DOC vs UV_{254} and TDS vs UV_{420}) for the four events. The red dot points indicate those occurring during the first flush and black data points show those occurring after the first flush. The rigid black line in the middle in Figure 3.14 represents the correlation line and the two outer lines represent the 95% confidence limits. The correlation graph shows that the data points within the first flush (Figure 3.14 a-d) displays anomaly (no correlation). Those data points after the first flush show good correlation. When re-plotted by excluding the data within the first flush, the correlation increased by 25-40% (DOC vs 254 nm increased from 0.863 to 0.901, DOC vs TDS increased from 0.521 to 0.628, DOC vs Conductivity from 0.545 to 0.716 and UV420 vs TDS 0.190 to 0.399). UV spectra can distinguish the change in the composition of samples within the first flush (and which do not correlate) and the samples in the remaining runoff in stormwater monitoring.

UV has been used in the past to detect organic matter. In this study, PCA analysis was used to detect pollutants that correlated with DOC and expected to behave similarly. Analysis of the UV spectra showed how it was able to detect a change in chemical composition and isosbestic point typically identifying the end of the flush. This applied to DOC as well as those pollutants that correlated with DOC as identified by PCA. The non-destructive nature of UV testing, its ease of use and rapid analysis, and interpretation lends itself to on-site testing and real-time testing. In this way, it could be integrated into treatment systems that are intended to treat the most polluted part of the runoff.

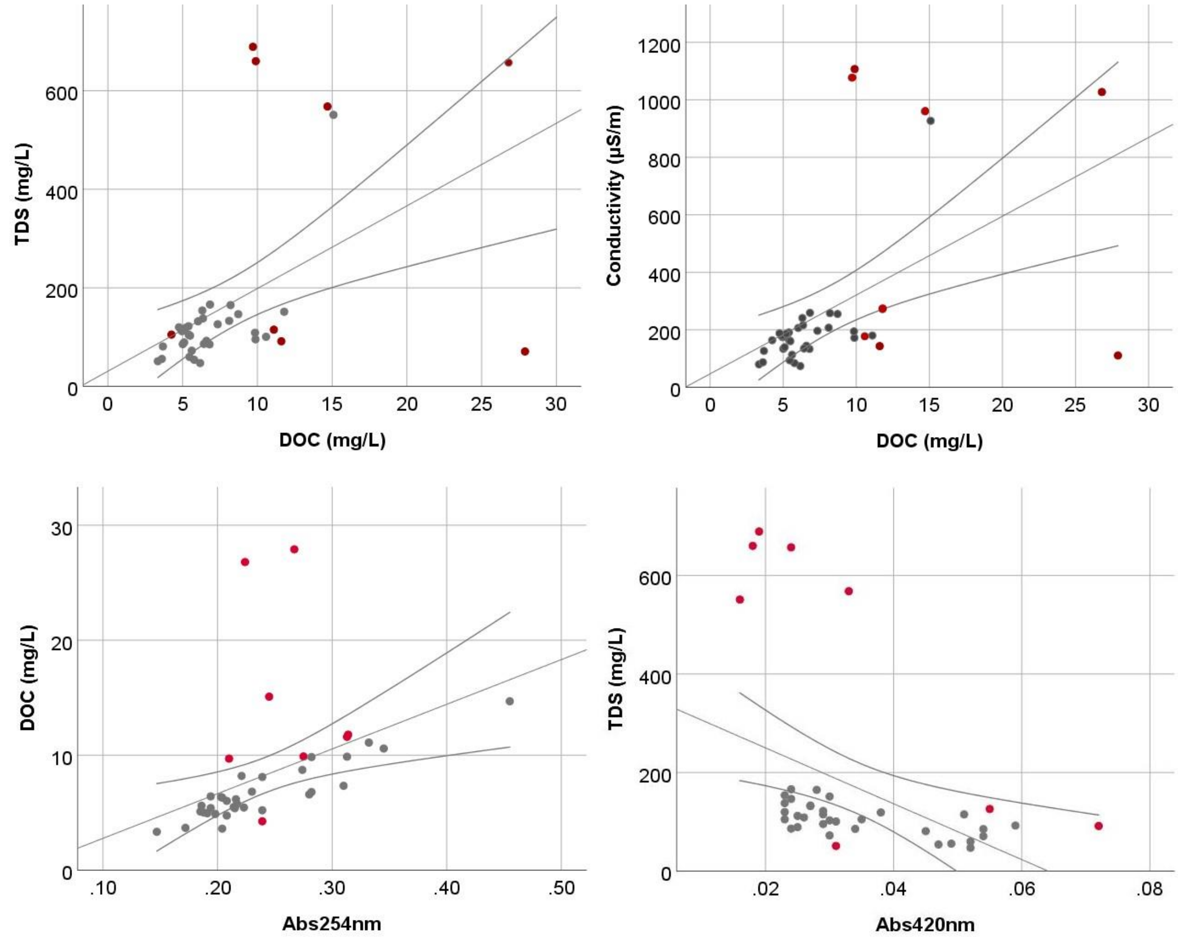

Figure 3.14 Relationship between measured parameters in the first flush (red dots indicate samples within the first flush and black dot indicates samples after the first flush)

3.4.5. TSS build-up measurements

Figure 3.15 shows the build-up of total suspended solids in the Angus Creek catchment. 10 rainfall events were considered based on the rainfall intensity and the intermittent periods of rainfall events. The TSS is one of the major indicators of water quality and governing factor for particle bound pollutants such as heavy metals, nutrients and organic pollutants (PAHs) (Aryal et al. 2005; Nie et al. 2008; Rügner et al. 2013; Wang et al. 2011). Hence TSS is used as an indicator for building the model. The collected data were within the dry weather period of 1 to 48 days. The data suggested that the build-up of total suspended solids becomes non-linear at the beginning and after 5 days, the build-up is virtually saturated.

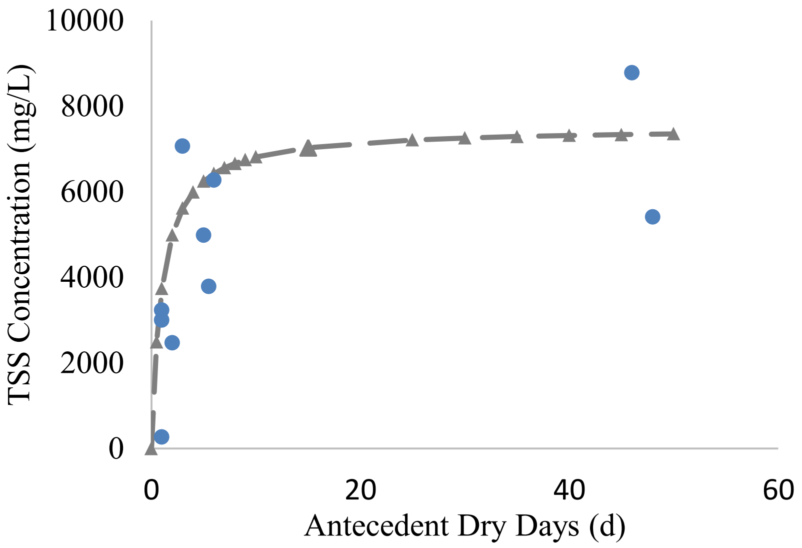

Figure 3.15 Total suspended solids build-up in Angus Creek catchment over period of time

3.5. Conclusions

Stormwater runoff samples were collected during 16 rainfall events covering three years (2016-2018) from Blacktown International Sportspark, Sydney, and analysed for water quality. The aim was to identify the relationships among the measured pollutants and the method to quantify the first flush runoff volume. The measured pollutants concentrations were within the range reported in previous studies. Mostly all events showed a first flush effect irrespective of the preceding dry weather period. This suggests that the first flush after a dry period carried the dissolved constituents, which had accumulated during the dry period, with the stormwater and increased the pollutant concentration.

The study on the relationship between measured pollutants showed that a simple linear (correlation) relationship may not completely explain the pollutants wash-off phenomenon. A Principal Component Analysis (PCA) showed two major components (C1 = TKN, TN, TP, NO3-N and C2= TDS, Cond, DOC) and the two components could explain 72% of the variability between parameters. Bi-plots show loadings of DOC, TDS, conductivity (Cond) are situated closely together and represent parameters that are highly correlated. The UV spectroscopy measurements on the stormwater samples revealed changes in the spectrum over time during runoff. In each rainfall event the UV spectrum produced two sets of spectral groups that intersected each other at wavelengths between 225 and 230 nm. The intersect which is called the isosbestic point indicates the end of the first flush. This information was exploited to separate the first flush from the remaining clean flush for DOC and for pollutants that behave similarly to it.

TDS and conductivity were substantially lower than the ANZECC guidelines levels at most events. However, during some of the first flush, these parameters were relatively high and much above the safety limit reported for salt sensitive/moderately sensitive crops. Large amounts of irrigation water that are high in salts can lead to poor turf performance due to salt accumulation impacts. In sensitive areas, it is therefore important to only harvest stormwater during storm events above 5 mm as this should dilute the salt content and avoid first flush waters that are high in salts. Both the Na and SAR values were also below the permissible guideline levels for Na/SAR-sensitive crops at most events except during the first flush periods in some instances. It is therefore important to only harvest stormwater avoiding first flush waters in most areas.

The concentrations of all heavy metals except Fe were within the safety levels. Fe concentrations were below the safety limit for short-term irrigation (20 years - the period reported in the safety-standard guidelines) but high enough to cause problems for long-term irrigation (100 years). Concentrations of polycyclic aromatic hydrocarbons (PAHs) and pharmaceutical and personnel care products (PPCPs) were below the quantifiable limits, therefore of no concern. There were strong positive correlations between conductivity and TDS (r = 0.99) and between TSS and turbidity (r = 0.91). Among other pollutants, there was a positive correlation between two aspects: DOC and conductivity (r = 0.55), and between DOC and TDS (r = 0.52).

This study reveals that the microbiological (E. coli and Faecal coliforms) component is much higher than the recommended levels suggested for irrigation and it should be closely monitored during future studies. Recognition of pathogenic microorganisms likely to be present is an advantage for secured application of stormwater management. The presence of waterborne pathogens, human biomarkers and faecal indicators must be analysed in future studies. Further pollutant build-up analysis revealed the relationship between TSS and the dry weather period. Number of dry days prior to a rainfall event can be used as an indicator to predict the pollutant loads of a rainfall event.

Chapter 4

Polycyclic aromatic hydrocarbons (PAH) removal from water using granular activated carbon: kinetic and equilibrium adsorption studies

This chapter publishsed as Eeshwarasinghe, D., Loganathan, P., Kalaruban, M. *et al.* 2018, Removing polycyclic aromatic hydrocarbons from water using granular activated carbon: kinetic and equilibrium adsorption studies. *Environ Sci Pollut Res* **25,** 13511–13524. https://doi.org/10.1007/s11356-018-1518-0

Chapter four

4.1. Introduction

In Chapter 2 it was reported that PAHs are a major group of pullutants generated from natural as well as anthropogenic activities and they can accumulate to dangerous levels in the environment over time (Makkar & Rockne 2003). In Chapter 3, which presented the concentrations of pollutants found in stormwater in Sydney, it was reported that PAH concentrations in the stormwater were below the detection limit of µg/L. Though PAHs were not detected in the stormwater at this site, scientists should not be complacent with these results because in many parts of the world toxic levels of PAHs have been reported (Chapter 2). Also, in many other places in Australia high levels of PAHs have been reported in stormwater(Duodu et al. 2017). It is expected that with the increase in population and industries, like other pollutants, PAHs concentrations in stormwater would increase and research information need to be obtained early to have technology in place to deal with this problem, and hence the initiation of the study reported in this Chapter.

To protect the environment, World Health Organization (WHO) has recommended concentration limits for various PAH in drinking water and the United States Environmental Protection Agency (USEPA) effluent guidelines division has included PAH in its list of priority pollutants to be monitored in industrial effluents**.** USEPA has categorised 16 PAHs in the priority list due to their adverse impact towards environment and human health (Yakout, Daifullah & El-Reefy 2013; Zhang et al. 2004).

Due to the toxic, mutagenic and carcinogenic natures of PAHs, significant interest has been raised in developing appropriate removal process for the PAHs

(Liu et al. 2016; Makkar & Rockne 2003; Yuan et al. 2010). Usually PAHs are difficult to remove efficiently by applying conventional physicochemical methods such as coagulation, flocculation, sedimentation, filtration or ozonation. However, adsorption process is a most promising technique in the removal of persistent organic pollutants and, in particular, activated carbon (AC) adsorbents are widely used for this purpose (Chen, Zhou & Zhu 2008; Cooney et al. 1999a; Crisafully et al. 2008; Valderrama et al. 2008). Some advantages AC possess are large internal specific surface area and highly developed porous structure, and efficient adsorption of pollutants even at low concentrations (Ania et al. 2007). Furthermore, PAHs are removed by AC from the water rather than being broken down by oxidation or reduction to potentially more dangerous metabolites (Valderrama et al. 2008).

Extensive research has been carried out on PAHs removal using AC for the removal of one or two PAHs, but only a very few studies have been conducted with a suit of PAHs (Khan, Khaodhir & Rotwiron 2007; Valderrama et al. 2007; Valderrama et al. 2009; Valderrama et al. 2008). Also, most of the studies on AC for removing PAHs have been conducted in static batch experiments, while only a few were done in dynamic column experiments (Khan, Khaodhir & Rotwiron 2007). The latter ones are more relevant to practical water treatment conditions in the field. The aims of this study, therefore, were: (1) to investigate the batch kinetic and equilibrium adsorption of five PAHs on to a granular activated carbon (GAC) and to explain the adsorption processes by using mathematical models, and (2) to investigate the adsorption of three PAHs on to GAC using dynamic fixed-bed column experiments and model the breakthrough curves using Thomas model. Concentrations of PAHs higher than those found in surface waters were used in the study to reliably measure the concentrations utilising a common analytical instrument. However, the concentrations used were similar to those of industrial effluents and therefore the results can be directly applied to treatment of these effluents.

4.2. Material and methods

4.2.1 Materials

Granular activated carbon used in the study was obtained from James Cummins P/L, Australia. It had a nominal size of 0.3–2.4 mm. To reduce the experimental variability, a narrow particle size range of 0.6-1 mm GAC was selected for the study. PAHs employed in the adsorption experiments were naphthalene, acenaphthylene, acenaphthene, fluorene and phenanthrene. The characteristics of the PAHs are presented in Table 4.1. Since PAHs had low solubility in water, experimental solutions were prepared from stock solutions of each PAH dissolved in acetonitrile (1%). Experimental solutions were prepared by diluting the stock solutions in MQ water for batch experiments and tap water for column experiments. The stock solutions contained 20 mg PAH in 40 mL acetonitrile (0.5 g/L). Experimental solutions were prepared by diluting the stock solutions in 1% acetonitrile made up with Milli-Q® water (ultra-pure water) for batch experiments and tap water for column experiments. To achieve the 6 mg/L used in the adsorption experiments, 13-mL stock solutions were diluted to 1 L using 1% acetonitrile for naphthalene, acenaphthylene and acenaphthene. concentration in the final solution was 2.3% for these PAHs. As fluorene and phenanthrene did not dissolve in the 1% acetonitrile, additional undiluted acetonitrile was added to the experimental solutions until they were dissolved. The final acetonitrile concentration for fluorene and phenanthrene was 4.5%. Acetonitrile and PAHs used were spectroscopically grade materials purchased from Sigma-Aldrich

4.2.1.1 GAC characteristics

Surface morphology of GAC particles was examined using a Hitachi S3400 Scanning Electron Microscope operated at 20 kV. Samples were sputter coated with gold prior to analysis. Surface area and porosity characteristics were measured using nitrogen adsorption-desorption isotherm by employing a Micrometrics TriStar 3000 Analyser (Micromeritics Instrument Co, USA). The specific surface area was determined using the nitrogen isotherm data measured at 77K from a relative pressure (p/p_o) of 10^{-5} to 0.99 by applying the BET equation. Before the analysis, the sample was vacuum dried for 3 h at 150 °C. The total pore volume was estimated to be the liquid volume of nitrogen at a relative pressure of 0.99. The micropore pore volume and the mesopore pore volume were calculated from the N_2 isotherms data by Dubinin-Astakov (DA) and BJH methods, respectively (Long et al. 2008; Sing 2004). The algorithm used in the TriStar 3000 Analyser is an implementation of these methods. Pore-size distributions were calculated by applying the density functional theory (DFT) to the N_2 isotherm data using the Micromeritics Software of the analyser (Long et al. 2008)

Table 4.1 Characteristics of the PAH used in the study (chapter 2) [1]Awoyemi (2011); [2]Miller et al. (1985); [3] Wammer & Peters (2006). [*]This value was estimated from Fig. 3 and Table 2 of the article by (Gustafson & Dickhut 1994)

PAH	Molecular formula	Molecular structure	Molecular weight (g/mol)	Aqueous solubility (25 ^{0}C) (mg/L)	Log K_{ow}	Molar volume[2] (cm^3/mol)	Molar dimensions [1,3] (Å)
Naphthalene	$C_{10}H_8$		128	31.7	3.30	148	9.1*7.3*3.8
Acenaphthylene	$C_{12}H_8$		152	16.1	3.94	168[*]	___
Acenaphthene	$C_{12}H_{10}$	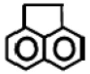	154	3.9	3.92	173	9.1*8.3*4.2
Fluorene	$C_{13}H_{10}$	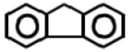	166	1.9	4.18	188	11.4*7.3*4.2
Phenanthrene	$C_{14}H_{10}$	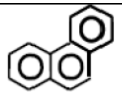	178	1.15	4.46	199	11.6*7.9*3.8

4.2.2 Method development

HPLC (Khan, Khaodhir & Rotwiron 2007; Walters & Luthy 1984) GAS chromatography (Awoyemi 2011; Crisafully et al. 2008; Lesage, Sperandio & Tiruta-Barna 2010), and GS/MS (Nguyen et al. 2014) techniques are popular methods for PAHs measurements. These advanced methods for the measurement of PAHs are specially used to measure very small concentrations (µg/L). However these methods are highly sophisticated, time consuming and the instruments are expensive. In this study, a simple and popular method of UV/VIS spectroscopy was used to obtain reliable measurements of PAHs (Ania et al. 2007; Awoyemi 2011; Valderrama et al. 2007; Valderrama et al. 2008). Most PAHs are insoluble in water; therefore a suitable organic solvent also should be selected to dissolve PAHs before diluting the PAHs solution with water. Use of suitable organic solvents proportionately in low quantities is very important.

4.2.2.1 Selecting a solvent

UV absorption was measured at different wave lengths for PAHs dissolved in three solvents, namely acetone, methanol and acetonitrile. The UV spectra were recorded in the range of 190-400 nm at medium scanning speed using 1cm quartz cuvette cell (UV1700, Shimadzu, Japan). From these experiments the solvent and wave length which gave the sharp and intense absorption peak was selected for measuring the concentration of each PAH. The results of these experiments are presented in Fig. 4.1 to 4.3. It is clearly visible from the figures that acetone as a solvent did not provide clear peaks for any of the three PAHs tested, whereas acetonitrile and methanol gave clearly distinguishable peaks for each tested PAH compound.

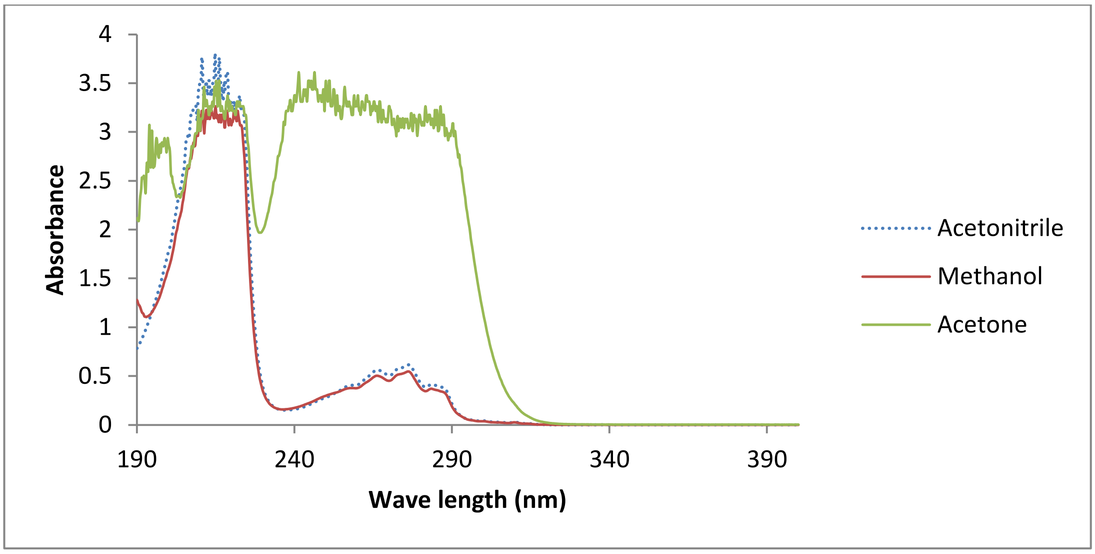

Figure 4.1 UV/ VIS spectrum for napthalene dissolved in acetonitrile, methanol and acetone

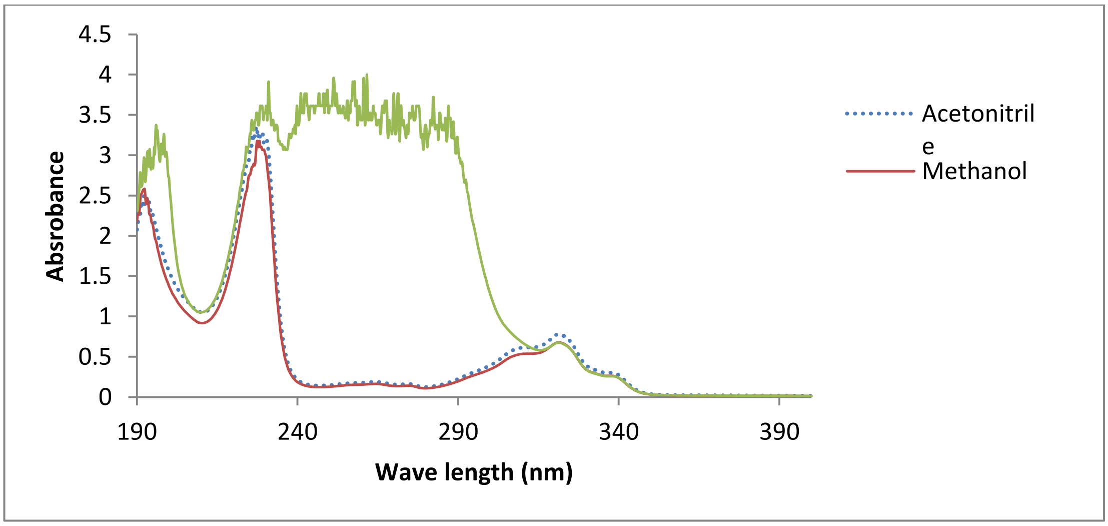

Figure 4.2 UV/VIS spectrum for acynapthylene dissolved in acetonitrile, methanol and acetone

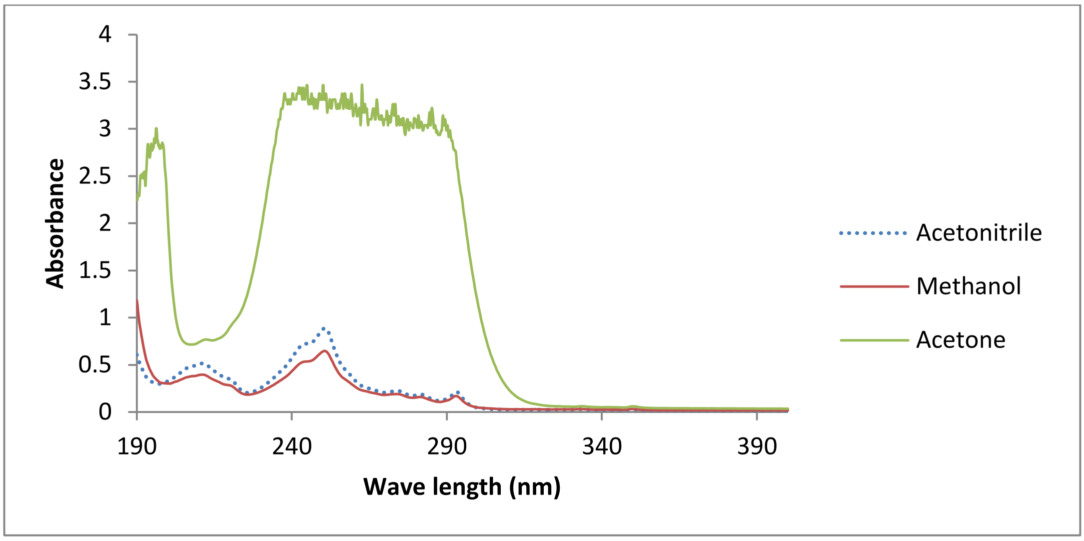

Figure 4.3 UV/VIS spectrum for phenanthrene dissolved in acetonitrile, methanol and acetone

Previous researchers have mostly used acetonitrile with UV/VIS spectroscopy (Valderrama et al. 2007). The advantages of using acetonitrile are it gives less noise in UV detection and less bulk peaking in the UV spectrum. Spectroscopic grade acetonitrile is best suited for high sensitivity analysis at short UV wavelengths. Because of these advantages and distinguishable peaks obtained from the UV /VIS spectrum, acetonitrile was selected as the solvent for the present study.

4.2.2.2 Selecting the best absorbance wavelengths

PAHs are generally measured using UV absorbance at a particular wave length. Previous researchers also have measured PAHs at different wavelengths such as 281 nm, acenaphthene; 261 nm, fluorene; 266 nm, naphthalene (Valderrama et al. 2009) , 275.5 nm, naphthalene (Ania et al. 2007) . The best wavelength was determined by measuring the absorbance for a range of PAHs concentrations. The results are presented in Figure. 4.4(a-e). Clear peaks were obtained at the following wave lengths and therefore these wave lengths were used for the measurement of the PAHs: Naphthalene, 219 nm; acenapthene, 226 nm; acenapthelene 228 nm; fluorene 263 nm; phenanthrene, 250 nm.

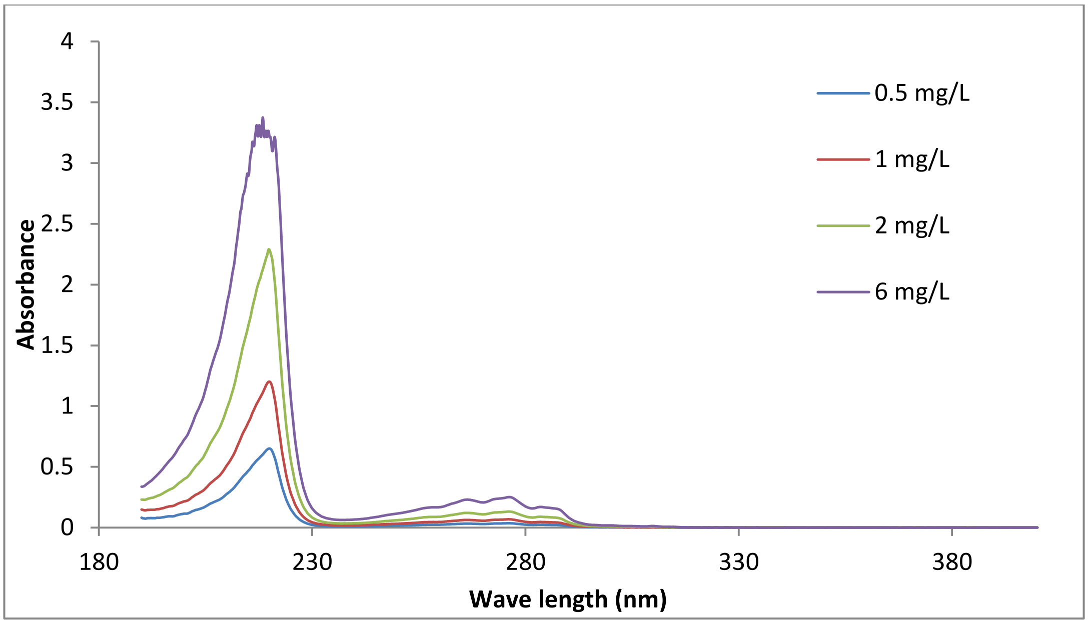

(a) Calibration curve for napthalene in acetonitrile

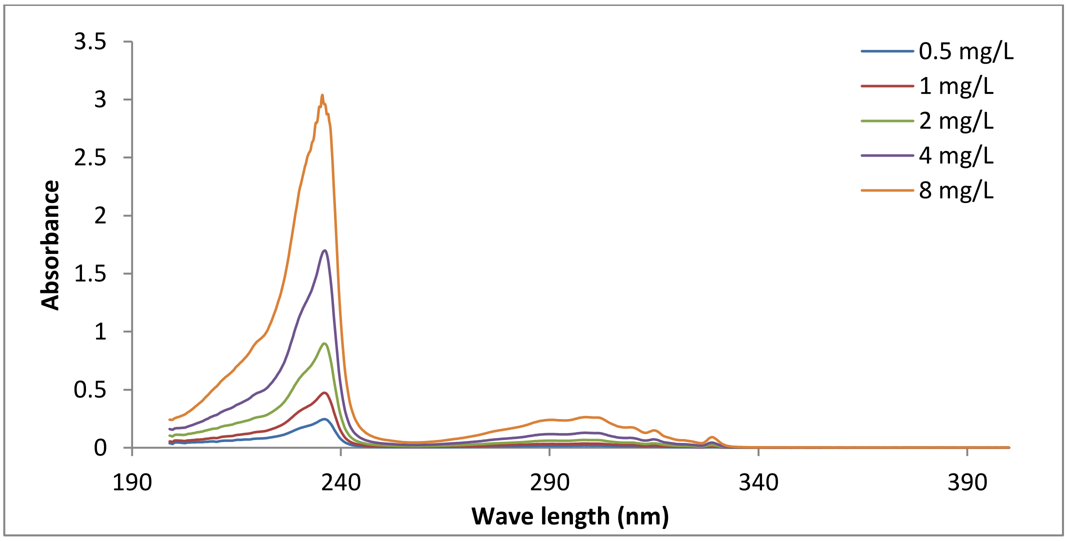

(b) Calibration curve for acenapthylene in acetonitrile

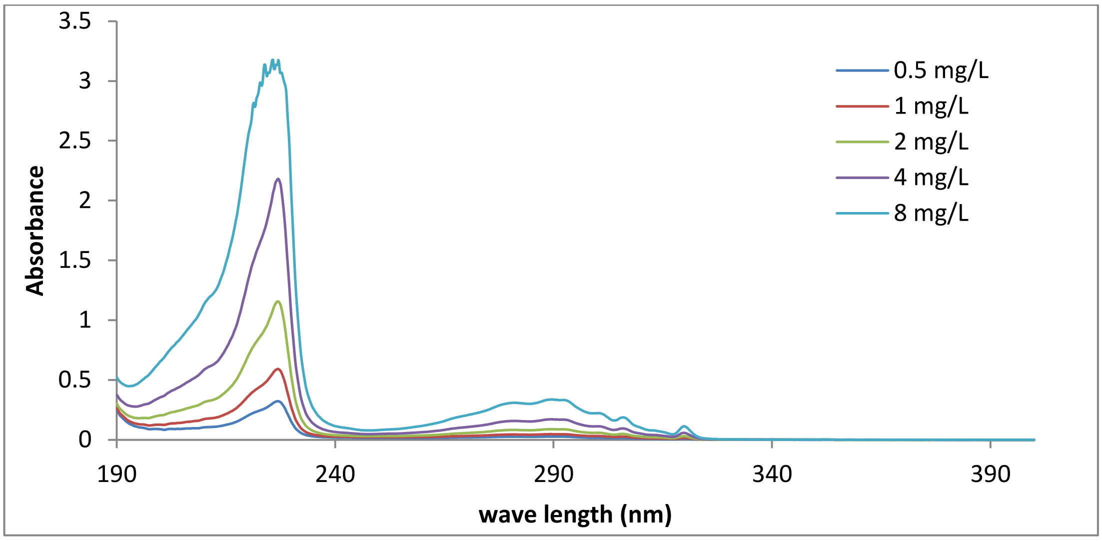

(c) Calibration curve for acenapthene in acetonitrile

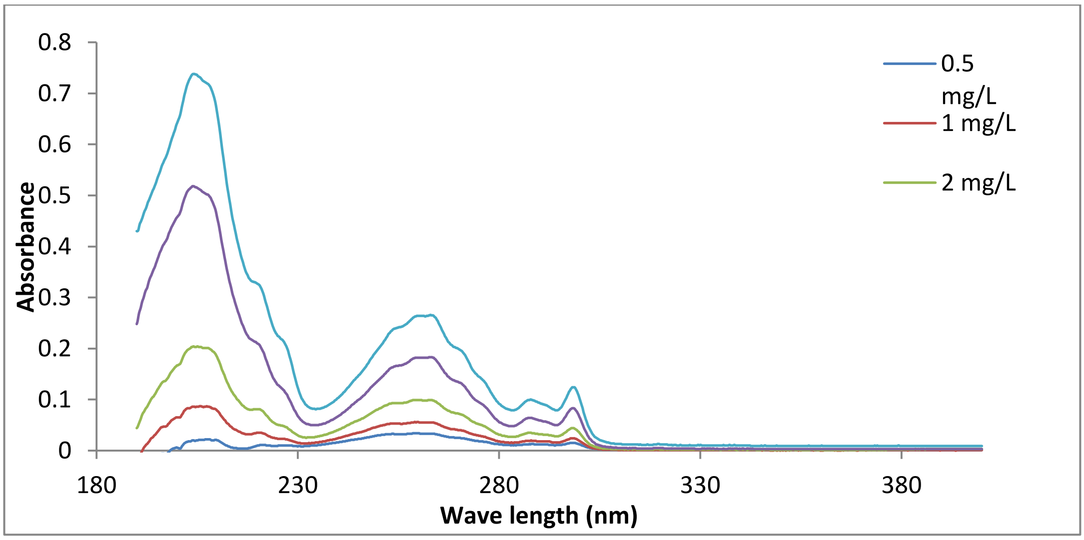

(d) Calibration curve for fluorene in acetonitrile

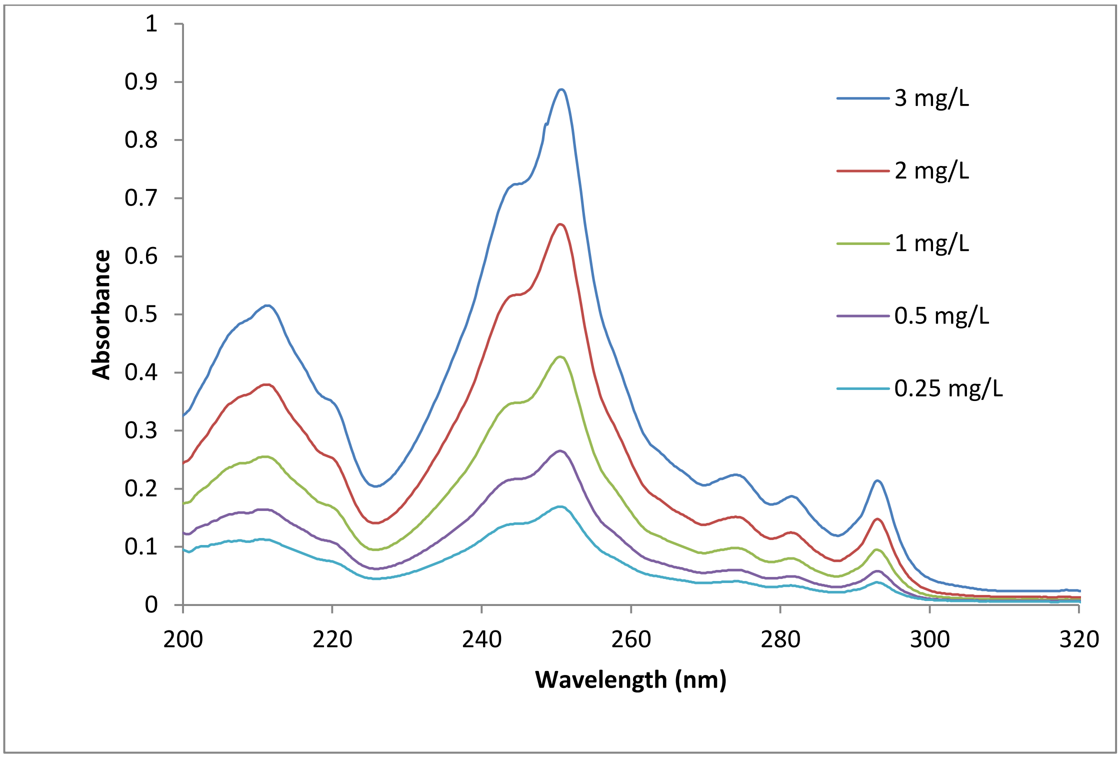

(e) Calibration curve of phenanthrene in acetonitrile

Figure 4. 4 (a-e) Calibration curves of tested PAHs in acetonitrile

As can be seen from the above figures, the PAHs spectrum gives two or three absorbance peaks. Instrumental setup, experimental conditions and organic solvents used, could be the reasons for obtaining peaks at different wavelengths compared to those in literature.

4.2.2.3. PAH analysis

All experiments were conducted on the five PAHs individually. PAHs concentrations were determined from standard curves of absorption vs concentrations of the standards. All glassware used in this study were specially cleaned to minimize contamination. Glassware were washed and rinsed with organic-free, deionized water and were soaked overnight in a 1: l HNO, acid bath before use. Losses by photodegradation were minimized by covering all containers used to hold PAH solutions with aluminium foil. To prevent volatilisation losses of PAH, all the containers were tightly closed by sealing the containers.

4.2.3. Batch kinetics adsorption experiments

Kinetic adsorption experiments were conducted in a set of glass flasks with 25 mg of GAC in 70 mL of solutions containing 6 mg/L of naphthalene, acenaphthene, acenaphthylene, fluorene or phenanthrene. The suspensions were agitated in a flat shaker at a shaking speed of 120 rpm for 24 h. Samples were taken at different time intervals periodically commencing at 5 min up to 24 h. The samples were filtered and the filtrates were analysed for the PAHs. PAH solutions without GAC were included as controls to account for the losses of PAH resulting from activities other than adsorption onto GAC such as volatilisation losses and adsorption on to glassware(Khan, Khaodhir & Rotwiron 2007). All adsorption experiments were conducted at 24±1 ^{o}C. The experiments were duplicated and the average values were taken for data analysis. The adsorption data were modelled using pseudo-first order (PFO), pseudo-second order (PSO) and Elovich models (Table 4.2). The amount of PAH adsorbed (q_t) at time t was calculated using equation (4.1).

$$q_t = \frac{(C_0 - C_t)V}{M} \qquad \boxed{4.1}$$

where C_0 is initial concentration of PAH (mg/L), C_t is concentration of PAH at time t (mg/L), V is volume of the solution (L) and M is mass of dry adsorbent (g).

4.2.4. Batch equilibrium adsorption experiments

To 70 mL of acetonitrile-water solution containing PAHs at a concentration of 6 mg/L in a set of glass flasks, different weights of GAC (0.6-0.8 mm) were added to provide GAC dosages of 2-50 mg/L. The flasks were agitated in a shaker at 120 rpm for 6-8 h at 24±1 °C. This period of shaking was found to be a sufficient period for the adsorption to reach equilibrium. Similarly, control samples without GAC were included and conducted. The experiments were duplicated and the average values were taken for data analysis. Once the equilibrium was attained, PAHs concentrations and amounts of PAHs adsorbed were determined as in the kinetics experiments. The data were modelled using Langmuir, Freundlich and Dubinin–Radushkevich adsorption isotherm models (Table 4.2). The amounts of PAHs adsorption at equilibrium, q_e (mg/g), were calculated using the equation given below (equation 4.2):

$$q_e = \frac{(C_0 - C_e).V}{M} \qquad \boxed{4.2}$$

where, C_0 is initial concentration of PAH (mg/L), C_e is equilibrium concentration of PAHs (mg/L), V is volume of solution (L) and M is mass of adsorbent (g). Percentage adsorption was calculated using equation 4.3 as follows;

$$\text{Percentage adsorption (\%)} = \frac{(C_0 - C_e)}{C_0} * 100 \qquad \boxed{4.3}$$

4.2.5. Column adsorption experiments

The fixed-bed column used in the study comprised of a 2-cm inner diameter pyrex glass tube. At the bottom of the column, a stainless-steel sieve was attached followed by a layer of glass beads to provide a uniform flow of the solution through the column. Different weight ratios of sand to GAC (24.5:0.5, 23.0:2.0, 21.5:3.5, 20.0:5.0) were used to determine acenaphthylene adsorption on to GAC. GAC and sand were mixed well and packed in the column to a bed height of 7-8 cm. Acenaphthylene (0.75 mg/L) spiked tap water solutions were pumped downward through the column at a filtration velocity of 18 m/h controlled by a peristaltic pump. Columns and tubes were closed tightly and externally covered with aluminium foils to minimise the losses due to other reasons. The effluents at the outlet of the column were collected at regular time intervals and the concentrations of acenaphthylene were measured. Similar column experiments were conducted using 25 to 30 g of only sand (0.6–2 mm) in the columns to investigate whether acenaphthylene is removed by sand alone in the column. Column experiments were also carried out using naphthalene (0.75 mg/L) and acenaphthene (0.75 mg/L) with sand to GAC ratio 24.5:0.5 and flow rate 18 m/h to compare the adsorption capacities of these PAHs on GAC.

The column experimental data were modelled using Thomas model (Table 4.2). The maximum adsorption of PAH (mg) in the fixed-bed was calculated from equation 4.4 given below:

$$q_{total} = \frac{Q}{1000} \int_{t=0}^{t-total} C_{ad} \, . dt \qquad \boxed{4.4}$$

where C_{ad} is the adsorbed PAHs concentration (C_{ad} = C_0-C_t) mg/L. The maximum adsorption capacity (mg/g) was calculated from Eq. (4.5):

$$q_{eq} = \frac{q_{total}}{M} \qquad \boxed{4.5}$$

where M is the mass of adsorbent (g) used in the fluidised-bed

Table 4. 2 Adsorption models Alade, Amuda & Ibrahim (2012); Kalaruban et al. (2016); [4]Nguyen et al. (2015); [1,4]Riahi, Chaabane & Thayer (2017); [3]Weber & Morris (1963)

Model	Equation	Model parameter
	Batch kinetics	
PFO[1]	$\frac{dq_t}{dt} = k_1(q_e - q_t)$	q_e = amount of PAH adsorbed at equilibrium (mg/g), q_t = amount of PAH adsorbed at time t(h), (mg/g), k_1 = equilibrium rate constant of pseudo-first order adsorption (1/h)
PSO[1]	$\frac{dq_t}{dt} = k_2(q_e - q_t)^2$	k_2 = equilibrium rate constant of pseudo-second order adsorption (g/mg.h)
Elovich[2]	$\frac{dq_t}{dt} = \alpha e^{-\beta q_t}$	α = initial adsorption rate (mg/g.h), β = related to extent of surface coverage and activation energy for chemisorption (g/mg), e = Elovich equilibrium constant (L/mg)
Webber and Morris[3]	$q_t = K_\mathrm{p} t^{1/2} + \mathrm{B}$	k_p = intra-particle diffusion rate constant (mg/(g.h$^{1/2}$)), B = constant which provides a measure of the boundary layer thickness (mg/g)
	Batch equilibrium	

Langmuir[1]	$q_e = \frac{q_m K_L C_e}{1 + K_L C_e}$	C_e = equilibrium concentration of PAH (mg/L), q = amount of PAH adsorbed per unit mass of adsorbent (mg/g), q_m = maximum amount of PAH adsorbed per unit mass of adsorbent (mg/g), K_L = Langmuir constant (L/mg) relates the energy of adsorption
Freundlich[1]	$q_e = K_f C_e^{1/n}$	k_f = Freundlich constant (mg/g)(L/mg)$^{1/n}$, n = Freundlich constant, q_e = the amount adsorbed per unit dosage of the adsorbent (mg/g)
Dubinin–Radushkevich[4]	$\ln(q_e) = \ln(q_m) - \beta\varepsilon^2$	q_m = the monolayer capacity, β = the activity coefficient related to mean adsorption energy and ε = Palanyi potential described as: $\varepsilon = RTln[1 + \frac{1}{C_e}]$ where R = universal gas constant 8.314 (J/mol.K), T = absolute temperature (K), From the plots of $\ln(q_e)$ versus ε^2 the values of β and q_m were determined
	Column adsorption	
Thomas model[1]	$\ln\left(\frac{c_0}{c_t} - 1\right) = \frac{k_{Th} q_0 M}{Q} - k_{Th} c_0 t$	k_{Th} = Thomas rate constant (mL/min.mg), q_o = equilibrium PAH uptake per g of adsorbent (mg/g), C_0 = inlet PAH concentration (mg/L), C_t = outlet PAH concentration at time t (mg/L), M = mass of adsorbent (g), Q = filtration velocity (mL/min), t = filtration time (min)

4.3.Results and discussion

4.3.1. GAC characteristics

Some physicochemical parameters of the GAC are listed in Table 4.3. Figure 4.5**a** shows that the GAC had the majority of pores between 1.8 and 15 nm. Figure 4.5b shows the pore size distribution of GAC. The average pore diameter was 3.2– 3.4 nm with micropore and mesopore volumes of 25–27 and 73–75%, respectively (Table 4.3). The scanning electron micrographs show the presence of large numbers of micropores and mesopores (Fig. 4.5 b) as indicated by the pore size distribution data (Fig. 4.5 a). Such large numbers of pores have provided the high surface area of GAC (Table 4.3) which is expected to produce high adsorption capacities for PAHs.

Table 4.3 Characteristics of GAC

Parameter	Values
Nominal size (mm)	0.3-3.28
BET surface area (m^2/g)	1218
Total pore volume obtained by BJH desorption method (cm^3/g)	0.60
Average pore diameter (nm)	3.2
% micro pore volume	25%
% meso pore volume	75%

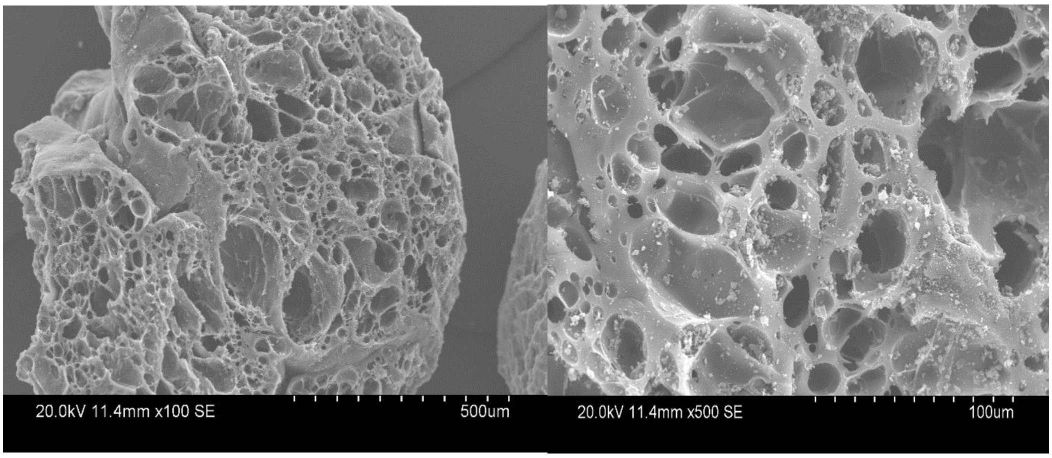

(a) Scanning electron micrographs of GAC

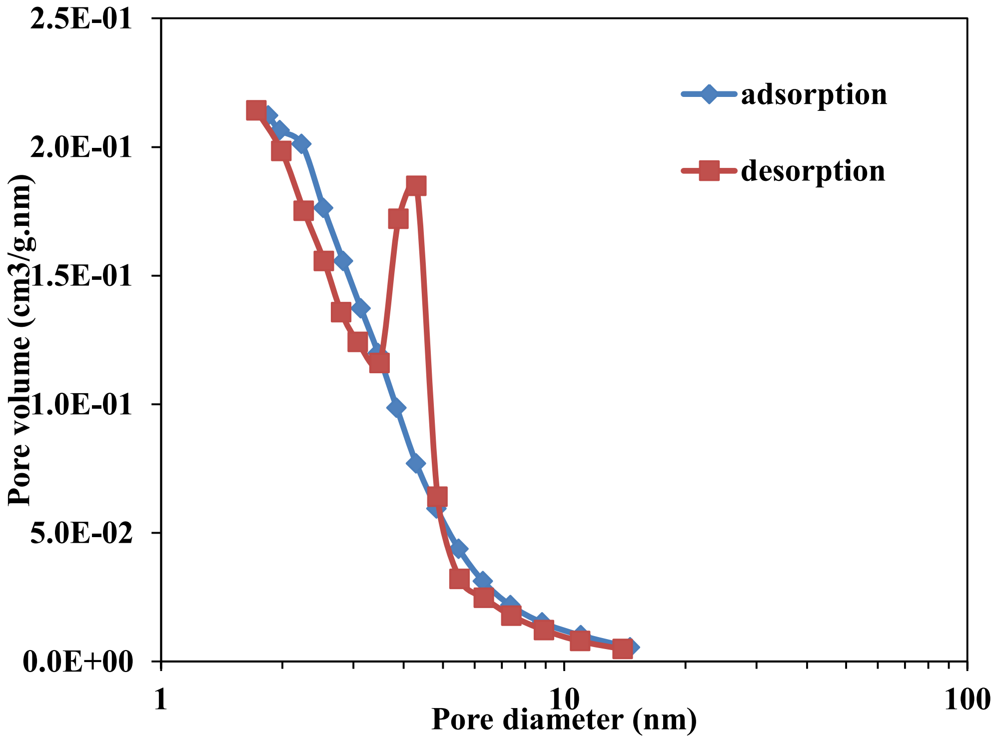

(b) Pore size distributions of GAC, calculated from the N_2 adsorption and desorption branches of the BJH plots. The desorption peak (hysteresis loop) at 4-6 nm is due to capillary condensation of N_2 in the mesopores (Wu et al. 2018).

Figure 4. 5 Characteristics of GAC

4.3.2. Kinetic adsorption experiments

For all PAHs, the rate of adsorption was fast within the first 2 h (Fig. 4.6), probably because of adsorption on the external surface and in the larger sized meso-pores of GAC. Subsequently, the rate of adsorbent progressively decreased reaching equilibrium after 4-5 h for naphthalene, 5-6 h for acenaphthylene, 8 h for acenaphthene, 16 h for fluorene, and 24 h for phenanthrene. The decrease in adsorption rate with time is due to a shift of PAH transport process from mesopores to micropores of GAC. As the molar volume of PAH increases, the penetration of PAH into the micropores became difficult. The time to reach adsorption equilibrium increased with increased molar volume (Table 4.1). Naphthalene, having the lowest molar volume and molecular dimension, was able to penetrate the micropores more easily than the other PAHs. The penetration of fluorene and phenanthrene having the largest molar volumes was much slower resulting in the lowest adsorption rate. Haro et al. (2011) also reported that the rate of adsorption of naphthalene on a AC was much faster than acenaphthalene and fluorene and ascribed the difference in the adsorption rate to their molecular dimensions. Awoyemi (2011) conducted a similar research using naphthalene and fluorene adsorption on to AC and explained the faster kinetic behaviour of naphthalene to its' lower molar volume and molecular dimensions as well.

4.3.2.1 Kinetic adsorption models

Kinetic adsorption data were modelled using PFO, PSO and Elovich with the aim of determining the best model to describe the adsorption data and understand the mechanism of adsorption (Fig. 4.6). Of the three models, PFO and PSO fitted the data the best with R^2 values of 0.983-0.999 (Table 4.4). But the model predicted values for the adsorption capacities (q_m) were close to the experimental values only for the PFO model fittings. In the PSO, the difference between experimental and model predicted values were approximately 25–30%. Therefore, PFO model is a better predictor of the adsorption kinetics than PSO model for the PAHs. The good agreement of the data with the PFO model suggests physical adsorption of the PAHs on GAC (Awoyemi 2011; Nur, Johir, et al. 2014) . The mechanism of physical adsorption is probably the van der Waals attractive forces occurring between instantaneous and induced dipole moments of PAH molecules and GAC (Valderrama et al. 2009). The PFO rate constant decreased with increase in molar volume for the PAHs (Table 4.4) due to increased resistance for the diffusion of larger sized PAHs as discussed earlier. This relationship was significant with a regression equation of PFO rate constant k_1 = -0.0039 x molar volume + 1.285, and an R^2 value of 0.7514.

Valderrama et al. (2007) also reported that adsorption of six PAHs on a GAC was described better by PFO although the PSO model provided an acceptable description of the adsorption process. Long et al. (2008) reported that both PFO and PSO models fit to the data for the kinetics of naphthalene adsorption on a AC had correlation coefficients larger than 0.99, but the estimated adsorption capacity was close to the experimental value only for PFO. Therefore, they concluded that PFO was a better model for predicting the adsorption kinetics.

Three consecutive stages in the kinetics of adsorption process for porous adsorbents have been presented by previous researchers (Haro et al. 2011; Valderrama et al. 2007; Valderrama et al. 2008) The first stage is the migration of PAH from the bulk solution to the GAC surface (boundary diffusion) which is very fast due to vigorous shaking of the suspensions and often cannot be measured. The main resistance to mass transfer occurs during the second stage where intra-particle diffusion due to movement of PAHs to the interior pores and channels of GAC takes place. The third stage is when adsorption reaches saturation.

The intra-particle diffusion model developed by Weber & Morris (1963) has been used to describe adsorption process in the second stage of PAHs adsorption (Fig. 4.7). If the Weber–Morris plot of q_t versus $t^{1/2}$ gives a straight line, then the adsorption process is considered to be solely controlled by intra-particle diffusion. The data in Fig. 4.7 cannot be described by a single linear trend line. However, if the data is divided into zones in which different transport processes might prevail, then distinct lines can be defined and used to analyse these transport processes. These plots for each of the five PAHs showed more than one straight line. This indicates that there is more than one diffusion rate for the PAHs, a faster rate followed by a slower rate as also found by Valderrama et al. (2008). The faster rate occurs in the mesopores and the slower rate in the micropores. The stage 2 of the adsorption kinetics process is divided into two zones representing the diffusion into the mesopores and micropores, respectively in Fig. 4.7. Zone 3 represents adsorption saturation plateau. The diffusion rates, K_{s1} and K_{s2} calculated from the corresponding slopes of each straight line in stage 2 process are presented in Table 4.5. It is obvious that the value for K_{s1} is much higher than that for K_{s2} for each PAH. It is interesting to note that phenanthrene has not completely reached the saturation stage within the experimental time of 24 h and continues to diffuse into the micropores with its very low diffusion rate of k_{s2} = 0.3 mg/g/min$^{1/2}$ (Table 4.5). This low diffusion rate is due to its large size (large molar volume, Table 1), which makes it difficult for it to penetrate into the pores. Steric hindrance might have also reduced the diffusion rate of phenanthrene (Haro et al. 2011). The diffusion rate in the mesopores (K_{s1}) has a significant negative correlation with molar volume (R^2 = 0.60) whereas such a relationship does not exist with $K_{s2.}$

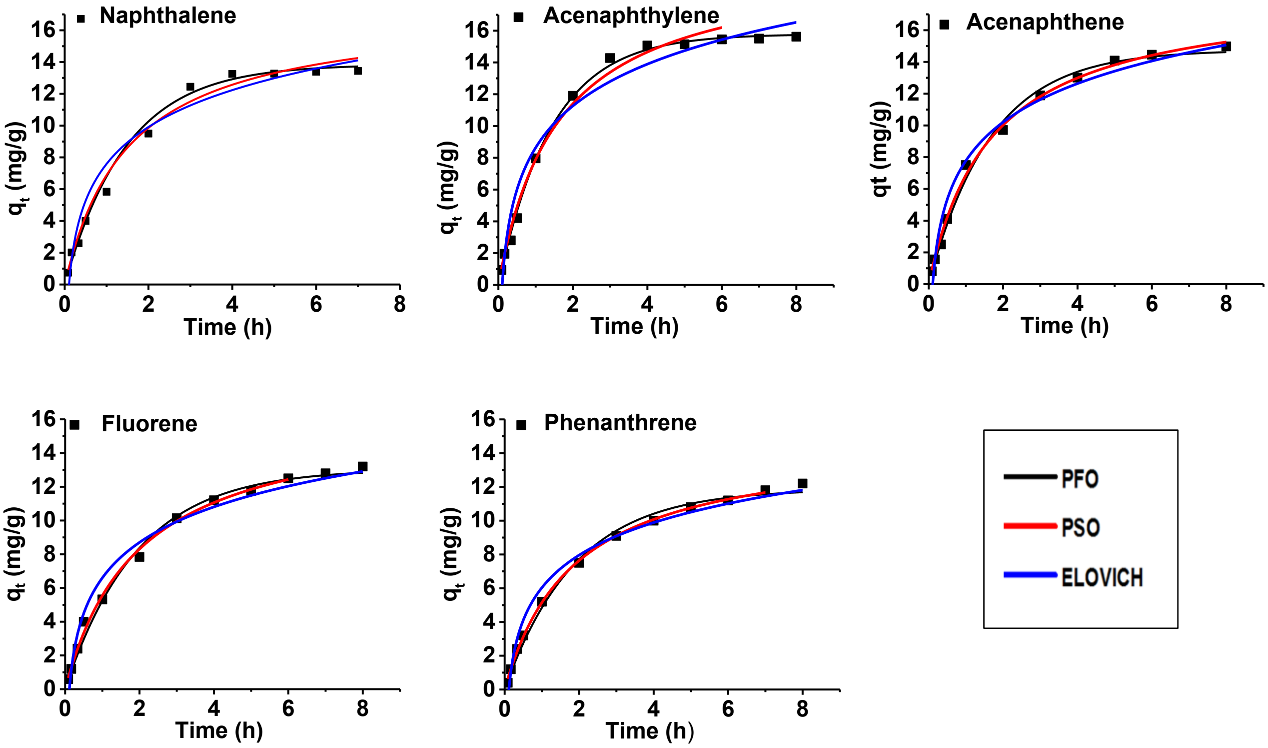

Figure 4.6 Kinetic of PAHs adsorption on GAC and models fit to the data

Table 4.4 Parameter values for batch kinetic adsorption models

Compound	Pseudo-first order (PFO)			Pseudo-second order (PSO)			Elovich			Experimental
	q_m mg/g	k_1 h^{-1}	R^2	q_m mg/g	K_2 g/mg h	R^2	α mg/g.h	β g/mg	R^2	q_m (mg/g)
Naphthalene	13.8	0.68	0.993	17.3	0.037	0.983	2.9	3.3	0.950	13.4
Acenaphthylene	15.7	0.70	0.997	20.5	0.030	0.991	2.5	3.8	0.963	15.6
Acenaphthene	14.7	0.60	0.995	18.5	0.032	0.997	2.6	3.5	0.974	15.0
Fluorene	13.0	0.51	0.993	16.5	0.031	0.996	2.9	3.0	0.974	13.2
Phenanthrene	11.8	0.52	0.994	14.8	0.036	0.999	3.2	2.8	0.980	12.1

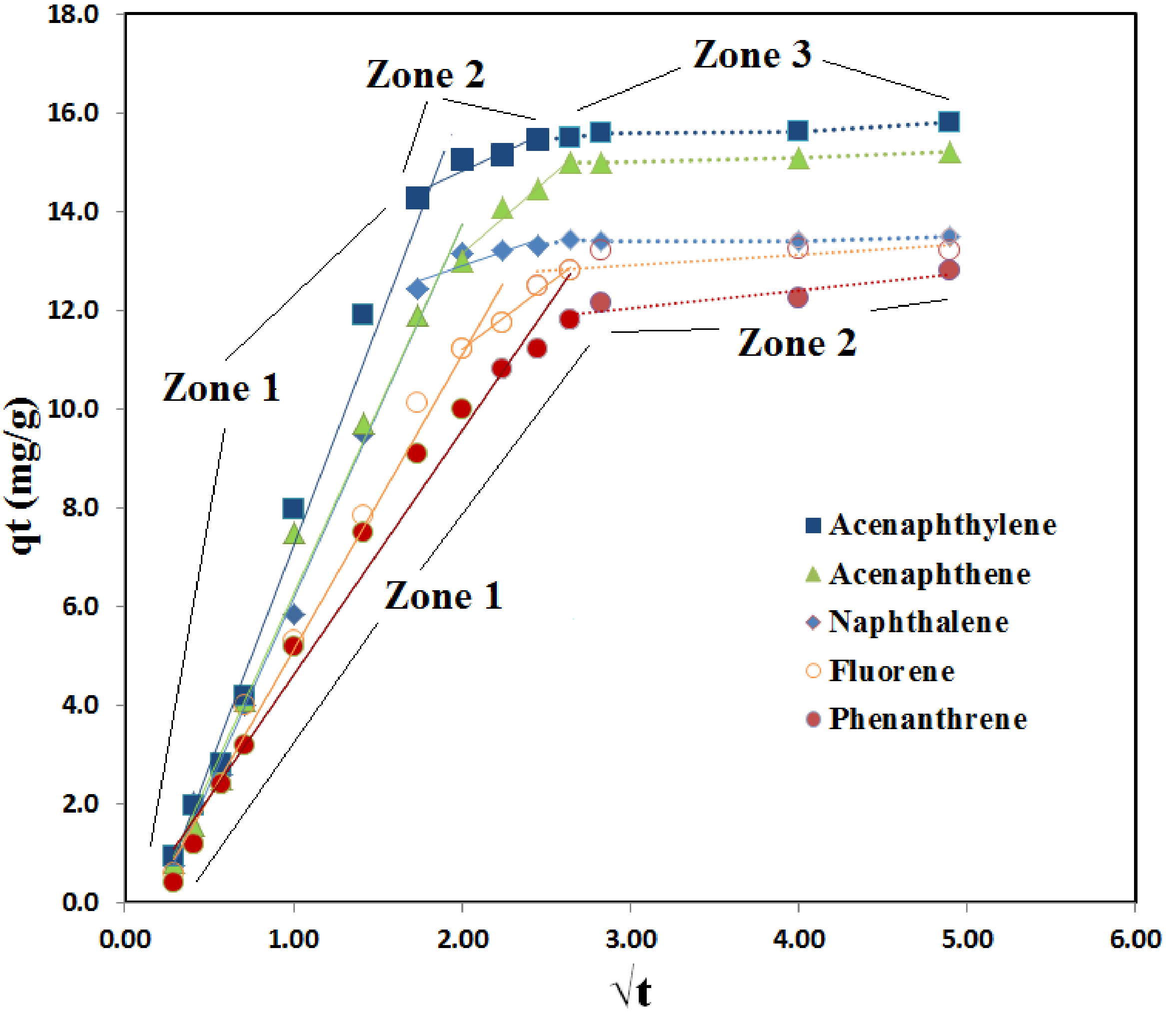

Figure 4.7 Webber and Morris intra-particle diffusion plots for the adsorption of PAH on GAC

Table 4. 5 Diffusion rates (ks1, ks2) and coefficient of determination (R2) obtained from the Webber and Morris plots

PAH	Webber-Morris short-term adsorption		Webber-Morris long-term adsorption	
	K_{s1} mg/g /min$^{1/2}$	R^2	k_{s2} mg/g /min$^{1/2}$	R^2
Naphthalene	7.6	0.992	1.0	0.809
Acenaphthylene	8.9	0.984	1.5	0.888
Acenaphthene	7.5	0.983	2.9	0.961
Fluorene	6.0	0.988	2.4	0.971
Phenanthrene	4.9	0.978	0.3	0.866

4.3.2.2. Equilibrium adsorption experiment

The removal efficiency of PAHs by adsorption on GAC generally increased with molecular weight and molar volume of the PAHs (Fig. 4.8). This trend under equilibrium adsorption conditions is the reverse of that obtained under adsorption kinetics conditions discussed previously. PAHs having the lowest molar volumes had the fastest adsorption rate but the total amount adsorbed at equilibrium was the lowest. The reason for this difference is that in kinetics of adsorption the larger sized PAHs resisted diffusion through the pores and channels in GAC unlike the smaller PAHs which had less resistance. At the end of sufficient period of adsorption when equilibrium of adsorption is attained, the total amount adsorbed is related to the affinity of PAHs towards GAC. This affinity is determined by the hydrophobicity of PAHs since GAC is mainly hydrophobic. In support of this reasoning, the amount of PAH adsorbed approximately followed the order of increasing log K_{ow} or decreasing water solubility of PAH (Table 4.1) as reported by others (Crisafully et al. 2008; Haro et al. 2011; Khan, Khaodhir & Rotwiron 2007; Valderrama et al. 2009). It was also reported that PAHs with higher K_{ow} had longer equilibrium time but had higher adsorption capacity (Haro et al. 2011; Khan, Khaodhir & Rotwiron 2007).

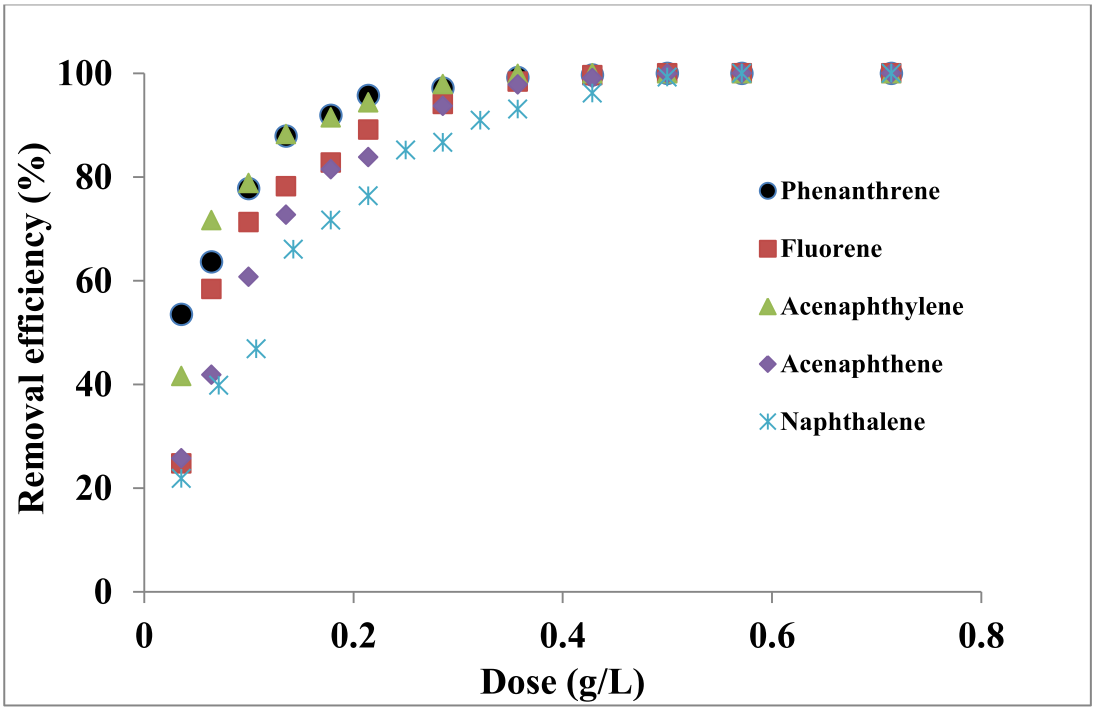

Figure 4. 8 Removal efficiency of PAH – Batch equilibrium adsorption experiment

Adsorption equilibrium data were modelled using Langmuir, Freundlich and Dubinin–Radushkevich isotherm models to obtain maximum adsorption capacity and affinity of adsorption of the PAHs (Fig. 4.9). The model parameters obtained from these fits are presented in Table 4.6. All three models described the adsorption data fairly well (R^2 = 0.801-0.992). However, Freundlich model fitted the data most satisfactorily (R^2 = 0.910-0.992) indicating probably that the process is heterogeneous adsorption due to the availability of different types of pores.

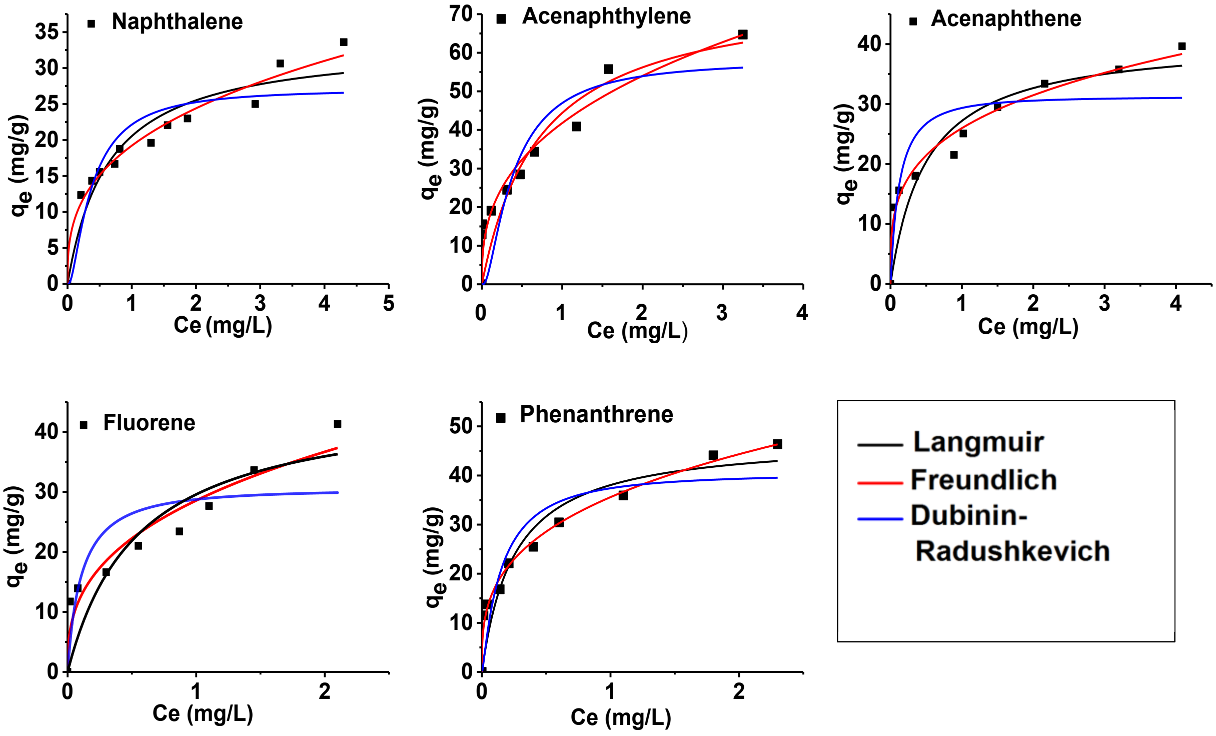

Figure 4.9 Experimental data and models fit to the data of PAHs adsorption on GAC

The Langmuir maximum monolayer adsorption capacity ranged from 34 to 77 mg/g. These values are lower than the values of 111, 140 and 145 mg/g reported by Valderrama et al. (2009) for acenaphthene, naphthalene, and fluorene adsorption, respectively on a GAC but comparable to the values of 50 and 64 mg/g reported by Yakout et al. (2013) for phenanthrene and naphthalene adsorption, respectively on a

AC. Lower values compared to the values of Valderrama et al. (2009) may be because of using much lower PAHs concentrations in our study (< 4 mg/L compared to values up to 100 mg/L equilibrium concentration in the study of Valderrama et al. (2009)). The study of Yakout et al. (2013) had equilibrium concentrations similar to those of ours.

The Langmuir constant related to the affinity of adsorption, K_L increased with increase in log K_{ow} as reported by others (Valderrama et al. 2009) but the relationship was not strong ($R^2 = 0.4664$). Boving & Zhang (2004) also reported a strong relationship between partition coefficient of PAHs between wood fiber adsorbent and solution and log K_{ow} for four PAHs. These results suggest that the affinity of GAC for the adsorption of PAHs increases with hydrophobicity of PAHs. Thus, the adsorptive behaviour of PAHs is controlled largely by the hydrophobicity of the PAHs.

In the Langmuir model, the value of R_L as calculated from the formula, $R_L = 1/(1 + C_mK_L)$ (where C_m is the maximum initial concentration of sorbate), indicates the favourability of the adsorption process, such as unfavourable ($R_L > 1$), favourable ($0 < R_L < 1$) or irreversible ($R_L = 0$) Naidu et al. (2016). The calculated R_L values for PAHs in the current study were in the 0.05–0.1 range (Table 6), indicating that the adsorption process is favourable for all tested PAHs. Similarly, the values of Freundlich constant 1/n were between 0.1 and 1 indicating a favourable adsorption and implying a stronger interaction between the GAC and PAHs (Yakout, Daifullah & El-Reefy 2013). The adsorption capacities obtained from the Dubinin–Radushkevich model for the PAHs generally followed the same order as the Langmuir adsorption capacities (Table 4.6). However, the magnitude of the values was approximately 10-30% lower than the Langmuir adsorption capacity values. Dubinin–Radushkevich model has the advantage of differentiating physical adsorption and chemical adsorption using the mean free energy of adsorption (kJ/mol) which is calculated as the reciprocal of the square root of 2 β. The mean free energy of adsorption (E) is defined as the free energy change when 1 mol of adsorbate is transferred to the surface of the solid from infinity in solution (El Nemr et al. 2009; Tripathy & Raichur 2008). From the magnitude of E, the type of adsorption such as chemisorption or physical sorption can be determined. If E = 8–16 kJ/mol, then the reaction is due to chemical adsorption; If E < 8 kJ/mol, then physical adsorption takes place (Tripathy & Raichur 2008). Values of E calculated for the five PAHs tested varied from 1.7 to 3.8 (kJ/mol) (Table 4.6), which showed that the type of adsorption involved in this study was mainly physical adsorption. This is consistent with the kinetics of adsorption study which showed PFO was the best predictive model of the data which indicated that the adsorption mechanism was mainly a physical process.

Table 4.6 Parameter values for batch equilibrium adsorption models

PAH	Langmuir model				Freundlich model				Dubinin–Radushkevich model			
	q_m mg/g	K_L L/mg	R^2	R_L	K_f $(mg/g)(L/mg)^{1/n}$	n	1/n	R^2	q_m mg/g	β (mol^2/kJ^2)	R^2	E (kJ/mol)
Naphthalene	33.7	1.6	0.918	0.13	19.2	2.9	0.34	0.977	23.6	0.05	0.894	3.0
Acenaphthylene	76.6	1.4	0.852	0.18	41.8	2.7	0.37	0.910	56.8	0.08	0.872	2.6
Acenaphthene	40.8	1.9	0.881	0.11	26.0	3.6	0.28	0.977	35.5	0.13	0.994	2.0
Fluorene	45.7	1.8	0.813	0.21	28.6	2.8	0.36	0.941	33.1	0.06	0.801	2.9
Phenanthrene	47.6	4.0	0.908	0.10	35.6	3.2	0.31	0.992	40.4	0.04	0.917	3.8

4.3.2.3 Column experiments

The dynamic column operation allows more efficient utilisation of the GAC adsorptive capacity than the static batch process and is more relevant to real operating systems on natural waters. The rational design of an adsorption system is therefore based on the accurate predictions of breakthrough curves for specified conditions. Use of GAC alone in large scale process in the treatment plant is costly. Mixing it with appropriate proportions of inert coarse-sized materials like sand may decrease the cost of operation without compromising much on the PAH removal efficiency. Mixing with sand also provides good hydraulic properties in the fixed-bed column adsorption process. Therefore, dynamic fixed-bed adsorption column experiments were conducted using GAC + sand mixtures for the removal of PAHs. To evaluate the contribution of sand in the mixture towards PAH adsorption, a column experiment was initially conducted with only sand. The breakthrough curves for the adsorption of acenaphthylene on sand at two filter velocities showed that sand had negligible adsorption capacity for acenaphthylene (Fig. 4.10).

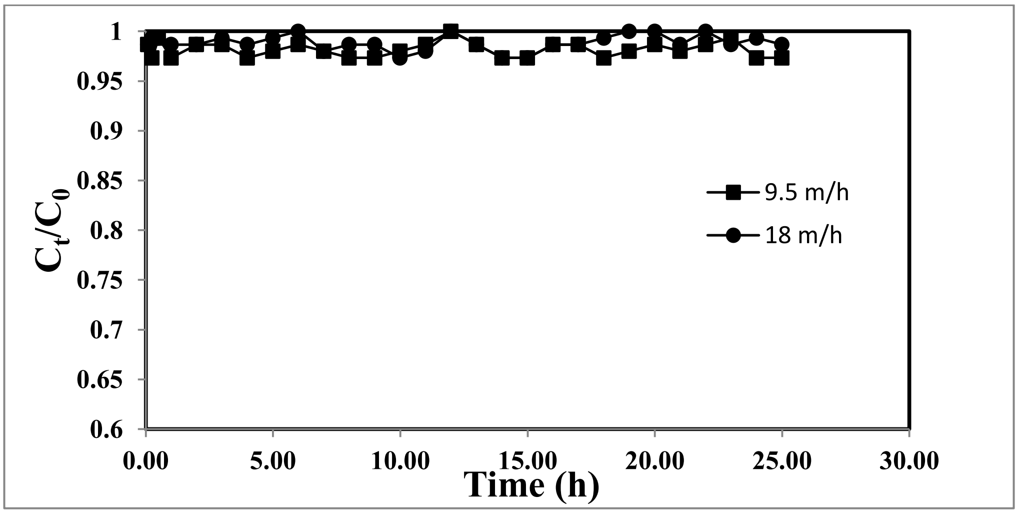

Figure 4.10 Breakthrough curves for acenaphthylene adsorption on sand at two flow velocitiesBreakthrough curves for acenaphthylene adsorption on sand at two flow velocities

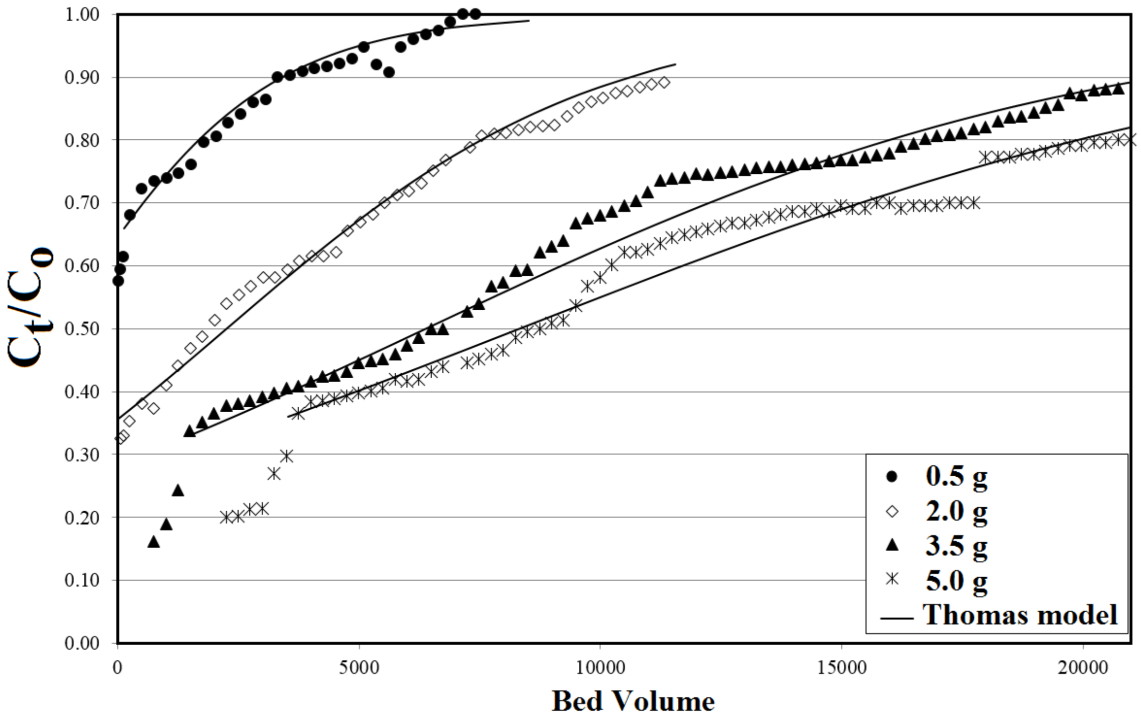

Figure 4.11 Breakthrough curves for acenaphthylene adsorption at different GAC to sand ratios (weight of GAC is shown in the legend. The balance of the total weight of 25 g in the column was sand) and Thomas model fits to the data

Following the experiment with column containing sand alone, four fixed-bed column experiments were conducted for the adsorption of acenaphthylene at different weight ratios of GAC to sand in the column (Table 4.7). The breakthrough curves are shown in Fig. 4.11. As the amount of GAC in the column increased, the breakthrough curve became less steep and took longer time to reach saturation indicating that the adsorption capacity increased. The breakthrough adsorption capacities calculated manually are presented in Table 4.7. Though the amount adsorbed increased with increased weight of GAC, the adsorption capacity expressed as amount adsorbed per unit weight of GAC remained approximately constant. Thomas model described the data very well (R^2 = 0.939-0.989) (Table 4.7, Fig. 4.11). The adsorption capacities calculated from the model were not too much different from those calculated manually.

Table 4. 7 Column adsorption parameters for acenaphthylene adsorption at different ratios of GAC to sand

GAC weight (g)	Sand weight (g)	Amount adsorbed in column (mg)	Adsorption capacity (mg/g GAC)	Thomas adsorption capacity (mg/g GAC)	Thomas model fit R^2
0.5	24.5	15.5	30.9	23.5	0.962
2	23	62.6	31.3	22.6	0.989
3.5	21.5	134.7	38.6	27.5	0.939
5	20	191.7	38.3	22.5	0.940

The breakthrough curves for the adsorption of naphthalene, acenaphthylene and acenaphthene showed that acenaphthylene took much longer time to reach column saturation than acenaphthene; acenaphthene took slightly longer time than naphthalene (Fig. 4.12). Adsorption capacities (mg/g) of acenaphthylene, acenaphthene and naphthalene calculated from the breakthrough curves were 31.0, 20.0 and 16.2, respectively. These values followed the same order as the batch equilibrium adsorption capacities for these three PAHs (Table 4.6). Thomas model fitted satisfactorily to the breakthrough curves ($R^2 = 0.94$-0.99, Table 4.7, Fig. 4.11). The Thomas model calculated adsorption capacities for the three PAHs (Table 4.8) were in the same order as the Langmuir adsorption capacities obtained in the batch adsorption study (Table 4.6). However, the Langmuir adsorption values were much higher than the column adsorption capacities. Nguyen et al. (2015) also reported lower column values than batch values for heavy metal adsorption on zeolite and iron-coated zeolite. They offered two reasons for this: firstly, adsorption did not attain equilibrium in the column study in contrast to that in the batch study; and secondly, the column adsorption was calculated at lower metal concentrations in the feed solution compared to higher metal concentrations in the batch study at which Langmuir adsorption maxima were calculated.

Table 4. 8 Column adsorption parameters for different PAHs (GAC weight (g): sand weight (g)

PAH	Amount adsorbed in column (mg)	Adsorption capacity (mg/g GAC)	Thomas adsorption capacity (mg/g GAC)	Thomas model fit R^2
Naphthalene	8.4	16.2	12.8	0.942
Acenaphthylene	15.5	31.0	23.6	0.962
Acenaphthene	10.1	20.0	13.6	0.992

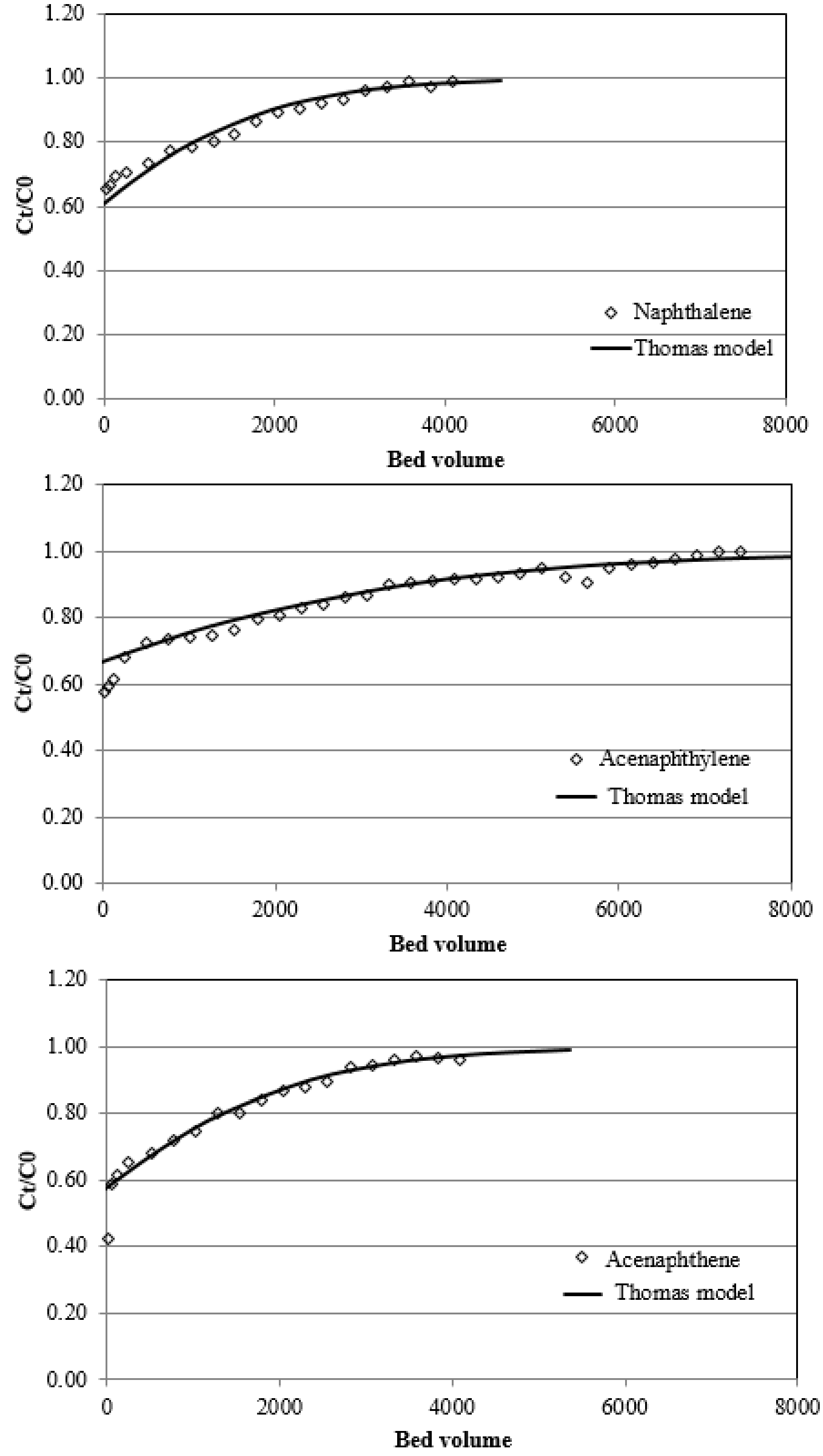

Figure 4.12 Thomas model fit for the breakthrough curves for naphthalene, acenaphthene and acenaphthylene adsorption at different GAC to sand ratios

4.4. Conclusions

Batch and column adsorption experiments on five PAHs showed that GAC can effectively remove PAHs from water. Batch kinetics adsorption was satisfactorily described by PFO, PSO, and Elovich models, with PFO model being the best of the three. Weber and Morris diffusion model produced two distinctive linear plots for amount adsorbed vs square root of time, indicating two consecutive intra-particle diffusion rates of adsorption, probably one through the mesopores and the other through the micropores of GAC. The diffusion rates were negatively related to molar volumes of PAHs; smaller PAHs diffused faster than the larger ones.

Batch equilibrium adsorption was satisfactorily described by Freundlich, Langmuir, and Dubinin–Radushkevich models, with the data fit being the best for Freundlich, indicating heterogeneous adsorption. The energy of adsorption calculated from the Dubinin–Radushkevich model confirmed the physical nature of adsorption suggested by the PFO kinetic model. The Langmuir adsorption affinity constants for the PAHs were in the reverse order as the rates of adsorption and depended mainly on the hydrophobicity of the PAHs.

Fixed-bed columns containing 2% GAC and 98% sand by weight removed substantial amounts of PAHs. The breakthrough curves were successfully simulated by Thomas model. The Thomas adsorption capacities had the same trend for the PAHs as the Langmuir adsorption capacities, though the Thomas values were lower

Chapter 5

Simultaneous removal of polycyclic aromatic hydrocarbons and heavy metals from water using granular activated carbon

This chapter is a major part of my published paper, Eeshwarasinghe, D., Loganathan, P. & Vigneswaran, S. 2019, 'Simultaneous removal of polycyclic aromatic hydrocarbons and heavy metals from water using granular activated carbon', *Chemosphere*, vol. 223, pp. 616-27

Chapter Five

5.1 Introduction

Chapter 4 presented data on the adsorptive removal of PAHs by GAC. Chapter 2 reviewed many studies conducted on the adsorptive removal of another important group of pollutants namely heavy metals (Ahmaruzzaman 2011; Bailey et al. 1999; Hua et al. 2012) and PAHs (Eeshwarasinghe et al. 2018; Lamichhane, Bal Krishna & Sarukkalige 2016; Valderrama et al. 2009; Yakout, Daifullah & El-Reefy 2013). However, very few studies have dealt with the simultaneous removal of both of these pollutants. Simultaneous removal is important because PAHs' and heavy metals' co-occurrence is very common in the environment, especially when the water contains both industrial and domestic waste discharges(Tao et al. 2013) and in stormwaters containing road-deposited sediments (Loganathan, Vigneswaran & Kandasamy 2013; Nguyen 2016) . Considering the importance of the simultaneous removal of these pollutants, in recent times more focus has been directed on conducting research on this topic.

Studies have reported both competitive and synergistic effects on the adsorption of PAHs and heavy metals. Chen, Zhu & Sun (2007) found that the presence of Cu decreased the adsorption of naphthalene by wood black carbon and explained this outcome as due to surface complexation of Cu to form hydration shells of dense water that competed with naphthalene for adsorption. They also stated that pore blockage by the hydrated Cu inhibited naphthalene adsorption. Huang, Fulton & Keller (2016) compared the individual and combined adsorption capacities of Cd and acenaphthene on a maghemite/mesoporous silica composite. They found that the adsorption capacities decreased from those of individual capacities when acenaphthene and Cd were present together. The competitive effect had a higher impact on Cd adsorption than on acenaphthene adsorption. Also, Huang, Fulton & Keller (2016) explained this as due to faster adsorption of acenaphthene which allowed it to occupy the adsorption sites first rather than Cd. In a study on the adsorption of Pb and pyrene in a soil, Pb curtailed the adsorption of pyrene and pyrene reduced the adsorption of Pb due to competitive adsorption (Aissaoui et al. 2017) .

In contrast to the competitive effects, synergistic effects of heavy metals and PAHs have also been reported in some studies. For example, Zhang & He (2015) found that Cu and pyrene adsorption capacities on Fe functionalised mesoporous silica were higher when they were present together than when they were present alone. They explained this observation as due to the formation of a Cu-pyrene complex through cation-π interaction (non-covalent binding force between metals and aromatic organic compounds) where the complex had stronger affinity to the adsorbent than the individual components. Formation of pyrene-Cu bridging was also suggested for the mutual promotion of the adsorption. The higher adsorption of PAHs (acenaphthene, fluorene and fluoranthene) and heavy metals (Ni, Pb, Zn) when they are present together compared to their individual presence was also reported for adsorption on clay minerals (Saeedi, Li & Grace 2018). This was explained as due to the formation of a cation-π bond with the effect being greater for the higher molecular weight PAHs. The reason for this was the larger number of benzene rings providing more electrons for π-interaction. Tao et al. (2014) and Tao et al. (2013)studied the effects of various metals on the adsorption of selected PAHs by aquatic dead phytoplankton biomass and reported that a change in the concentration of the metals had different effects on the adsorption behaviour of the

PAHs. Sorption enhancement which occurred at medium metal concentrations, was reportedly caused by these cation- π interactions, and increased with the order of softness of the metals, and the π-donor strength of the PAHs.

Simultaneous adsorption of PAHs and heavy metals has not been studied in detail on activated carbon (AC) adsorbent, which is one of the most popular and reliable adsorbents used for removing both heavy metals(Kurniawan et al. 2006; Loganathan et al. 2018; Tao et al. 2013; Tao et al. 2014) and PAHs (Alade, Amuda & Ibrahim 2012; Eeshwarasinghe et al. 2018; Valderrama et al. 2009; Yakout, Daifullah & El-Reefy 2013). Inner-sphere complexation of heavy metals adsorption on AC has been established in previous studies using zeta potential data (Loganathan et al. 2018) and this might have relevance to the simultaneous adsorption of PAHs and heavy metals on AC. We have also shown earlier that the porosity of granular AC (GAC) did influence PAH adsorption kinetics(Eeshwarasinghe et al. 2018) , which could in turn have an impact on the mutual adsorption of PAH and heavy metals. These aspects will be used to explain the simultaneous adsorption of heavy metals having different affinities to GAC and PAHs in the study presented here. The aims of the study, therefore, were to: firstly, determine the effects of different concentrations of Cu, Cd, and Zn on the equilibrium and kinetics of acenaphthylene and phenanthrene adsorption on GAC; secondly, determine the effect of these two PAHs on the equilibrium and kinetics of adsorption of the three heavy metals; thirdly, explain the mechanism of adsorption using zeta potential data; and fourthly, model the adsorption behaviour of the heavy metals and PAHs when they occur separately and together. Such modelling has not been previously reported for simultaneous adsorption of PAHs and heavy metals.

5.2. Materials and methods

5.2.1 Materials

GAC (0.3–2.4 mm) for this study was the same as the one used in Chapter 4. A particle size range of 400-800 μm was separated from the original material and used in the experiments. The BET surface area, pore volume and average pore diameter of the GAC were 1010 m^2/g, 0.69 cm^3/g and 2.7 nm, respectively (Eeshwarasinghe et al. 2018). The scanning electron micrographs of the GAC (Fig. 5.1) revealed the presence of large numbers of micropores and mesopores which may have resulted in GAC having high surface area.

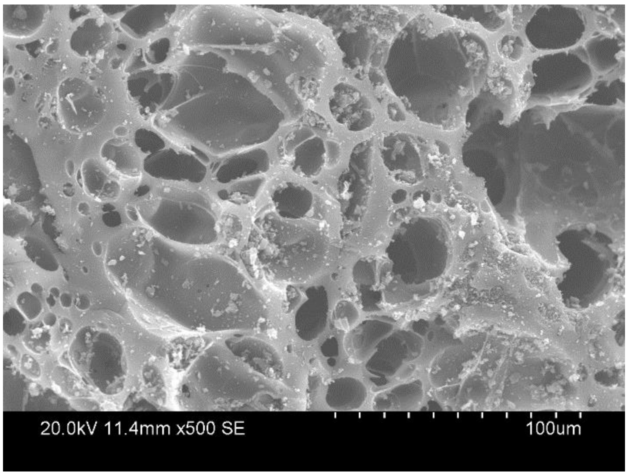

Figure 5.1 Scanning electron micrographs of GAC (Eeshwarasinghe et al. 2018)

The PAHs used in the study were acenaphthylene ($C_{12}H_8$, $\log K_{ow}$ 3.94, molar volume 168 cm^3/mol) and phenanthrene ($C_{14}H_{10}$, $\log K_{ow}$ 4.46, molar volume 199 cm^3/mol) (Eeshwarasinghe et al. 2018). As the PAHs were only partially soluble in water, their solutions were prepared from concentrated stock solutions of each PAH dissolved in acetonitrile. The stock solutions contained 20 mg PAH in 20 mL acetonitrile (1 g/L). Solutions employed for the studies were prepared by diluting the stock solutions in 1% acetonitrile in Milli-Q® water. Acetonitrile and PAHs used were spectroscopic grade materials purchased from Sigma-Aldrich, USA. Heavy metals studied were Cu, Cd and Zn. Analytical grade (99% purity) nitrate salts of these metals were employed in the experiments to prepare the heavy metals solution. These salts were also purchased from Sigma-Aldrich (USA).

5.2.2 Chemical analysis

PAH concentration in the solution was determined using UV–VIS Spectrophotometry (Shimadzu UV-1700). The absorbance values of acenaphthylene and phenanthrene were determined at the wavelengths of 322 nm and 250 nm, respectively. These wavelengths proved to be the optimum values for measuring the concentrations of these PAHs, both in the presence and absence of heavy metals (Appendix B; Figs. B.1, B.3-B.6). These PAHs' concentrations were determined from standard curves of absorption vs concentrations of the standards (Appendix B; Figs. B.2, B.7, B.8). The glassware used in the experiments were initially washed and rinsed with deionised water and then soaked overnight in dilute nitric acid bath before use. PAH losses caused by photodegradation were minimised by covering all flasks containing PAH solutions with aluminium foil. The flasks were also tightly sealed to prevent any losses occurring through volatilisation. Heavy metal concentrations were determined using a Microwave Plasma-Atomic Emission Spectrometer (Agilent 4100 MP-AES).

5.2.3 Zeta potential

The zeta potential of GAC was conducted in the presence of 10^{-3} M of $NaNO_3$ at pH levels of 4, 5, and 6 with and without additions of heavy metals and PAHs using a Zetasizer nano instrument (Nano ZS Zen3600, Malvern, UK). 10^{-3} M of $NaNO_3$ was used to keep the ionic strength of all solutions constant. The concentrations of GAC (< 0.075 mm particle size), heavy metals, and PAHs in the suspensions were 0.6 g/L, 20 mg/L, and 1 mg/L, respectively. The measurements were made after the suspensions were agitated in a flat shaker at a speed of 120 rpm for 22 h. As the pH level changed from the initial pH during PAHs and heavy metals adsorption, the pH levels were adjusted back to the initial pH after 3 h of shaking. pH adjustments were made by adding diluted HCl or NaOH. The initial pH, pH after 3 h and the final pH were measured using a pH meter.

5.2.4 Adsorption experiments

A series of glass flasks containing 70 mL solutions at pH 5 in the presence of PAHs and heavy metals together or individually were agitated with different GAC doses ranging from 0.05 to 0.8 g/L in a flat shaker at 120 rpm for 5 h at room temperature (24 ± 1 °C). The concentration of PAHs was 1 mg/L whereas that of heavy metals was 5, 20 or 50 mg/L. Much higher concentrations were used for heavy metals to be in consistent with the difference in concentrations between PAHs and heavy metals found in industrial and domestic wastewaters where the concentrations of heavy metals are 10-1000 times those of PAHs (Lawal 2017; Manjuladevi & Sri 2017; Westholm, Repo & Sillanpää 2014). All solutions contained 0.005 M $NaNO_3$ to ensure the ionic strength remained constant. The suspensions were then filtered and subsequently the filtrates were analysed for

PAHs and heavy metals. The amount of PAH and heavy metal adsorption at equilibrium, q_e (mg/g), was calculated using the equation given below:

$$q_e = \frac{(C_0 - C_e).V}{M} \qquad \boxed{5.1}$$

where, C_0 is initial concentration of PAH or heavy metal (mg/L), C_e is equilibrium concentration of PAH or heavy metal (mg/L), V is volume of solution (L) and M is mass of adsorbent (g). Percentage adsorption was calculated using the following equation and the data were fitted to the mathematical models described in Table 1:

$$\text{Percentage adsorption (\%)} = \frac{(C_0 - C_e)}{C_0} \times 100 \qquad \boxed{5.2}$$

The kinetics of adsorption was conducted at pH 5 in the presence of 0.005 M $NaNO_3$ with an adsorbent dose of 0.3 g/L, PAHs concentration of 1 mg/L, and heavy metals concentration of 20 mg/L, by shaking the suspensions at 120 rpm in a flat shaker at room temperature. Samples were taken at different periods of time (10 min – 24 h), and after filtration of the suspensions, the filtrates were analysed for PAHs and heavy metals. The amount of PAH or heavy metal adsorption (q_t) at time t was estimated as described below:

$$q_t = \frac{(C_0 - C_t)V}{M} \qquad \boxed{5.3}$$

where, C_0 is initial concentration of PAH or heavy metal (mg/L), C_t is concentration of PAH or heavy metal at time t (mg/L), V is volume of the solution (L) and M is mass of adsorbent (g). Both the equilibrium and kinetic adsorption data were fitted to the mathematical models presented in Chapter 4.

5.3. Results and discussion

5.3.1 Equilibrium adsorption

The adsorptive removals of PAHs in the presence and absence of heavy metals are shown as percentage removal of initially added PAHs for the initial PAHs concentration of 1 mg/L and heavy metals concentration of 20 mg/L in Fig. 5.2. For comparative purposes the percentage of removal of heavy metals alone and in the presence of PAHs are also shown in the same figure as well as in Fig. 5.3 where the results are illustrated more clearly by expanding the Y-axis scale. Similar results are presented in Fig. B.9 (Appendix B) for the initial PAHs concentration of 1 mg/L and heavy metals concentration of 5 mg/L. The data show that the percentages of PAHs removed are many times higher than those of the heavy metals despite the latter having 20 times larger concentrations in solution. This indicates that PAHs have higher affinity to GAC than heavy metals do. This is because the hydrophobic interaction and H-bonding of the PAHs with the hydrophobic GAC surface and functional groups (Chen, Zhu & Sun 2007; Eeshwarasinghe et al. 2018) are more dominant than the cationic heavy metal ions' exchange/chelation/complexation ability with the limited negatively charged functional groups on GAC (Chen, Zhu & Sun 2007; Dong et al. 2018; Loganathan et al. 2018). The removal percentages fell when PAH and heavy metals were present together compared to their respective individual presence (Fig. 5.2 and 5.3), indicating there was competition for adsorption between PAHs and heavy metals. The competitive effect of PAHs on heavy metals adsorption is higher than the heavy metals' effect on PAHs adsorption. Enhancement of PAHs adsorption by heavy metals presence reported for other adsorbents due to metal cation - π interaction (Saeedi, Li & Grace 2018; Zhang et al.

2017) seems to be less important than the competitive adsorption effect in the case of GAC.

Because the percentage removal of PAHs and heavy metals presented in Fig. 5.2, 5.4 and B.9 (Appendix B) depend on their initial concentrations the results are also presented as amounts adsorbed (amounts removed) in Fig. 5.3, 5.5 (Appendix B; B.10 and B.11). These figures show that in the case of 20 mg/L of heavy metals the amounts of metals adsorbed are nearly twice those of acenaphthylene, because the heavy metals concentrations were 20 times that of acenaphthylene. For phenanthrene which has a higher affinity to GAC, the amounts adsorbed were nearly the same as the heavy metals. However, when the heavy metals concentrations were reduced to 5 mg/L the amounts adsorbed for both the PAHs were higher than those of heavy metals, indicating that the PAHs have higher affinity than heavy metals towards GAC.

At all GAC doses the adsorptive removal of phenanthrene was higher than that of acenaphthylene, both in the presence and absence of metals. This is probably due to the higher hydrophobicity of the phenanthrene (log K_{ow} 4.46; K_{ow} 28,840) than that of acenaphthylene (log K_{ow} 3.94; K_{ow} 8709), though pH changes during adsorption might have also influenced the hydrophobicity difference between the two PAHs. This is consistent with the findings of other studies which reported that the adsorption capacity of PAHs increased with increasing log K_{ow} (Eeshwarasinghe et al. 2018; Valderrama et al. 2009; Yakout, Daifullah & El-Reefy 2013). Another reason could be the higher number of benzene rings in phenanthrene (3 rings) compared to those in acenaphthylene (2 rings). Ge et al. (2016) reported that PAHs' adsorption capacity increased when the number of benzene rings also increased in

PAH. This can be explained as being due to increased π-π complex formation between the π-electrons of benzene rings and the active sites on an AC surface.

Generally, the adsorption of PAHs was reduced by the metals in the order of Cu ≥ Zn > Cd which is closely related to the metals' adsorption capacity (Fig. 5.3). Sounthararajah et al. (2015b) reported that the adsorption capacities of metals on GAC, both in batch and column experiments, followed the order Cu > Zn > Cd. They explained this as due to Cu having the lowest pK_1 (first hydrolysis constant K_1, highest tendency to form $Cu(OH)^+$) and highest hydroxide precipitate solubility product pK_{so} (metal hydroxide precipitation potential high when pK_{so} is high) and Cd having the highest pK_1 and lowest pK_{so}. Erto et al. (2015) also reported similar explanations for the higher adsorption of Zn than Cd. They also stated that Zn^{2+} being smaller in size than Cd^{2+} was able to penetrate smaller pores in AC and furthermore it was less affected by steric hindrance during adsorption. McBride (1989) provided another explanation for the metal affinity order based on ionic potential (Z^2/r) (Z is charge and r is radius of the metal ion) which followed the same order as the affinity. The metals' reaction with the functional groups can also influence the adsorption behaviour. The strength of this reaction is reported to be higher for Cu than Zn (McBride 1989).

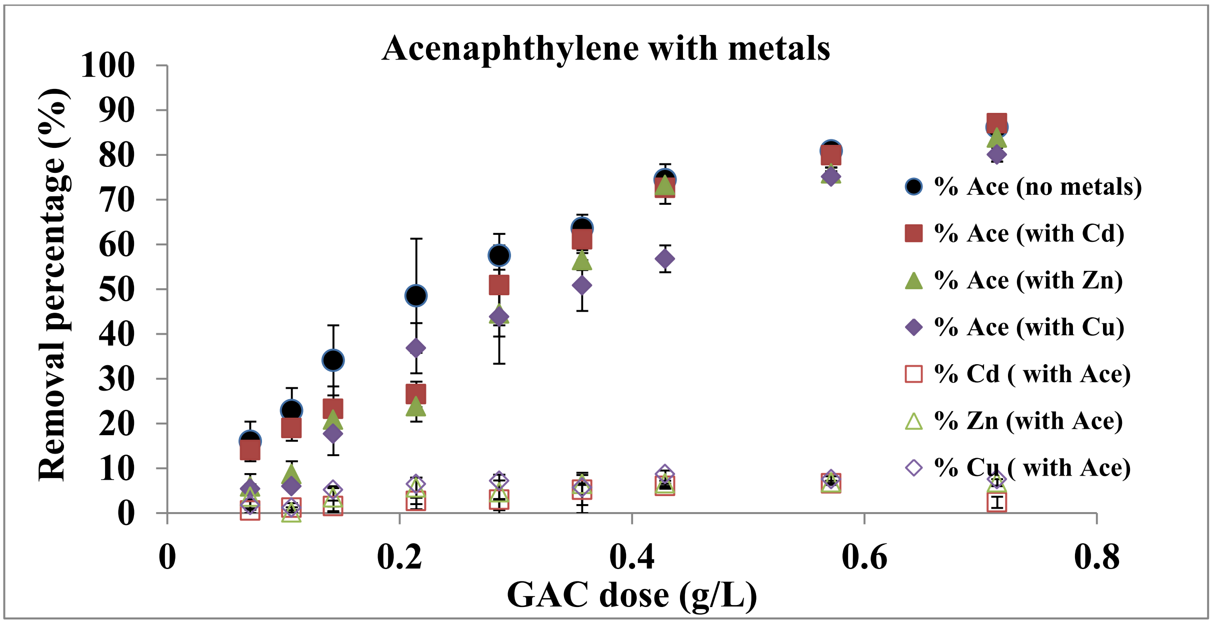

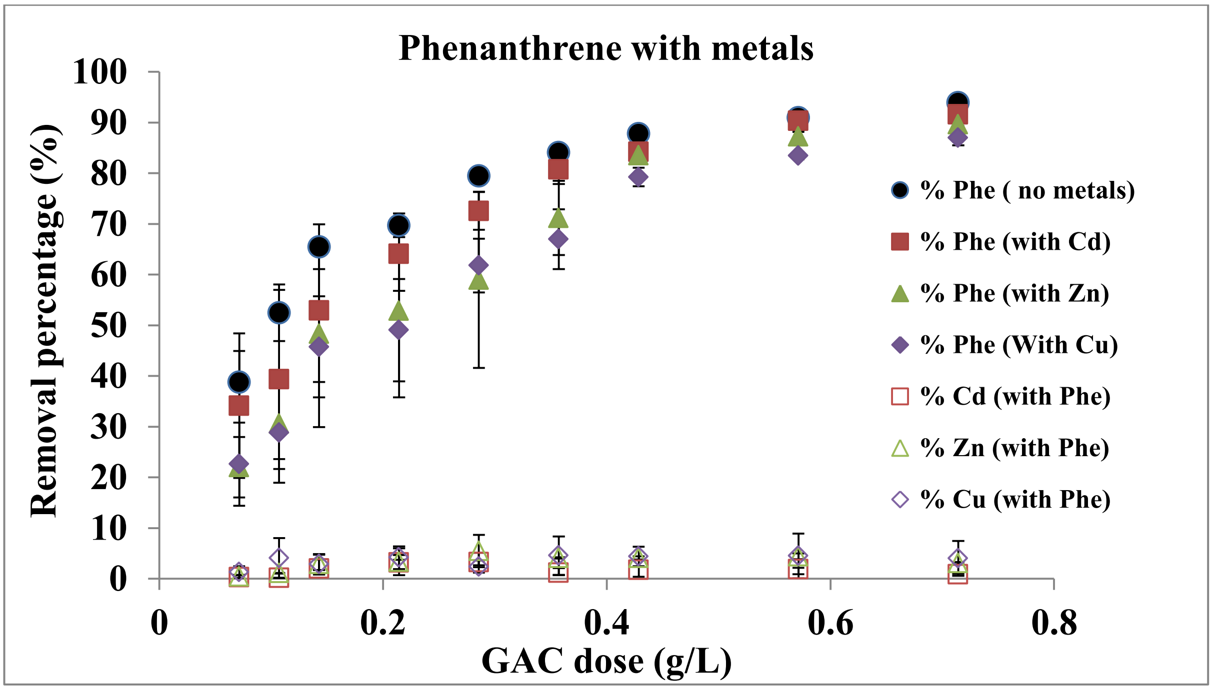

Figure 5.2 Percentage removal of acenaphthylene and phenanthrene compared with percentage removal of heavy metals during their simultaneous adsorption on GAC in the presence of 0.005 M NaNO3 (PAH concentration 1 mg/L, metal concentration 20 mg/L).

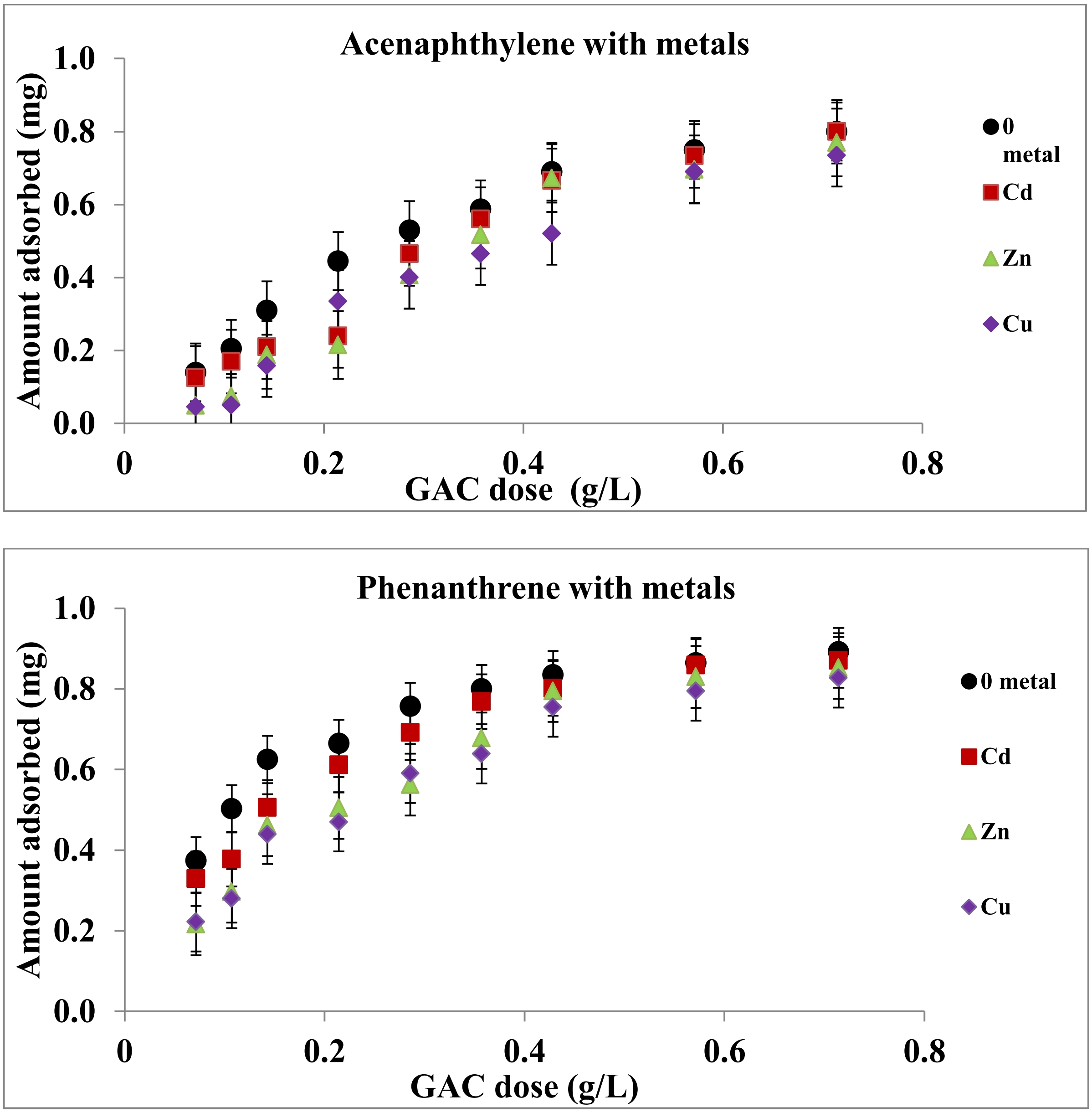

Figure 5.3 Amount of acenaphthylene and phenanthrene removed compared with amount of heavy metal removal during their simultaneous adsorption on GAC in the presence of 0.005 M NaNO3 (PAH concentration 1 mg/L, metal concentration 20 mg/L

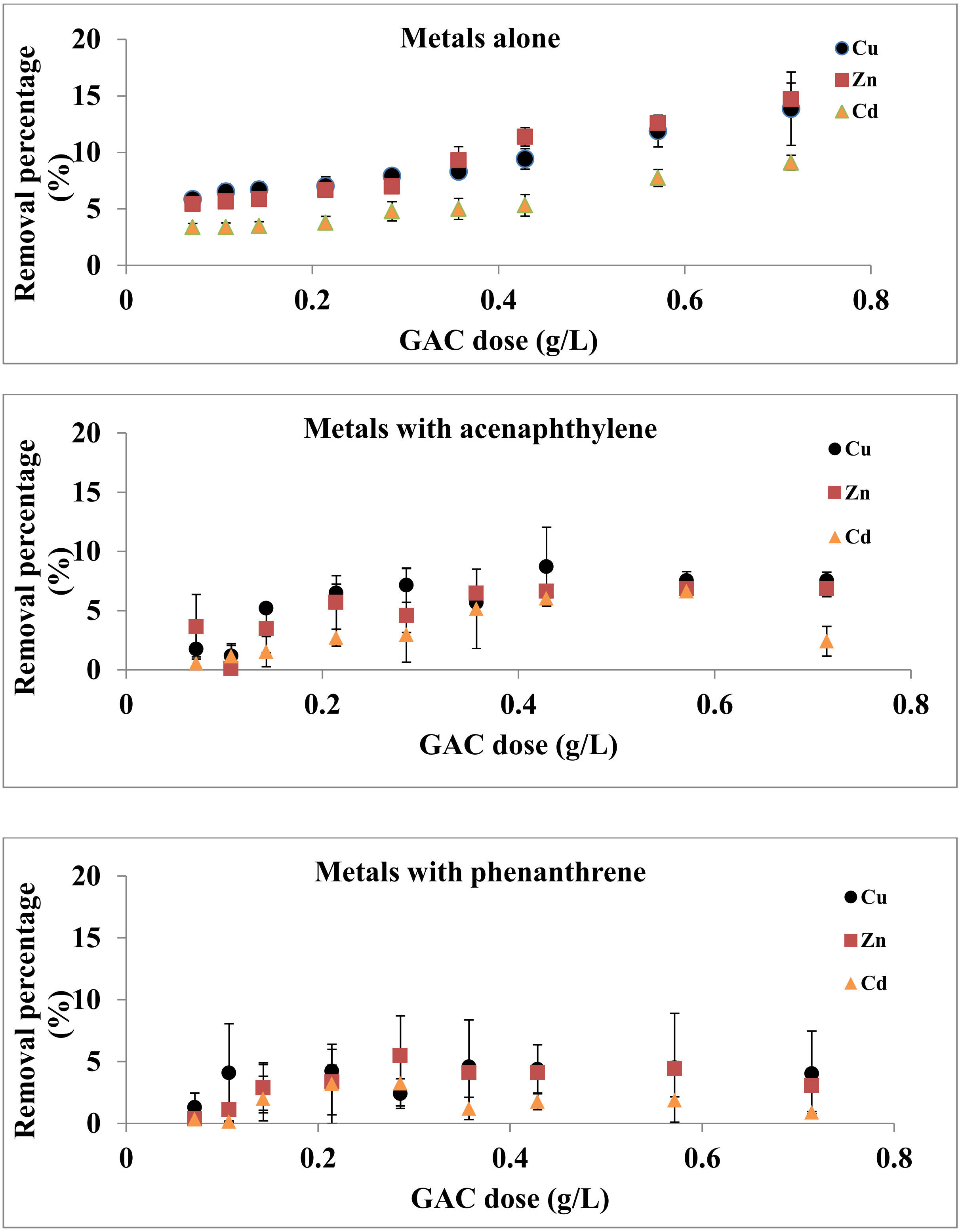

Figure 5.4 Percentage removal of heavy metals from solutions with and without the presence of acenaphthylene and phenanthrene (solutions with initial concentrations: 0.005 M NaNO3, PAH 1 mg/L, metal 20 mg/L)

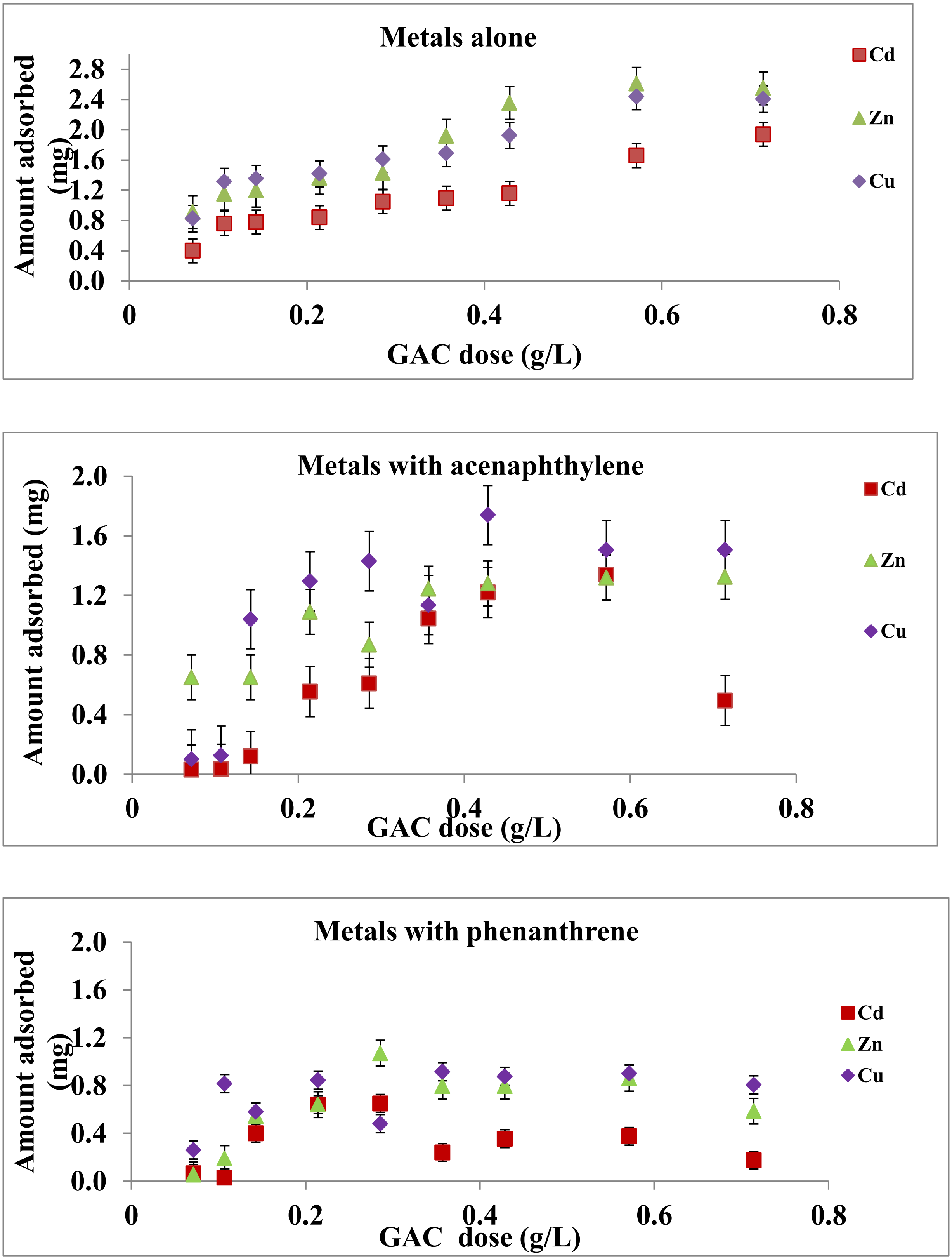

Figure 5.5 Amount of heavy metals adsorbed from solutions with and without the presence of acenaphthylene and phenanthrene (solutions with initial concentrations: 0.005 M NaNO3, PAH 1 mg/L, metal 20 mg/L))

5.3.2. Zeta potential

Since the adsorption of heavy metals is governed by metals' electrostatic interaction with the GAC surface, the zeta potential of GAC which reflects the surface charge, was studied at various pH levels in the presence of heavy metals and PAHs. The negative zeta potential of GAC in the absence of metals had the highest values (Fig. 5.6 and 5.7) which favours the adsorption of the positively charged metals and it increased with pH due to increased deprotonation of acidic functional groups. The data showed that the zero point of charge (ZPC, pH at which the net charge is zero) of GAC was 4.2. The low zero point of charge suggests that the GAC surface predominantly comprises -COOH functional groups (Park et al. 2007).

The addition of PAHs to GAC suspensions had little effect on the zeta potential because the PAHs had very few charges (Fig. 5.6 and 5.7). However, the addition of heavy metals had strong effects on the zeta potential of GAC by drastically reducing the negative surface potential. Addition of Cu reversed the negative zeta potential of GAC to positive values at all pH values and Zn alone or with acenaphthylene either changed the negative potential to zero or to positive values at pH values less than 5.5. The extent of reduction of the negative zeta potential followed the same order of the adsorption capacity of the metals (Cu > Zn > Cd) (Fig. 5.5). The strong reduction in the negative zeta potential indicates that the metals were adsorbed by inner-sphere complexation (specific adsorption) by exchanging with the protons on the GAC surface functional groups (Loganathan et al. 2018). The possible reasons for the differences between the metals in alteration of the zeta potential were same as the metals' adsorption capacity differences discussed in the earlier section.

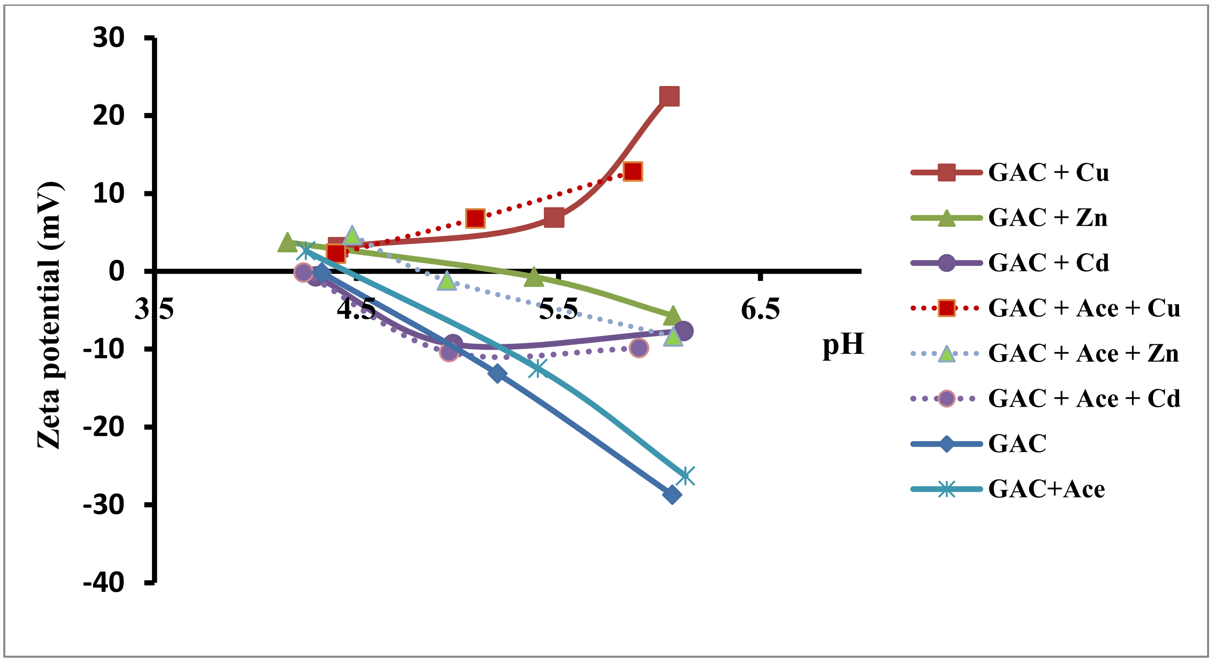

Figure 5.6 Effect of pH on the zeta potential of GAC (0.6 g/L) with and without metals (20 mg/L) and acenaphthylene (1 mg/L)

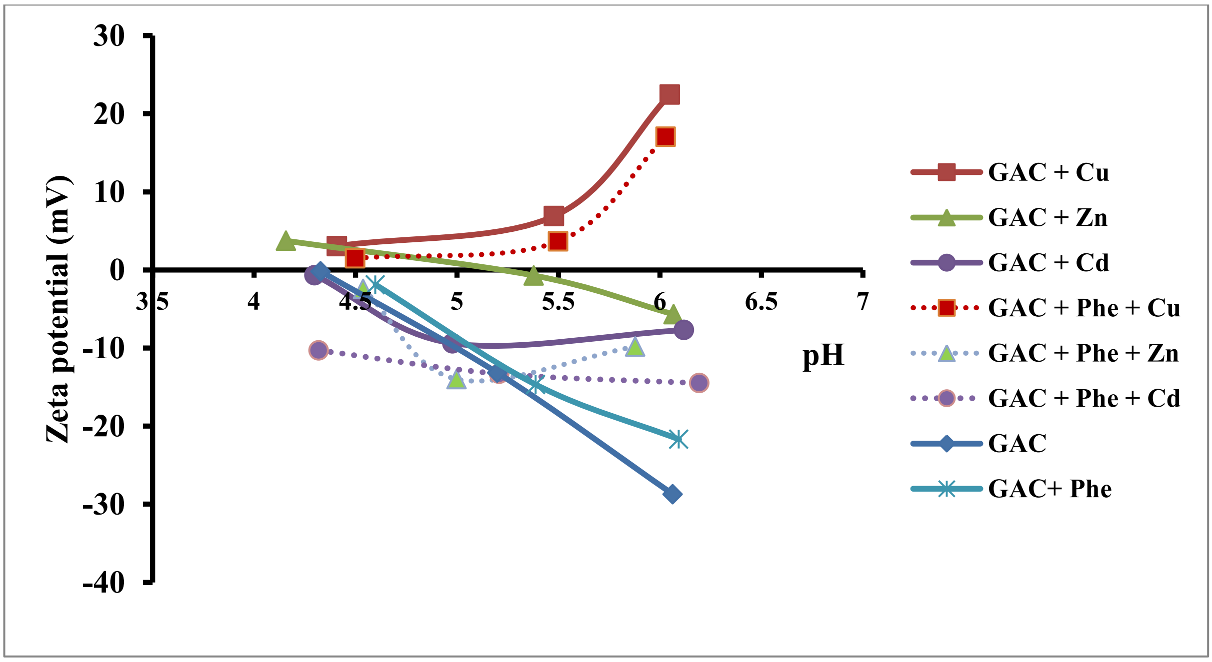

Figure 5.7 Effect of pH on the zeta potential of GAC (0.6 g/L) with and without metals (20 mg/L) and phenanthrene (1 mg/L)

5.3.3. pH changes during adsorption

At all initial pH levels, the pH increased for all treatments (ΔpH positive) (Fig. 5.8). The ΔpH was highest for the lowest initial pH of 4 because, at this low pH, the protons (H^+) which are at high concentration in solution, adsorb onto the negatively charged sites on GAC. This causes a decrease in their concentration in solution, thus producing a higher pH (Park et al. 2007). However, this increase in pH is lowered when heavy metals are added to the GAC because: firstly, the metals compete with protons for adsorption; and secondly, protons are released to the solution by exchanging with the metals adsorbed (Dastgheib & Rockstraw 2001; Kalaruban et al. 2016). In the presence of PAHs, heavy metals adsorption declined due to competition for adsorption with PAHs and therefore the increase in pH remained approximately the same as in the GAC alone treatment except for Cu which has higher adsorption capacity than the other metals even when PAHs are present. Consistent with this data, the zeta potential of GAC was reversed from negative to positive values in the presence of Cu and Cu + PAH (Fig. 5.6 and 5.7).

As the initial pH increased, ΔpH was reduced because the adsorption of protons declined due to the presence of lower proton concentration in solution and the higher adsorption of metals releasing more protons (Dastgheib & Rockstraw 2001; Park et al. 2007). This is more striking for Cu than Cd and Zn because Cu was adsorbed in higher quantities.

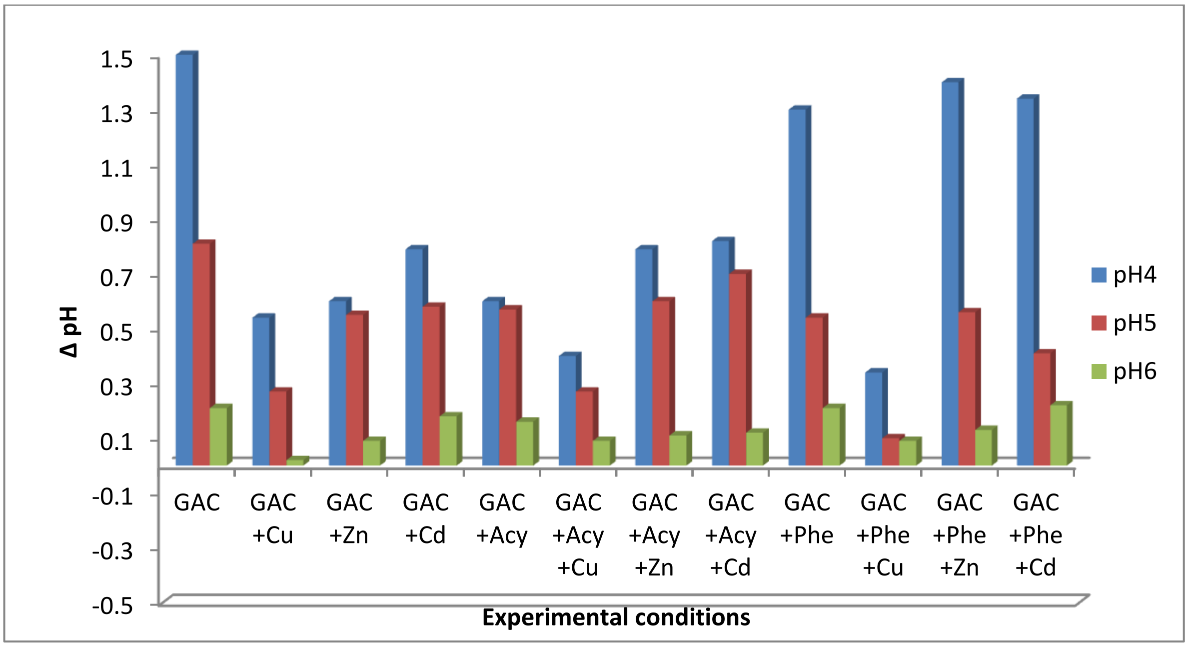

Figure 5. 8 Effect of initial pH, heavy metal, and PAH on change in pH (ΔpH = final pH – initial pH) during adsorption on GAC

Fig. 5.9 shows that there is a negative relationship between ΔpH and Δzeta potential (zeta potential of GAC in the presence of heavy metals with and without PAHs – zeta potential of GAC alone). As the initial pH increased from 4 to 6, Δzeta potential increased because specific adsorption (inner-sphere complexation) of metals, especially Cu and Zn, increased (Loganathan et al. 2018). During the specific adsorption of metals, protons (H^+) are released from the functional groups on the GAC surface. The final pH was thus reduced and ΔpH decreased. At the initial pHs of 5 and 6, Δzeta potential followed the order Cu > Zn > Cd but ΔpH followed the reverse order of Cd ≥ Zn > Cu, regardless of the presence or absence of PAHs.

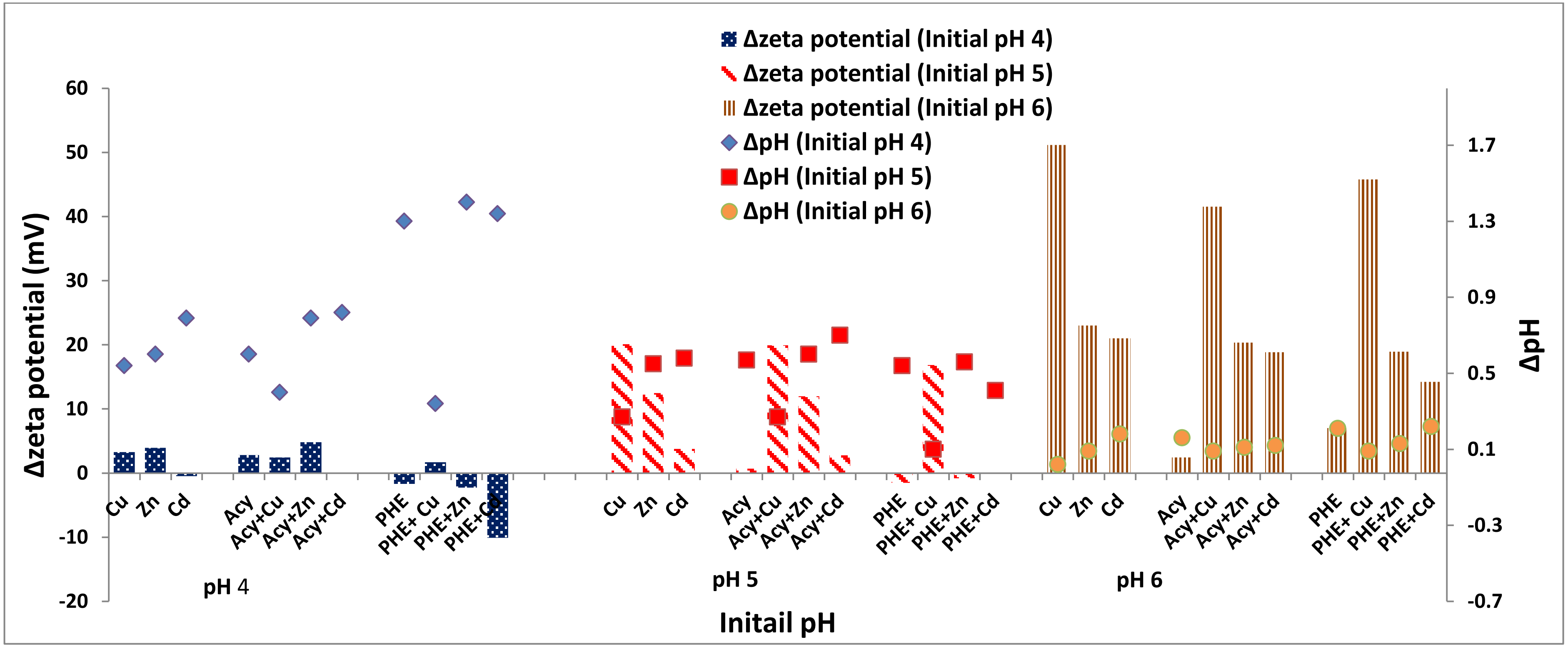

Figure 5. 9 Relationship between ΔpH (Final pH - initial pH) and Δzeta potential (zeta potential of GAC with heavy metals and PAHs – zeta potential of GAC alone) at three initial pHs during adsorption

(▨ ▨ ▥ - Δzeta potential; ◆ , ■ and ● - ΔpH)

5.3.4. Equilibrium adsorption modelling

Three adsorption models, namely Langmuir, Freundlich and Dubinin–Radushkevick models were used to describe the equilibrium adsorption data. Of these models, Langmuir model satisfactorily described the data for both PAHs with and without metals at different concentrations (Tables 5.1 and 5.2). The R^2 values ranged from 0.60 to 0.88 for a degree of freedom of data points of 8 (9 data points). This means that the model explained 60-88% of the variation of data. R^2 value > 0.76 (correlation coefficient, r = 0.87) for a degree of freedom of 8 indicates a very highly significant relationship (Little & Hills 1978). R^2 value > 0.59 (r = 0.76) indicates a highly significant relationship. Freundlich model fitted well to the data for phenanthrene (Table 5.2) except for phenanthrene with 50 mg/L concentration of metals. But it failed to satisfactorily describe the data for acenaphthylene. Dubinin–Radushkevick model satisfactorily described the data for both PAHs in the absence of metals but the data fit to this model was poor in the presence of metals at most of the concentrations.

The fairly satisfactory data fit to Langmuir model may indicate that the PAHs were adsorbed as monolayers on the GAC. The Langmuir maximum adsorption capacity of phenanthrene (7.36 mg/g) was higher than that of acenaphthylene (2.63 mg/g) due to the higher hydrophobicity of the former (log K_{ow} 4.46) than the latter (log K_{ow} 3.94). The presence of metals decreased the adsorption capacity with this effect becoming stronger as the metal concentration increased because of competitive adsorption. The decrease in adsorption capacity reached its highest point in the presence of Cu and its lowest when Cd was present for reasons explained earlier. From the Langmuir model parameter K_L, another parameter R_L can be calculated by using the formula $R_L = 1 / (1+C_mK_L)$ (where C_m is the maximum initial concentration of sorbate) to assess whether the adsorption process is favourable or not. The calculated R_L values for the two PAHs in the presence of all concentrations of heavy metals were in the range of 0.05 - 0.26. As these values are between 0 and 1, the adsorption process can be considered a favourable one (Rusmin et al. 2015).

Unlike PAHs adsorption, the adsorption of heavy metals alone or in the presence of PAHs did not fit to either of the two adsorption models. This is because the percentage removal of these metals was low at the low GAC doses used in the study and the intense competition of PAHs with heavy metals for adsorption.

Table 5. 1 Model parameters for the adsorption of acenaphthylene on GAC at three metals concentrations in the presence of 0.005 M NaNO3.

	Metals	Langmuir model			Freundlich model			Dubinin–Radushkevick model			
		q_m	K_L	R^2	K_f	n	R^2	q_m	β	R^2	E
	mg/L	mg/g	L/mg		mg/g(L/mg)$^{1/n}$			mg/g	(mol^2/kJ^2)		(kJ/mol)
	0	2.63	6.40	0.75	2.63	2.69	0.58	3.2	0.04	0.88	3.5
Cu	5	0.81	7.87	0.73	1.79	3.59	0.39	1.4	0.05	0.65	3.1
Zn		0.88	9.32	0.75	2.35	2.11	0.58	2.0	0.03	0.40	3.9
Cd		1.98	9.29	0.73	1.87	4.35	0.33	4.4	0.14	0.36	1.9
Cu	20	0.54	4.84	0.74	1.19	3.17	0.20	1.2	0.04	0.53	3.4
Zn		0.57	5.44	0.64	1.09	4.10	0.18	1.9	0.09	0.73	2.4
Cd		1.87	13.08	0.88	1.59	9.93	0.12	1.7	0.08	0.20	2.4
Cu	50	0.31	2.88	0.67	2.79	0.76	0.48	2.9	0.05	0.78	3.3
Zn		0.51	3.55	0.60	1.91	11.38	0.26	1.9	0.01	0.51	6.3
Cd		0.96	10.66	0.62	1.15	2.28	0.17	2.7	0.09	0.46	2.3

Table 5. 2 Model parameters for the adsorption of phenanthrene on GAC at three metals concentrations in the presence of 0.005 M NaNO3.

	Metals	Langmuir model			Freundlich model			Dubinin–Radushkevick model			
		q_m	K_L	R^2	K_f	n	R^2	q_m	β	R^2	E
	mg/L	mg/g	L/mg		mg/g(L/mg)$^{1/n}$			mg/g	(mol^2/kJ^2)		(kJ/mol)
	0	7.36	3.15	0.80	7.35	1.61	0.92	5.4	0.03	0.90	4
Cu	5	5.95	2.93	0.84	5.99	1.56	0.86	5.1	0.04	0.87	3.5
Zn		5.46	3.19	0.80	5.19	1.77	0.84	3.3	0.03	0.66	3.8
Cd		6.17	3.43	0.78	5.81	1.80	0.87	1.5	0.03	0.39	4
Cu	20	2.18	24.84	0.81	3.63	2.36	0.71	4.1	0.03	0.74	4.2
Zn		2.25	14.50	0.73	4.34	2.19	0.76	2.4	0.02	0.40	5.1
Cd		2.74	19.42	0.85	4.34	2.19	0.76	2.0	0.03	0.29	4.3
Cu	50	0.74	6.07	0.67	1.02	2.91	0.22	4.9	0.03	0.79	4.1
Zn		1.29	18.23	0.80	2.85	1.77	0.42	2.7	0.02	0.67	4.5
Cd		2.20	8.09	0.82	3.18	2.50	0.60	1.6	0.05	0.39	3.1

5.3.5. Kinetic adsorption modelling

The pseudo-first order model fitted better to the adsorption kinetic data of PAHs in the presence of heavy metals compared to the pseudo-second order model (Appendix B; Table B.1). Conversely, the opposite trend occurred for the adsorption of heavy metals in the presence of PAHs (Appendix B; table B.2). This indicates that PAHs are adsorbed generally by physical interaction with GAC through hydrophobic interaction and van der Waals forces whereas heavy metals are adsorbed chemically through exchange with protons in the functional groups on GAC. These results are consistent with the zeta potential findings where heavy metals adsorption markedly decreased the negative charges on GAC and even Cu reversed them into positive charges (Figs. 5.6 and 5.7). In comparison, PAHs adsorption had only little effect on the zeta potential of GAC.

Because the GAC has numerous pores and channels, the kinetics of adsorption would have been influenced by PAHs' and metals' diffusion rates into these pores and channels. This was investigated by fitting the data to the Weber and Morris model (Weber & Morris 1963) . The fit of the data showed two distinct sets of straight lines with high R^2 values (0.89-0.99) (Figs. 5.10 and 5.11, Table 5.3). The straight-line relationships' and the initial line going through the origin in the graph show that the rate of adsorption is controlled by intra-particle diffusion. The straight-line plots indicate that initially the rate of adsorption was fast (high K_{s1}) followed by a slower rate of adsorption (low K_{s2}) (Table 5.3). The faster rate of adsorption was probably due to intra-particle diffusion into the mesopores and the slower rate was into the micropores. Haro et al. (2011) reported three straight lines when the data for the adsorption of acenaphthene and fluorene on activated carbon were plotted according to Weber and Morris model. They attributed the first line up to 10 min to external mass transfer and the other two from 10 min to 4 h to intra-particle diffusion similar to our interpretation. The allocation of the data to the two straight lines is arbitrary by eye-estimate using the limited data which is clear for PAHs but not so much for the metals. Therefore, more data are required especially at longer times in future studies to confirm the above explanations.

The diffusion rate into the mesopores (K_{s1}) was faster for acynaphthylene (molar volume 168 cm^3/mol) than that for phenanthrene (molar volume 199 cm^3/mol) irrespective of the type of metals present because of its smaller size. However, this pattern was not noticed in the rate of diffusion into the micropores (K_{s2}). With reference to the metals, generally, no difference in the rate of diffusion into the mesopores was observed, but in the micropores the heavy metals' rate of diffusion was higher than that of PAHs.

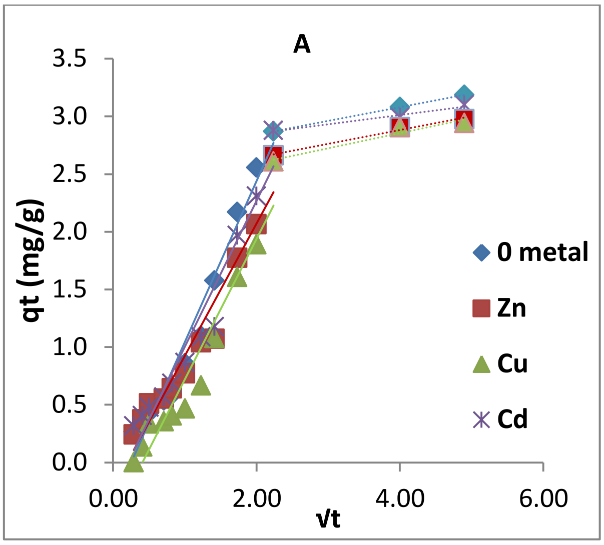

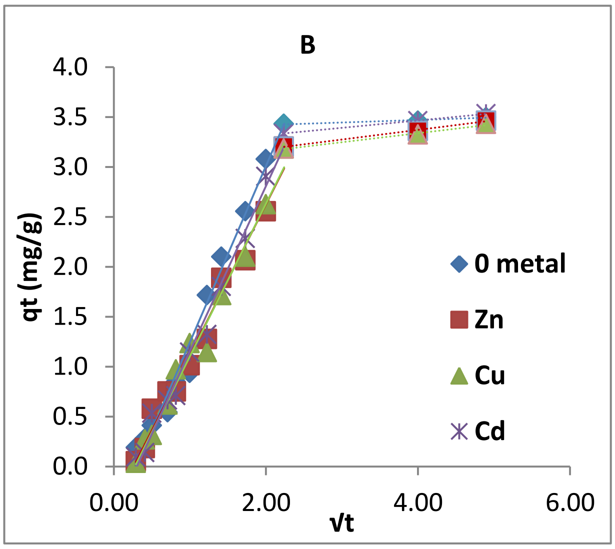

Figure 5.10 Weber and Morris plots of (A) rate of adsorption of phenanthrene in the presence of heavy metals; (B) rate of adsorption of acynaphthylene in the presence of heavy metals (PAH 1 mg/L, metals 20 mg/L, GAC dose 0.3 g/L)

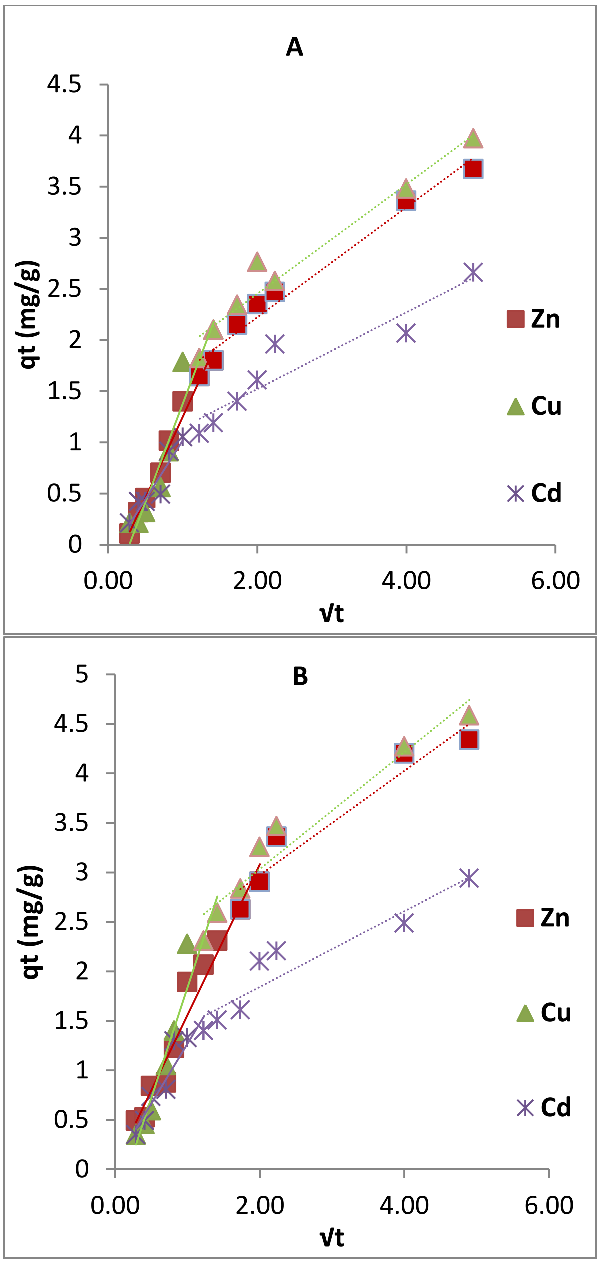

Figure 5.11 Weber and Morris plots of (A) rate of adsorption of metals in the presence of phenanthrene; (B) rate of adsorption of metals in the presence of acynaphthylene (1 mg/L) (PAH 1 mg/L, metals 20 mg/L, GAC dose 0.3 g/L)

Table 5.3 Weber-Morris plot parameters for the adsorption of PAHs and heavy metals in the presence of each otherTable 5. 4 Weber-Morris plot parameters for the adsorption of PAHs and heavy metals in the presence of each other

PAH	Metal	Weber-Morris short-term adsorption K_{s1} mg/g /min$^{1/2}$	R^2	Weber-Morris long-term adsorption K_{s2} mg/g /min$^{1/2}$	R^2
Acenaphthylene	0	1.76	0.985	0.025	0.966
	Cd	1.66	0.987	0.075	0.999
	Zn	1.51	0.979	0.096	0.995
	Cu	1.52	0.982	0.09	0.989
Phenanthrene	0	1.39	0.968	0.12	1.000
	Cd	1.26	0.949	0.08	0.969
	Zn	1.15	0.947	0.12	0.984
	Cu	1.19	0.926	0.13	0.942
Metals with acenaphthylene	Cd	1.14	0.894	0.38	0.887
	Zn	1.47	0.980	0.51	0.979
	Cu	1.92	0.932	0.53	0.957
Metals with phenanthrene	Cd	1.24	0.913	0.27	0.987
	Zn	1.16	0.977	0.40	0.969
	Cu	1.28	0.960	0.43	0.935

5.4 Conclusions

In solutions containing both PAHs (acenaphthylene or phenanthrene) and heavy metals (Cd, Cu or Zn) the adsorptive removal of PAHs using GAC was greater than those of heavy metals, even with the latter at 20 times higher concentration. The adsorptive capacities of both PAHs and heavy metals were reduced in the presence of both compared to their capacities when they were present separately. This was due to competition for adsorption, despite their adsorption mechanisms being different. Copper and Zn reduced the adsorption of PAHs more than Cd did. Similarly, PAHs reduced the adsorption of Cd more than the other metals. These results were explained using zeta potential data where Cu and Zn reduced the negative charges on the GAC more than Cd did – the negative charges were even reversed to positive values in the presence of Cu. The adsorption capacity was higher for phenanthrene than for acenaphthylene, which was consistent with the higher hydrophobicity of phenanthrene. The Langmuir adsorption capacity for both the PAHs decreased with increased concentration of metals, the effect being in the order Cu > Zn > Cd. The kinetic adsorption data fitted to the Weber and Morris plots indicating intra-particle diffusion of both PAHs and heavy metals into the mesopores and micropores in GAC. The diffusion rate was higher in all cases in the mesopores which occurred when the adsorption process began. The rate of diffusion into mesopores was faster for acenaphthylene than phenanthrene irrespective of the type of metal present, consistent with their size difference. The rate of diffusion in both mesopores and micropores was in the order Cu > Zn > Cd in the presence of either of the PAHs.

Chapter 6

Enhanced removal of nutrients, heavy metals, and PAH from synthetic stormwater by incorporating different adsorbents into a filter media

This chapter is a major part of my published paper, Ekanayake, D., Loganathan, P., Johir, M.A.H. *et al.* Enhanced Removal of Nutrients, Heavy Metals, and PAH from Synthetic Stormwater by Incorporating Different Adsorbents into a Filter Media. *Water Air Soil Pollut* **232,** 96 (2021).

Chapter Six

6.1. Introduction

Biofiltration systems are comparatively a new technique in the treatment of stormwater to remove pollutants and its becoming more popular in the field application due to its simplicity and cost effectiveness (Hsieh & Davis 2005). In the earlier chapters the characteristics of stormwater was determined from field samplings of stormwater during several rainfall events. In two chapters, GAC adsorbent was shown to effectively remove PAHs and heavy metals. The information gathered in those chapters are used in this chapter to prepare a synthetic stormwater solution containing the pollutants at concentrations relevant to field conditions and to enhance the removal of pollutants by a biofilter media by incorporation of GAC into the biofilter media.

Biofiltration systems are configured as vegetated filtration trenches or basins with an underlying porous collection pipe and are designed to remove fine suspended solids and dissolved pollutants. Biofilters differ from simple filtration systems in that they aim to reproduce natural physical, chemical, and biological processes. Many studies have been carried out on vegetated biofiltration systems for removal of nutrients (Chen et al. 2013; Kim, Seagren & Davis 2003), and heavy metals (Li & Davis 2008b). However, pollutant removal capacities of the filter medium below the vegetation level is poorly understood. Treatment reliability is an important issue highlighted by the number of studies that report significant variations in pollutant removal rates. Pollution retention through bio-filter systems occurs mainly by evaporation, filtration, adsorption to the medium, precipitation and biological intakes by plants and microbes. However, the short contact time between pollutants and vegetation may reduce the biological uptake of nutrients and heavy metals from the stormwater (Denman, May & Breen 2006). Hence it is important to improve the medium of the biofiltration system to enhance pollutant removal by adsorption or precipitation when stormwater percolates through the medium.

The present study evaluated the performance of a soil medium (R165) proposed for use as a filter below the vegetation in biofiltration basins in Blacktown, New South Wales, Australia to remove targeted pollutants. Apart from the performance of R165, other filter media such as zeolite and granular activated carbon (GAC) were mixed in with R165 to evaluate if pollutant removal could be further improved. Zeolite is well known for removing specific types of heavy metals (Nguyen et al. 2015) and ammonium (Cooney et al. 1999a, 1999b) by cation exchange mechanism (Wang & Peng 2010). GAC is one of the most abundant adsorbent commonly used in water treatment and very effective in removing a wide range of organic pollutants including polycyclic aromatic hydrocarbons (PAH) and heavy metals through hydrophobic and electrostatic interactions, hydrogen bonding and chelation mechanisms (Eeshwarasinghe et al. 2018; Valderrama et al. 2008). The results of this study provide an in-depth knowledge on the application of zeolite and GAC as biofilter media for stormwater harvesting and reuse. The originality of this study is the development of a novel experimental protocol to estimate the efficiency of a filter medium for the treatment of stormwater pollutants from 1-3 years rainfall experienced in the field using a laboratory column-set-up over short-term duration. The pollutants removals by the filter medium were estimated by incorporating three adsorbents of contrasting properties which is another novelty of the study.

6.2. Materials and Methods

The laboratory testing mimics the current design of biofiltration under rainfall conditions experienced in Blacktown. Column studies were carried out to assess the performance of the R165 soil media, which is proposed for use in Blacktown's bio retention basins. The improvements in pollutant removal by incorporating small amounts of GAC (0.1-2%) and Zeolite (1-10%) with R165 was also evaluated.

6.2.1. Materials

6.2.1.1 Zeolite

The zeolite used in the study is a locally available material, one that demonstrates a good capacity to adsorb heavy metals (Nguyen et al. 2015) . The zeolite was sourced from a natural deposit at Werris Creek, New South Wales and supplied by Zeolite Australia Pty Ltd., Australia. The Brunauer–Emmett–Teller (**BET**) surface area of zeolite amounted to 15.4 g/m^2, according to Nguyen et al. (2015). Nguyen (2016) produced XRD spectra of Australian natural zeolite and they revealed that zeolite primarily consisted of heulandite (2θ: 10.0o, 19.0o, 22.7o, 30.0o) and a small amount of quartz (2θ: 21.0o, 27.0o, 36.5o). Morphology of the Australian zeolite was also documented by Nguyen (2016) and is presented in Fig. 6.1. Furthermore, her findings from the FTIR spectra of zeolite indicated the presence of Si or Al and hydroxyl groups and adsorbed water molecules. The zero point of charge (ZPC, the pH at which the net surface charge is zero) of zeolite was 2.2 (Nguyen et al. 2015), suggesting that at the pH of most stormwaters (which is 6-7) the net surface charge on this material is negative and favours the adsorption of positively charged metals and ammonium. The zeta potential value of zeolite is -17 mv at pH 6.5 (Nguyen et al. 2015; Sounthararajah et al. 2016).

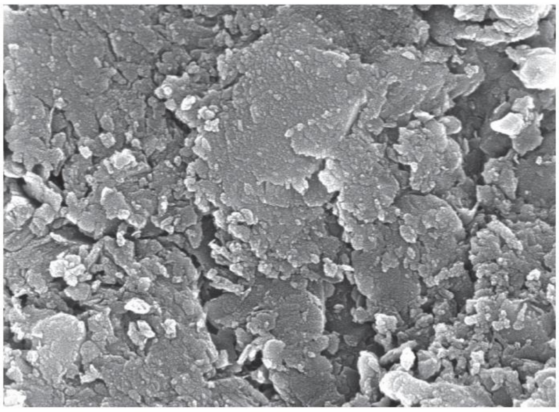

Figure 6.1 SEM images of zeolite; adopted from the thesis (Nguyen 2016)

6.2.1.2 GAC

GAC (particle size ranging from 0.3 to 2.4 mm) was purchased from James Cummins P/L, Australia. A particle size varying from 0.4 -2 mm was separated from the original material and used in the experiments. The BET surface area, pore volume and average pore diameter of the GAC were 1000 m^2/g, 0.69 cm^3/g and 2.7 nm, respectively. The scanning electron micrographs of the GAC revealed the presence of many micropores and mesopores, which may have given the GAC a high surface area (Eeshwarasinghe et al. 2018). Details of the characteristics of used GAC are reported in Chapter 4.

6.2.1.3 R165

Table 6.1 Characteristics of the bio retention media (R165)

Characteristics	**Result**	**Result_Unit**
Electrical Conductivity @ 25°C	15	µS/cm
pH Value	6.8	pH Unit
Total Phosphorus as P	101	mg/kg
Total Nitrogen as N	220	mg/kg
Total Kjeldahl Nitrogen as N	220	mg/kg
Nitrite + Nitrate as N (Sol.)	1.5	mg/kg
Organic Matter	0.5	%
Total Organic Carbon	0.5	%
+150µm	93	%
+300µm	62	%
+425µm	26	%
+600µm	6	%
+1180µm	2	%
+2.36mm	2	%
+4.75mm	1	%
Clay (<2 µm)	5	%
Gravel (>4750 µm)	1	%
Silt (2-60 µm)	1	%
Sand (60-150 µm)	2	%
Sand (150-300 µm)	31	%
Sand (300-425 µm)	36	%
Sand (425-600 µm)	20	%
Sand (600-1180 µm)	4	%
Sand (1180-2360 µm)	1	%
Gravel (2360-4750 µm)	1	%
Moisture Content	5.3	%
Copper	<5	mg/kg
Lead	5	mg/kg
Nickel	<2	mg/kg
Zinc	9	mg/kg
Arsenic	<5	mg/kg
Cadmium	<1	mg/kg
Chromium	3	mg/kg
Mercury	<0.1	mg/kg

The characteristics of this biofiltration media are presented in Table 6.1. It shows that the media is loamy sand containing 95% sand. Further R165 is composed of small content of nutrients, organic carbon and traces of heavy metals. Possible leaching of these compounds were tested using distilled water at the beginning of the experiment.

6.2.1.4 Synthetic stormwater

Analytical grade nitrate salts of heavy metals used for heavy metals. Polycyclic aromatic hydrocarbons (PAHs) employed in the adsorption experiments were acenaphthene, phenanthrene and pyrene. All chemicals were obtained from Sigma-Aldrich (USA).

Synthetic stormwater was used for testing. The use of synthetic stormwater circumvents the need to collect large qualities of stormwater in the field in Blacktown, store and transport to the laboratory for testing. The concentrations of the constituents of interest in the synthetic stormwater were adjusted to the expected range that occurs in Blacktown. The concentrations remain the same throughout the testing providing an easier comparison of performance of different media used in the various column studies. This would not be possible if actual stormwater collected in the field is used. The composition of synthetic stormwater is shown in Table 6.2.

Table 6.2 Characteristics of synthetic stormwater

Compound	Pollutant	Concentration (mg/L)	Compound	Pollutant	Concentration (mg/L)
KNO_3	NO_3^-- N	3	$Ni(NO_3)_2$	Ni^{2+}	0.002
KH_2PO_4	PO_4^{3-}- P	1.5	$Cd(NO_3)_2$	Cd^{2+}	0.01
NH_4Cl	NH_4^+- N	0.65	$Pb(NO_3)_2$	Pb^{2+}	0.04
NaCl	Na^+	75-80	$Cu(NO_3)_2$	Cu^{2+}	0.08
$CaCl_2$	Ca^{2+}	25	$Zn(NO_3)_2$	Zn^{2+}	0.1
$MgCl_2.6H_2O$	Mg^{2+}	13.5	$AlCl_3.6H_2O$	Al^{3+}	0.1
Humic acid	DOC	5-10	$FeCl_3$	Fe^{3+}	0.15
Pyrene	pyrene	0.03	Na_3AsO_4	AsO_4^{3+}	0.05
Phenanthrene	Phenanthrene	0.03	$Mn(NO_3)_2$	Mn^{2+}	0.03
Acenaphthene	Acenaphthene	0.03		pH	6.8
Kaolin clay	Turbidity (NTU)	40		Conductivity (µS/cm)	650-700

6.2.2. Methods

6.2.2.1 Column experiment

Column with dimensions 18.5 cm (diameter) x 18.5 cm (height) was used in the experiments. The R165 media was packed to a depth of 50 mm in the column. Coarse sand layers and gravels were placed above and below R165 as shown in Fig. 6.2. The stormwater was passed through the column at a flow velocity of 100 mm/h for most experiments and at 300 mm/h for a few experiments. Downflow mode of operation was employed and effluent was collected at the bottom of the column at various times during the experiment. Pollutant concentrations in the influent solution

(C_0) and in the effluent solution at various times (t) (C) were measured and the breakthrough curves (C_0/C vs time) were plotted. The breakthrough curves show the time-wise progress in pollutants removal by the column. The experimental set-up is illustrated in Fig. 6.2 a & b

The breakthrough data for NH_4^+ and PO_4^{3-} were simulated using Thomas model (Eeshwarasinghe et al. 2018; Nur et al. 2015; Thomas 1944). Thomas model equation is given below equation (6.1).

$$\ln\left(\frac{C_o}{C}-1\right)=\frac{k_T q_o m_c}{Q}-k_T C_o t \qquad \boxed{6.1}$$

where, k_T is the Thomas rate constant (mL/min.mg), q_0 is the maximum solid-phase concentration of the solute (mg/g), m_C is the mass of adsorbent in the column (g), Q is the volumetric flow rate (mL/min), C_o (mg P/L) is the inlet phosphate concentration; C (mg P/L) is the outlet phosphate concentration at time t (min). The values for k_T and q_0 were determined from the slope and intercept of a linear plot of ln (C_0/C -1) vs t.

6.2.2.1.1 Rainfall intensity

Laboratory testing was conducted to mimic rainfall experienced in Blacktown. The annual rainfall in Blacktown is 800 mm. At a flow velocity of 100 mm/hr, and 8-hour run of the column test, the water flow in the column is equivalent to 1 year of rainfall (800 mm/year).The rate of stormwater inflow to column at the rainfall intensity of 0.1 m/hr and 0.3 m/hr used in the study were 45 ml min^{-1} and 135 ml min^{-1} , respectively as explained below:

The surface area of the column is 22/7 x 0.185/2 x 0.185/2 m^2 = 0.0269 m^2

For the rainfall intensity of 0.1 m/hr, the rate of stormwater inflow to the column is 0.1 m/hr x 0.0269 m^2 = 0.00269 x 10^6 cm^3 = 2690 ml/hr = 2690/60 ml/min or 45 ml/min

Similarly, for the rainfall intensity of 0.3 m/hr, the rate would be 135 ml/min

The experiments were run until the media exhausted for up to 25-30 hours representing intermittent rainfall.

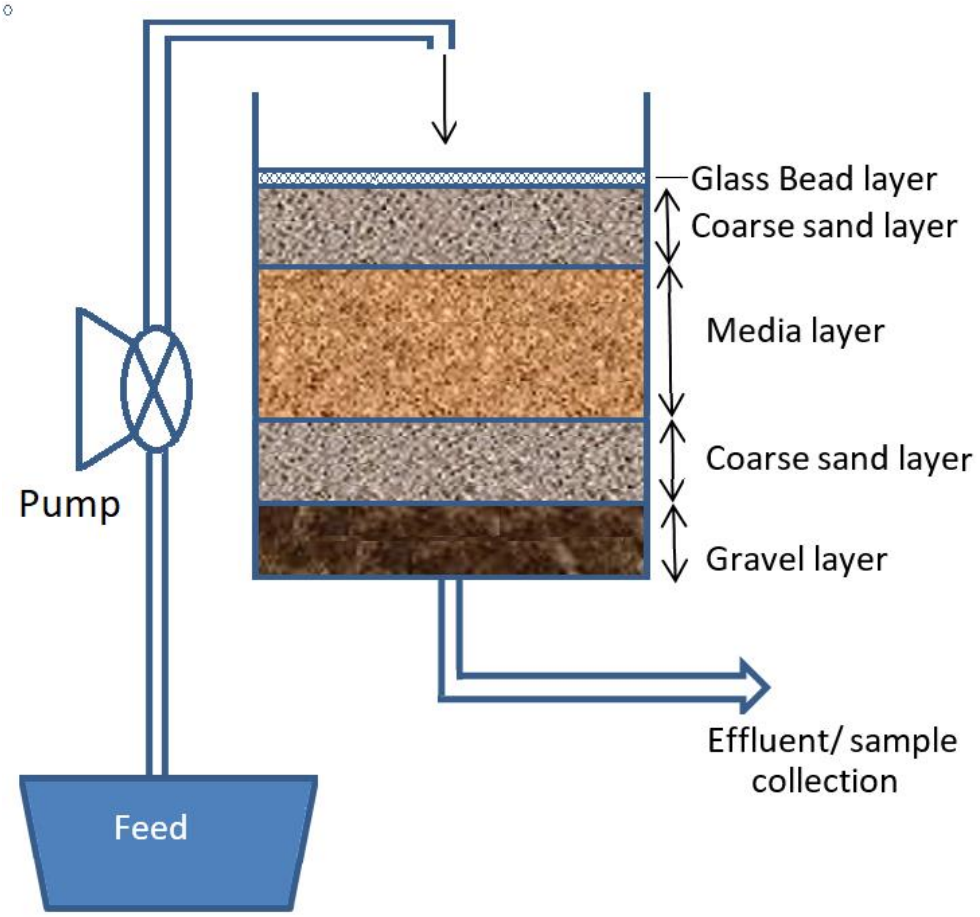

(**a**) Schematic diagram of the column experiments

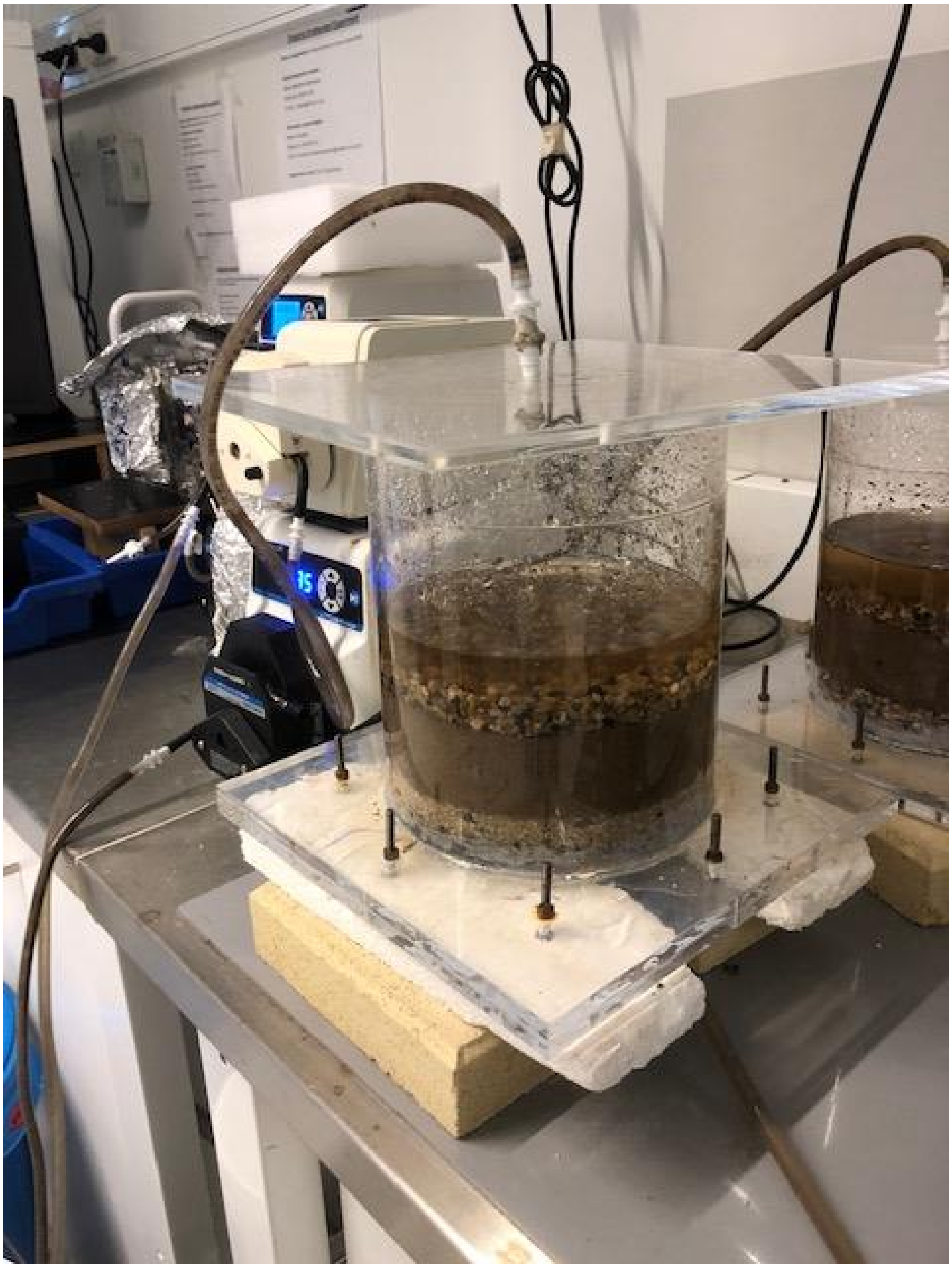

(**b)** The laboratory set up of the experiment

Figure 6.2 Column Experiment

6.2.2.2 Enhancing the performances using additives (GAC, zeolite)

Experiments were carried out by using two separate columns of 1% Zeolite+R165 and 1% GAC+R165 at a flow velocity of 100 mm/hr to evaluate the possible improvement of the bio-retention media. Initially PAHs, heavy metals, DOC, phosphate and turbidity were tested. 100% removal of PAHs observed from the column1% GAC+R165. There weren't significant reductions in any other tested pollutants by both columns. The percentage of GAC was reduced from that used in the initial experiments to reduce the cost of a filter that would be installed in the field. Hence zeolite was selected to remove the majority of pollutants and a small percentage of GAC for the removal of organic pollutants. Further column experiments were carried out by mixing in with R165, 5%, 10%, 20% of zeolite. The media depth in the column was 50 mm. Experiments carried out in the study are summarized in Table 6.3.

Table 6.3 Summary of all experiments

No	Filter Media	Media Height (mm)	Rainfall intensity	Flow velocity
1	R165	50	1 (800 mm/year)	100 mm/hr (8 hr; 45 mL/min)
2	1% GAC mixed with R165	50	1 (800 mm/year)	100 mm/hr (8 hr; 45 mL/min)
3	1% Zeolite mixed with R165	50	1 (800 mm/year)	100 mm/hr (8 hr; 45 mL/min)
4	5% zeolite mixed with R165	50	1 (800 mm/year)	100 mm/hr (8 hr; 45 mL/min)
5	10% Zeolite mixed with R165	50	1 (800 mm/year)	100 mm/hr (8 hr; 45 mL/min)
6	20% Zeolite mixed with R165	50	1 (800 mm/year)	100 mm/hr (8 hr; 45 mL/min)
7	0.3% GAC+10% Zeolite mixed with R165	50	1 (800 mm/year)	100 mm/hr (8 hr; 45 mL/min)
8	0.3% GAC+10% Zeolite mixed with R165	50	1 (800 mm/year)	300 mm/hr (8 hr; 135 mL/min)

6.2.2.3 Measured parameters

Concentrations of dissolved nutrients (TN, NH_4, TKN, TP), and metals (Na, K, Ca, Mg, , Pb, Cu, Zn, As, Fe, Mn, Al, Ni) in the influent and effluent were measured. Hydrocarbons (Acenaphthene, Phenanthrene and Pyrene) were measured only 2 times per test (initially at the start of the experiment and finally at the end) to avoid expensive cost of analysis. Other physical parameters (pH, turbidity, DO, EC) and DOC were measured on an hourly basis. Analytical methods used in this study are shown in Table 6.4. The variation of flow rate over monitored continuously.

Table 6.4 Analytical methods for measuring stormwater parameters

Parameter	**Measurement Method**
Heavy Metals	ICP-MS (7900 - Agilent Technologies)Agilent Technologies)
PAHs	Gas chromatography–mass spectrometry (GCMS)
Total nitrogen and NH_3	EN ISO 11905-1 and DIN 38405-9 (Photometric method)
DOC	APHA 5310B-High temperature combustion method (using a Multi N/C 3100 analyser (Analytik Jena AG))
PO4-P	Photometric method using HACH DR3900
Na, Ca, Mg	APHA 3120 using 4100 MP-AES (microwave plasma - atomic emission spectrometry)
Electrical conductivity	HACH HQ40d meter and CDC40101 probe
Turbidity	Turbidity meter
pH	HACH HQ40d meter and CDC40101 probe

6.3. Results

6.3.1 Nutrients removal

6.3.1.1 PO_4-P removal

The removal rates of PO_4-P during four columns test run at 100 mm/h are shown in Fig. 6.3a. The results show that the proportion of PO_4-P removed decreased with time. The R165 media was exhausted within 15 h (equivalent to less than 2 years rainfall) in terms of removing PO_4-P. The addition of zeolite in larger amounts (or higher percentages) improved PO_4-P removal rates extending the life of the R165 media up to more than 40 h (equivalent to 5 years rainfall) depending on the amount of zeolite used. More than 50% of the PO_4 was removed by R165 + 10 % zeolite media for up to 20 h (equivalent to 2.5 years rainfall).

6.3.1.2 NH4-N removal

The removal of NH_4-N during four columns test runs at 100 mm/h is shown in Fig. 6.3b. As in the case of PO_4-P removal, the tests show that the R165 media was exhausted within 15 h. The addition of zeolite at increasing percentages improved NH_4-N removal rates. The life of the media in the case of a 20% zeolite addition to R165 was extended to over 40 h (equivalent to 5 years rainfall).

Previous research concluded that NH_4^+ and PO_4^{3-} were simultaneously removed from an aqueous solution using zeolites (Sun et al. 2011; Wild, Kisliakova & Siegrist 1996). NH_4^+ was removed by a cation exchange reaction on the zeolite, whereas the Ca^{2+} in zeolite contributed to the removal of PO_4^{3-} due to the formation of the surface precipitate of $Ca_3(PO_4)_2$. Another explanation for the enhanced adsorption of PO_4^{3-} is bridge provided by the positively charged Ca (Ca^{2+}) between the negatively charged zeolite and PO_4^3- (Zhan et al. 2017). Cooney et al. (1999a) investigated the capability of using Australian natural zeolite to remove NH_4^+ employing a fixed-bed ion-exchange process and achieved high removal efficiencies from wastewater. Furthermore, they observed a reduction of adsorption capacity of NH_4^+ in the presence of Ca^{2+}, Mg^{2+} and K^+ because these cations competed with NH_4^+ for adsorption.

Nutrients (NH4-N and PO_4-P) removal by the 10% Zeolite+R165 media at a flow velocity of 300 mm/h was also investigated (Fig.6.4). According to the breakthrough curve, the removal capacity decreased over the time and the column became saturated within 5 h. This means that the media would only be sufficient to remove a two year equivalent pollution load under this flow velocity. This is because at higher flow rate, a larger amount of nutrients enters the column per unit time and the media's capacity to adsorb nutrients becomes more quickly exhausted. The results of the nutrients adsorption study showed that the column with R165 alone is not satisfactorily for removing both NH_4^+ and PO_4^{3-} for water discharge into a freshwater body to comply with the recommended Australian guidelines (Anzecc 2000). In contrast, the R165 column mixed with at least 10% zeolite is capable of sufficiently removing the nutrients for safe water discharge into a freshwater body (Chapter 2).

The Thomas model satisfactorily described the NH_4^+ and PO_4^{3-} breakthrough at the two flow velocities tested (Fig. 6.3 and 6.4) as shown by the high coefficient of determinations (R^2) (0.72-0.99, Tables 6.5 and 6.6). Increased percentage of zeolite in the filter medium increased the Thomas adsorption capacity for both NH_4^+ and PO_4^{3-} at the flow velocity of 100 mm/h (Table 6.5). When the flow velocity was increased, the adsorption capacity decreased for the 10% zeolite column (Table 6.5

and 6.6). This is probably because at higher flow velocity the nutrients had less time to interact with zeolite and get adsorbed (Nur et al. 2015).

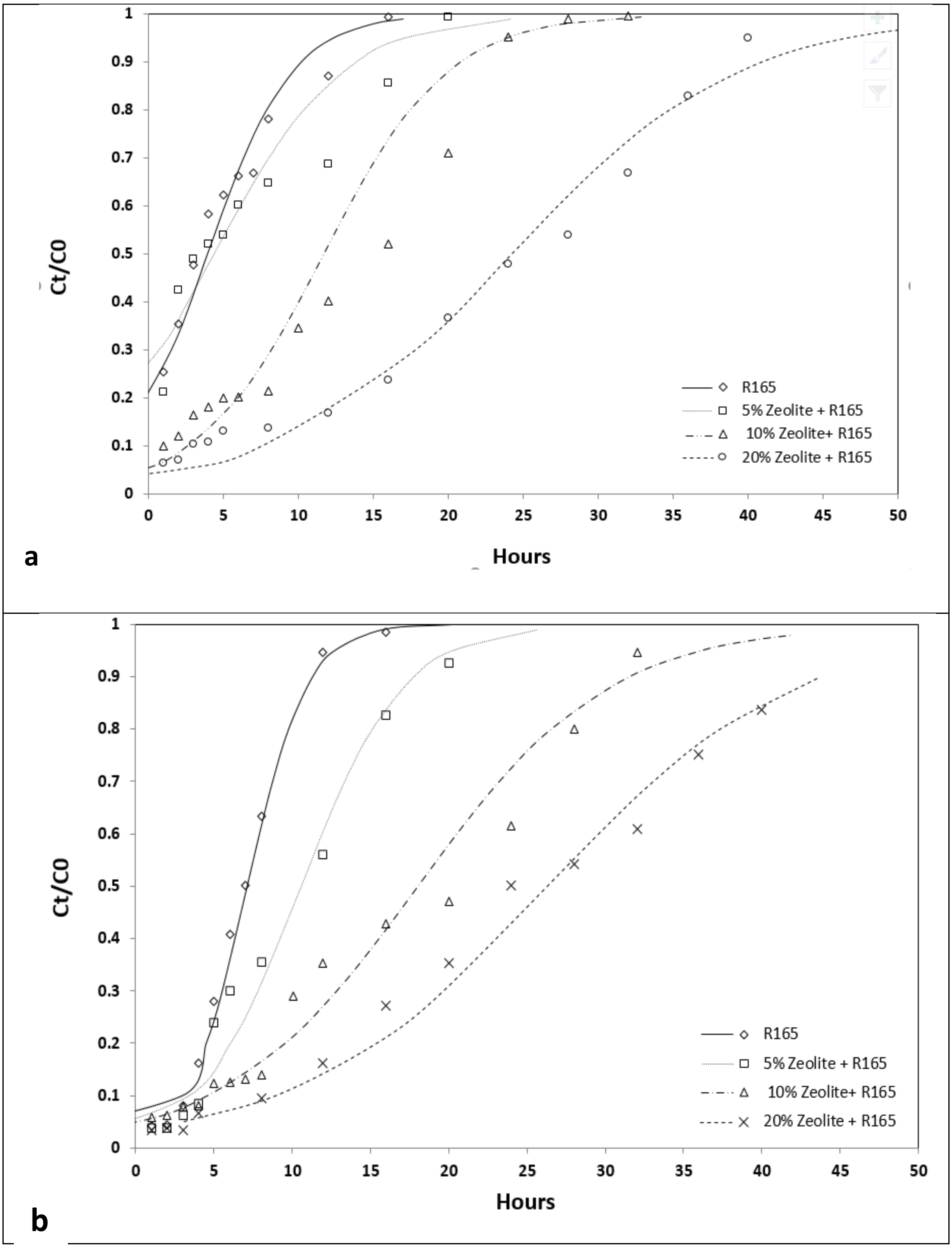

Figure 6.3 The breakthrough curve for (a) PO_4-P and (b) NH_4-N removal by four columns at a flow velocity of 100 mm/h. Lines show the Thomas model simulation.

Table 6.5 Thomas model parameters for the simulation of breakthrough curves in Fig.6.3

		Co mg/L	**M** g	**Q** mL/min	**q_o** mg/g	**K_T** mL/min.mg	**R^2**
NH_4-N	R165	0.6	1800	45	3.6	0.0098	0.93
	R165+5% Zeolite	0.6	1890	45	3.8	0.0064	0.79
	R165+10% Zeolite	0.6	1980	45	9.6	0.0067	0.95
	R165+20% Zeolite	0.6	2160	45	18.2	0.0037	0.72
PO_4-P	R165	1.5	1800	45	16.1	0.0058	0.99
	R165+5% Zeolite	1.5	1890	45	22.7	0.0034	0.92
	R165+10% Zeolite	1.5	1980	45	36.9	0.0018	0.97
	R165+20% Zeolite	1.5	2160	45	49.4	0.0014	0.98

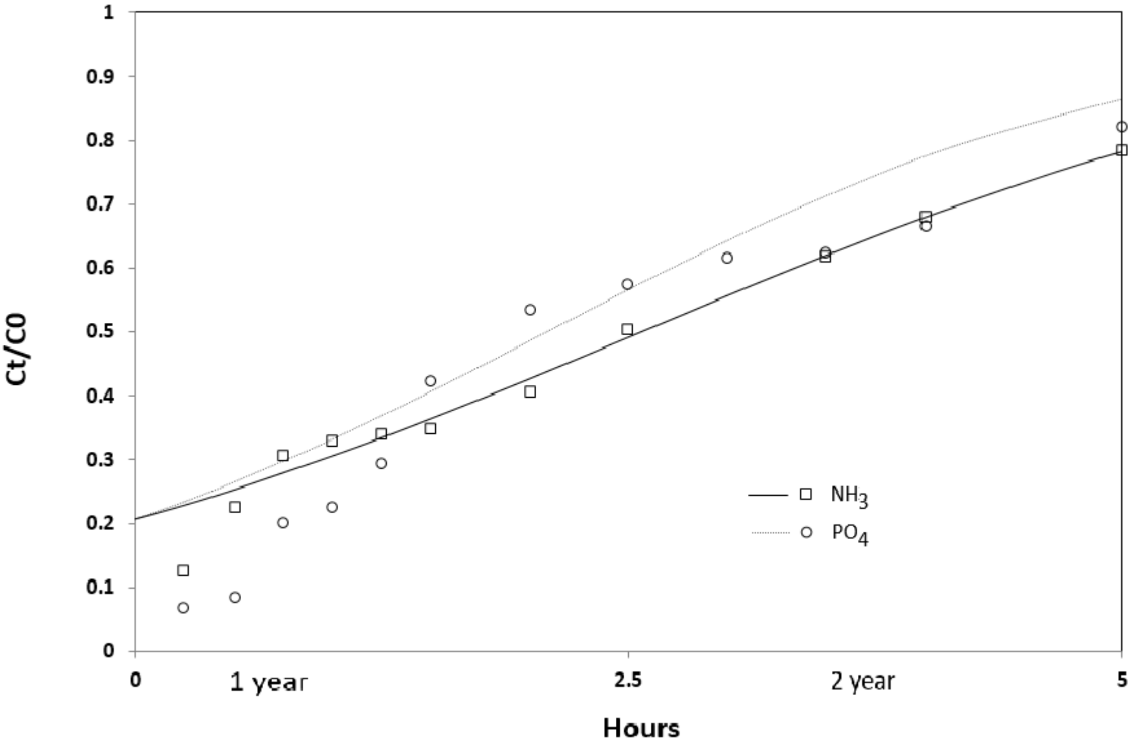

Figure 6.4 The breakthrough curves for NH_4-N and PO_4-P removals by the 10% Zeolite + R165 column test at a flow velocity of 300 mm/h. Lines show the Thomas model simulation.

Table 6.6 Thomas model parameters for the simulation of breakthrough curves in Fig.6.4

	Co **mg/L**	**M** **g**	**Q** **mL/min**	**q_o** **mg/g**	**K_T** **mL/min.mg**	**R^2**
NH_4-N	0.56	1980	135	5.8	0.0156	0.98
PO_4-P	1.2	1980	135	12.1	0.0089	0.87

Previous researchers have observed effective removal of total P (TP) by bio-filter media in laboratory scale experiments (Davis et al. 2003; Fletcher et al. 2007; Henderson, Greenway & Phillips 2007). However, they reported high variability in total N (TN) removal from the media. Hatt, Fletcher & Deletic (2009b) conducted a field scale experiment on bio-filtration filter media (soil based) and while observing effective removal of TP, reported significant variability of TN concentrations in the effluent. Furthermore, they emphasized the need to use media containing low concentrations of P to prevent possible leaching of P from the medium. In the present study, R165 contained considerable amount of P (101 mg/kg) (Table 1), however TP was not detected in the leachate when R165 was leached with distilled water. TN and NO_3-N removals by R165 were not significant and highly variable. This remained so even with the addition of zeolite to R165 (Appendix Table C.1).

Sonstrom, Clausen & Askew (2002) reported that a bio-filtration system retained 49% total suspended solids, 74% total P, 44% total Kjeldahl-N (TKN), 45% total Zn, 29% total Cu, 2% total Pb on a mass basis, and 99% faecal coliform on a concentration basis in a field study conducted at a commercial parking lot in

Connecticut, USA. In Victoria, Australia, Hatt, Fletcher & Deletic (2009a) conducted a field scale study on the removal of pollutants using bio-filters from urban run-off and stated that nutrient retention was variable, and ranged from consistent leaching to effective and reliable removal, depending on the bio-filter design. Of the pollutants, nitrogen was found to be more difficult to remove because it is highly soluble and strongly influenced by the variable wetting and drying regime that is inherent in bio-filter operation. However, they reported that average removal efficiencies of total TKN and TP were 9% and 12%, respectively. They suggested that soil-based bio-filters especially those which were low in P content were suitable in removing TP.

6.3.2 DOC removal

The concentration of DOC in the feed was 8-9 mg/L. There was only a slight reduction in the concentration of DOC in the effluent and no significant removal was observed for DOC by R165. This remained so even with the addition of zeolite (Appendix Table C.2). Even though GAC is known to remove DOC (Sounthararajah et al. 2016), there was hardly any improvement in DOC removal in the column with the addition of GAC to the media and likely because of the low GAC dosage (0.3%) used in the experiment.

6.3.3 Heavy metals removal

Heavy metals removal by R165 was good for up to 3 h (40-90% for all heavy metals) (Fig. 6.5a). After 16 h the percentages of removal reduced to 45% for Zn, 30% for Cu, 20% for Pb and less than 10% for the remainder of the heavy metals. The addition of 10% zeolite to R165 significantly increased the removal rates of most heavy metals and the life of the R165 media (Fig. 6.5b). The removal percentages of Ni, Fe, and Mn remained the lowest even after the addition of zeolite.

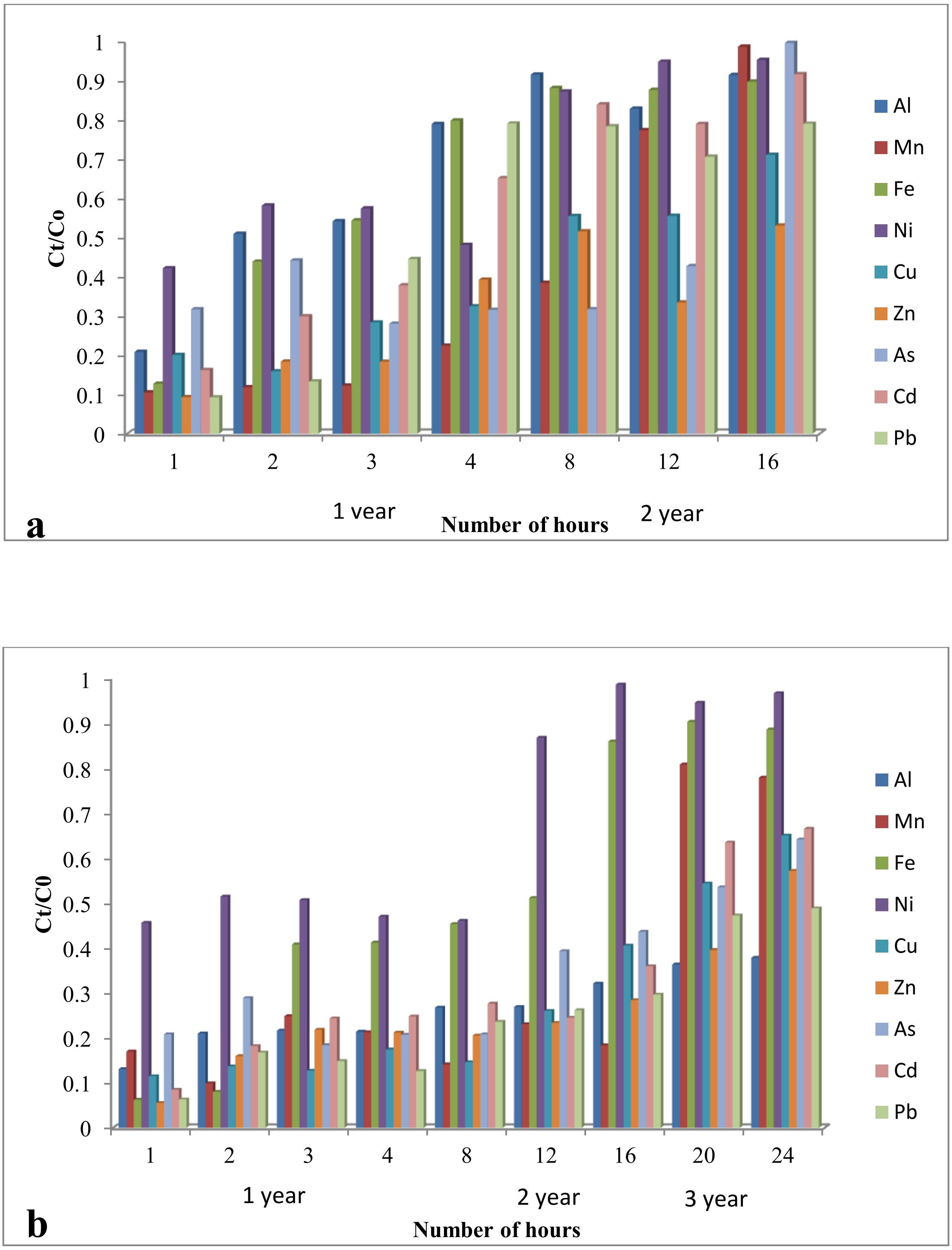

Figure 6.5 Metals removal by (a) R165 (b) R165+10% zeolite at a flow velocity of 100 mm/h.

Of the heavy metals, R165+10% zeolite had the highest removal percentages for Pb, Cu, Zn, Cd and As and the lowest for Ni, Mn and Fe (Fig. 6.5b). Pitcher, Slade & Ward (2004) conducted batch experiments using two zeolites, a synthetic zeolite and a natural mordenite to test their ability to remove dissolved heavy metals from simulated and spiked motorway stormwaters. They reported up to 42-89% reduction of heavy metals from the stormwater by mordenite and, also stated the percentage reduction order was Pb > Cu > Zn and Cd. Removal of heavy metals mainly took place by ion exchange mechanism on the zeolite and through the impurities present in natural zeolites (Ćurković, Cerjan-Stefanović & Filipan 1997). The difference in the removal of heavy metals in percent terms depend on the concentrations of the heavy metals in the stormwater and the chemical characteristics of the heavy metals. The first hydrolysis constant of the metals (M) (MOH^+ formation) and solubility product of the metal hydroxides control the adsorption affinity of the metals (Nguyen et al. 2015). The lower the first hydrolysis constant, the greater the proportion of MOH^+ which has stronger adsorption than M^{2+} among the various metal species in solution. High solubility product favours precipitation of metals, especially on the surface of the adsorbent. Of the heavy metals tested, Pb has the lowest hydrolysis constant and the highest solubility product and therefore the highest removal percentage at 24 h (Fig. 6.5b), the longest filtration time that was tested. This agrees with the results of heavy metals adsorption on other adsorption media(Nguyen et al. 2015; Sounthararajah et al. 2015b) .

The results of the heavy metals removal study show that use of R165 without additives as filter medium can remove only a one-year heavy equivalent metal load from stormwater to comply with the water quality required for safe disposal to natural waters. An addition of 10% zeolite to the medium increased the capacity of the filter to remove heavy metals and produce safe water for a period longer than two years.

6.3.4 Turbidity and conductivity removals

Fig. 6.6 shows the turbidity removal by the column experiments at 100 mm/h flow velocity. R165 reduced the turbidity by 68-78 % whereas the column of R165 mixed with 10% zeolite removed turbidity by 83-86%. When the flow rate increased (300 mm/h) in the latter column, the removal percentage decreased to 65-75%. This is due to the entry of a larger quantity of turbidity into the column per unit time.

The column containing R165 without additives and that containing R165 mixed with 10% zeolite decreased conductivity only during the first 4 h at the infiltration rate of 100 mm/h, and thereafter the turbidity remained the same as the influent solution (Appendix Table C.3). However, the reduction in conductivity was much higher in the latter column.

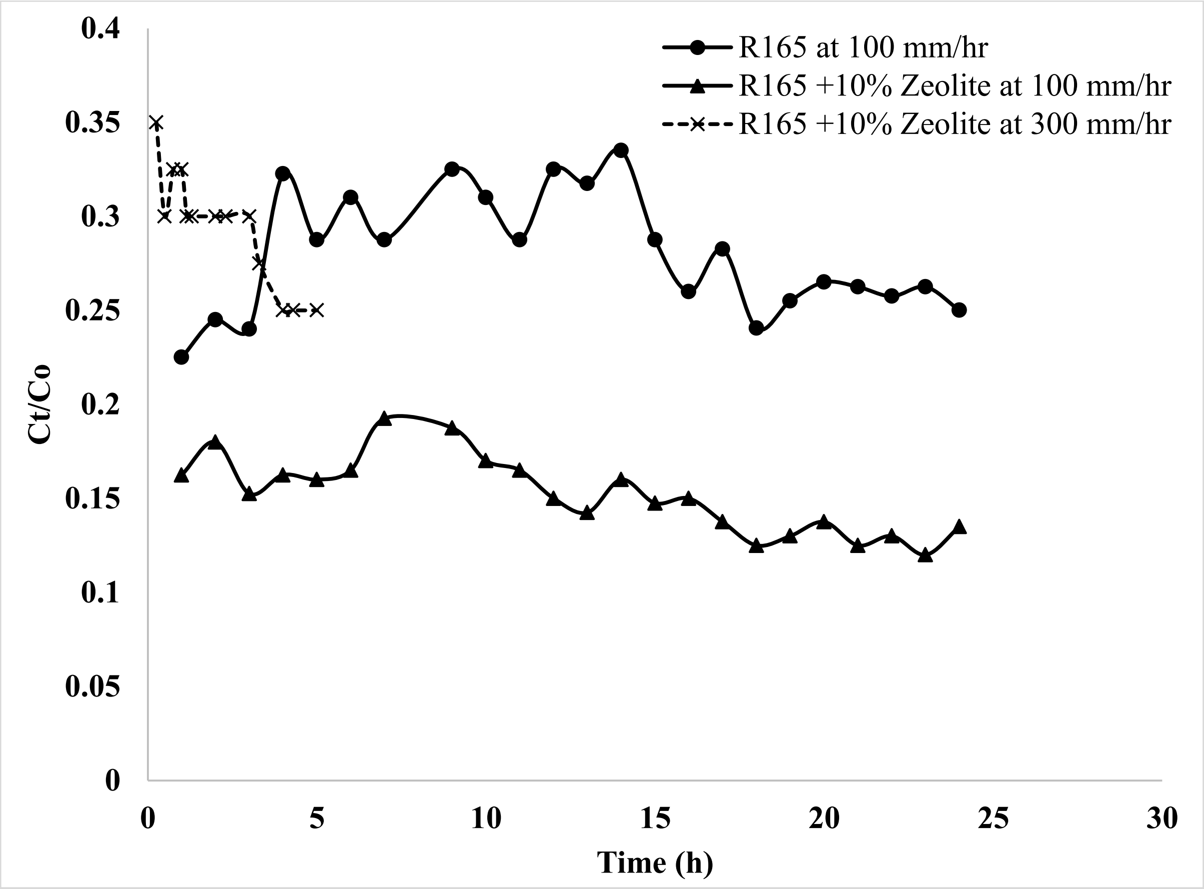

Figure 6.6 Turbidity removal by two filter columns at flow velocities of 100 and 300 mm/h

6.3.5 Polycyclic aromatic hydrocarbons (PAH) removal

PAH removal by R165 at a flow velocity of 100 mm/h was 30-99% for acenaphthene, 50-99% for phenanthrene and 50-92% for pyrene (Fig. 6.7a). The lowest removal for each PAH was, as expected, at the highest time of testing (20 h) at between 30 and 50% removal. The adsorbent medium was increasingly saturated with PAH as time progressed resulting in decrease in the available sites for further adsorption.

However, when 0.3% GAC and 10 % zeolite were mixed with R165, higher percentages of the PAHs were removed at both 100 and 300 mm/h flow velocities

(Figs 6.7 b, c). The percentage removals at 20 h for the flow velocity of 100 mm/h ranged 65 to > 99% (Fig .6.7b) compared to 30-50% in the column with only R165. Phenanthrene and pyrene were almost completely removed. The higher percentage removals at the lower flow rate compared to the higher velocity is due to a lower amount of PAH entering the filter per unit time. The higher removals of PAHs even with the addition of a very small amount of GAC to the filter media was due to the high affinity of PAHs to GAC (Eeshwarasinghe et al. 2018) and not likely to be due to adsorption onto zeolite in the filter. Preliminary batch experiments on adsorption of phenanthrene on R165, zeolite and GAC at an equilibrium phenanthrene concentration of 0.5 mg/L showed that their adsorption capacities were 0.05, 0.05 and 20 mg/g, respectively. This indicates that the adsorption capacity of GAC is nearly 400 times that of zeolite. Therefore, zeolite even with 33 times the weight of GAC (10% vs 0.3% GAC) in the filter media would not have made any significant contribution towards the removal of the PAHs. Huttenloch, Roehl & Czurda (2001) also reported that the adsorption capacity of a natural zeolite, clinoptilolite for the PAH, naphthalene was almost zero. The inability of zeolite to adsorb PAHs is due to its low degree of hydrophobicity. To overcome this problem others have modified the surface of zeolite by grafting hydrophobic organic groups such as quaternary ammonium groups and surfactants which made the modified zeolite an attractive adsorbent for removing PAHs (Lemić et al. 2007; Wołowiec et al. 2017).

The removal percentage of acenaphthene was lower than that of phenanthrene and pyrene because the hydrophobicity of acenaphthene (log Kow 3.92) was lower than the other two PAHs (phenanthrene log Kow 4.46, pyrene log Kow 5.18) (Eeshwarasinghe et al. 2018). Acenaphthene appears to progress towards saturation of the three columns faster at both flow velocities than phenanthrene and pyrene, because of its lower adsorption capacity. Media containing 0.3 % GAC +10% Zeolite+ R165 at 100 mm/h resulted in nearly 100% removal of both phenanthrene and pyrene for an estimated period of three years equivalent rainfall.

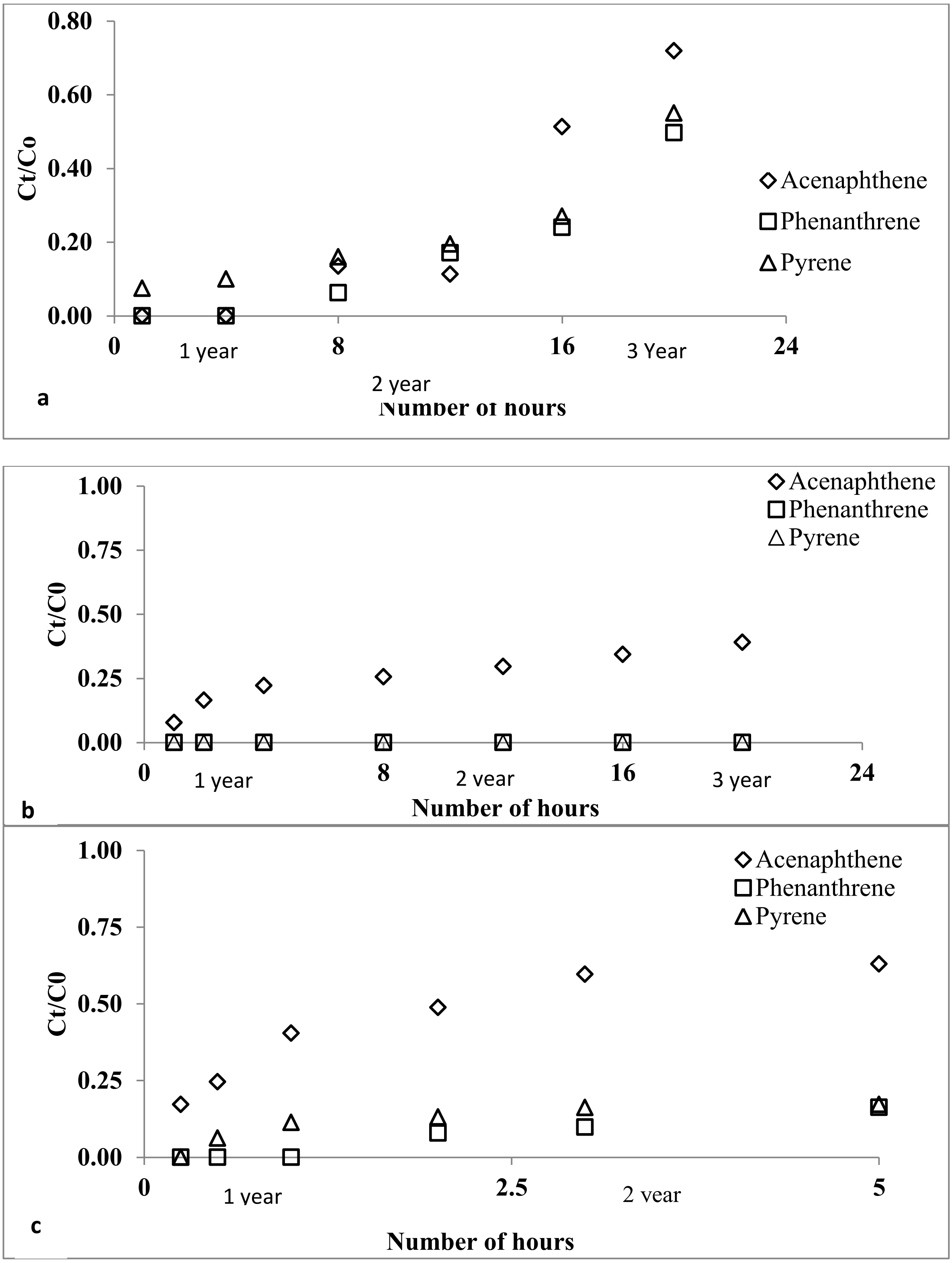

Figure 6.7 The breakthrough curve for PAH removal by the column with (a) R165 at flow velocity100 mm/h; (b) 0.3% GAC +10% Zeolite+ R165 at flow velocity 100 mm/h; (c) 0.3 % GAC +10% Zeolite+ R165 at flow velocity 300 mm/h.

6.4 Conclusions

A column with a soil-based filter medium (R165) is able to remove PO_4-P and NH_4-N for up to 8 h at a flow velocity of 100 mm/h which is a time-equivalent of one year of rainfall at Blacktown. Adding 10% of zeolite to R165 extended the column saturation period to three years. The breakthrough data for PO_4-P and NH_4-N were satisfactorily described by the Thomas model. However, the tested media were unable to remove TN and NO_3-N even with the addition of 10% zeolite, with higher variability of these pollutants in effluent concentrations. More than 50% of the majority of the nine heavy metals tested were removed in a process lasting up to 4 h in the soil-based filter. This level of removal increased to 16 h (rainfall equivalent to 2 years) when 10% zeolite was added to the filter. The column with R165 + 10% zeolite showed higher affinity towards Pb, Cu, Zn and As - regardless of their initial concentrations - and less affinity towards Ni.

The column with R165+10% zeolite removed considerable amounts of PAHs (30-50%) while a column with R165+10% zeolite+0.3% GAC removed 65- > 99% of PAHs from the influent when operated for 20 h; phenanthrene and pyrene were almost completely removed. The percentage of acenaphthene removed was smaller than phenanthrene and pyrene because the hydrophobicity of acenaphthene (log Kow 3.92) was lower than that of the other two PAHs (phenanthrene log Kow 4.46, pyrene log Kow 5.18). Overall, the results indicated that modification of the soil-based filter medium with zeolite and GAC can increase the removal of nutrients (PO_4-P, NH_4^+), heavy metals and PAHs from stormwater. This application will greatly facilitate the reduction of pollutant concentration in biofilter-treated stormwater in many stormwater harvesting projects, which are currently experiencing difficulties in achieving clean reusable water.

The present study used synthetic stormwater based on the characteristics of the stormwater which was monitored over three years at Angus Creek catchment, Blacktown City Council, Sydney, Australia. The results of this research provide useful information and guidelines for engineering professionals and councils on how biofilters should be operating over an extended period of time. In particular they provide useful information on the life span of the filter material and typically how long they can usefully remove pollutants to meet specified pollutant removal thresholds. Furthermore the research provides information on how the life of the filter can be extended by adding a small amount of adsorbent to the filter material. This provides an option for extending the life of the filter which in some circumstances is viable on a cost-effective basis. This information feeds directly into the design of biofilters that stormwater design engineers can adopt and which councils can choose to incorporate in their design guides and specifications

Chapter 7

Key findings of each chapter and recommendations for future studies

Chapter Seven

7.1. Summary of key findings

This study began with stormwater monitoring and characterisation at Angus Creek, Blacktown City Council, Sydney, the aim being to develop a new stormwater harvesting system to benefit the Blacktown International Sportspark. The main objective was to establish relationships between the concentrations of a number of critical stormwater pollutants, and rainfall. Here, the effect of rainfall intensity and duration of dry period prior to the rainfall was investigated to decide what was the best time to harvest stormwater and the appropriate treatment necessary to remove pollutants. Since first flush of stormwater is the most critical period of stormwater sampling, a simple spectroscopic technique was devised to identify the first flush. Removing selected PAHs from water was investigated by adsorption onto granular activated carbon (GAC) with the aim to identify the adoptability of adsorption using low cost-based absorbents. Doing so will enhance field-scale bio-infiltration techniques and it is discussed in Chapter 6.

7.1.1 Stormwater characterisation

First flush is the most important scenario which must be characterised for effective stormwater treatment system. Extensive amounts of pollutants can be transported during the first flush compared to the remaining stages of a storm. In urban stormwater management, first flush management is crucial since it carries a very high concentration of pollutants. The first flush constitutes 20-30% of runoff yet carries up to 80% of the pollutant load which can be very expensive treatment-wise, and lead to higher variability in treated stormwater. Generating field-scale data using a rapid methodology is subsequently very important. Detection of first flush constituents is one of the main objectives of the thesis. Stormwater monitoring was conducted from June 2016 to November 2018 at the Angus Creek catchment, Blacktown City Council, Sydney, Australia. Identifying the relationships between pollutants and rainfall is a method to design a very versatile stormwater harvesting strategy. Similarly, understanding the relationship between dry weather periods and pollutant build up in a particular catchment zone, may help modelling. Specifically, it helps to predict the nature of expected pollutant load in various rainfall events depending on the number of dry days.

The UV spectroscopy measurements on the stormwater samples revealed changes in the spectrum over time during runoff. In each rainfall event, the UV spectrum produced two sets of spectral groups that intersected each other at wavelengths between 225 and 230 nm. The intersect which is called the isosbestic point indicates the end of the first flush. This information was exploited to separate the first flush from the remaining clean flush for DOC and for pollutants behaving similarly to it. Results indicated the great adaptability of this method to develop an on-site rapid test to capture the first flush.

7.1.2 Laboratory adsorption experiments

Mostly anthropogenic activities and some naturally occurring activities release significant amounts of PAHs into the environment. PAHs are regarded as widespread and persistent organic compounds which can be accumulated to dangerous levels in the environment over time. There are huge concerns about the health of the ecosystem and that of humanity, given the ubiquitous nature and geographical reach of organic pollutants. There are several treatment methods to remove PAHs from aqueous solutions. However, most of the methods studied are unable to completely remove PAHs from their source and can consequently generate dangerous metabolics. Of these methods, adsorption was found to be a simple and most effective one with less maintenance for removing PAHs. Five common PAHs chosen for the experiments were naphthalene, acenaphthylene, acenaphthylene, fluorene and phenanthrene. GAC was used as the adsorbent and batch equilibrium, kinetics and fixed columns experiments were conducted to investigate the adsorption capacity of PAHs on to GAC. PAHs measured using the UV-VIS technique was found to be a simple, rapid and low-cost method to measure PAHs. Adsorption experiments on the five PAHs showed that GAC can effectively remove them from water. Batch kinetics adsorption was satisfactorily described by PFO, PSO, and Elovich models, with the PFO model being the best of the three. Weber and Morris diffusion model produced two distinctive linear plots for the amount adsorbed vs square root of time, indicating two consecutive intra-particle diffusion rates of adsorption, probably one through the mesopores and the other through the micropores of GAC.

Batch equilibrium adsorption was satisfactorily described by Freundlich, Langmuir, and Dubinin–Radushkevich models, with the data fit being the best for the Freundlich version, indicating heterogeneous adsorption. The Langmuir adsorption affinity constants for the PAHs were in the reverse order as the rates of adsorption depended mainly on the hydrophobicity of the PAHs. The energy of adsorption calculated from the Dubinin–Radushkevich model confirmed the physical nature of adsorption suggested by the PFO kinetic model. Fixed-bed columns containing 2% GAC and 98% sand (by weight) removed substantial amounts of PAHs. The breakthrough curves were successfully simulated by the Thomas model and indicated that a small amount of GAC can sufficiently remove PAHs from stormwater. The Thomas adsorption capacities had the same trend for the PAHs as the Langmuir adsorption capacities, though the Thomas values were lower.

Both PAHs and heavy metals are found in stormwater runoff. However, very few studies have dealt with the simultaneous removal of both of these pollutants. Simultaneous removal is important because PAHs' and heavy metals' co-occurrence is very common in the environment. Simultaneous adsorption of PAHs and heavy metals has not been studied in detail on activated carbon (AC) adsorbent, which is one of the commonly available and reliable adsorbents with adsorptive capacity. In solutions containing both PAHs (acenaphthylene or phenanthrene) and heavy metals (Cd, Cu or Zn), the adsorptive removal of PAHs using GAC was higher than those of heavy metals, even with the latter at 20 times higher concentration. The adsorptive capacities of both PAHs and heavy metals were reduced in the presence of both compared to their capacities when they were present individually. The Langmuir adsorption capacity for both PAHs decreased when the concentration of metals increased, the effect being in the order Cu > Zn > Cd. The kinetic adsorption data fitted to the Weber and Morris plots indicating intra-particle diffusion of both PAHs and heavy metals into the mesopores and micropores in GAC.

7.1.3 Column experiments with bio-retention media

In Chapter 3, important characteristics of stormwater were determined from field samplings of stormwater during several rainfall events at Blacktown

International Sportspark. GAC adsorbent was found to effectively remove PAHs and heavy metals. At present, bio-retention (bio-filter) basins with natural media are widely used in Australia. However, application of bio-filters is found to be less reliable and highly variable when treating stormwater. Chapter 6 evaluated the performance of R165, a soil medium proposed for use in Blacktown City Council's bioretention basins in New South Wales bio retention basins to remove targeted pollutants. In view of improving the performance of R165, other filter media such as zeolite and granular activated carbon (GAC) in small proportions were incorporated with R165.

Columns with bio-retention medium (R165) can remove PO_4-P and NH_3-N for up to 8 hours at a flow velocity of 100 mm/hr (which is a time-equivalent of one year of rainfall at Blacktown). An addition of 10% of zeolite to R165 extended the column saturation period up to three times higher (which is a time-equivalent of four years of rainfall at Blacktown). However, the tested columns were unable to remove TN even with 10% of zeolite, with higher variability of TN in effluent concentrations. Most of the heavy metals were removed by R165 alone, however, the column became saturated within 8 hours (rainfall equivalent to one year). The column with R165+10% zeolite showed higher affinity to Pb, Cu, Zn and As regardless of their initial concentrations. Less affinity was shown towards Ni. Meanwhile the column with R165+10% zeolite increased the column saturation time from 8 hours with only R165 to 36 hours with zeolite addition.

The column with R165+10% zeolite removed considerable amounts of PAHs whereas the column with R165+10% zeolite + 0.3% GAC removed 90% to 100% of PAHs from the influent. Overall, the results indicated that modification of the sand-based bio-retention medium with small quantities of zeolite and GAC increased the removal of nutrients (PO-P, NH4), heavy metals and PAHs from stormwater. This application will greatly facilitate the reduction of pollutant concentration in stormwater. Many stormwater harvesting projects are currently experiencing difficulties in producing reliable output due to higher variability of the stormwater. A stormwater treatment system has to deal with larger volumes of stormwater all at once. Also the contact time during the filtration process is much less than the laboratory experiment. Technically advanced treatment processes are not economically viable for most stormwater managers and institutions to deal with. Furthermore these systems demand high levels of technical expertise and constant maintenance.

The methodology used in this chapter is adsorption and a very passive treatment method which needs less operational requirements and maintenance. As well the bio-retention treatment systems are very popular among water treatment professionals working for urban councils. GAC and zeolite are easily available low-cost adsorbents which can remove a lot of pollutants at the same time. Zeolite's presence may help with the clogging of a bio-retention system but more experimental data are required to confirm this assertion. Mostly, bio-retention systems receive runoff from car parks, roads and commercial areas, a situation which contributes to the contamination of PAHs and certain heavy metals. The significance of these pollutants in the stormwater and the rate at which they are increasing reflects the rapid growth of the world's population and what it demands. Outcomes of Chapters 4, 5 and 6 established the advantage of using GAC and zeolite which identified more efficient adsorbent for removing PAHs, heavy metals and certain nutrients present in stormwater.

7.2 Recommendations

As discussed in the early chapters the major drawback of current stormwater treatment is the lack of consistency in producing purified stormwater to the required standards that users expect. Secondly, bio-retention systems used for treating stormwater fail to operate due to clogging which can occur within a very short period of time. The following serious problems have to be taken into account: (i) pollutant loads are highly variable in receiving waters; (ii) a large quantity of water is needed to be treated and this increases the flow velocity into the bio-retention systems; and (iii) the required area of land and operational costs can be obstacles. At present, although local councils may accept stormwater harvesting systems that have been designed for their own circumstances, the following recommendations are suggested to mitigate the above-mentioned problems when establishing stormwater treatment systems. Most treatment systems are composed of physical treatment systems such as gross pollutant litter basket, sand filters, grassed swales and sediment ponds, then secondary treatment systems such as swales, infiltration trenches, porous paving and bio-retention systems and tertiary or polishing treatment systems (bio-retention/ bio-infiltration systems/high rate filtration and wetlands). Usually the primary treatment system is followed by the secondary or tertiary treatment system, which functions to remove sediments and trap other pollutants via the filtration method.

Designing small-scale bio-retention/wetland systems for a particular area based on the nature of runoff followed by a final water harvesting system can produce much cleaner water. Categorising them into small groups based on the common characteristics will help to treat the water more specifically and meaningfully. As illustrated in Fig. 7.1 a residential area can have a couple of small bioretention/wetland operations per 10 houses in a residential scheme. Water generated from residential areas may be contaminated with biological pathogens. In this case the treatment system should be composed of a pathogen-removing method such as UV treatment backed up by physical filtration systems. Treatment systems which can adsorb additional amounts of nutrients must be designed and implemented. Industrial areas and commercial areas contain large amounts of PAHs and heavy metals from their runoff and they have to be urgently removed. Locations prone to erosion must have a more capable physical treatment system that can trap more sediments and particles.

Even though most of these treatment systems are currently operating, creating more such small-scale treatment systems will reduce the load that has to be managed by the final step of bio-retention treatment systems. Operational, functional and maintenance times and the costs of stormwater harvesting schemes can be reduced. Early removal of particles can prevent unexpected clogging of the media of a bio-retention system. Identifying site-specific characteristics and systems by generating a lot of meaningful data is vital for easier management of the harvesting system. Chapter 3 discussed several relationships between rainfall and pollutants, pollutants build-up and number of dry days. This should be addressed in more detail to understand the pollutant build-up and wash-off principles of particular catchments.

Field-scale investigation is required to test the capacity of biofilters' media mixed with various low-cost adsorbents such as pine needles, saw dust, charcoal, biochar, almond nut shells, coconut shells, orange peel, and agricultural waste. Importantly, spent filter media is currently sent to landfill at considerable cost. Through accelerated column tests and media characterisation, it is important to develop a guideline for councils to safely transform the spent media into a useful product to avoid expensive and ruinous landfill disposal.

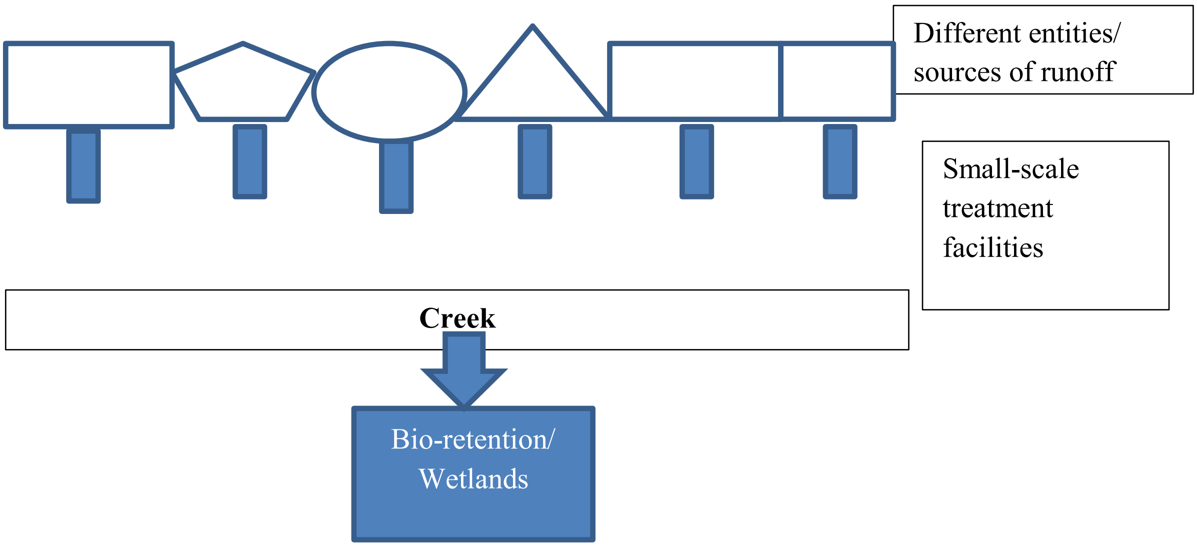

Figure 7.1 Schematic diagram of proposed small-scale treatment systems

I strongly believe that the following recommendations, if implemented will improve future research projects on remediation of water:

1. It is necessary to have improved sampling techniques to capture more diverse storm events. The major drawback of the present study was the lack of automated sampling methodology which automatically operates according to the storm run-off base flow of the creek. The study failed to capture many storm events, and also the important first flush of events which occurred during after-work hours, weekends and holidays because staff were not available to collect the required samples. Therefore, a **better automated sampler with a sensor** is required in future studies. It is very important to collect more representative samples from the start through to the end of a storm. More storm events with more samples are necessary to better understand pollutant accumulation and transport in the catchment. Additionally, having more data will help to apply mathematical models that can explain the trends and patterns of the catchment with respect to various storm events and hydrology.
2. **Accurate rainfall (every minute**) records during the storm events are necessary in future studies. Also, accurate dry weather periods must be documented prior to every sampling event. These data will help to obtain more reliable and accurate relationships between pollutant load and rainfall, and also between dry weather duration and pollution load.
3. The study revealed that the microbiological component is much higher and it should be closely monitored during future studies. Recognition of pathogenic microorganisms likely to be present is an advantage for proper stormwater management. The presence of waterborne pathogens, human biomarkers and faecal indicators must be analysed in future research.

4. Future studies can focus on field-scale approaches to how stormwater treatment facilities function, in order to further test the UV/VIS technique when differentiating the first flush from what happens next.

References

Adams, B.J. 2000, 'Urban stormwater management planning with analytical probabilistic models'.

Ahmaruzzaman, M. 2011, 'Industrial wastes as low-cost potential adsorbents for the treatment of wastewater laden with heavy metals', *Advances in colloid and interface science*, vol. 166, no. 1-2, pp. 36-59.

Aissaoui, J., Kacem, M., Dubujet, P. & Mgaidi, A. 2017, 'Study of multicompound sorption of Lead and Pyrene on a reconstituted soil: batch and fixed bed column tests', *Soil and Sediment Contamination: An International Journal*, vol. 26, no. 4, pp. 404-25.

Alade, A.O., Amuda, O.S. & Ibrahim, A.O. 2012, 'Isothermal studies of adsorption of acenaphthene from aqueous solution onto activated carbon produced from rice (Oryza sativa) husk', *Desalination and Water Treatment*, vol. 46, no. 1-3, pp. 87-95.

Alley, W.M. 1981, 'Estimation of impervious-area Washoff Parameters', *Water Resources Research*, vol. 17, no. 4, pp. 1161-6.

Alley, W.M. & Smith, P.E. 1981, 'Estimation of accumulation parameters for urban runoff quality modeling', *Water resources research*, vol. 17, no. 6, pp. 1657-64.

Altmann, J., Massa, L., Sperlich, A., Gnirss, R. & Jekel, M. 2016, 'UV254 absorbance as real-time monitoring and control parameter for micropollutant removal in advanced wastewater treatment with powdered activated carbon', *Water research*, vol. 94, pp. 240-5.

Ania, C., Cabal, B., Pevida, C., Arenillas, A., Parra, J., Rubiera, F. & Pis, J. 2007, 'Removal of naphthalene from aqueous solution on chemically modified activated carbons', *Water research*, vol. 41, no. 2, pp. 333-40.

Anzecc, A. 2000, 'Australian and New Zealand guidelines for fresh and marine water quality', *Australian and New Zealand Environment and Conservation Council and Agriculture and Resource Management Council of Australia and New Zealand, Canberra*, pp. 1-103.

Aryal, R., Beecham, S., Vigneswaran, S., Kandasamy, J. & Naidu, R. 2013, 'Spatial variation of polycyclic aromatic hydrocarbons and equivalent toxicity in Sydney Harbour, Australia', *Journal of Water and Climate Change*, vol. 4, no. 4, pp. 364-72.

Aryal, R., Chong, M.N., Beecham, S. & Mainali, B. 2017, 'Identifying the first flush in stormwater runoff using UV spectroscopy', *Desalination and Water Treatment*, vol. 96, pp. 231-6.

Aryal, R., Furumai, H., Nakajima, F., Beecham, S. & Lee, B.K. 2015, 'Analysis of the built-up processes for volatile organics and heavy metals in suspended solids from road run-off', *Desalination and Water Treatment*, vol. 54, no. 4-5, pp. 1254-9.

Aryal, R., Furumai, H., Nakajima, F. & Jinadasa, H. 2007, 'The role of inter-event time definition and recovery of initial/depression loss for the accuracy in quantitative simulations of highway runoff', *Urban Water Journal*, vol. 4, no. 1, pp. 53-8.

Aryal, R., Grinham, A. & Beecham, S. 2014, 'Tracking inflows in Lake Wivenhoe during a major flood using optical spectroscopy', *Water*, vol. 6, no. 8, pp. 2339-52.

Aryal, R., Vigneswaran, S. & Kandasamy, J. 2011, 'Application of Ultraviolet (UV) spectrophotometry in the assessment of membrane bioreactor performance for monitoring water and wastewater treatment', *Applied Spectroscopy*, vol. 65, no. 2, pp. 227-32.

Aryal, R.K., Furumai, H., Nakajima, F. & Boller, M. 2006a, 'Characteristics of particle-associated PAHs in a first flush of a highway runoff', *Water science and technology*, vol. 53, no. 2, pp. 245-51.

Aryal, R.K., Furumai, H., Nakajima, F. & Boller, M. 2006b, 'Characteristics of particle-associated PAHs in a first flush of a highway runoff', *Water Science & Technology*, vol. 53, no. 2, pp. 245-50.

Aryal, R.K., Jinadasa, H.K.P.K., Furumai, H. & Nakajima, F. 2005, 'A long-term suspended solids runoff simulation in a highway drainage system', *Water Science and Technology*, Article, vol. 52, pp. 159-67, <https://www.scopus.com/inward/record.uri?eid=2-s2.0-27244438014&partnerID=40&md5=ab48f48ed4c25cf20eb090cabc0912b5>.

Aryal, R.K. & Lee, B.K. 2009, 'Characteristics of suspended solids and micropollutants in first-flush highway runoff', *Water, Air, and Soil Pollution: Focus*, vol. 9, no. 5-6, pp. 339-46.

Aryal, R.K., Murakami, M., Furumai, H., Nakajima, F. & Jinadasa, H.K.P.K. 2006, 'Prolonged deposition of heavy metals in infiltration facilities and its possible threat to groundwater contamination', *Water Science & Technology*, vol. 54, no. 6-7, pp. 205-12.

Awad, J., Fisk, C.A., Cox, J.W., Anderson, S.J. & van Leeuwen, J. 2018, 'Modelling of THM formation potential and DOM removal based on drinking water catchment characteristics', *Science of The Total Environment*, vol. 635, pp. 761-8.

Awoyemi, A. 2011, 'Understanding the adsorption of polycyclic aromatic hydrocarbons from aqueous phase onto activated carbon'.

Baccar, R., Bouzid, J., Feki, M. & Montiel, A. 2009, 'Preparation of activated carbon from Tunisian olive-waste cakes and its application for adsorption of heavy metal ions', *Journal of Hazardous Materials*, vol. 162, no. 2-3, pp. 1522-9.

Bach, P.M., McCarthy, D.T. & Deletic, A. 2010, 'Redefining the stormwater first flush phenomenon', *Water research*, vol. 44, no. 8, pp. 2487-98.

Bailey, S.E., Olin, T.J., Bricka, R.M. & Adrian, D.D. 1999, 'A review of potentially low-cost sorbents for heavy metals', *Water research*, vol. 33, no. 11, pp. 2469-79.

Barber, S.A. 1995, *Soil nutrient bioavailability: a mechanistic approach*, John Wiley & Sons.

Barbosa, A.E., Fernandes, J.N. & David, L.M. 2012, 'Key issues for sustainable urban stormwater management', *Water research*, vol. 46, no. 20, pp. 6787-98.

Becouze-Lareure, C., Dembélé, A., Coquery, M., Cren-Olivé, C. & Bertrand-Krajewski, J.L. 2019, 'Assessment of 34 dissolved and particulate organic and metallic micropollutants discharged at the outlet of two contrasted urban catchments', *Science of the Total Environment*, vol. 651, pp. 1810-8.

Bhatnagar, A. & Sillanpää, M. 2011, 'A review of emerging adsorbents for nitrate removal from water', *Chemical Engineering Journal*, vol. 168, no. 2, pp. 493-504.

Birch, G.F., Matthai, C., Fazeli, M.S. & Suh, J.Y. 2004, 'Efficiency of a constructed wetland in removing contaminants from stormwater', *Wetlands*, vol. 24, no. 2, p. 459.

Boving, T.B. & Zhang, W. 2004, 'Removal of aqueous-phase polynuclear aromatic hydrocarbons using aspen wood fibers', *Chemosphere*, vol. 54, no. 7, pp. 831-9.

Brannvall, E., Mažeikienė, A. & Valentukevičienė, M. 2006, 'Experimental research on sorption of petroleum products from water by natural clinoptilolite and vermiculite', *Geologija*, no. 56, pp. 5-12.

Bratieres, K., Fletcher, T.D., Deletic, A. & Zinger, Y. 2008, 'Nutrient and sediment removal by stormwater biofilters: A large-scale design optimisation study', *Water research*, vol. 42, no. 14, pp. 3930-40.

Brown, J.N. & Peake, B.M. 2006, 'Sources of heavy metals and polycyclic aromatic hydrocarbons in urban stormwater runoff', *Science of the total environment*, vol. 359, no. 1-3, pp. 145-55.

Brown, R. & Hunt, W. 2009, 'Bioretention performance in the upper coastal plain of North Carolina', *Low Impact Development for Urban Ecosystem and Habitat Protection*, pp. 1-10.

Brown, R. & Hunt, W. 2011, 'Underdrain configuration to enhance bioretention exfiltration to reduce pollutant loads', *Journal of Environmental Engineering*, vol. 137, no. 11, pp. 1082-91.

Brown, R.A. & Hunt, W.F. 2012, 'Improving bioretention/biofiltration performance with restorative maintenance', *Water Science and Technology*, vol. 65, no. 2, pp. 361-7.

Budai, P. & Clement, A. 2011, 'Refinement of national-scale heavy metal load estimations in road runoff based on field measurements', *Transportation Research Part D: Transport and Environment*, vol. 16, no. 3, pp. 244-50.

Cahill, R. & Lund, J. 2013, 'Residential water conservation in Australia and California', *Journal of Water Resources Planning and Management*, vol. 139, no. 1, pp. 117-21.

Chang, C.-F., Chang, C.-Y., Chen, K.-H., Tsai, W.-T., Shie, J.-L. & Chen, Y.-H. 2004, 'Adsorption of naphthalene on zeolite from aqueous solution', *Journal of colloid and Interface Science*, vol. 277, no. 1, pp. 29-34.

Chen, B., Zhou, D. & Zhu, L. 2008, 'Transitional adsorption and partition of nonpolar and polar aromatic contaminants by biochars of pine needles with different pyrolytic temperatures', *Environmental science & technology*, vol. 42, no. 14, pp. 5137-43.

Chen, J., Zhu, D. & Sun, C. 2007, 'Effect of heavy metals on the sorption of hydrophobic organic compounds to wood charcoal', *Environmental science & technology*, vol. 41, no. 7, pp. 2536-41.

Chen, J.P. 2012, *Decontamination of heavy metals: processes, mechanisms, and applications*, Crc Press.

Chen, X., Peltier, E., Sturm, B.S. & Young, C.B. 2013, 'Nitrogen removal and nitrifying and denitrifying bacteria quantification in a stormwater bioretention system', *Water Research*, vol. 47, no. 4, pp. 1691-700.

Cimino, G., Cappello, R., Caristi, C. & Toscano, G. 2005, 'Characterization of carbons from olive cake by sorption of wastewater pollutants', *Chemosphere*, vol. 61, no. 7, pp. 947-55.

Cooney, E.L., Booker, N.A., Shallcross, D.C. & Stevens, G.W. 1999a, 'Ammonia removal from wastewaters using natural Australian zeolite. I. Characterization of the zeolite', *Separation science and technology*, vol. 34, no. 12, pp. 2307-27.

Cooney, E.L., Booker, N.A., Shallcross, D.C. & Stevens, G.W. 1999b, 'Ammonia removal from wastewaters using natural Australian zeolite. II. Pilot-scale study using continuous packed column process', *Separation Science and Technology*, vol. 34, no. 14, pp. 2741-60.

Cooper, W.J., Nickelsen, M.G., Green, R.V. & Mezyk, S.P. 2002, 'The removal of naphthalene from aqueous solutions using high-energy electron beam irradiation', *Radiation Physics and chemistry*, vol. 65, no. 4-5, pp. 571-7.

Crisafully, R., Milhome, M.A.L., Cavalcante, R.M., Silveira, E.R., De Keukeleire, D. & Nascimento, R.F. 2008, 'Removal of some polycyclic aromatic hydrocarbons from petrochemical wastewater using low-cost adsorbents of natural origin', *Bioresource technology*, vol. 99, no. 10, pp. 4515-9.

Ćurković, L., Cerjan-Stefanović, Š. & Filipan, T. 1997, 'Metal ion exchange by natural and modified zeolites', *Water research*, vol. 31, no. 6, pp. 1379-82.

Dastgheib, S.A. & Rockstraw, D.A. 2001, 'Pecan shell activated carbon: synthesis, characterization, and application for the removal of copper from aqueous solution', *Carbon*, vol. 39, no. 12, pp. 1849-55.

Davis, A.P. 2007, 'Field performance of bioretention: Water quality', *Environmental Engineering Science*, vol. 24, no. 8, pp. 1048-64.

Davis, A.P., Shokouhian, M. & Ni, S. 2001, 'Loading estimates of lead, copper, cadmium, and zinc in urban runoff from specific sources', *Chemosphere*, vol. 44, no. 5, pp. 997-1009.

Davis, A.P., Shokouhian, M., Sharma, H., Minami, C. & Winogradoff, D. 2003, 'Water quality improvement through bioretention: Lead, copper, and zinc removal', *Water Environment Research*, vol. 75, no. 1, pp. 73-82.

Davis, B. & Birch, G. 2009, 'Catchment-wide assessment of the cost-effectiveness of stormwater remediation measures in urban areas', *Environmental Science & Policy*, vol. 12, no. 1, pp. 84-91.

Davis, J.A. 1984, 'Complexation of trace metals by adsorbed natural organic matter', *Geochimica et Cosmochimica acta*, vol. 48, no. 4, pp. 679-91.

De-Bashan, L.E. & Bashan, Y. 2004, 'Recent advances in removing phosphorus from wastewater and its future use as fertilizer (1997–2003)', *Water research*, vol. 38, no. 19, pp. 4222-46.

DeBusk, K. & Wynn, T. 2011, 'Storm-water bioretention for runoff quality and quantity mitigation', *Journal of Environmental Engineering*, vol. 137, no. 9, pp. 800-8.

Deletic, A., McCarthy, D., Chandresena, G., Li, Y., Hatt, B., Payne, E., Zhang, K., Henry, R., Kolotelo, P. & Randjelovic, A. 2014, 'Biofilters and wetlands for stormwater treatment and harvesting', *Cooperative Research Centre for Water Sensitive Cities, Monash University, Melbourne*, p. 67.

Denman, L., May, P. & Breen, P. 2006, 'An investigation of the potential to use street trees and their root zone soils to remove nitrogen from urban stormwater', *Australasian Journal of Water Resources*, vol. 10, no. 3, pp. 303-11.

Dietz, M.E. 2007, 'Low impact development practices: A review of current research and recommendations for future directions', *Water, air, and soil pollution*, vol. 186, no. 1-4, pp. 351-63.

Dillon, P. & Ellis, D. 2004, 'Australian water conservation and reuse research program', *Water(Australia)*, vol. 31, no. 1, pp. 36-9.

Dong, L., Hou, L.a., Wang, Z., Gu, P., Chen, G. & Jiang, R. 2018, 'A new function of spent activated carbon in BAC process: removing heavy metals by ion exchange mechanism', *Journal of hazardous materials*, vol. 359, pp. 76-84.

Douben, P.E. 2003, *PAHs: an ecotoxicological perspective*, John Wiley & Sons.

Duodu, G.O., Ogogo, K.N., Mummullage, S., Harden, F., Goonetilleke, A. & Ayoko, G.A. 2017, 'Source apportionment and risk assessment of PAHs in Brisbane River sediment, Australia', *Ecological Indicators*, vol. 73, pp. 784-99.

Eeshwarasinghe, D., Loganathan, P., Kalaruban, M., Sounthararajah, D.P., Kandasamy, J. & Vigneswaran, S. 2018, 'Removing polycyclic aromatic hydrocarbons from water using granular activated carbon: kinetic and equilibrium adsorption studies', *Environmental Science and Pollution Research*, vol. 25, no. 14, pp. 13511-24.

El Nemr, A., Abdelwahab, O., El-Sikaily, A. & Khaled, A. 2009, 'Removal of direct blue-86 from aqueous solution by new activated carbon developed from orange peel', *Journal of hazardous materials*, vol. 161, no. 1, pp. 102-10.

Erto, A., Di Natale, F., Musmarra, D. & Lancia, A. 2015, 'Modeling of single and competitive adsorption of cadmium and zinc onto activated carbon', *Adsorption*, vol. 21, no. 8, pp. 611-21.

Fabris, R., Braun, K., Morran, J.Y., Ho, L. & Drikas, M. 2015, 'The evolution of organic character in a drought-and flood-impacted water source and the relationship with drinking water treatment', *Journal of Water and Climate Change*, vol. 6, no. 3, pp. 401-13.

Fletcher, T.D., Mitchell, V., Deletic, A., Ladson, T.R. & Seven, A. 2007, 'Is stormwater harvesting beneficial to urban waterway environmental flows?', *Water Science and Technology*, vol. 55, no. 4, pp. 265-72.

Furumai, H. 2008, 'Rainwater and reclaimed wastewater for sustainable urban water use', *Physics and Chemistry of the Earth, Parts A/B/C*, vol. 33, no. 5, pp. 340-6.

Gachanja, A. 2005a, 'Polycyclic aromatic hydrocarbons determination and environmental application in: Encyclopedia of Analytical Science', USA: Elsevier Science Ltd.

Gachanja, A.N. 2005b, 'POLYCYCLIC AROMATIC HYDROCARBONS | Determination A2 - Worsfold, Paul', in A. Townshend & C. Poole (eds), *Encyclopedia of Analytical Science (Second Edition)*, Elsevier, Oxford, pp. 225-34.

Ge, X., Wu, Z., Wu, Z., Yan, Y., Cravotto, G. & Ye, B.-C. 2016, 'Enhanced PAHs adsorption using iron-modified coal-based activated carbon via microwave radiation', *Journal of the Taiwan Institute of Chemical Engineers*, vol. 64, pp. 235-43.

Ghane, E., Ranaivoson, A.Z., Feyereisen, G.W., Rosen, C.J. & Moncrief, J.F. 2016, 'Comparison of contaminant transport in agricultural drainage water and urban stormwater runoff', *PloS one*, vol. 11, no. 12.

GHOSH, K. & Schnitzer, M. 1979, 'UV and visible absorption spectroscopic investigations in relation to macromolecular characteristics of humic substances', *Journal of Soil Science*, vol. 30, no. 4, pp. 735-45.

Gil, K. & Kim, T.-w. 2012, 'Determination of first flush criteria from an urban residential area and a transportation land-use area', *Desalination and Water Treatment*, vol. 40, no. 1-3, pp. 309-18.

Goldberg, S., Tabatabai, M., Sparks, D., Al-Amoodi, L. & Dick, W. 2005, 'Equations and models describing adsorption processes in soils', *Soil Science Society of America Book Series*, vol. 8, p. 489.

Gottschalk, C., Libra, J.A. & Saupe, A. 2009, *Ozonation of water and waste water: A practical guide to understanding ozone and its applications*, John Wiley & Sons.

Graves, G.A., Wan, Y. & Fike, D.L. 2004, 'Water quality characteristics of storm water from major land uses in South Florida', *Journal of the American Water Resources Association*, vol. 40, no. 6, pp. 1405-19.

Gupta, V.K., Carrott, P., Ribeiro Carrott, M. & Suhas 2009, 'Low-cost adsorbents: growing approach to wastewater treatment—a review', *Critical reviews in environmental science and technology*, vol. 39, no. 10, pp. 783-842.

Gustafson, K.E. & Dickhut, R.M. 1994, 'Molecular diffusivity of polycyclic aromatic hydrocarbons in aqueous solution', *Journal of Chemical and Engineering Data*, vol. 39, no. 2, pp. 281-5.

Han, Y., Lau, S., Kayhanian, M. & Stenstrom, M.K. 2006, 'Correlation analysis among highway stormwater pollutants and characteristics', *Water Science and Technology*, vol. 53, no. 2, pp. 235-43.

Hang, Y., Yin, H., Wang, A., Shen, L., Feng, Y. & Liu, R. 2014, 'Preparation of titanate whiskers starting from metatitanic acid and their adsorption performances for Cu (II), Pb (II), and Cr (III) ions', *Water, Air, & Soil Pollution*, vol. 225, no. 9, p. 2095.

Haro, M., Cabal, B., Parra, J.B. & Ania, C.O. 2011, 'On the Adsorption Kinetics and Equilibrium of Polyaromatic Hydrocarbons from Aqueous Solution', *Adsorption Science & Technology*, vol. 29, no. 5, pp. 467-78.

Hathaway, J., Hunt, W., Graves, A. & Wright, J. 2011, 'Field evaluation of bioretention indicator bacteria sequestration in Wilmington, North Carolina', *Journal of Environmental Engineering*, vol. 137, no. 12, pp. 1103-13.

Hatt, B., Deletic, A. & Fletcher, T. 2007, 'Stormwater reuse: designing biofiltration systems for reliable treatment', *Water Science and Technology*, vol. 55, no. 4, pp. 201-9.

Hatt, B.E., Deletic, A. & Fletcher, T.D. 2006, 'Integrated treatment and recycling of stormwater: a review of Australian practice', *Journal of environmental management*, vol. 79, no. 1, pp. 102-13.

Hatt, B.E., Fletcher, T.D. & Deletic, A. 2009a, 'Hydrologic and pollutant removal performance of stormwater biofiltration systems at the field scale', *Journal of Hydrology*, vol. 365, no. 3-4, pp. 310-21.

Hatt, B.E., Fletcher, T.D. & Deletic, A. 2009b, 'Pollutant removal performance of field-scale stormwater biofiltration systems', *Water science and technology*, vol. 59, no. 8, pp. 1567-76.

He, J., Valeo, C., Chu, A. & Neumann, N.F. 2010, 'Characterizing physicochemical quality of storm-water runoff from an urban area in Calgary, Alberta', *Journal of Environmental Engineering*, vol. 136, no. 11, pp. 1206-17.

Headley, T. & Tanner, C.C. 2012, 'Constructed wetlands with floating emergent macrophytes: an innovative stormwater treatment technology', *Critical Reviews in Environmental Science and Technology*, vol. 42, no. 21, pp. 2261-310.

Henderson, C., Greenway, M. & Phillips, I. 2007, 'Removal of dissolved nitrogen, phosphorus and carbon from stormwater by biofiltration mesocosms', *Water Science and Technology*, vol. 55, no. 4, pp. 183-91.

Hoffman, E.J., Mills, G.L., Latimer, J.S. & Quinn, J.G. 1984, 'Urban runoff as a source of polycyclic aromatic hydrocarbons to coastal waters', *Environmental science & technology*, vol. 18, no. 8, pp. 580-7.

Holman, H.-Y.N., Nieman, K., Sorensen, D.L., Miller, C.D., Martin, M.C., Borch, T., McKinney, W.R. & Sims, R.C. 2002, 'Catalysis of PAH biodegradation by humic acid shown in synchrotron infrared studies', *Environmental science & technology*, vol. 36, no. 6, pp. 1276-80.

Howarth, R.W. 1988, 'Nutrient limitation of net primary production in marine ecosystems', *Annual review of ecology and systematics*, vol. 19, no. 1, pp. 89-110.

Hsieh, C.-h. & Davis, A.P. 2005, 'Evaluation and optimization of bioretention media for treatment of urban storm water runoff', *Journal of Environmental Engineering*, vol. 131, no. 11, pp. 1521-31.

Hua, M., Zhang, S., Pan, B., Zhang, W., Lv, L. & Zhang, Q. 2012, 'Heavy metal removal from water/wastewater by nanosized metal oxides: a review', *Journal of hazardous materials*, vol. 211, pp. 317-31.

Huang, J., Du, P., Ao, C., Ho, M., Lei, M., Zhao, D. & Wang, Z. 2007, 'Multivariate analysis for stormwater quality characteristics identification from different urban surface types in Macau', *Bulletin of environmental contamination and toxicology*, vol. 79, no. 6, pp. 650-4.

Huang, Y., Fulton, A.N. & Keller, A.A. 2016, 'Simultaneous removal of PAHs and metal contaminants from water using magnetic nanoparticle adsorbents', *Science of the Total Environment*, vol. 571, pp. 1029-36.

Huber, W.C., Dickinson, R.E., Barnwell Jr, T.O. & Branch, A. 1988, 'Storm water management model; version 4', *Environmental Protection Agency, United States*.

Hunt, W., Jarrett, A., Smith, J. & Sharkey, L. 2006, 'Evaluating bioretention hydrology and nutrient removal at three field sites in North Carolina', *Journal of Irrigation and Drainage Engineering*, vol. 132, no. 6, pp. 600-8.

Hunt, W., Smith, J., Jadlocki, S., Hathaway, J. & Eubanks, P. 2008, 'Pollutant removal and peak flow mitigation by a bioretention cell in urban Charlotte, NC', *Journal of Environmental Engineering*, vol. 134, no. 5, pp. 403-8.

Huttenloch, P., Roehl, K.E. & Czurda, K. 2001, 'Sorption of nonpolar aromatic contaminants by chlorosilane surface modified natural minerals', *Environmental science & technology*, vol. 35, no. 21, pp. 4260-4.

Hvitved-Jacobsen, T., Vollertsen, J. & Nielsen, A.H. 2010, *Urban and highway stormwater pollution: concepts and engineering*, CRC press.

Inglezakis, V.J. 2005, 'The concept of “capacity” in zeolite ion-exchange systems', *Journal of Colloid and Interface Science*, vol. 281, no. 1, pp. 68-79.

Islam, M. & Patel, R. 2010, 'Synthesis and physicochemical characterization of Zn/Al chloride layered double hydroxide and evaluation of its nitrate removal efficiency', *Desalination*, vol. 256, no. 1-3, pp. 120-8.

Jaishankar, M., Tseten, T., Anbalagan, N., Mathew, B.B. & Beeregowda, K.N. 2014, 'Toxicity, mechanism and health effects of some heavy metals', *Interdisciplinary toxicology*, vol. 7, no. 2, pp. 60-72.

Järup, L. 2003, 'Hazards of heavy metal contamination', *British medical bulletin*, vol. 68, no. 1, pp. 167-82.

Jiminez, A.L.F. 2014, *Environmental assessment of used motor oil in the Ciudad Juarez-el Paso area*, The University of Texas at El Paso.

Johnsen, A.R. & Karlson, U. 2005, 'PAH degradation capacity of soil microbial communities—does it depend on PAH exposure?', *Microbial ecology*, vol. 50, no. 4, pp. 488-95.

Kalaruban, M., Loganathan, P., Shim, W., Kandasamy, J., Ngo, H. & Vigneswaran, S. 2016, 'Enhanced removal of nitrate from water using amine-grafted agricultural wastes', *Science of the Total Environment*, vol. 565, pp. 503-10.

Kandasamy, J., Beecham, S. & Dunphy, A. 2008, 'Stormwater sand filters in water-sensitive urban design', *Proceedings of the Institution of Civil Engineers: Water Management*.

Karapınar, N. 2009, 'Application of natural zeolite for phosphorus and ammonium removal from aqueous solutions', *Journal of hazardous materials*, vol. 170, no. 2-3, pp. 1186-91.

Kavitha, D. & Namasivayam, C. 2008, 'Capacity of activated carbon in the removal of acid brilliant blue: Determination of equilibrium and kinetic model parameters', *Chemical Engineering Journal*, vol. 139, no. 3, pp. 453-61.

Khan, E., Khaodhir, S. & Rotwiron, P. 2007, 'Polycyclic aromatic hydrocarbon removal from water by natural fiber sorption', *Water Environment Research*, vol. 79, no. 8, pp. 901-11.

Kim, H.-C. & Yu, M.-J. 2005, 'Characterization of natural organic matter in conventional water treatment processes for selection of treatment processes focused on DBPs control', *Water research*, vol. 39, no. 19, pp. 4779-89.

Kim, H., Seagren, E.A. & Davis, A.P. 2003, 'Engineered bioretention for removal of nitrate from stormwater runoff', *Water Environment Research*, vol. 75, no. 4, pp. 355-67.

Korshin, G.V., Li, C.-W. & Benjamin, M.M. 1997, 'Monitoring the properties of natural organic matter through UV spectroscopy: a consistent theory', *Water Research*, vol. 31, no. 7, pp. 1787-95.

Kurniawan, T.A., Chan, G.Y., Lo, W.-h. & Babel, S. 2006, 'Comparisons of low-cost adsorbents for treating wastewaters laden with heavy metals', *Science of the total environment*, vol. 366, no. 2-3, pp. 409-26.

Kus, B., Kandasamy, J., Vigneswaran, S., Shon, H. & Moody, G. 2012, 'Two stage filtration for stormwater treatment: A pilot scale study', *Desalination and Water Treatment*, vol. 45, no. 1-3, pp. 361-9.

Lambert, M., Leven, B. & Green, R. 2000, 'New methods of cleaning up heavy metal in soils and water', *Environmental science and technology briefs for citizens. Kansas State University, Manhattan, KS*.

Lamichhane, S., Bal Krishna, K.C. & Sarukkalige, R. 2016, 'Polycyclic aromatic hydrocarbons (PAHs) removal by sorption: A review', *Chemosphere*, vol. 148, pp. 336-53.

Larsen, T., Broch, K. & Andersen, M.R. 1998, 'First flush effects in an urban catchment area in Aalborg', *Water Science and Technology*, vol. 37, no. 1, p. 251.

Lau, S.L., Han, Y., Kang, J.H., Kayhanian, M. & Stenstrom, M.K. 2009, 'Characteristics of highway stormwater runoff in Los Angeles: Metals and polycyclic aromatic hydrocarbons', *Water Environment Research*, vol. 81, no. 3, pp. 308-18.

Lawal, A.T. 2017, 'Polycyclic aromatic hydrocarbons. A review', *Cogent Environmental Science*, vol. 3, no. 1, p. 1339841.

Lee, E., Maniquiz, M., Gorme, J. & Kim, L. 2010, 'Determination of cost-effective first flush criteria for BMP sizing', *Desalination and Water Treatment*, vol. 19, no. 1-3, pp. 157-63.

Lee, J., Bang, K., Ketchum Jr, L., Choe, J. & Yu, M. 2002, 'First flush analysis of urban storm runoff', *Science of the Total Environment*, vol. 293, no. 1-3, pp. 163-75.

Lee, J.H. & Bang, K.W. 2000, 'Characterization of urban stormwater runoff', *Water research*, vol. 34, no. 6, pp. 1773-80.

Lemić, J., Tomašević-Čanović, M., Adamović, M., Kovačević, D. & Milićević, S. 2007, 'Competitive adsorption of polycyclic aromatic hydrocarbons on organo-zeolites', *Microporous and Mesoporous Materials*, vol. 105, no. 3, pp. 317-23.

Lerner, D.N. 1986, 'Leaking pipes recharge ground water', *Groundwater*, vol. 24, no. 5, pp. 654-62.

Lesage, G., Sperandio, M. & Tiruta-Barna, L. 2010, 'Analysis and modelling of non-equilibrium sorption of aromatic micro-pollutants on GAC with a multi-compartment dynamic model', *Chemical Engineering Journal*, vol. 160, no. 2, pp. 457-65.

Li, D., Wan, J., Ma, Y., Wang, Y., Huang, M. & Chen, Y. 2015, 'Stormwater runoff pollutant loading distributions and their correlation with rainfall and catchment characteristics in a rapidly industrialized city', *PloS one*, vol. 10, no. 3, p. e0118776.

Li, H. & Davis, A.P. 2008a, 'Heavy metal capture and accumulation in bioretention media', *Environmental science & technology*, vol. 42, no. 14, pp. 5247-53.

Li, H. & Davis, A.P. 2008b, 'Urban particle capture in bioretention media. I: Laboratory and field studies', *Journal of Environmental Engineering*, vol. 134, no. 6, pp. 409-18.

Li, H. & Davis, A.P. 2009, 'Water quality improvement through reductions of pollutant loads using bioretention', *Journal of Environmental Engineering*, vol. 135, no. 8, pp. 567-76.

Li, H., Sharkey, L.J., Hunt, W.F. & Davis, A.P. 2009, 'Mitigation of impervious surface hydrology using bioretention in North Carolina and Maryland', *Journal of Hydrologic Engineering*, vol. 14, no. 4, pp. 407-15.

Little, T.M. & Hills, F.J. 1978, *Agricultural experimentation: design and analysis*.

Liu, J., Sample, D.J., Bell, C. & Guan, Y. 2014, 'Review and research needs of bioretention used for the treatment of urban stormwater', *Water*, vol. 6, no. 4, pp. 1069-99.

Liu, L., Liu, A., Li, D., Zhang, L. & Guan, Y. 2016, 'Characterizing polycyclic aromatic hydrocarbon build-up processes on urban road surfaces', *Environmental pollution*, vol. 214, pp. 185-93.

Loganathan, P., Shim, W.G., Sounthararajah, D.P., Kalaruban, M., Nur, T. & Vigneswaran, S. 2018, 'Modelling equilibrium adsorption of single, binary, and ternary combinations of Cu, Pb, and Zn onto granular activated carbon', *Environmental Science and Pollution Research*, vol. 25, no. 17, pp. 16664-75.

Loganathan, P., Vigneswaran, S. & Kandasamy, J. 2013, 'Road-deposited sediment pollutants: a critical review of their characteristics, source apportionment, and management', *Critical reviews in environmental science and technology*, vol. 43, no. 13, pp. 1315-48.

Loganathan, P., Vigneswaran, S., Kandasamy, J. & Bolan, N.S. 2014, 'Removal and Recovery of Phosphate From Water Using Sorption', *Critical Reviews in Environmental Science and Technology*, vol. 44, no. 8, pp. 847-907.

Loh, M. & Coghlan, P. 2003, *Domestic water use study in Perth, Western Australia, 1998-2001*, Water Corporation Perth.

Long, C., Lu, J., Li, A., Hu, D., Liu, F. & Zhang, Q. 2008, 'Adsorption of naphthalene onto the carbon adsorbent from waste ion exchange resin: equilibrium and kinetic characteristics', *Journal of Hazardous Materials*, vol. 150, no. 3, pp. 656-61.

Lucas, W.C. 2009, 'Design of integrated bioinfiltration-detention urban retrofits with design storm and continuous simulation methods', *Journal of hydrologic Engineering*, vol. 15, no. 6, pp. 486-98.

Madzivhandila, V.A. & Chirwa, E. 2017, 'Modeling chlorine decay in drinking water distribution systems using aquasim'.

Majumdar, D. & Gupta, N. 2000, 'Nitrate pollution of groundwater and associated human health disorders', *Indian journal of environmental health*, vol. 42, no. 1, pp. 28-39.

Makkar, R.S. & Rockne, K.J. 2003, 'Comparison of synthetic surfactants and biosurfactants in enhancing biodegradation of polycyclic aromatic hydrocarbons', *Environmental Toxicology and Chemistry: An International Journal*, vol. 22, no. 10, pp. 2280-92.

Manjuladevi, M. & Sri, M.O. 2017, 'Heavy metals removal from industrial wastewater by nano adsorbent prepared from cucumis melopeel activated carbon', *Journal of Nanomedicine Research*, vol. 5, pp. 1-4.

Manoli, E. & Samara, C. 1999, 'Polycyclic aromatic hydrocarbons in natural waters: sources, occurrence and analysis', *TrAC Trends in Analytical Chemistry*, vol. 18, no. 6, pp. 417-28.

Martin, S. & Griswold, W. 2009, 'Human health effects of heavy metals', *Environmental Science and Technology briefs for citizens*, vol. 15, pp. 1-6.

Massoudieh, A., Abrishamchi, A. & Kayhanian, M. 2008, 'Mathematical modeling of first flush in highway storm runoff using genetic algorithm', *Science of the total environment*, vol. 398, no. 1-3, pp. 107-21.

Mažeikiene, A., Valentukevičiene, M., Rimeika, M., Matuzevičius, A.B. & Dauknys, R. 2008, 'Removal of nitrates and ammonium ions from water using natural sorbent zeolite (clinoptilolite)', *Journal of Environmental Engineering and Landscape Management*, vol. 16, no. 1, pp. 38-44.

McBride, M. 1989, 'Reactions controlling heavy metal solubility in soils', *Advances in soil science*, Springer, pp. 1-56.

McCready, S., Slee, D.J., Birch, G.F. & Taylor, S.E. 2000, 'The Distribution of Polycyclic Aromatic Hydrocarbons in Surficial Sediments of Sydney Harbour, Australia', *Marine Pollution Bulletin*, vol. 40, no. 11, pp. 999-1006.

McKay, C.P. 1996, 'Elemental composition, solubility, and optical properties of Titan's organic haze', *Planetary and Space Science*, vol. 44, no. 8, pp. 741-7.

Menichini, E. & Bocca, B. 2003, 'POLYCYCLIC AROMATIC HYDROCARBONS A2 - Caballero, Benjamin', *Encyclopedia of Food Sciences and Nutrition (Second Edition)*, Academic Press, Oxford, pp. 4616-25.

Miguntanna, N.S., Egodawatta, P., Kokot, S. & Goonetilleke, A. 2010, 'Determination of a set of surrogate parameters to assess urban stormwater quality', *Science of the Total Environment*, vol. 408, no. 24, pp. 6251-9.

Miller, M.M., Wasik, S.P., Huang, G.L., Shiu, W.Y. & Mackay, D. 1985, 'Relationships between octanol-water partition coefficient and aqueous solubility', *Environmental science & technology*, vol. 19, no. 6, pp. 522-9.

Mitchell, V., McMahon, T.A. & Mein, R.G. 1999, *The reuse potential of urban stormwater and wastewater*, CRC for Catchment Hydrology.

Mitchell, V.G., Mein, R.G. & McMahon, T.A. 2002, 'Utilising stormwater and wastewater resources in urban areas', *Australasian Journal of Water Resources*, vol. 6, no. 1, pp. 31-43.

Monteiro, M.T., Oliveira, S.M., Luizão, F.J., Cândido, L.A., Ishida, F.Y. & Tomasella, J. 2014, 'Dissolved organic carbon concentration and its relationship to electrical conductivity in the waters of a stream in a forested Amazonian blackwater catchment', *Plant Ecology & Diversity*, vol. 7, no. 1-2, pp. 205-13.

Mostofa, K.M., Wu, F., Liu, C.-Q., Vione, D., Yoshioka, T., Sakugawa, H. & Tanoue, E. 2011, 'Photochemical, microbial and metal complexation behavior of fluorescent dissolved organic matter in the aquatic environments', *Geochemical Journal*, vol. 45, no. 3, pp. 235-54.

Murphy, L.U., Cochrane, T.A. & O'Sullivan, A. 2015, 'Build-up and wash-off dynamics of atmospherically derived Cu, Pb, Zn and TSS in stormwater runoff as a function of meteorological characteristics', *Science of The Total Environment*, vol. 508, pp. 206-13.

Musikavong, C. & Wattanachira, S. 2007, 'Reduction of dissolved organic matter in terms of DOC, UV-254, SUVA and THMFP in industrial estate wastewater treated by stabilization ponds', *Environmental monitoring and assessment*, vol. 134, no. 1-3, pp. 489-97.

Naidu, G., Nur, T., Loganathan, P., Kandasamy, J. & Vigneswaran, S. 2016, 'Selective sorption of rubidium by potassium cobalt hexacyanoferrate', *Separation and Purification Technology*, vol. 163, pp. 238-46.

Nguyen, T.C. 2016, 'Pollutants in road-deposited sediments: characteristics, mobility, bioavailability and remediation'.

Nguyen, T.C., Loganathan, P., Nguyen, T.V., Vigneswaran, S., Kandasamy, J. & Naidu, R. 2015, 'Simultaneous adsorption of Cd, Cr, Cu, Pb, and Zn by an iron-coated Australian zeolite in batch and fixed-bed column studies', *Chemical Engineering Journal*, vol. 270, pp. 393-404.

Nguyen, T.C., Loganathan, P., Nguyen, T.V., Vigneswaran, S., Kandasamy, J., Slee, D., Stevenson, G. & Naidu, R. 2014, 'Polycyclic aromatic hydrocarbons in road-deposited sediments, water sediments, and soils in Sydney, Australia: comparisons of concentration distribution, sources and potential toxicity', *Ecotoxicology and environmental safety*, vol. 104, pp. 339-48.

NHMRC, N. 2011, 'Australian drinking water guidelines', *Commonwealth of Australia*.

Nie, F.-h., Li, T., Yao, H.-f., Feng, M. & Zhang, G.-k. 2008, 'Characterization of suspended solids and particle-bound heavy metals in a first flush of highway runoff', *Journal of Zhejiang University-Science A*, vol. 9, no. 11, pp. 1567-75.

Nixon, S., Ammerman, J., Atkinson, L., Berounsky, V., Billen, G., Boicourt, W., Boynton, W., Church, T., Ditoro, D. & Elmgren, R. 1996, 'The fate of nitrogen and phosphorus at the land-sea margin of the North Atlantic Ocean', *Biogeochemistry*, vol. 35, no. 1, pp. 141-80.

Novotny, V. 1995, *Non point pollution and urban stormwater management*, vol. 9, CRC Press.

NSW, D. 2006, 'Managing Urban Stormwater. Harvesting and Reuse. DEC', *New South Wales, Australia*, vol. 137.

Nur, T. 2014, 'Nitrate, phosphate and fluoride removal from water using adsorption process'.

Nur, T., Johir, M., Loganathan, P., Nguyen, T., Vigneswaran, S. & Kandasamy, J. 2014, 'Phosphate removal from water using an iron oxide impregnated strong base anion exchange resin', *Journal of Industrial and Engineering Chemistry*, vol. 20, no. 4, pp. 1301-7.

Nur, T., Loganathan, P., Nguyen, T., Vigneswaran, S., Singh, G. & Kandasamy, J. 2014, 'Batch and column adsorption and desorption of fluoride using hydrous ferric oxide: solution chemistry and modeling', *Chemical Engineering Journal*, vol. 247, pp. 93-102.

Nur, T., Shim, W., Loganathan, P., Vigneswaran, S. & Kandasamy, J. 2015, 'Nitrate removal using Purolite A520E ion exchange resin: batch and fixed-bed column adsorption modelling', *International journal of environmental science and technology*, vol. 12, no. 4, pp. 1311-20.

Papanikolaou, N.C., Hatzidaki, E.G., Belivanis, S., Tzanakakis, G.N. & Tsatsakis, A.M. 2005, 'Lead toxicity update. A brief review', *Medical science monitor*, vol. 11, no. 10, pp. RA329-RA36.

Park, K.-H., Lee, C.-H., Ryu, S.-K. & Yang, X. 2007, 'Zeta-potentials of oxygen and nitrogen enriched activated carbons for removal of copper ion', *Carbon letters*, vol. 8, no. 4, pp. 321-5.

Persson, A., Welander, T., Hinchee, R., Alleman, B., Hoeppel, R. & Miller, R. 1994, 'Biotreatment of petroleum hydrocarbon containing sludges by land application. A case history and prospects for future treatment', *Hudrocarbon Bioremediation Boca Raton, FL, USA CRC Press, Inc*, pp. 334-42.

Philp, M., McMahon, J., Heyenga, S., Marinoni, O., Jenkins, G., Maheepala, S. & Greenway, M. 2008, 'Review of stormwater harvesting practices', *Urban Water Security Research Alliance Technical Report*, no. 9.

Pitcher, S., Slade, R. & Ward, N. 2004, 'Heavy metal removal from motorway stormwater using zeolites', *Science of the Total Environment*, vol. 334, pp. 161-6.

Pope, L.M. & Bevans, H.E. 1984, *Relation of urban land-use and dry-weather, storm, and snowmelt flow characteristics to stream-water quality, Shunganunga Creek basin, Topeka, Kansas*, 2331-1258, US Geological Survey.

Premiers, N. 1997, 'Report to the NSW Government on the Proposal by Sydney Water Corporation for Sewage Overflow Abatement in Sydney Harbour. Waterways Advisory Panel Report. NSW Premiers Department'.

Price, M. 2002, 'Who needs sustainability?', *Geological Society, London, Special Publications*, vol. 193, no. 1, pp. 75-81.

Radcliffe, J.C. & Page, D. 2020, 'Water reuse and recycling in Australia-history, current situation and future perspectives', *Water Cycle*, vol. 1, pp. 19-40.

RANGES, H.M.O.L.F. 2017, 'POLLUTION PREVENTION GUIDELINE HEAVY METALS ON LIVE FIRING RANGES'.

Read, J., Wevill, T., Fletcher, T. & Deletic, A. 2008, 'Variation among plant species in pollutant removal from stormwater in biofiltration systems', *Water research*, vol. 42, no. 4-5, pp. 893-902.

Riahi, K., Chaabane, S. & Thayer, B.B. 2017, 'A kinetic modeling study of phosphate adsorption onto Phoenix dactylifera L. date palm fibers in batch mode', *Journal of Saudi Chemical Society*, vol. 21, pp. S143-S52.

Roig, B. & Thomas, O. 2003, 'UV spectrophotometry: a powerful tool for environmental measurement', *Management of Environmental Quality: An International Journal*, vol. 14, no. 3, pp. 398-404.

Rügner, H., Schwientek, M., Beckingham, B., Kuch, B. & Grathwohl, P. 2013, 'Turbidity as a proxy for total suspended solids (TSS) and particle facilitated pollutant transport in catchments', *Environmental earth sciences*, vol. 69, no. 2, pp. 373-80.

Rusmin, R., Sarkar, B., Liu, Y., McClure, S. & Naidu, R. 2015, 'Structural evolution of chitosan–palygorskite composites and removal of aqueous lead by composite beads', *Applied Surface Science*, vol. 353, pp. 363-75.

RWCC, N. 1993, 'NSW guidelines for urban and residential use of reclaimed water', *NSW Recycled Water Coordination Committee*.

Saeedi, M., Li, L.Y. & Grace, J.R. 2018, 'Effect of organic matter and selected heavy metals on sorption of acenaphthene, fluorene and fluoranthene onto various clays and clay minerals', *Environmental Earth Sciences*, vol. 77, no. 8, p. 305.

Shafique, M. & Kim, R. 2015, 'Low impact development practices: a review of current research and recommendations for future directions', *Ecological Chemistry and Engineering S*, vol. 22, no. 4, pp. 543-63.

Shaheen, D.G. 1975, *Contributions of urban roadway usage to water pollution*, vol. 1, Office of Research and Development, US Environmental Protection Agency.

Shammaa, Y. & Zhu, D.Z. 2001, 'Techniques for controlling total suspended solids in stormwater runoff', *Canadian Water Resources Journal*, vol. 26, no. 3, pp. 359-75.

Sharifi, S., Massoudieh, A. & Kayhanian, M. 2011, 'A Stochastic Stormwater Quality Volume-Sizing Method with First Flush Emphasis', *Water environment research*, vol. 83, no. 11, pp. 2025-35.

Shie, J.-L., Chang, C.-Y., Chen, J.-H., Tsai, W.-T., Chen, Y.-H., Chiou, C.-S. & Chang, C.-F. 2005, 'Catalytic oxidation of naphthalene using a Pt/Al2O3 catalyst', *Applied Catalysis B: Environmental*, vol. 58, no. 3-4, pp. 289-97.

Singh, N., Kumar, D. & Sahu, A.P. 2007, 'Arsenic in the environment: effects on human health and possible prevention', *Journal of Environmental Biology*, vol. 28, no. 2, p. 359.

Singh, R., Gautam, N., Mishra, A. & Gupta, R. 2011, 'Heavy metals and living systems: An overview', *Indian journal of pharmacology*, vol. 43, no. 3, p. 246.

Smirnova, A.A. 2011, 'Use of numerical symbols by birds', *Zoologichesky Zhurnal*, vol. 90, no. 7, pp. 803-10.

Sonstrom, R.S., Clausen, J.C. & Askew, D.R. 2002, 'Treatment of parking lot stormwater using a StormTreat system', *Environmental science & technology*, vol. 36, no. 20, pp. 4441-6.

Sounthararajah, D., Loganathan, P., Kandasamy, J. & Vigneswaran, S. 2015a, 'Effects of humic acid and suspended solids on the removal of heavy metals from water by adsorption onto granular activated carbon', *International journal of environmental research and public health*, vol. 12, no. 9, pp. 10475-89.

Sounthararajah, D.P. 2016, 'Mitigation of pollutants for beneficial use of stormwater'.

Sounthararajah, D.P., Loganathan, P., Kandasamy, J. & Vigneswaran, S. 2015b, 'Effects of humic acid and suspended solids on the removal of heavy metals from water by adsorption onto granular activated carbon', *International journal of environmental research and public health*, vol. 12, no. 9, pp. 10475-89.

Sounthararajah, D.P., Loganathan, P., Kandasamy, J. & Vigneswaran, S. 2016, 'Column studies on the removal of dissolved organic carbon, turbidity and heavy metals from stormwater using granular activated carbon', *Desalination and Water Treatment*, vol. 57, no. 11, pp. 5045-55.

Strassler, E., Pritts, J. & Strellec, K. 1999, 'Preliminary data summary of urban storm water best management practices', *United States Environmental Protection Agency, Office of Water*.

Strategy, Q.W.R. 2001, 'Queensland water recycling strategy', *Brisbane, Australia: Department of Natural Resources, Queensland State Government*.

Sun, S., Wang, L., Huang, S., Tu, T. & Sun, H. 2011, 'The effect of capping with natural and modified zeolites on the release of phosphorus and organic contaminants from river sediment', *Frontiers of Chemical Science and Engineering*, vol. 5, no. 3, pp. 308-13.

Tao, Y., Li, W., Xue, B., Zhong, J., Yao, S. & Wu, Q. 2013, 'Different effects of copper (II), cadmium (II) and phosphate on the sorption of phenanthrene on the biomass of cyanobacteria', *Journal of hazardous materials*, vol. 261, pp. 21-8.

Tao, Y., Xue, B., Yang, Z., Yao, S. & Li, S. 2014, 'Effects of Heavy Metals on the Sorption of Polycyclic Aromatic Hydrocarbons by Microcystis aeruginosa', *Journal of environmental quality*, vol. 43, no. 6, pp. 1953-62.

Thomas, H.C. 1944, 'Heterogeneous ion exchange in a flowing system', *Journal of the American Chemical Society*, vol. 66, no. 10, pp. 1664-6.

Thomas, O., Causse, J., Jung, A.-V. & Thomas, M.-F. 2017, 'Natural water', *UV-Visible Spectrophotometry of Water and Wastewater*, Elsevier, pp. 225-59.

Tripathy, S.S. & Raichur, A.M. 2008, 'Abatement of fluoride from water using manganese dioxide-coated activated alumina', *Journal of Hazardous Materials*, vol. 153, no. 3, pp. 1043-51.

Vaillant, S., Pouet, M. & Thomas, O. 2002, 'Basic handling of UV spectra for urban water quality monitoring', *Urban Water*, vol. 4, no. 3, pp. 273-81.

Valderrama, C., Cortina, J., Farran, A., Gamisans, X. & Lao, C. 2007, 'Kinetics of sorption of polyaromatic hydrocarbons onto granular activated carbon and Macronet hyper-cross-linked polymers (MN200)', *Journal of Colloid and Interface Science*, vol. 310, no. 1, pp. 35-46.

Valderrama, C., Gamisans, X., Cortina, J.L., Farrán, A. & de las Heras, F.X. 2009, 'Evaluation of polyaromatic hydrocarbon removal from aqueous solutions using activated carbon and hyper-crosslinked polymer (Macronet MN200)', *Journal of Chemical Technology & Biotechnology: International Research in Process, Environmental & Clean Technology*, vol. 84, no. 2, pp. 236-45.

Valderrama, C., Gamisans, X., De las Heras, X., Farran, A. & Cortina, J. 2008, 'Sorption kinetics of polycyclic aromatic hydrocarbons removal using granular activated carbon: intraparticle diffusion coefficients', *Journal of Hazardous Materials*, vol. 157, no. 2-3, pp. 386-96.

Walters, R.W. & Luthy, R.G. 1984, 'Equilibrium adsorption of polycyclic aromatic hydrocarbons from water onto activated carbon', *Environmental science & technology*, vol. 18, no. 6, pp. 395-403.

Wammer, K.H. & Peters, C.A. 2006, 'A molecular modeling analysis of polycyclic aromatic hydrocarbon biodegradation by naphthalene dioxygenase', *Environmental Toxicology and Chemistry: An International Journal*, vol. 25, no. 4, pp. 912-20.

Wang, L., Lyons, J., Kanehl, P. & Bannerman, R. 2001, 'Impacts of urbanization on stream habitat and fish across multiple spatial scales', *Environmental management*, vol. 28, no. 2, pp. 255-66.

Wang, L., Wei, J., Huang, Y., Wang, G. & Maqsood, I. 2011, 'Urban nonpoint source pollution buildup and washoff models for simulating storm runoff quality in the Los Angeles County', *Environmental Pollution*, vol. 159, no. 7, pp. 1932-40.

Wang, S. & Peng, Y. 2010, 'Natural zeolites as effective adsorbents in water and wastewater treatment', *Chemical engineering journal*, vol. 156, no. 1, pp. 11-24.

Watson, K., Farré, M.J., Leusch, F.D. & Knight, N. 2018, 'Using fluorescence-parallel factor analysis for assessing disinfection by-product formation and natural organic matter removal efficiency in secondary treated synthetic drinking waters', *Science of the Total Environment*, vol. 640, pp. 31-40.

Weber, W.J. & Morris, J.C. 1963, 'Kinetics of adsorption on carbon from solution', *Journal of the Sanitary Engineering Division*, vol. 89, no. 2, pp. 31-60.

Weiss, P.T., Gulliver, J.S. & Erickson, A.J. 2007, 'Cost and pollutant removal of storm-water treatment practices', *Journal of Water Resources Planning and Management*, vol. 133, no. 3, pp. 218-29.

Westholm, L.J., Repo, E. & Sillanpää, M. 2014, 'Filter materials for metal removal from mine drainage—a review', *Environmental Science and Pollution Research*, vol. 21, no. 15, pp. 9109-28.

Wild, D., Kisliakova, A. & Siegrist, H. 1996, 'P-fixation by Mg, Ca and zeolite A during stabilization of excess sludge from enhanced biological P-removal', *Water Science and Technology*, vol. 34, no. 1-2, pp. 391-8.

Wołowiec, M., Muir, B., Zięba, K., Bajda, T., Kowalik, M. & Franus, W. 2017, 'Experimental study on the removal of VOCs and PAHs by zeolites and surfactant-modified zeolites', *Energy & Fuels*, vol. 31, no. 8, pp. 8803-12.

Wu, X., Fan, M., Mclaughlin, J.F., Shen, X. & Tan, G. 2018, 'A novel low-cost method of silica aerogel fabrication using fly ash and trona ore with ambient pressure drying technique', *Powder Technology*, vol. 323, pp. 310-22.

Yakout, S., Daifullah, A. & El-Reefy, S. 2013, 'Adsorption of naphthalene, phenanthrene and pyrene from aqueous solution using low-cost activated carbon derived from agricultural wastes', *Adsorption Science & Technology*, vol. 31, no. 4, pp. 293-302.

Yeoman, S., Stephenson, T., Lester, J. & Perry, R. 1988, 'The removal of phosphorus during wastewater treatment: a review', *Environmental Pollution*, vol. 49, no. 3, pp. 183-233.

Yuan, M., Tong, S., Zhao, S. & Jia, C.Q. 2010, 'Adsorption of polycyclic aromatic hydrocarbons from water using petroleum coke-derived porous carbon', *Journal of Hazardous Materials*, vol. 181, no. 1-3, pp. 1115-20.

Zafiriou, O.C., Joussot-Dubien, J., Zepp, R.G. & Zika, R.G. 1984, 'Photochemistry of natural waters', *Environmental Science & Technology*, vol. 18, no. 12, pp. 358A-71A.

Zhan, Y., Zhang, H., Lin, J., Zhang, Z. & Gao, J. 2017, 'Role of zeolite's exchangeable cations in phosphate adsorption onto zirconium-modified zeolite', *Journal of Molecular Liquids*, vol. 243, pp. 624-37.

Zhang, M. & He, Z. 2015, 'Characteristics of Dissolved Organic Carbon Revealed by Ultraviolet-Visible Absorbance and Fluorescence Spectroscopy: The Current Status and Future Exploration', *Labile organic matter—chemical compositions, function, and significance in soil and the environment*, vol. 62, pp. 1-21.

Zhang, Z., Hong, H., Zhou, J. & Yu, G. 2004, 'Phase association of polycyclic aromatic hydrocarbons in the Minjiang River Estuary, China', *Science of the Total Environment*, vol. 323, no. 1-3, pp. 71-86.

Zhang, Z., Hou, X., Zhang, X. & Li, H. 2017, 'The synergistic adsorption of pyrene and copper onto Fe (III) functionalized mesoporous silica from aqueous solution', *Colloids and Surfaces A: Physicochemical and Engineering Aspects*, vol. 520, pp. 39-45.

Appendix A

Table A.1. List of the polycyclic hydrocarbons (PAHs) tested

PAHs tested	
2-Fluorobiphenyl	Pyrene
Naphthalene (Ex SVOC)	Benz(a)anthracene
Anthracene-d10	Chrysene
Phenol-d6	Benzo(b+j)fluoranthene
2-Chlorophenol-D4	Benzo(k)fluoranthene
4-Terphenyl-d14	Benzo(a)pyrene
2.4.6-Tribromophenol	Indeno(1.2.3.cd)pyrene
Acenaphthylene	Dibenz(a.h)anthracene
Acenaphthene	Benzo(g.h.i)perylene
Fluorene	Benzo(a)pyrene
Phenanthrene	
Anthracene	
Fluoranthene	

Table A.2. Concentrations of pharmaceutical and personnel care products (PPCPs)

Compound name	analyte limit	**E9**		**E11**	
	ng/L	Rep 1	Rep 2	Rep 1	Rep 2
saccharin	5	N.Q.	127	< LOQ	9
Salicyclic acid	20	N.Q.	N.Q.	< LOQ	18
Ketoprofen	5	N.Q.	< LOQ	< LOQ	7
Naproxen	5	59	< LOQ	< LOQ	9
Bisphenol A	10	1646	240	< LOQ	23
diclofenac	5	27	11	< LOQ	8
propylparaben	20	< LOQ	< LOQ	< LOQ	7
Diuron	5	268	168	< LOQ	8
Ibuprofen	5	310	286	< LOQ	9
phenylphenol	10	41	20	< LOQ	8
Gemfibrozil	5	51	< LOQ	< LOQ	10
triclocarban	10	< LOQ	< LOQ	< LOQ	9
Triclosan	5	8	< LOQ	< LOQ	7
4-n-nonylphenol	10	14	< LOQ	< LOQ	12
PFOA	5	33	25	< LOQ	9

PFOS	5	24	19	< LOQ	8
Atenolol	5	< LOQ	< LOQ	< LOQ	8
Paracetamol	5	1998	362	< LOQ	9
Sulfamethoxazole	5	< LOQ	< LOQ	< LOQ	8
Caffeine	5	4800	1212	< LOQ	10
Trimethoprim	5	< LOQ	< LOQ	< LOQ	8
benzotriazole	5	2980	626	< LOQ	10
triamterene	5	< LOQ	< LOQ	< LOQ	9
primidone	10	< LOQ	< LOQ	< LOQ	6
carazolol	5	< LOQ	< LOQ	< LOQ	9
TCEP	5	134	46	< LOQ	8
Dilantin	10	N.Q.	N.Q.	< LOQ	13
Simazine	5	153	29	< LOQ	8
Carbamazepine	5	< LOQ	< LOQ	< LOQ	7
omeprazole	5	< LOQ	< LOQ	< LOQ	8
Atrazine	5	19	7	< LOQ	8
Verapamil	5	< LOQ	< LOQ	< LOQ	9
Linuron	5	< LOQ	< LOQ	< LOQ	7
diazepam	5	< LOQ	< LOQ	< LOQ	8
benzophenone	20	< LOQ	< LOQ	< LOQ	14
clozapine	5	< LOQ	< LOQ	< LOQ	8
amtriptyline	5	< LOQ	< LOQ	< LOQ	8
hydroxyzine	10	< LOQ	< LOQ	< LOQ	7
oxybenzone	50	< LOQ	< LOQ	< LOQ	2
Diazinon	5	< LOQ	< LOQ	< LOQ	8
LOQ: analyte limit of quantitation ng/L		N.Q:Not quantifiable			

Figure A.1-16 Hydrographs which were generated using X-prats software along with the pollutant concentration variation for each sampling events

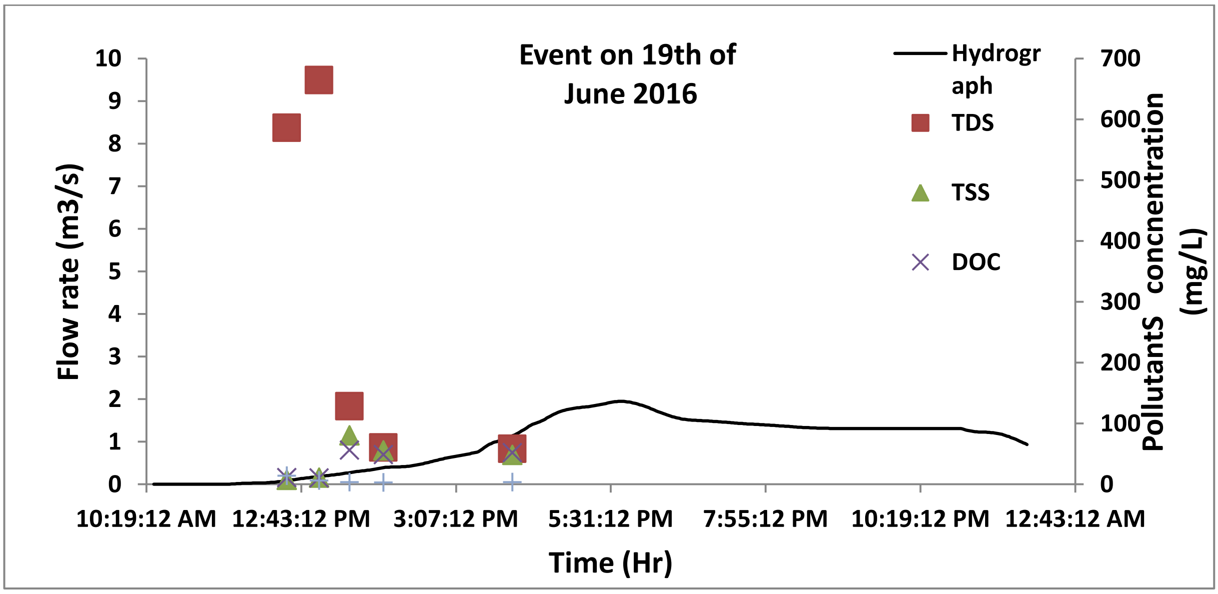

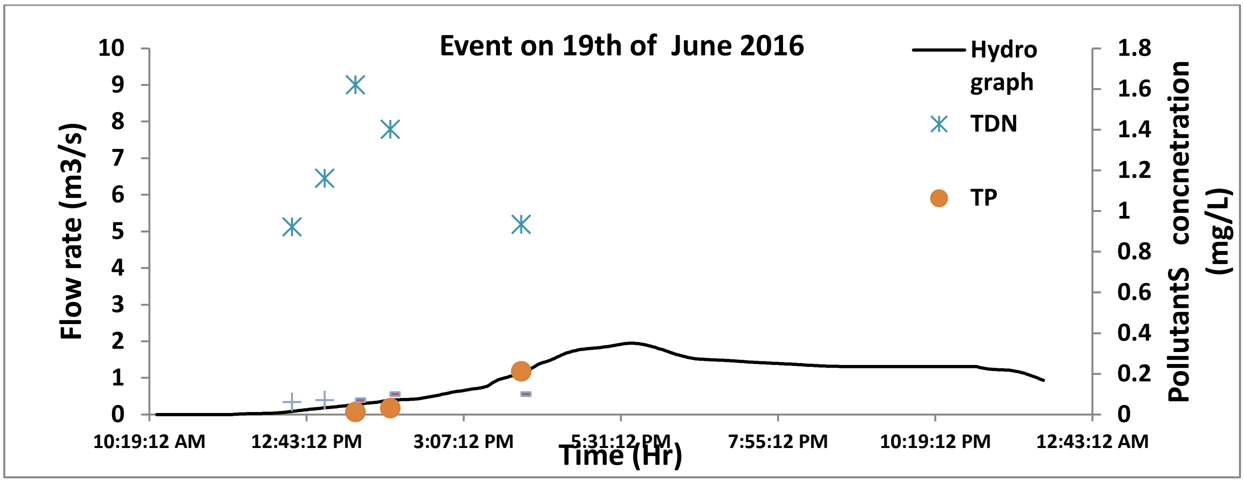
Event on 19th of June 2016
Flow rate (m3/s)
PollutantS concnetration (mg/L)
Time (Hr)
Hydro graph
TDN
TP
10
9
8
7
6
5
4
3
2
1
0
1.8
1.6
1.4
1.2
1
0.8
0.6
0.4
0.2
0
10:19:12 AM
12:43:12 PM
3:07:12 PM
5:31:12 PM
7:55:12 PM
10:19:12 PM
12:43:12 AM

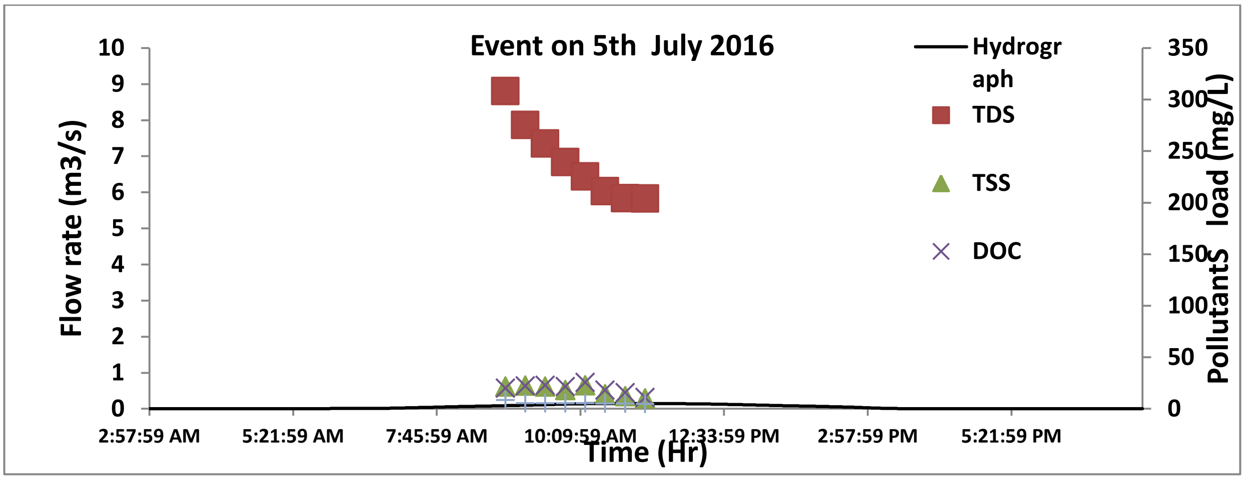
Event on 5th July 2016
Flow rate (m3/s)
PollutantS load (mg/L)
Time (Hr)
Hydrograph
TDS
TSS
DOC
10
9
8
7
6
5
4
3
2
1
0
350
300
250
200
150
100
50
0
2:57:59 AM
5:21:59 AM
7:45:59 AM
10:09:59 AM
12:33:59 PM
2:57:59 PM
5:21:59 PM

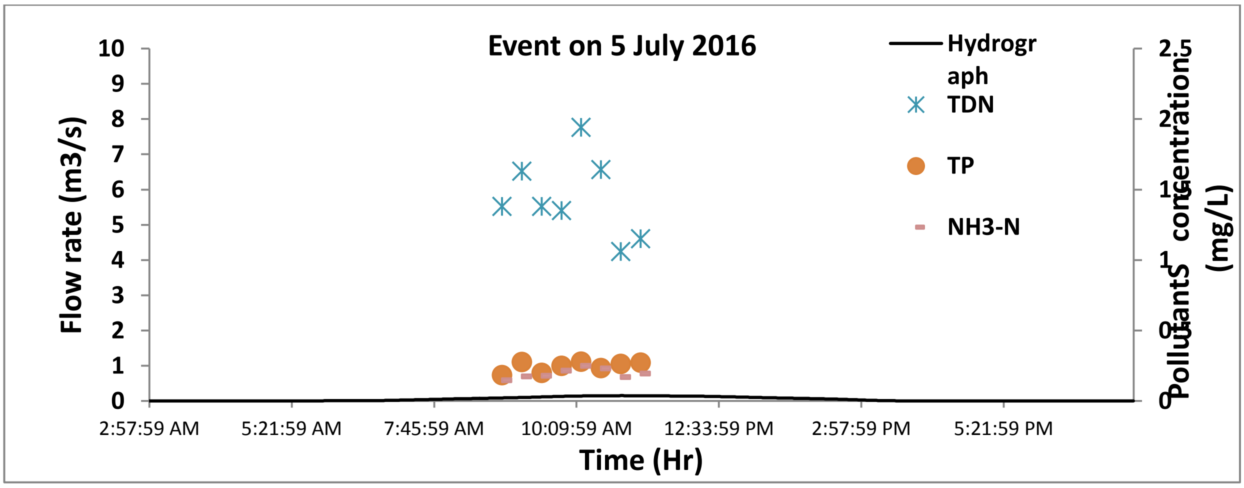
Event on 5 July 2016
Flow rate (m3/s)
PollutantS concentration (mg/L)
Time (Hr)
Hydrograph
TDN
TP
NH3-N
10
9
8
7
6
5
4
3
2
1
0
2.5
2
1.5
1
0.5
0
2:57:59 AM
5:21:59 AM
7:45:59 AM
10:09:59 AM
12:33:59 PM
2:57:59 PM
5:21:59 PM

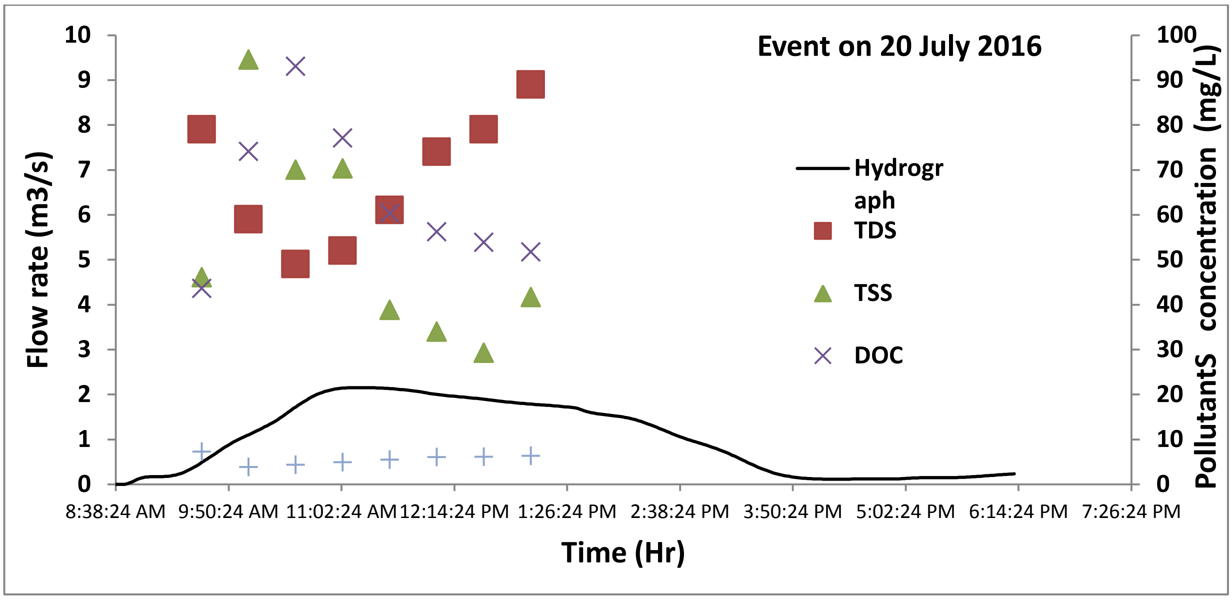
Event on 20 July 2016
Flow rate (m3/s)
PollutantS concentration (mg/L)
Time (Hr)
Hydrograph
TDS
TSS
DOC
0
1
2
3
4
5
6
7
8
9
10
0
10
20
30
40
50
60
70
80
90
100
8:38:24 AM
9:50:24 AM
11:02:24 AM
12:14:24 PM
1:26:24 PM
2:38:24 PM
3:50:24 PM
5:02:24 PM
6:14:24 PM
7:26:24 PM

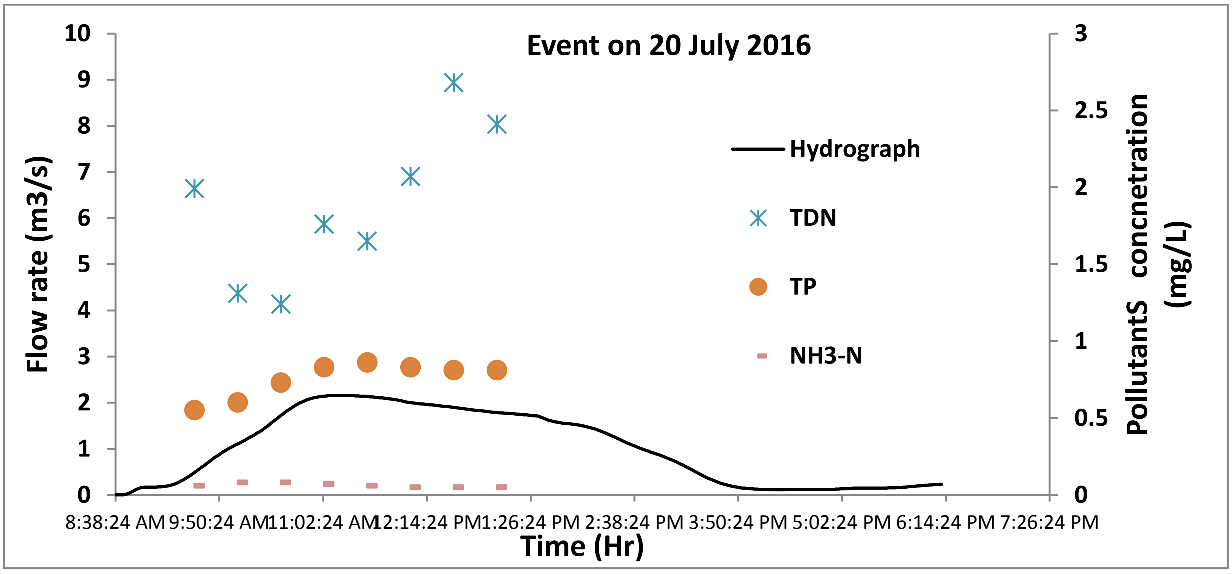
Event on 20 July 2016
Flow rate (m3/s)
PollutantS concnetration (mg/L)
Time (Hr)
Hydrograph
TDN
TP
NH3-N
0
1
2
3
4
5
6
7
8
9
10
0
0.5
1
1.5
2
2.5
3
8:38:24 AM
9:50:24 AM
11:02:24 AM
12:14:24 PM
1:26:24 PM
2:38:24 PM
3:50:24 PM
5:02:24 PM
6:14:24 PM
7:26:24 PM

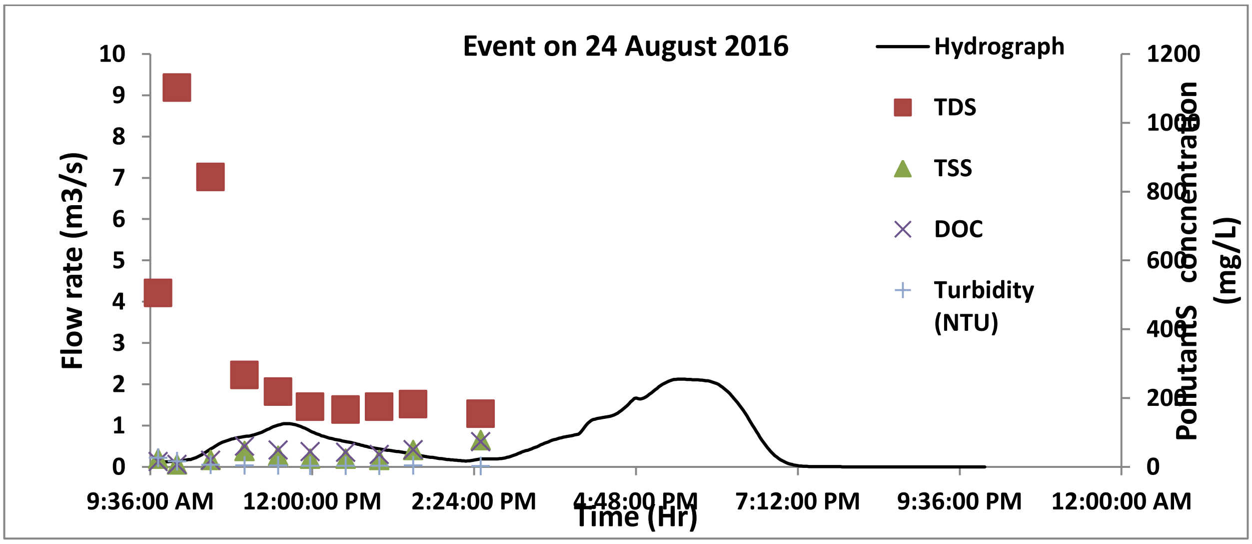
Event on 24 August 2016
Flow rate (m3/s)
PollutantS concnetration (mg/L)
Time (Hr)
Hydrograph
TDS
TSS
DOC
Turbidity (NTU)
0
1
2
3
4
5
6
7
8
9
10
0
200
400
600
800
1000
1200
9:36:00 AM
12:00:00 PM
2:24:00 PM
4:48:00 PM
7:12:00 PM
9:36:00 PM
12:00:00 AM

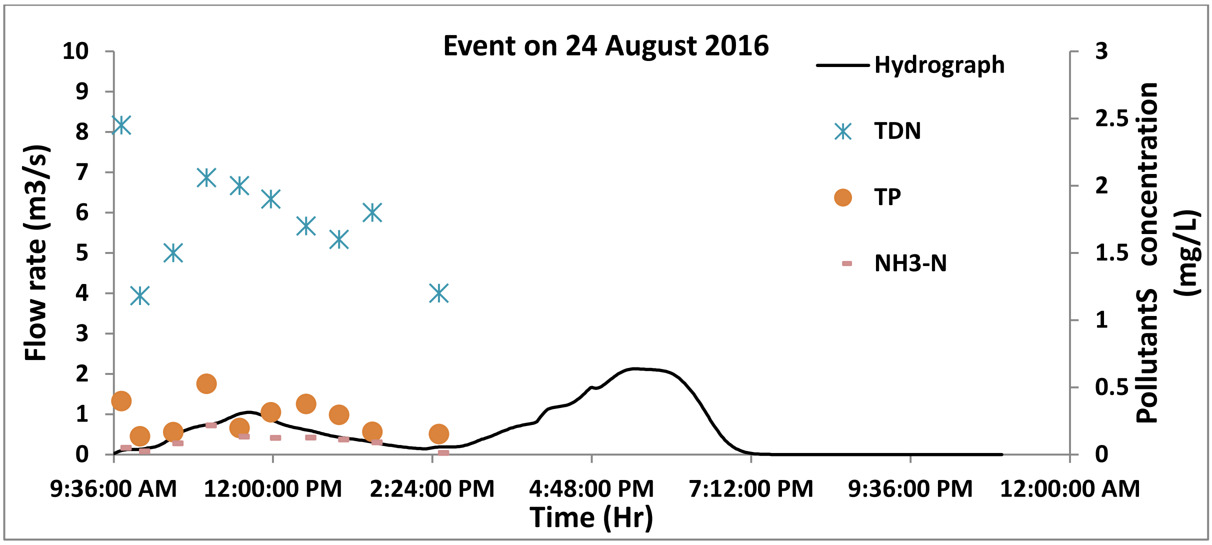
Event on 24 August 2016
Hydrograph
TDN
TP
NH3-N
Flow rate (m3/s)
PollutantS concentration (mg/L)
10
9
8
7
6
5
4
3
2
1
0
3
2.5
2
1.5
1
0.5
0
9:36:00 AM
12:00:00 PM
2:24:00 PM
4:48:00 PM
7:12:00 PM
9:36:00 PM
12:00:00 AM
Time (Hr)

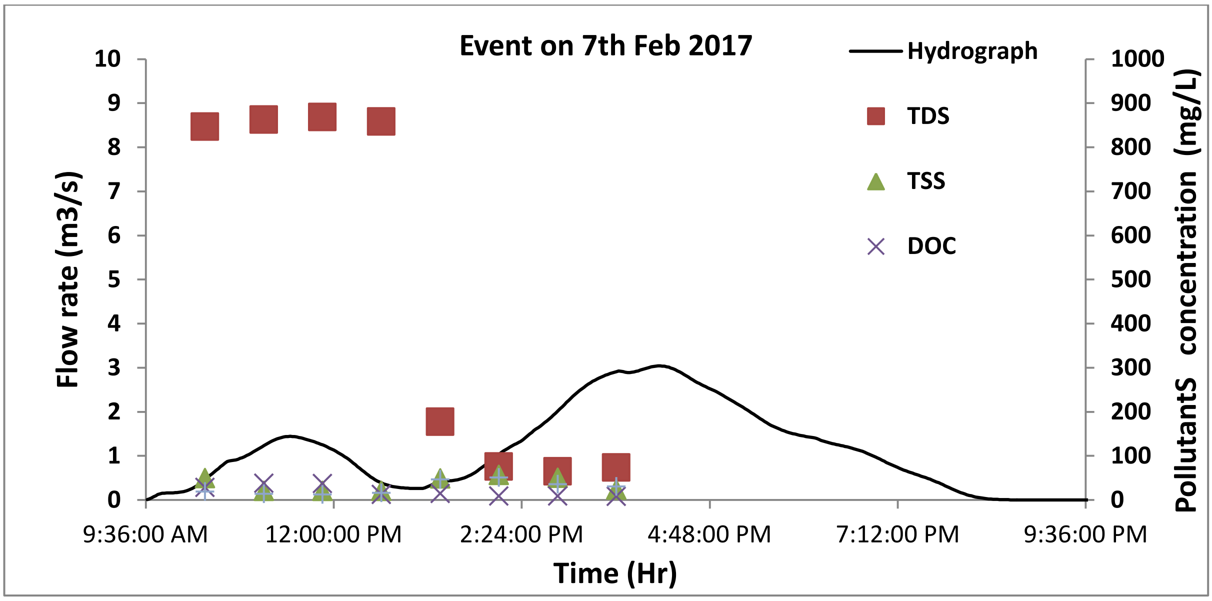
Event on 7th Feb 2017
Hydrograph
TDS
TSS
DOC
Flow rate (m3/s)
PollutantS concentration (mg/L)
10
9
8
7
6
5
4
3
2
1
0
1000
900
800
700
600
500
400
300
200
100
0
9:36:00 AM
12:00:00 PM
2:24:00 PM
4:48:00 PM
7:12:00 PM
9:36:00 PM
Time (Hr)

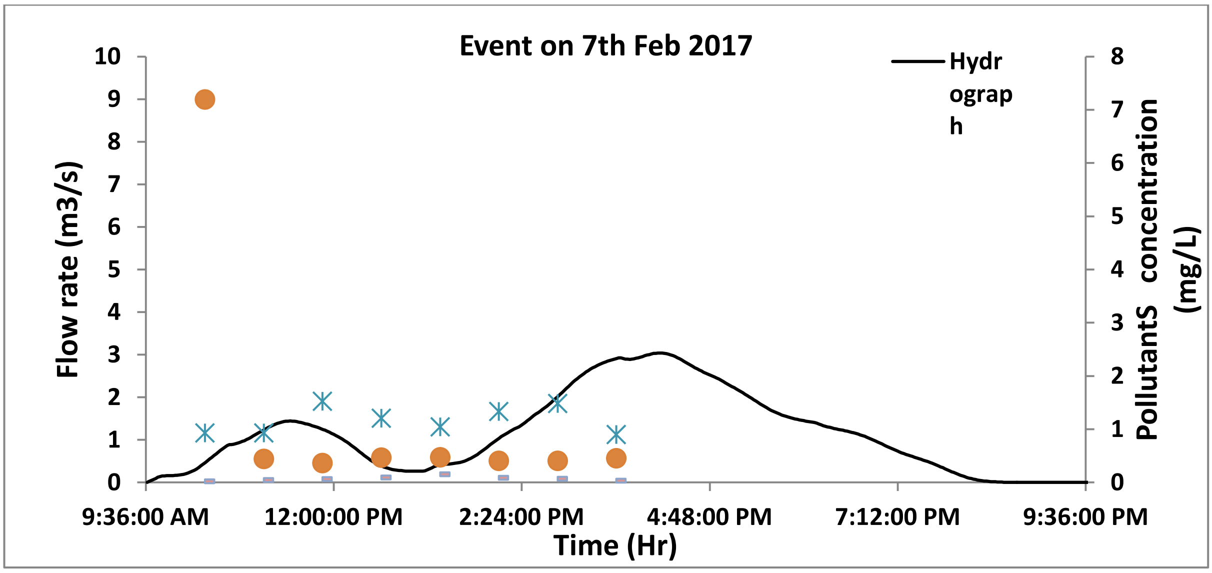
Event on 7th Feb 2017
Hydr ograp h
Flow rate (m3/s)
PollutantS concentration (mg/L)
10
9
8
7
6
5
4
3
2
1
0
8
7
6
5
4
3
2
1
0
9:36:00 AM
12:00:00 PM
2:24:00 PM
4:48:00 PM
7:12:00 PM
9:36:00 PM
Time (Hr)

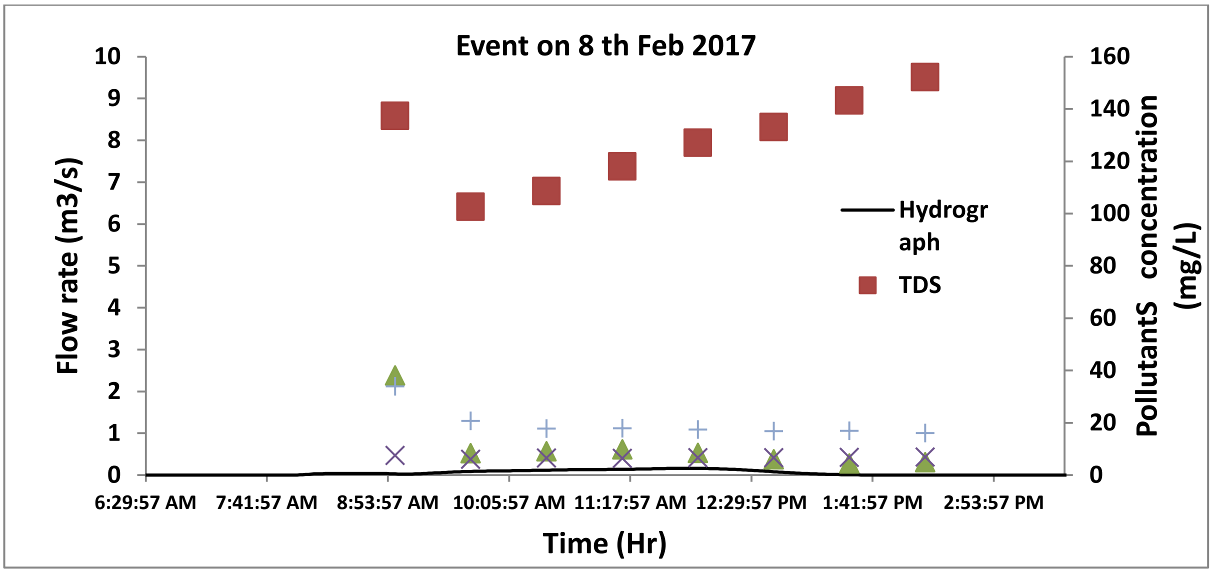
Event on 8 th Feb 2017
Flow rate (m3/s)
10
9
8
7
6
5
4
3
2
1
0
160
140
120
100
80
60
40
20
0
PollutantS concentration (mg/L)
Hydrograph
TDS
6:29:57 AM
7:41:57 AM
8:53:57 AM
10:05:57 AM
11:17:57 AM
12:29:57 PM
1:41:57 PM
2:53:57 PM
Time (Hr)

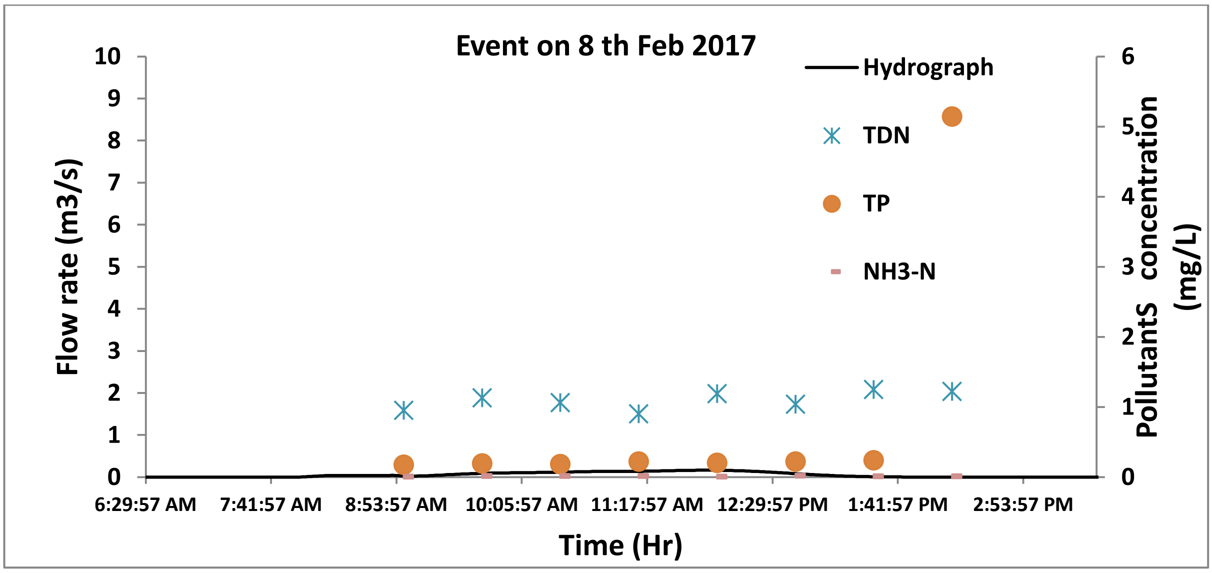
Event on 8 th Feb 2017
Flow rate (m3/s)
10
9
8
7
6
5
4
3
2
1
0
6
5
4
3
2
1
0
PollutantS concentration (mg/L)
Hydrograph
TDN
TP
NH3-N
6:29:57 AM
7:41:57 AM
8:53:57 AM
10:05:57 AM
11:17:57 AM
12:29:57 PM
1:41:57 PM
2:53:57 PM
Time (Hr)

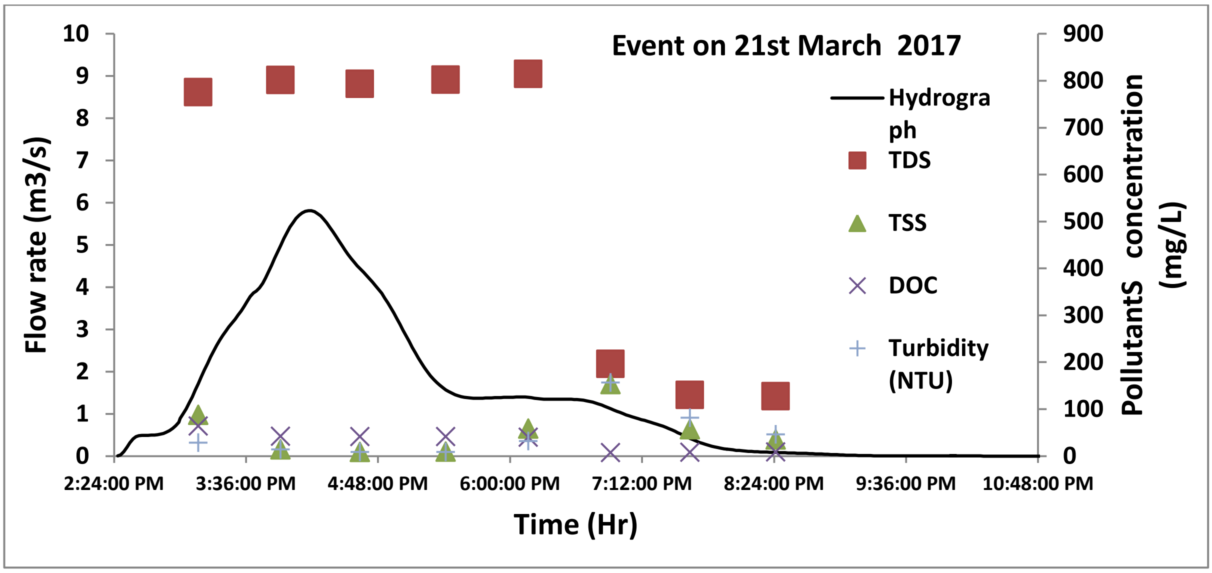
Event on 21st March 2017
Flow rate (m3/s)
10
9
8
7
6
5
4
3
2
1
0
900
800
700
600
500
400
300
200
100
0
PollutantS concentration (mg/L)
Hydrograph
TDS
TSS
DOC
Turbidity (NTU)
2:24:00 PM
3:36:00 PM
4:48:00 PM
6:00:00 PM
7:12:00 PM
8:24:00 PM
9:36:00 PM
10:48:00 PM
Time (Hr)

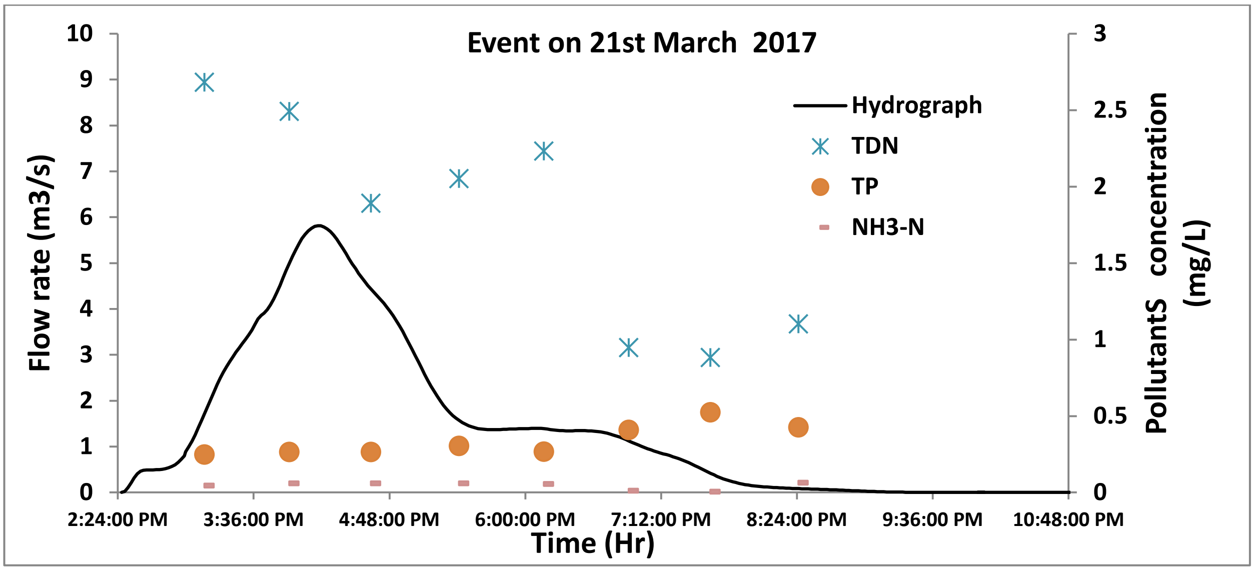
Event on 21st March 2017
Flow rate (m3/s)
PollutantS concentration (mg/L)
Time (Hr)
Hydrograph
TDN
TP
NH3-N
0
1
2
3
4
5
6
7
8
9
10
0
0.5
1
1.5
2
2.5
3
2:24:00 PM
3:36:00 PM
4:48:00 PM
6:00:00 PM
7:12:00 PM
8:24:00 PM
9:36:00 PM
10:48:00 PM

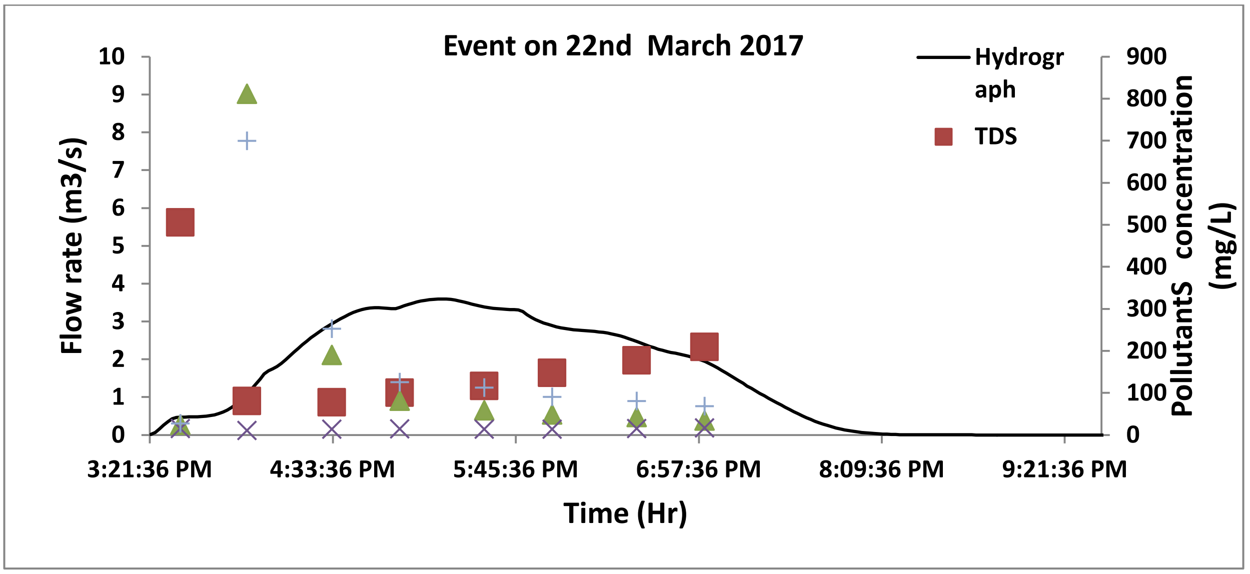
Event on 22nd March 2017
Flow rate (m3/s)
PollutantS concentration (mg/L)
Time (Hr)
Hydrograph
TDS
0
1
2
3
4
5
6
7
8
9
10
0
100
200
300
400
500
600
700
800
900
3:21:36 PM
4:33:36 PM
5:45:36 PM
6:57:36 PM
8:09:36 PM
9:21:36 PM

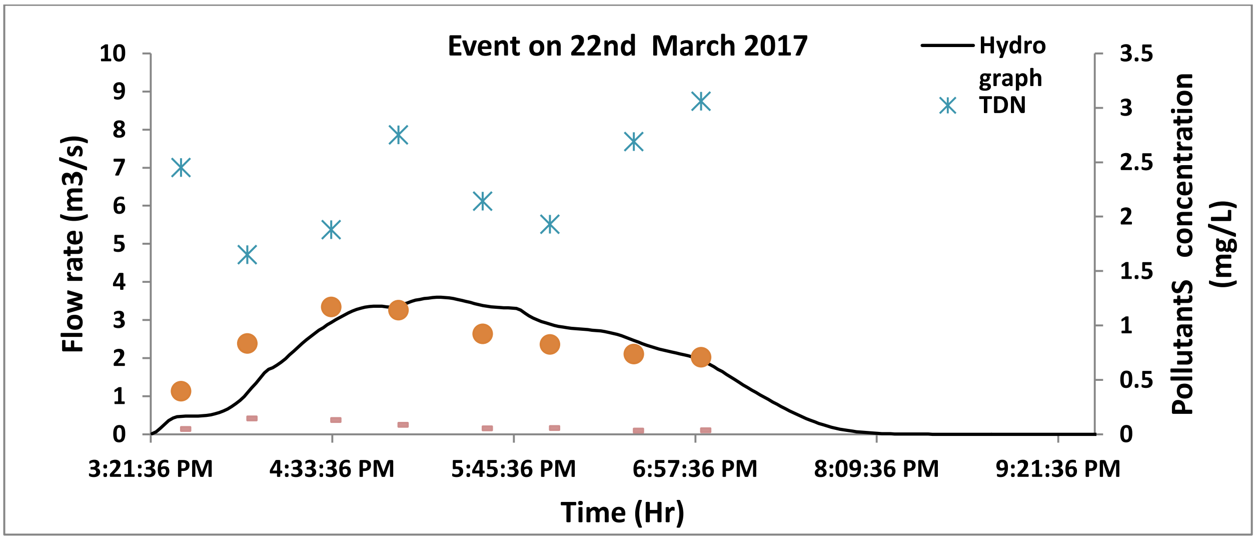
Event on 22nd March 2017
Flow rate (m3/s)
PollutantS concentration (mg/L)
Time (Hr)
Hydrograph
TDN
0
1
2
3
4
5
6
7
8
9
10
0
0.5
1
1.5
2
2.5
3
3.5
3:21:36 PM
4:33:36 PM
5:45:36 PM
6:57:36 PM
8:09:36 PM
9:21:36 PM

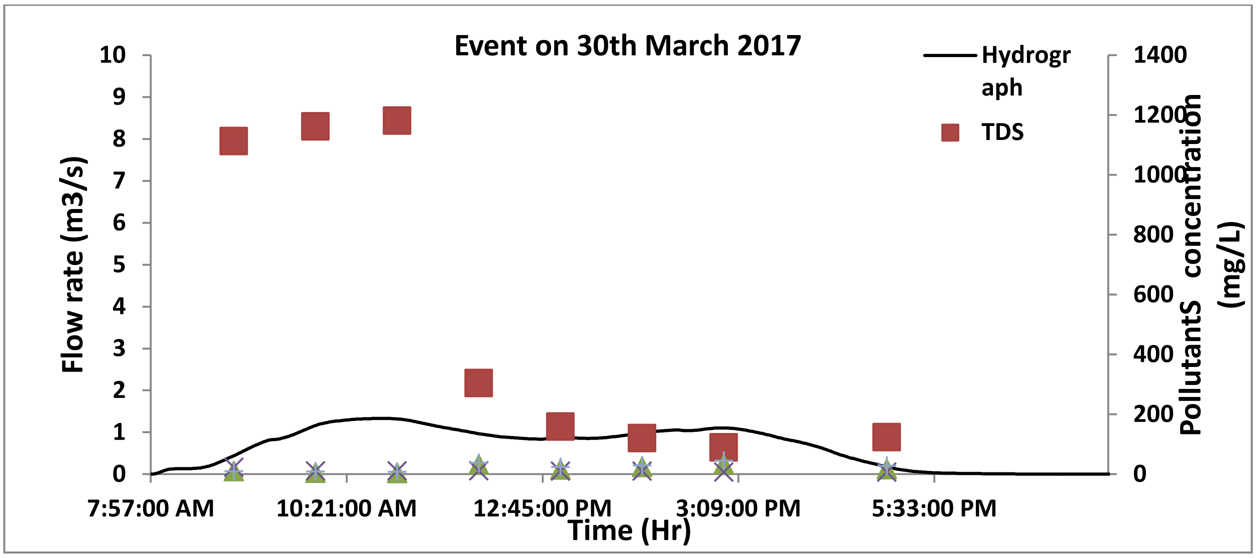
Event on 30th March 2017
Flow rate (m3/s)
Time (Hr)
PollutantS concentration (mg/L)
Hydrograph
TDS
0
1
2
3
4
5
6
7
8
9
10
0
200
400
600
800
1000
1200
1400
7:57:00 AM
10:21:00 AM
12:45:00 PM
3:09:00 PM
5:33:00 PM

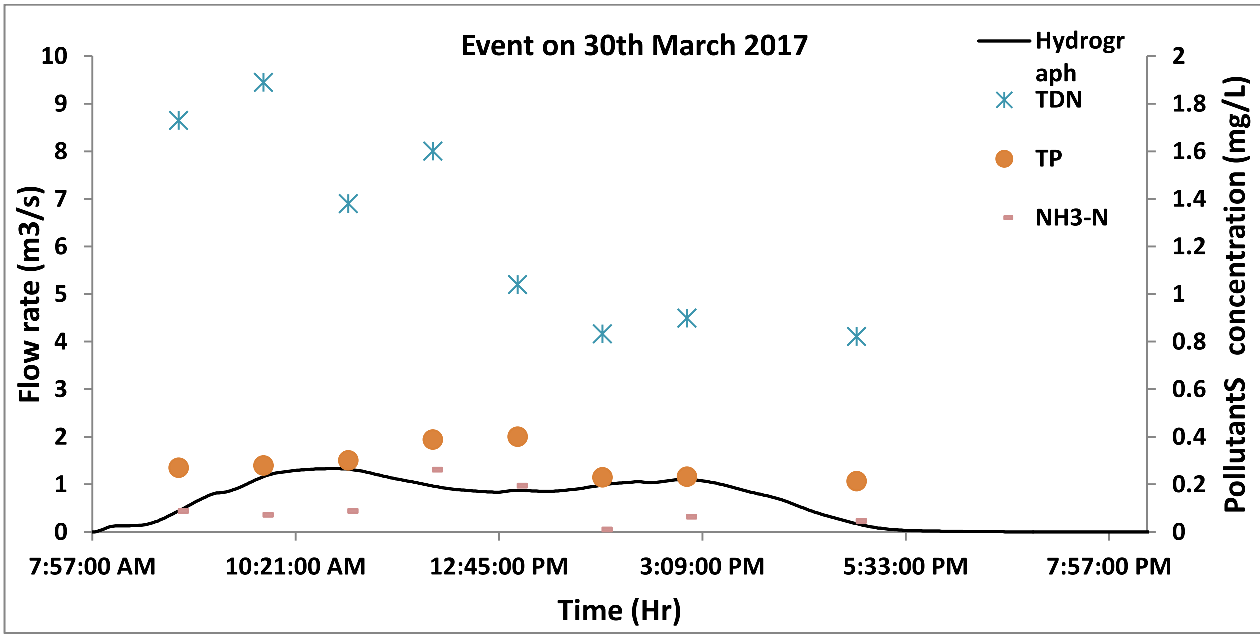
Event on 30th March 2017
Flow rate (m3/s)
Time (Hr)
PollutantS concentration (mg/L)
Hydrograph
TDN
TP
NH3-N
0
1
2
3
4
5
6
7
8
9
10
0
0.2
0.4
0.6
0.8
1
1.2
1.4
1.6
1.8
2
7:57:00 AM
10:21:00 AM
12:45:00 PM
3:09:00 PM
5:33:00 PM
7:57:00 PM

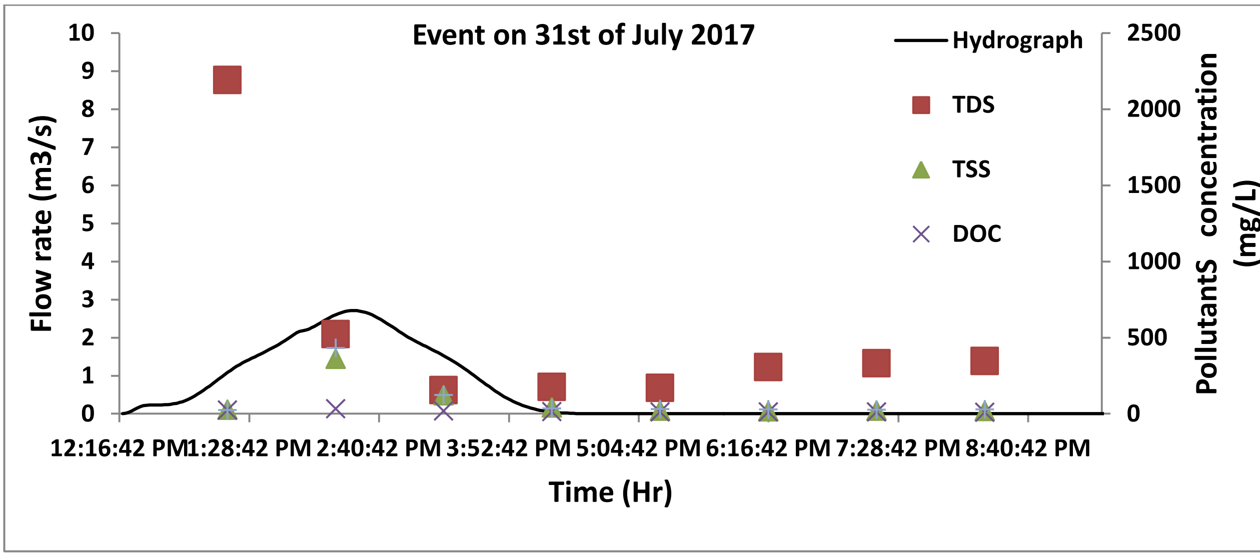
Event on 31st of July 2017
Flow rate (m3/s)
Time (Hr)
PollutantS concentration (mg/L)
Hydrograph
TDS
TSS
DOC
0
1
2
3
4
5
6
7
8
9
10
0
500
1000
1500
2000
2500
12:16:42 PM
1:28:42 PM
2:40:42 PM
3:52:42 PM
5:04:42 PM
6:16:42 PM
7:28:42 PM
8:40:42 PM

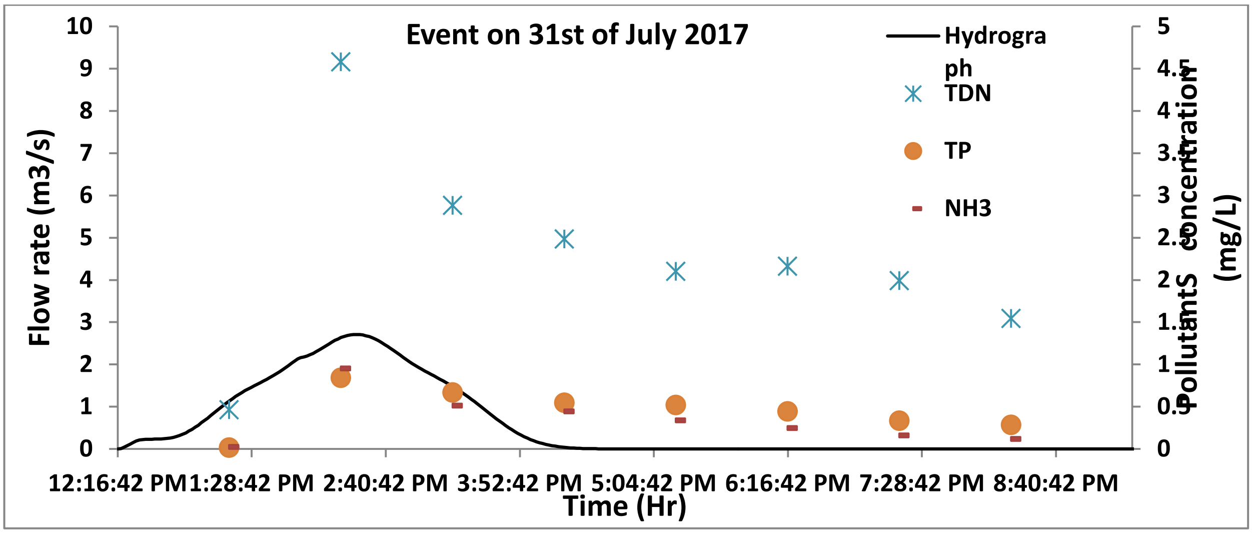
Event on 31st of July 2017
Flow rate (m3/s)
10
9
8
7
6
5
4
3
2
1
0
12:16:42 PM
1:28:42 PM
2:40:42 PM
3:52:42 PM
5:04:42 PM
6:16:42 PM
7:28:42 PM
8:40:42 PM
Time (Hr)
5
4.5
4
3.5
3
2.5
2
1.5
1
0.5
0
PollutantS concentration (mg/L)
Hydrograph
TDN
TP
NH3

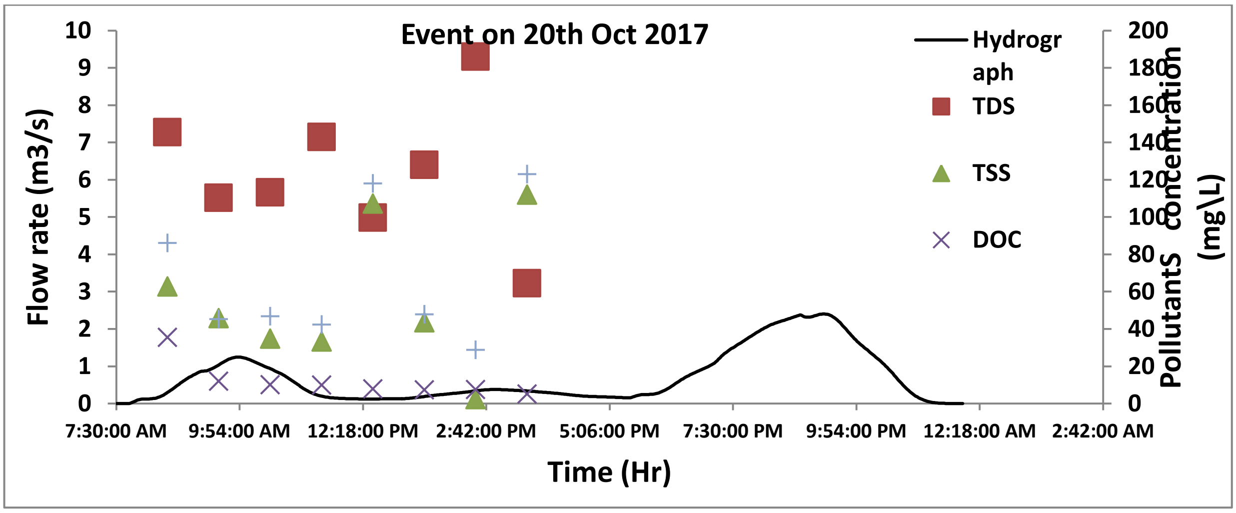
Event on 20th Oct 2017
Flow rate (m3/s)
10
9
8
7
6
5
4
3
2
1
0
7:30:00 AM
9:54:00 AM
12:18:00 PM
2:42:00 PM
5:06:00 PM
7:30:00 PM
9:54:00 PM
12:18:00 AM
2:42:00 AM
Time (Hr)
200
180
160
140
120
100
80
60
40
20
0
PollutantS concentration (mg\L)
Hydrograph
TDS
TSS
DOC

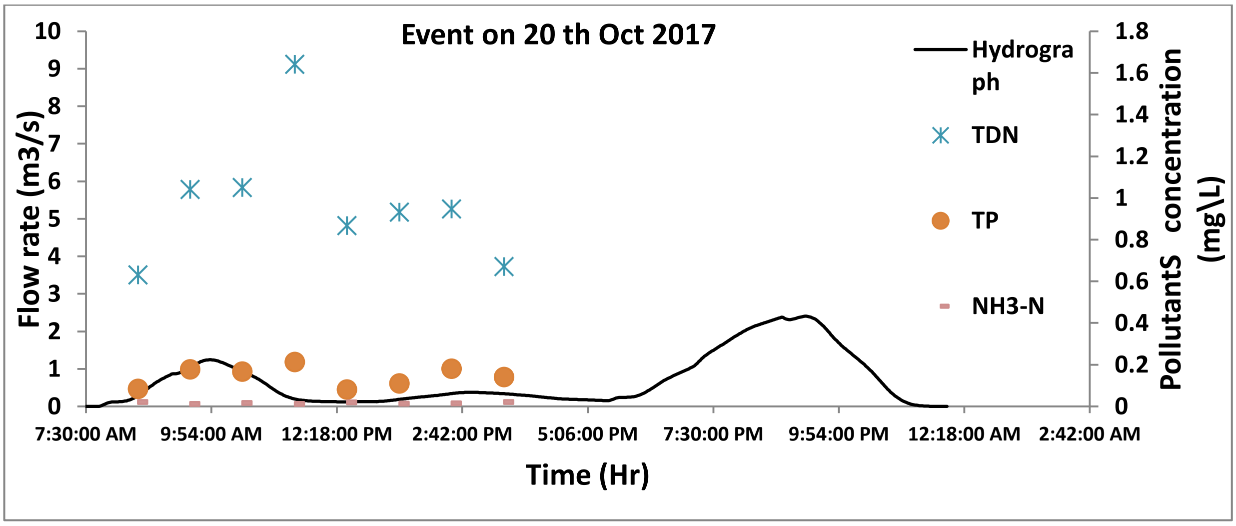
Event on 20 th Oct 2017
Flow rate (m3/s)
10
9
8
7
6
5
4
3
2
1
0
7:30:00 AM
9:54:00 AM
12:18:00 PM
2:42:00 PM
5:06:00 PM
7:30:00 PM
9:54:00 PM
12:18:00 AM
2:42:00 AM
Time (Hr)
1.8
1.6
1.4
1.2
1
0.8
0.6
0.4
0.2
0
PollutantS concentration (mg\L)
Hydrograph
TDN
TP
NH3-N

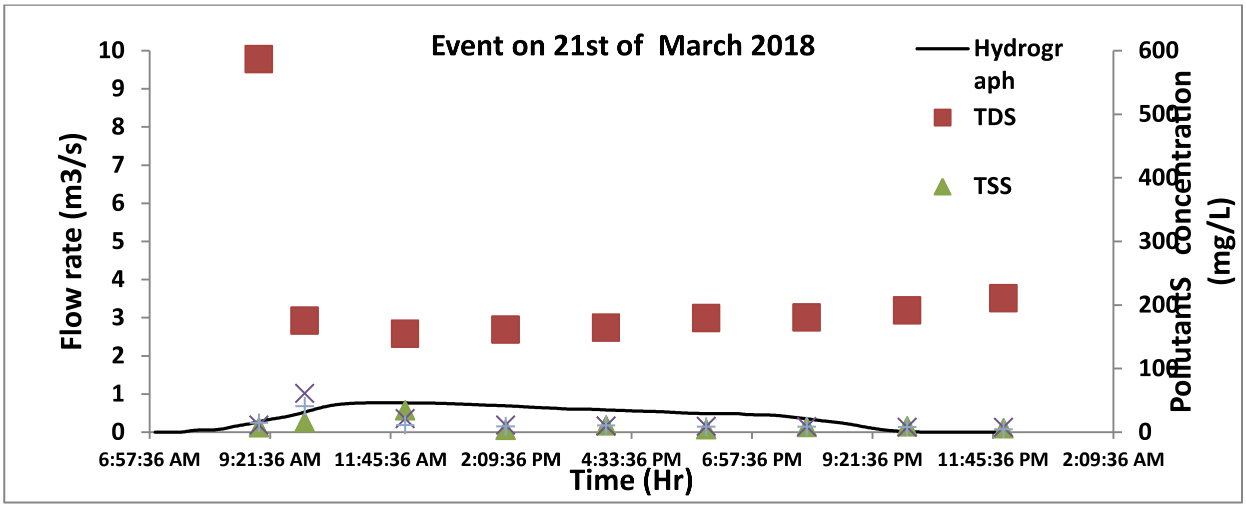
Event on 21st of March 2018
Hydrograph
TDS
TSS
Flow rate (m3/s)
10
9
8
7
6
5
4
3
2
1
0
600
500
400
300
200
100
0
Pollutants concentration (mg/L)
6:57:36 AM
9:21:36 AM
11:45:36 AM
2:09:36 PM
4:33:36 PM
6:57:36 PM
9:21:36 PM
11:45:36 PM
2:09:36 AM
Time (Hr)

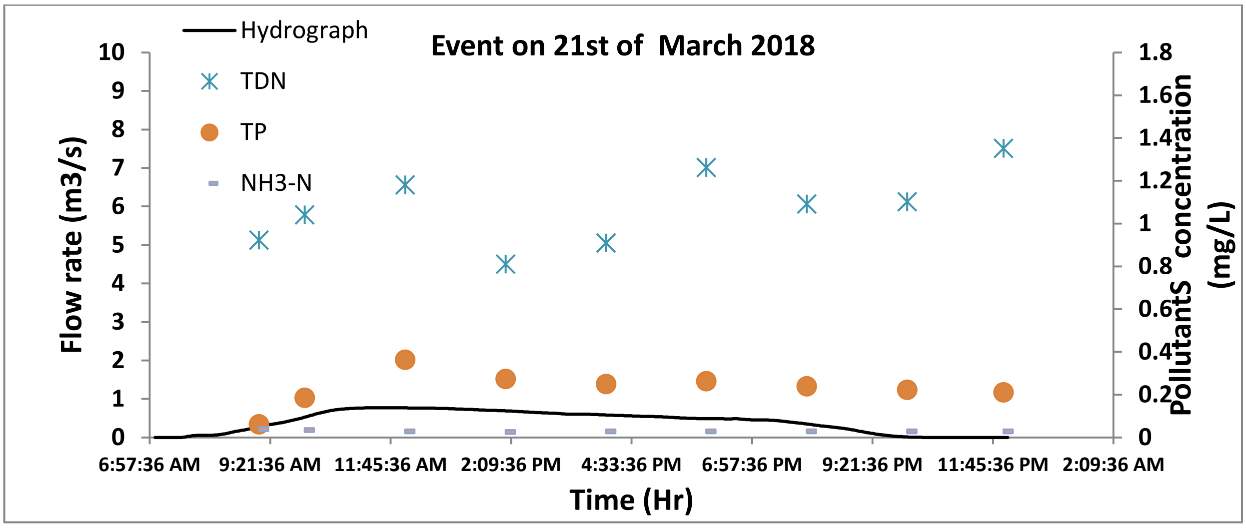
Event on 21st of March 2018
Hydrograph
TDN
TP
NH3-N
Flow rate (m3/s)
10
9
8
7
6
5
4
3
2
1
0
1.8
1.6
1.4
1.2
1
0.8
0.6
0.4
0.2
0
Pollutants concentration (mg/L)
6:57:36 AM
9:21:36 AM
11:45:36 AM
2:09:36 PM
4:33:36 PM
6:57:36 PM
9:21:36 PM
11:45:36 PM
2:09:36 AM
Time (Hr)

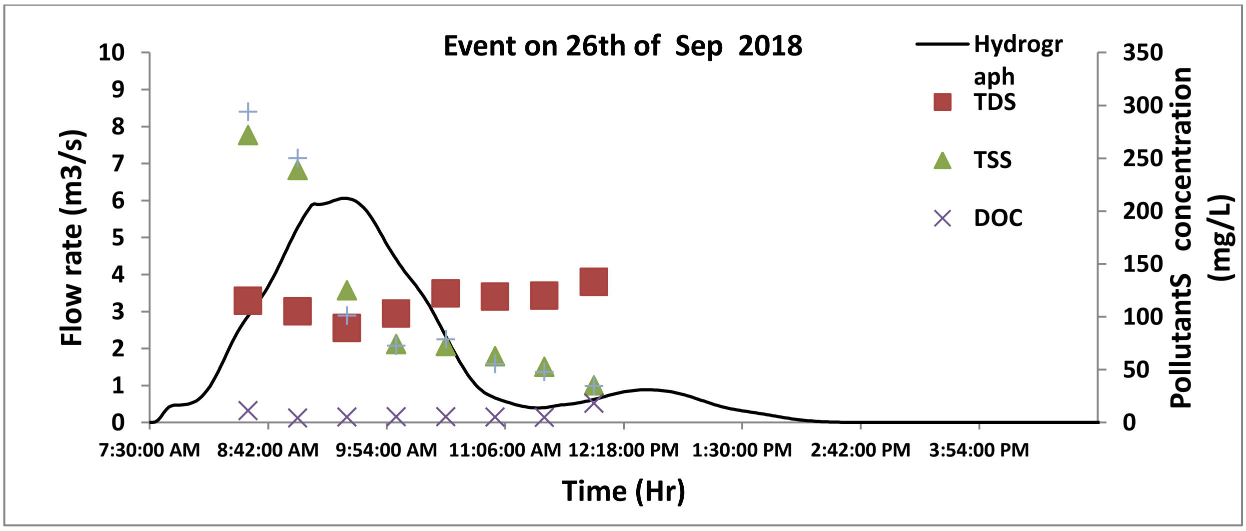
Event on 26th of Sep 2018
Hydrograph
TDS
TSS
DOC
Flow rate (m3/s)
10
9
8
7
6
5
4
3
2
1
0
350
300
250
200
150
100
50
0
Pollutants concentration (mg/L)
7:30:00 AM
8:42:00 AM
9:54:00 AM
11:06:00 AM
12:18:00 PM
1:30:00 PM
2:42:00 PM
3:54:00 PM
Time (Hr)

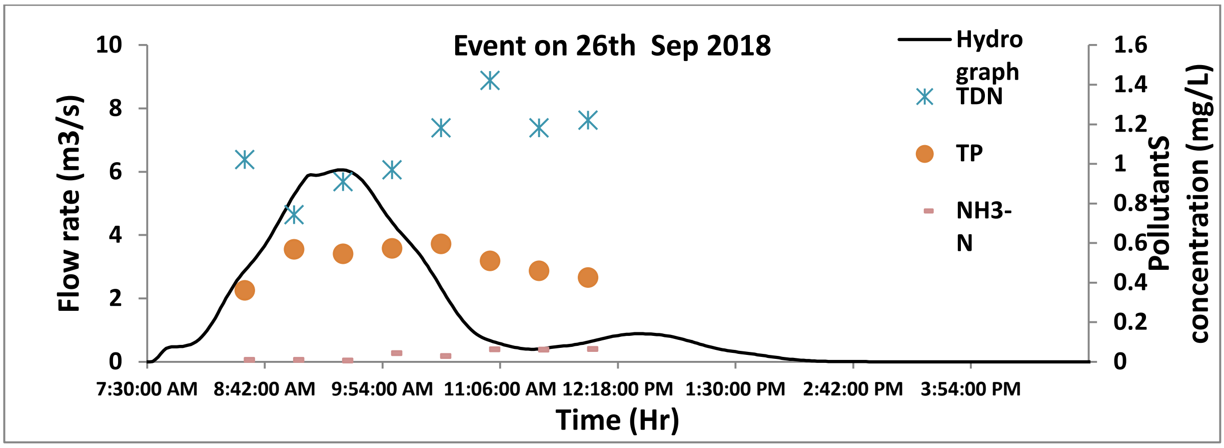
Event on 26th Sep 2018
Flow rate (m3/s)
0
2
4
6
8
10
PollutantS concentration (mg/L)
0
0.2
0.4
0.6
0.8
1
1.2
1.4
1.6
7:30:00 AM
8:42:00 AM
9:54:00 AM
11:06:00 AM
12:18:00 PM
1:30:00 PM
2:42:00 PM
3:54:00 PM
Time (Hr)
Hydrograph
TDN
TP
NH3-N

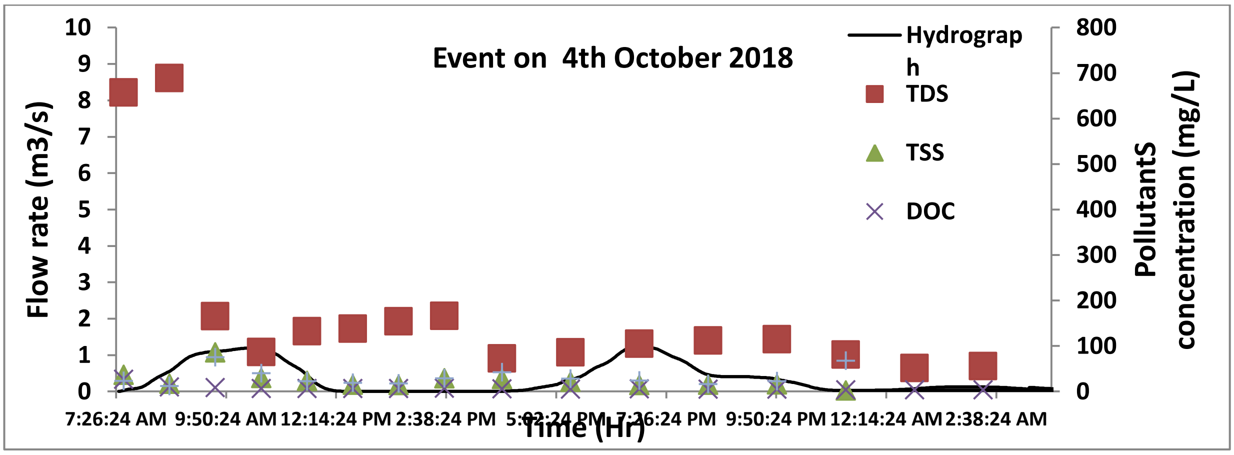
Event on 4th October 2018
Flow rate (m3/s)
0
1
2
3
4
5
6
7
8
9
10
PollutantS concentration (mg/L)
0
100
200
300
400
500
600
700
800
7:26:24 AM
9:50:24 AM
12:14:24 PM
2:38:24 PM
5:02:24 PM
7:26:24 PM
9:50:24 PM
12:14:24 AM
2:38:24 AM
Time (Hr)
Hydrograph
TDS
TSS
DOC

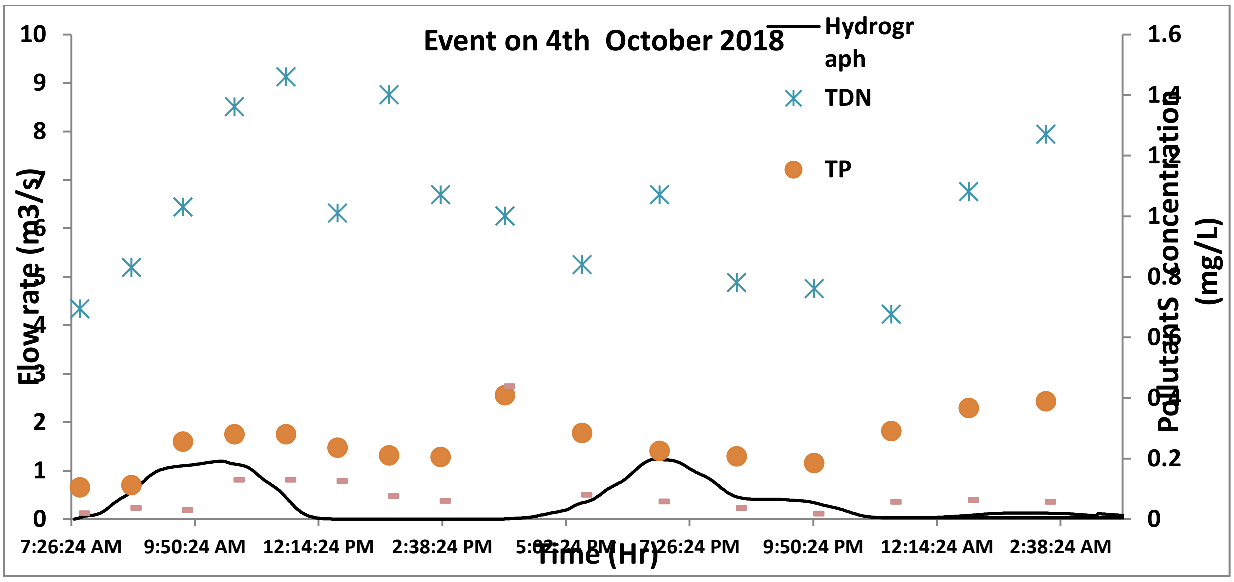
Event on 4th October 2018
Flow rate (m3/s)
0
1
2
3
4
5
6
7
8
9
10
PollutantS concentration (mg/L)
0
0.2
0.4
0.6
0.8
1
1.2
1.4
1.6
7:26:24 AM
9:50:24 AM
12:14:24 PM
2:38:24 PM
5:02:24 PM
7:26:24 PM
9:50:24 PM
12:14:24 AM
2:38:24 AM
Time (Hr)
Hydrograph
TDN
TP

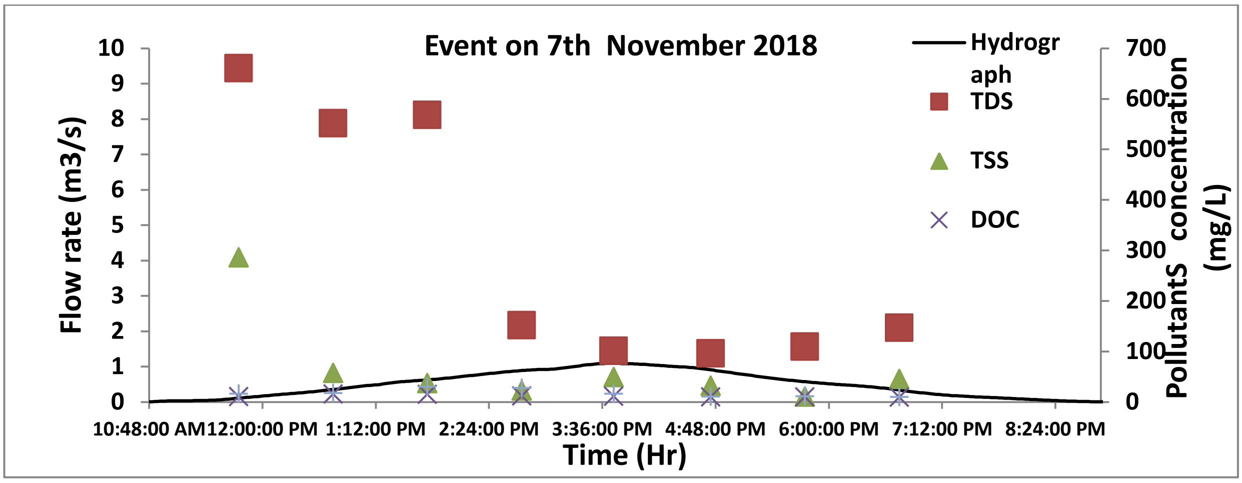
Event on 7th November 2018
Hydrograph
TDS
TSS
DOC
Flow rate (m3/s)
PollutantS concentration (mg/L)
Time (Hr)
0
1
2
3
4
5
6
7
8
9
10
0
100
200
300
400
500
600
700
10:48:00 AM
12:00:00 PM
1:12:00 PM
2:24:00 PM
3:36:00 PM
4:48:00 PM
6:00:00 PM
7:12:00 PM
8:24:00 PM

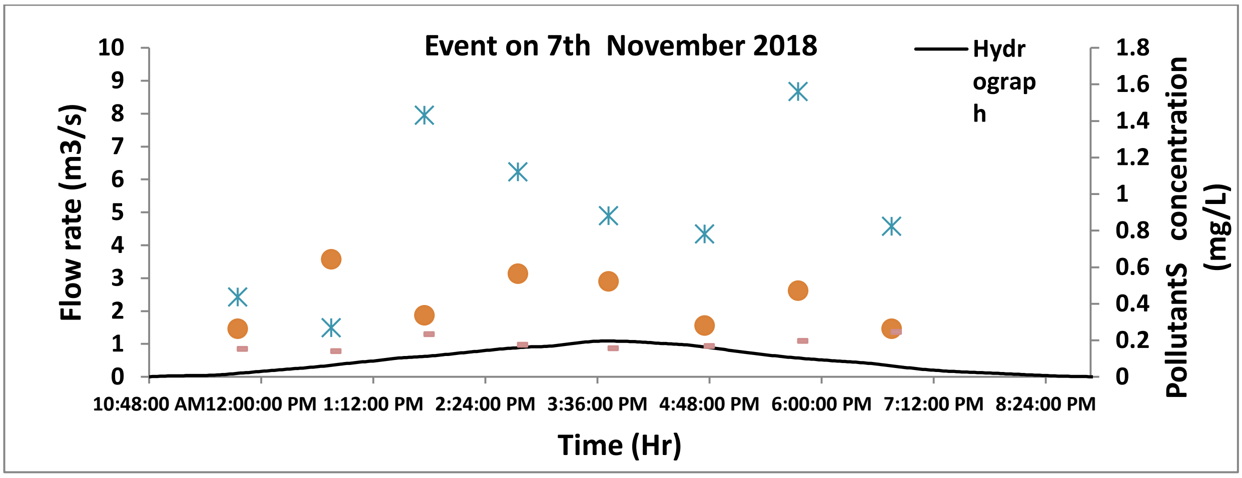
Event on 7th November 2018
Hydrograph
Flow rate (m3/s)
PollutantS concentration (mg/L)
Time (Hr)
0
1
2
3
4
5
6
7
8
9
10
0
0.2
0.4
0.6
0.8
1
1.2
1.4
1.6
1.8
10:48:00 AM
12:00:00 PM
1:12:00 PM
2:24:00 PM
3:36:00 PM
4:48:00 PM
6:00:00 PM
7:12:00 PM
8:24:00 PM

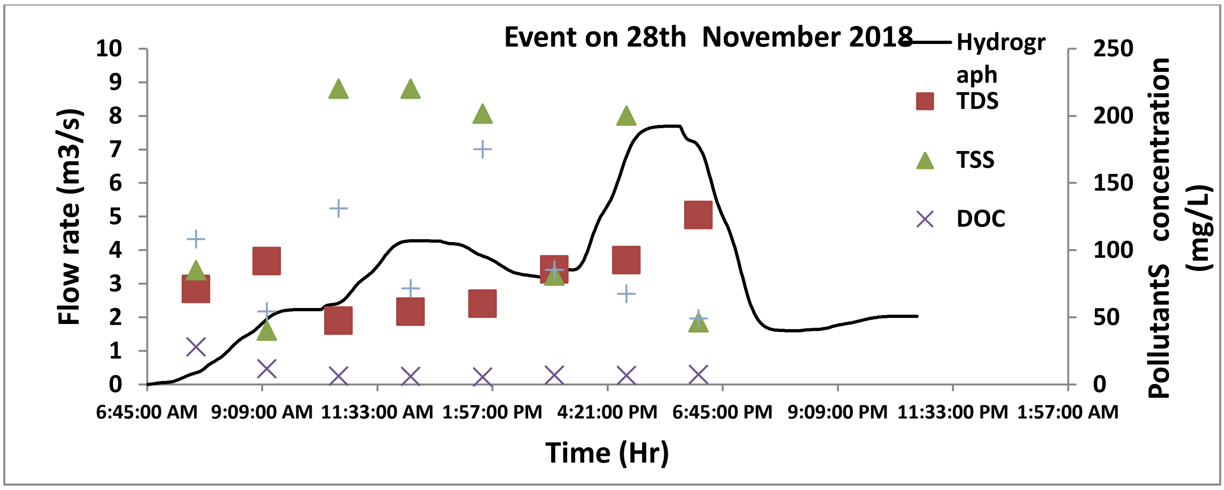
Event on 28th November 2018
Hydrograph
TDS
TSS
DOC
Flow rate (m3/s)
PollutantS concentration (mg/L)
Time (Hr)
0
1
2
3
4
5
6
7
8
9
10
0
50
100
150
200
250
6:45:00 AM
9:09:00 AM
11:33:00 AM
1:57:00 PM
4:21:00 PM
6:45:00 PM
9:09:00 PM
11:33:00 PM
1:57:00 AM

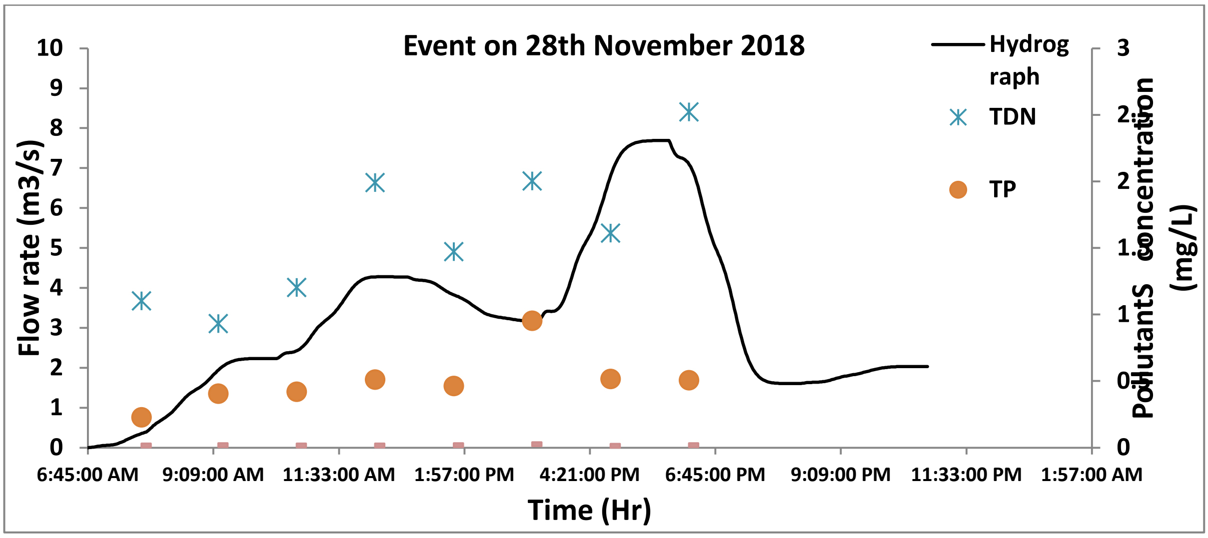
Event on 28th November 2018
Hydrograph
TDN
TP
Flow rate (m3/s)
Pollutants concentration (mg/L)
Time (Hr)
10
9
8
7
6
5
4
3
2
1
0
3
2.5
2
1.5
1
0.5
0
6:45:00 AM
9:09:00 AM
11:33:00 AM
1:57:00 PM
4:21:00 PM
6:45:00 PM
9:09:00 PM
11:33:00 PM
1:57:00 AM

Appendix B

Simultaneous removal of polycyclic aromatic hydrocarbons and heavy metals from water using granular activated carbon

Table B.1. Kinetic model parameter values for the adsorption of acenaphthylene and phenanthrene on GAC in the presence of 0.005 M $NaNO_3$ (GAC 0.3 g/L, PAH 1 mg/L, Metals 20 mg/L).

PAH	Metal	Pseudo-first order			Pseudo-second order			Experimental
		q_m mg/g	k_1 h^{-1}	R^2	q_m mg/g	k_2 g/mg/h	R^2	q_m (mg/g)
Acenaphthylene	0	3.70	0.56	0.973	5.89	3.7	0.973	3.43
	Cu	3.25	0.37	0.974	4.00	0.34	0.809	3.18
	Zn	3.85	0.56	0.846	5.9	0.26	0.812	3.20
	Cd	4.30	0.66	0.872	6.93	0.18	0.642	3.34
Phenanthrene	0	3.05	0.56	0.948	3.66	0.42	0.686	2.87
	Cu	2.68	0.32	0.967	3.35	0.16	0.459	2.61
	Zn	2.34	0.25	0.825	3.57	0.43	0.794	2.66
	Cd	3.89	0.72	0.755	3.57	0.43	0.732	2.80

Table B.2. Kinetic model parameter values for the adsorption of metals on GAC in the presence of acenaphthylene, phenanthrene and 0.005 M $NaNO_3$ (GAC 0.3 g/L, PAH 1 mg/L, Metals 20 mg/L)

Metal		Pseudo-first order			Pseudo-second order			Experimental
		q_m mg/g	k_1 h^{-1}	R^2	q_m mg/g	k_2 g/mg/h	R^2	q_m (mg/g)
Cu	0	3.94	0.29	0.919	4.64	0.66	0.996	4.67
Zn	0	3.7	0.26	0.969	4.54	0.61	0.989	4.34
Cd	0	2.31	0.24	0.894	2.42	1.17	0.961	2.94
Cu	Acenaphthylene	2.41	0.38	0.615	4.72	0.36	0.858	4.09
Zn	Acenaphthylene	2.22	0.38	0.615	4.29	0.42	0.914	3.95
Cd	Acenaphthylene	1.91	0.47	0.893	2.21	0.79	0.939	2.66
Cu	Phenanthrene	2.00	0.25	0.727	2.69	0.63	0.944	3.08
Zn	Phenanthrene	2.04	0.32	0.645	3.29	0.53	0.91	3.45
Cd	Phenanthrene	1.68	0.18	0.799	1.62	0.84	0.958	1.96

Fig. B.1. Absorbance spectra for different concentrations of acenaphthylene and phenanthrene

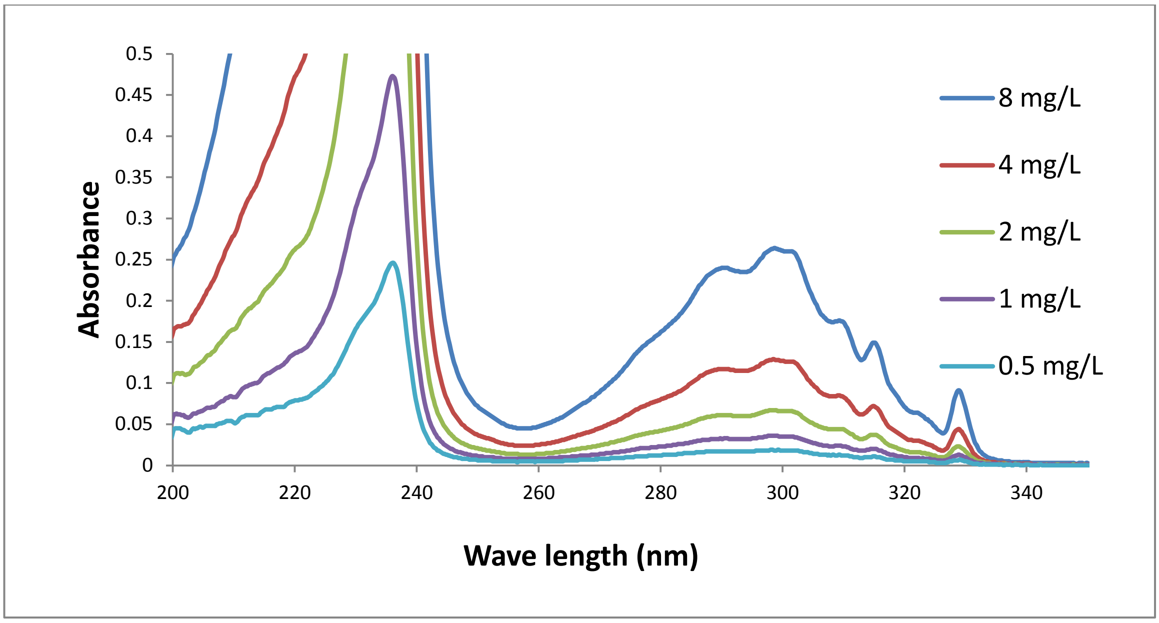

Acenaphthylene

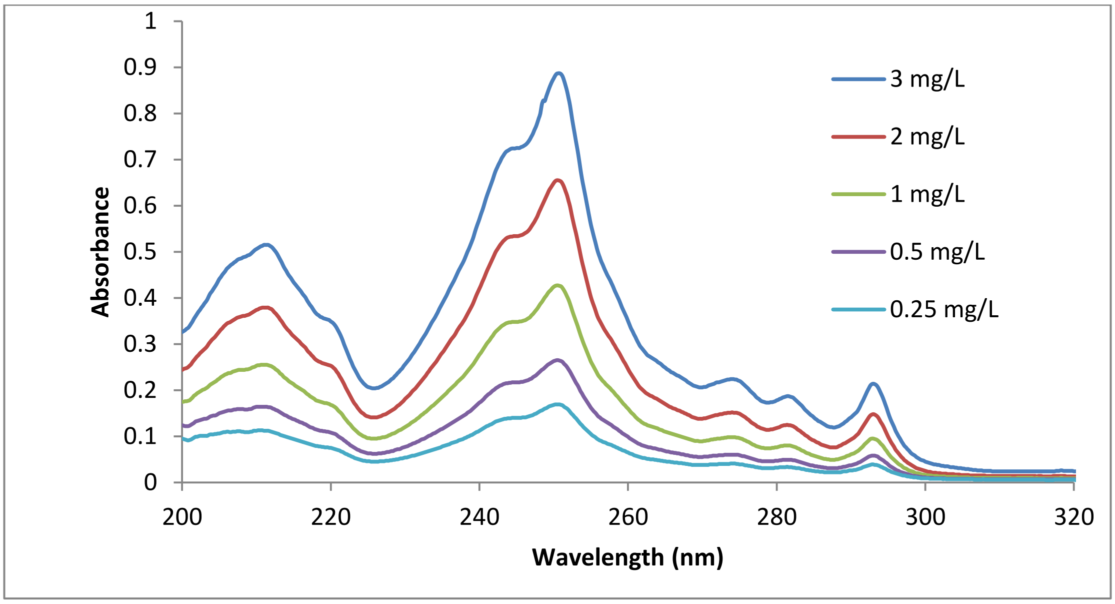

Phenanthrene

Fig. B.2. Calibration graphs of absorbance vs PAH concentration

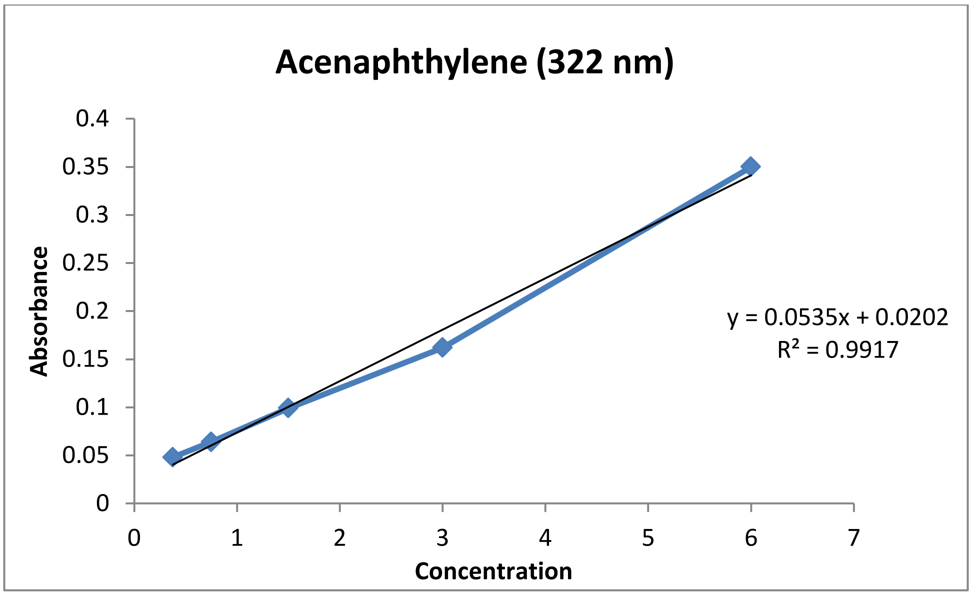

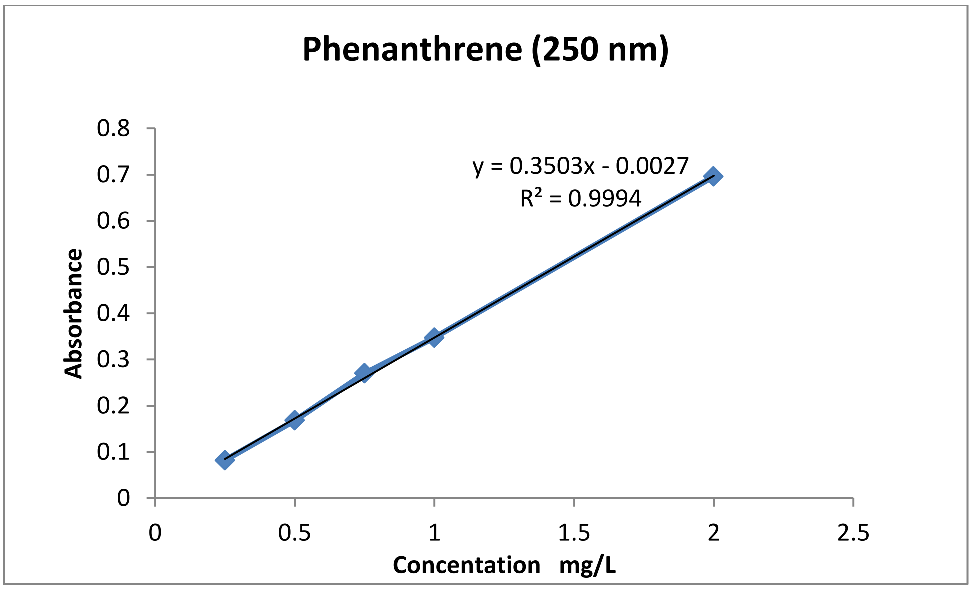

Fig. B.3. Absorbance spectra for acenaphthylene (1 mg/L) in the presence of different concentrations of Cu, Zn, and Cd

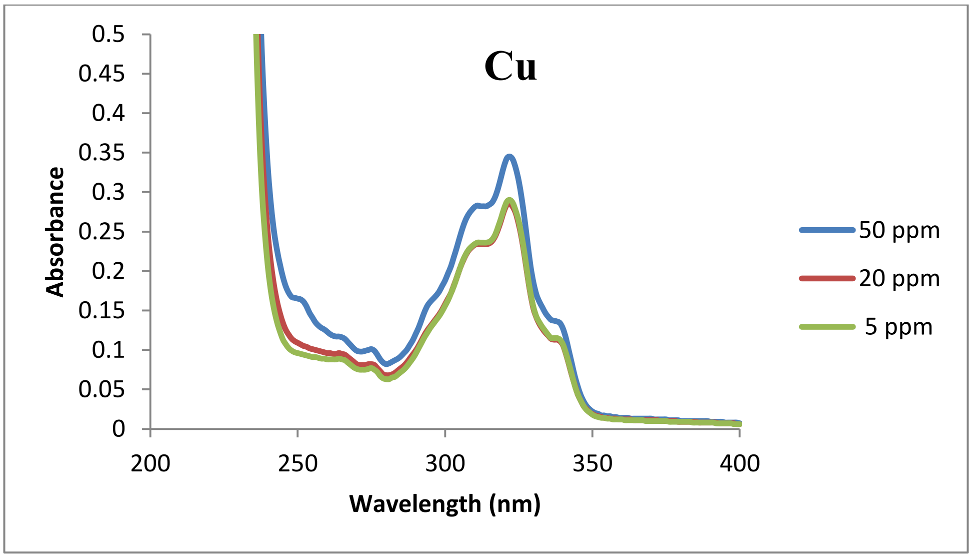
Cu
Absorbance
0.5
0.45
0.4
0.35
0.3
0.25
0.2
0.15
0.1
0.05
0
200
250
300
350
400
Wavelength (nm)
50 ppm
20 ppm
5 ppm

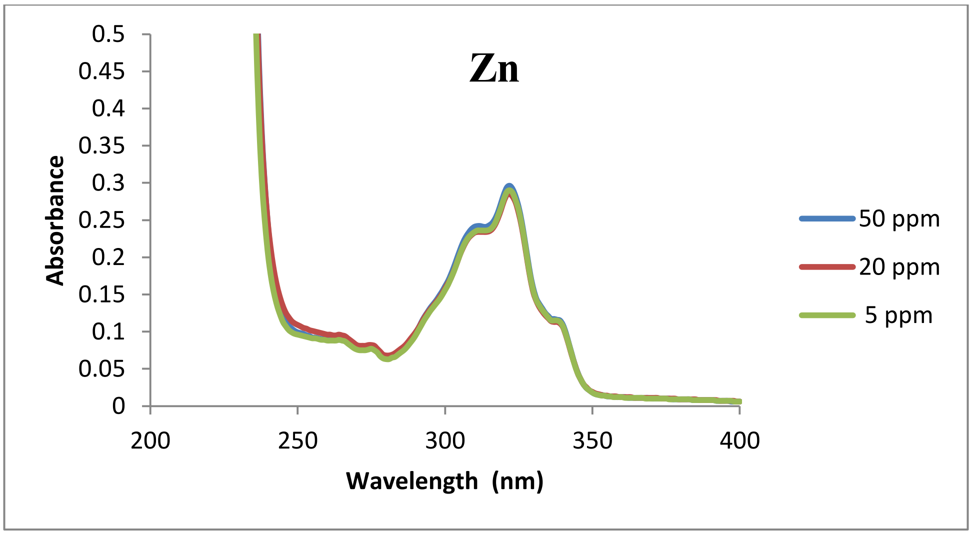
Zn
Absorbance
0.5
0.45
0.4
0.35
0.3
0.25
0.2
0.15
0.1
0.05
0
200
250
300
350
400
Wavelength (nm)
50 ppm
20 ppm
5 ppm

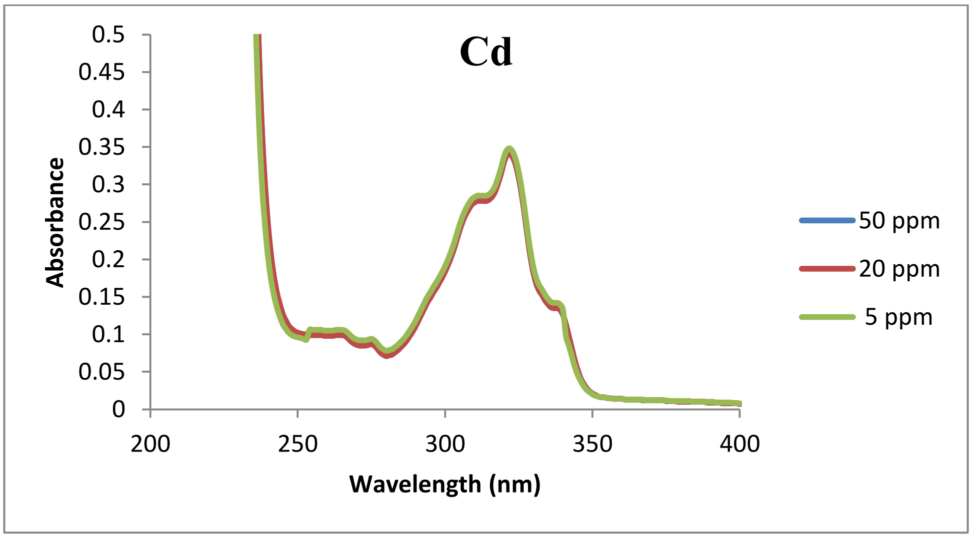
Cd
Absorbance
0.5
0.45
0.4
0.35
0.3
0.25
0.2
0.15
0.1
0.05
0
200
250
300
350
400
Wavelength (nm)
50 ppm
20 ppm
5 ppm

Fig. B.4. Absorbance spectra for phenanthrene (1 mg/L) in the presence of different concentrations of Cu, Zn, and Cd

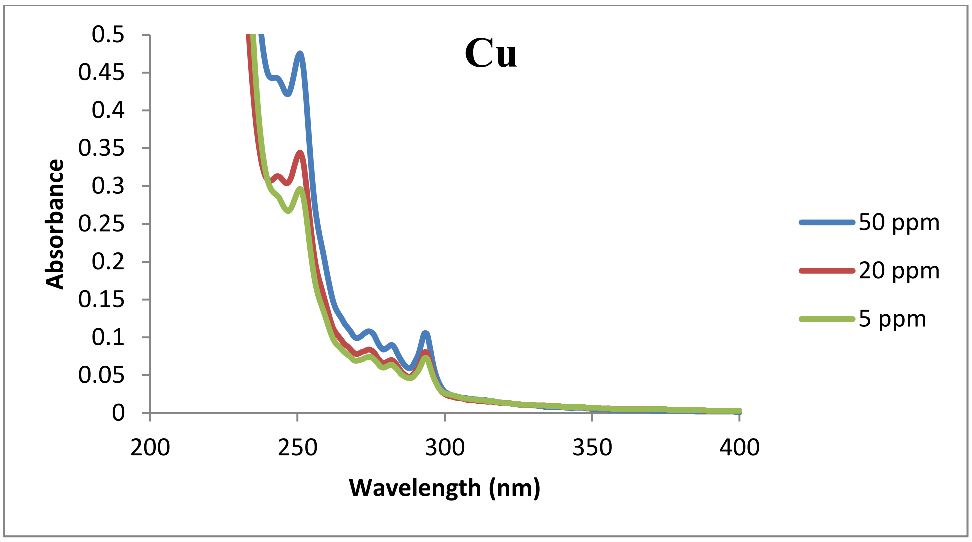

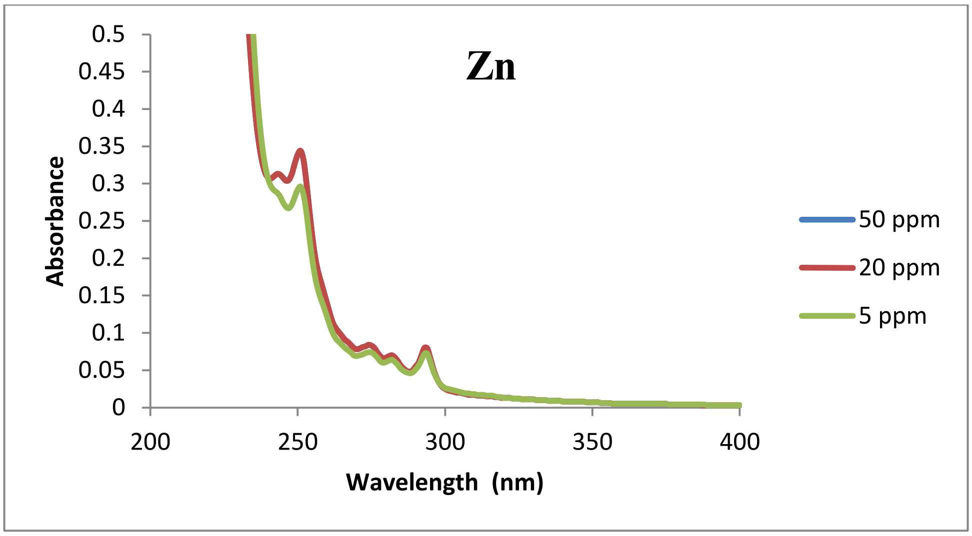

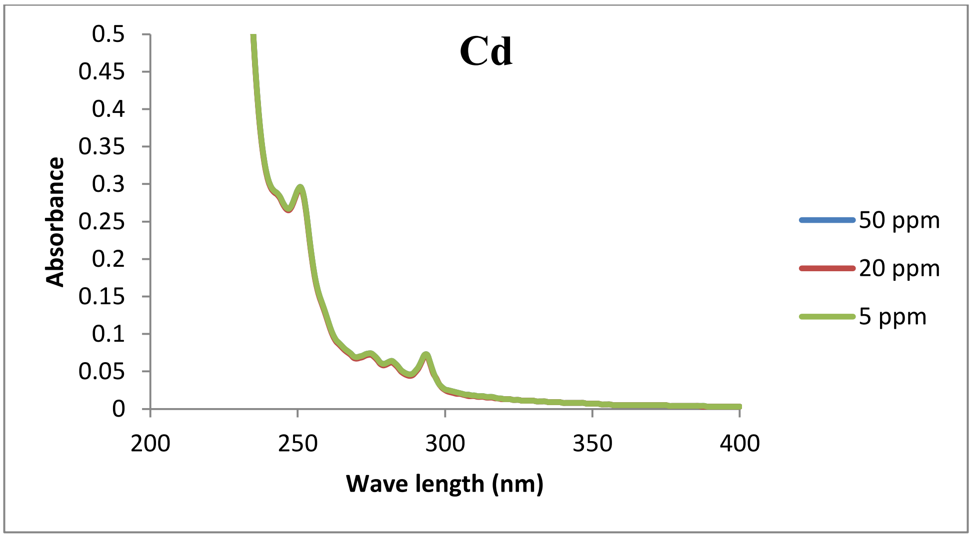

Fig. B.5. Absorbance spectra of different concentrations of acenaphthylene in the presence of 50 mg/L of metals

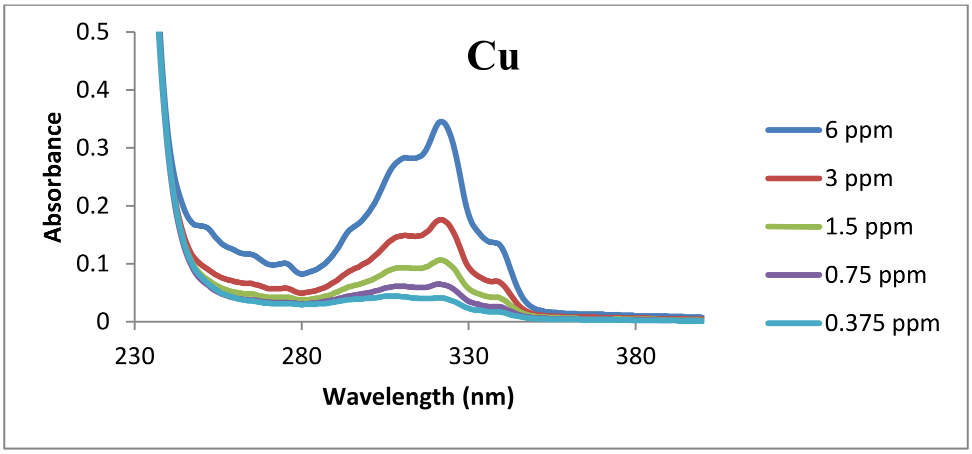

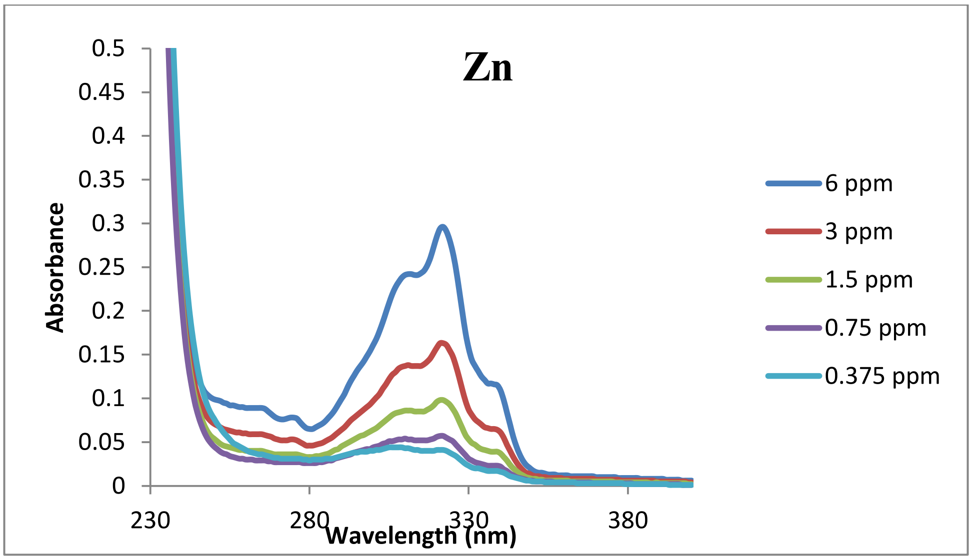

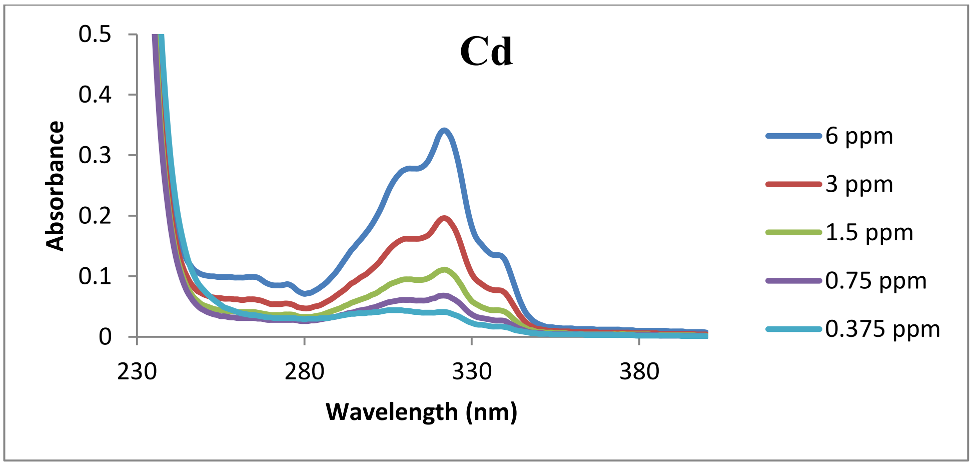

Fig. B.6. Absorbance spectra of different concentrations of phenanthrene in the presence of 50 mg/L of metals

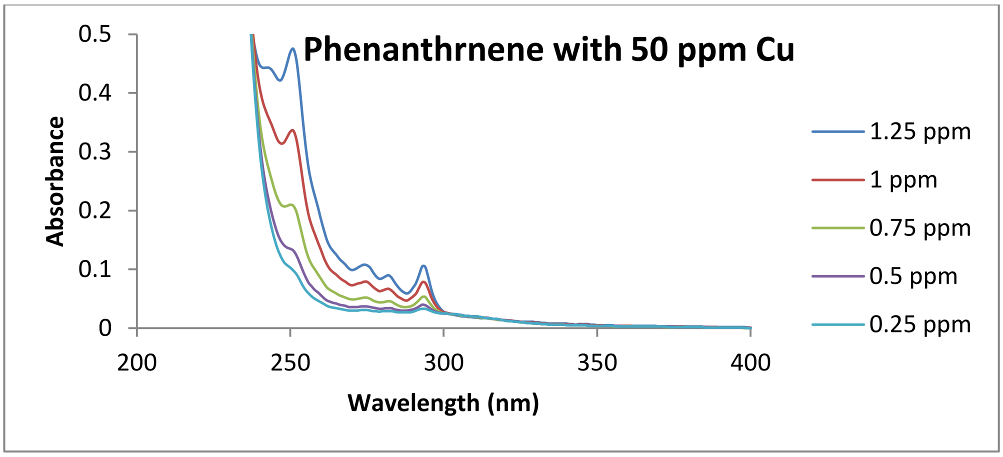

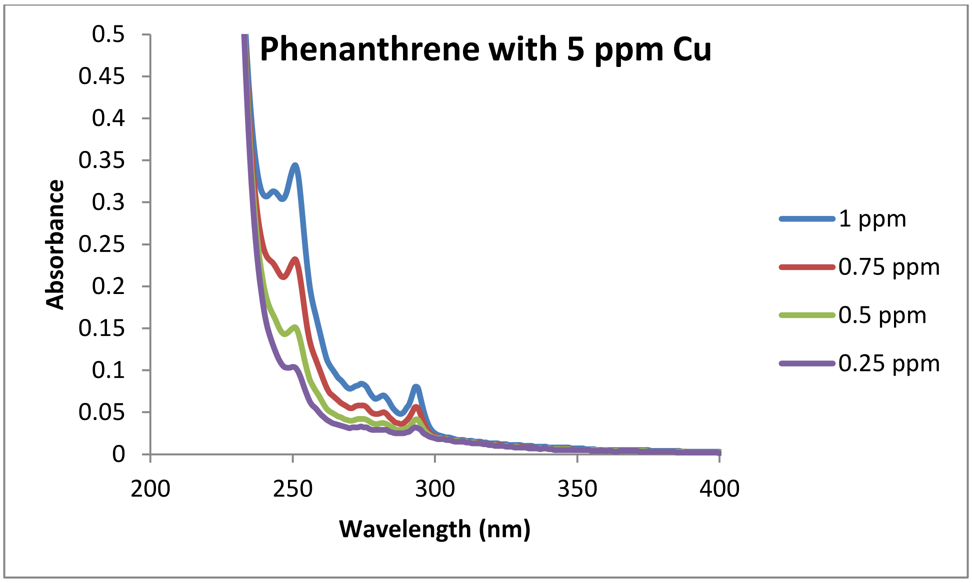

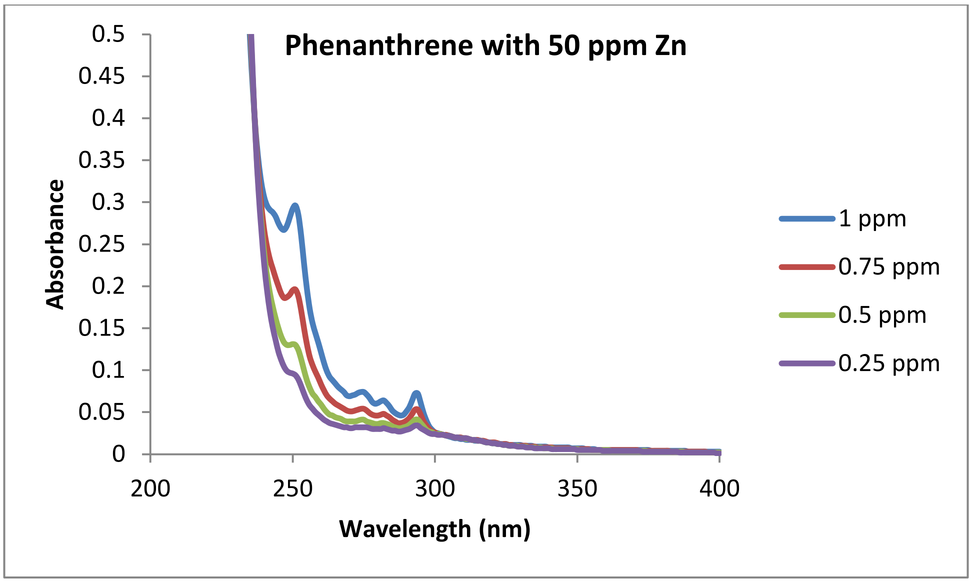
Phenanthrene with 50 ppm Zn
Absorbance
0.5
0.45
0.4
0.35
0.3
0.25
0.2
0.15
0.1
0.05
0
200
250
300
350
400
Wavelength (nm)
1 ppm
0.75 ppm
0.5 ppm
0.25 ppm

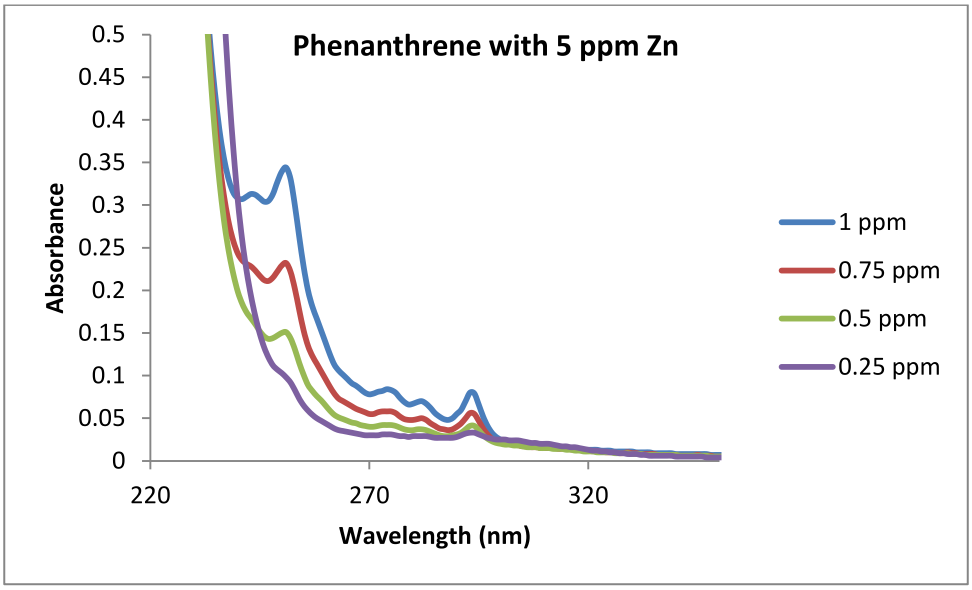
Phenanthrene with 5 ppm Zn
Absorbance
0.5
0.45
0.4
0.35
0.3
0.25
0.2
0.15
0.1
0.05
0
220
270
320
Wavelength (nm)
1 ppm
0.75 ppm
0.5 ppm
0.25 ppm

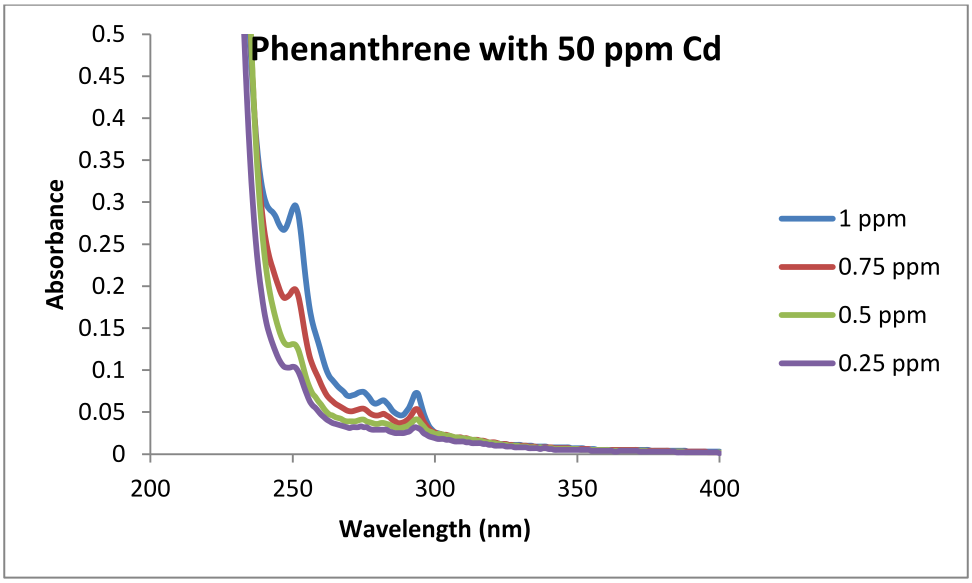
Phenanthrene with 50 ppm Cd
Absorbance
0.5
0.45
0.4
0.35
0.3
0.25
0.2
0.15
0.1
0.05
0
200
250
300
350
400
Wavelength (nm)
1 ppm
0.75 ppm
0.5 ppm
0.25 ppm

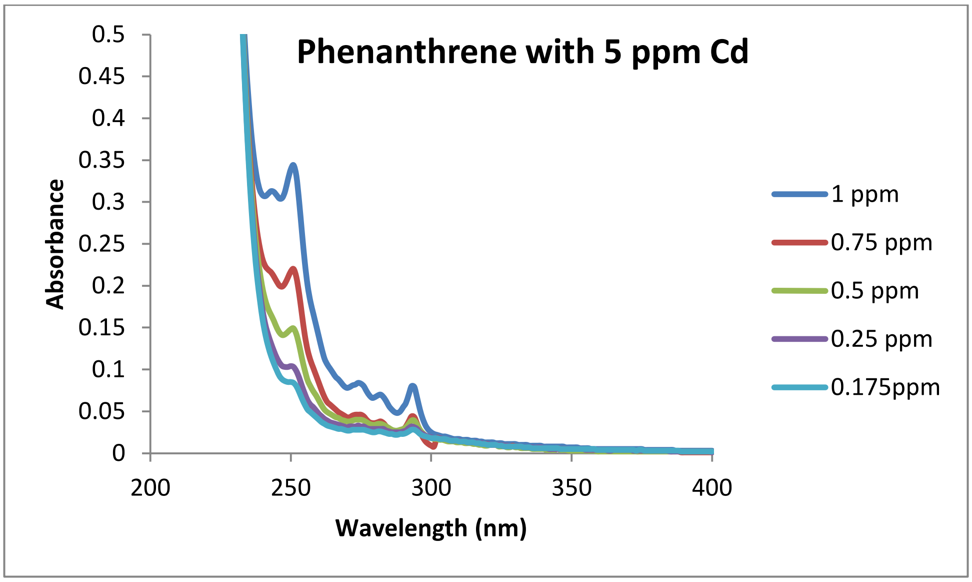
Phenanthrene with 5 ppm Cd
Absorbance
0.5
0.45
0.4
0.35
0.3
0.25
0.2
0.15
0.1
0.05
0
200
250
300
350
400
Wavelength (nm)
1 ppm
0.75 ppm
0.5 ppm
0.25 ppm
0.175ppm

Fig. B.7: Standard calibration curves for acenaphthylene

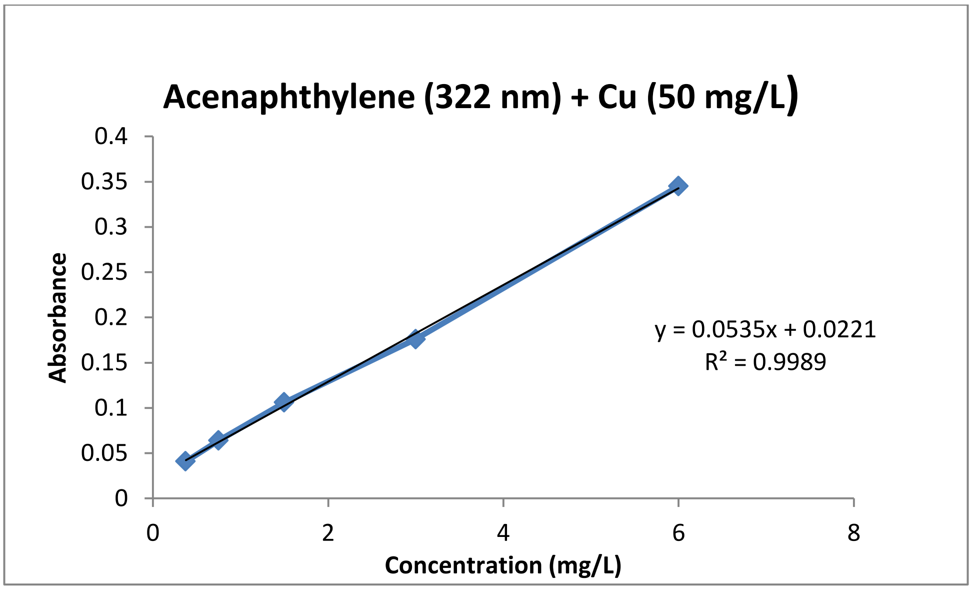

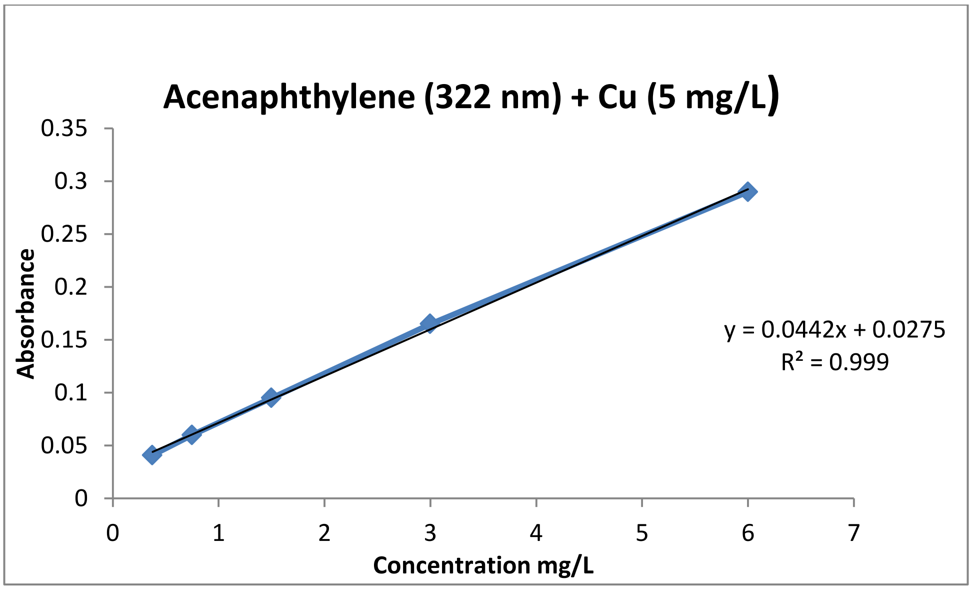

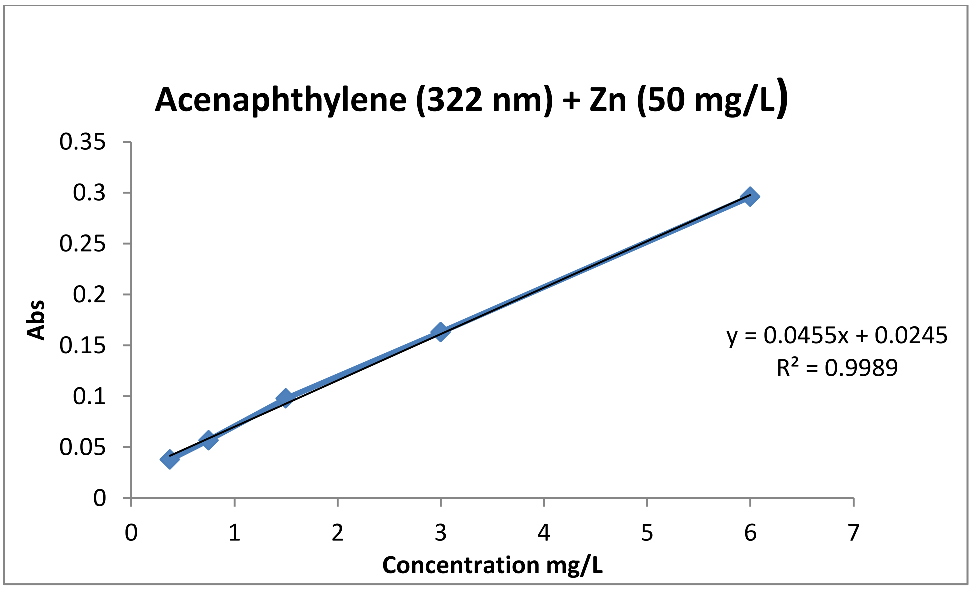
Acenaphthylene (322 nm) + Zn (50 mg/L)
Abs
0.35
0.3
0.25
0.2
0.15
0.1
0.05
0
0
1
2
3
4
5
6
7
Concentration mg/L
y = 0.0455x + 0.0245
R² = 0.9989

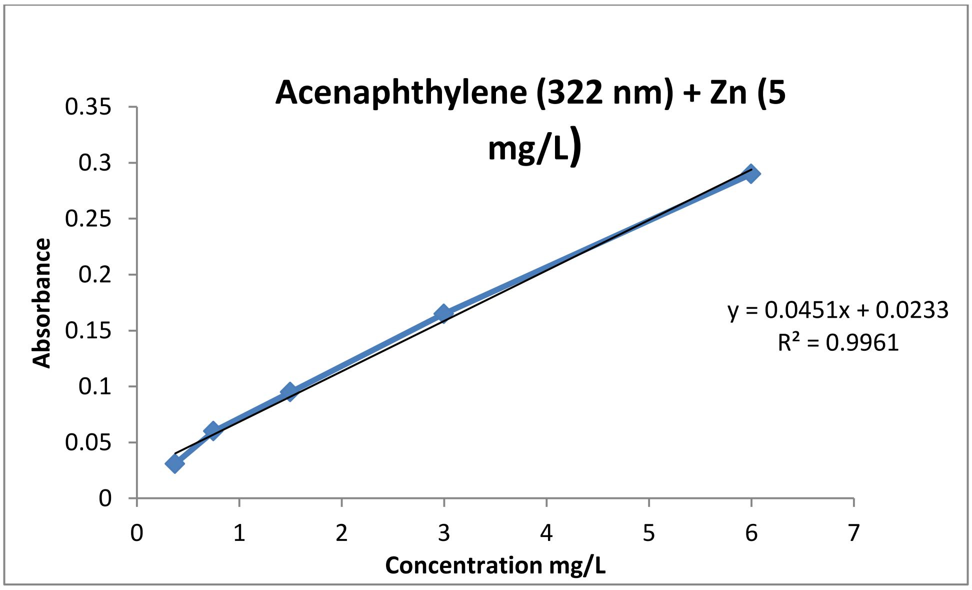
Acenaphthylene (322 nm) + Zn (5 mg/L)
Absorbance
0.35
0.3
0.25
0.2
0.15
0.1
0.05
0
0
1
2
3
4
5
6
7
Concentration mg/L
y = 0.0451x + 0.0233
R² = 0.9961

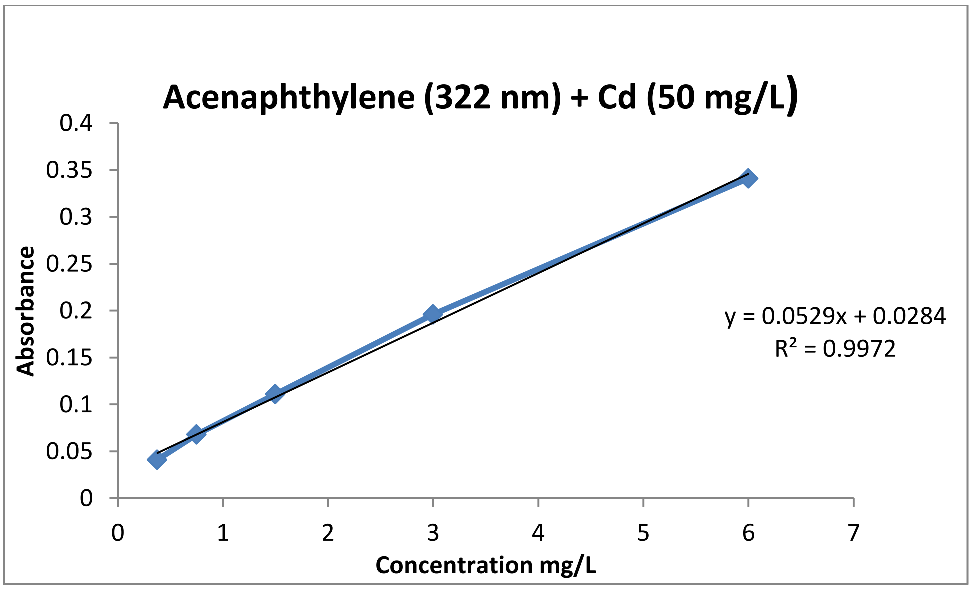
Acenaphthylene (322 nm) + Cd (50 mg/L)
Absorbance
0.4
0.35
0.3
0.25
0.2
0.15
0.1
0.05
0
0
1
2
3
4
5
6
7
Concentration mg/L
y = 0.0529x + 0.0284
R² = 0.9972

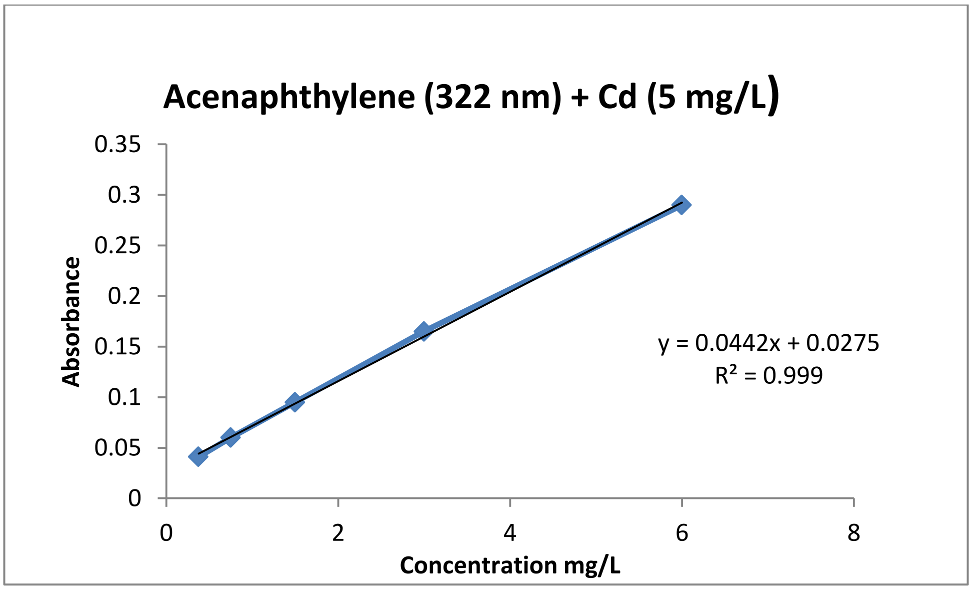
Acenaphthylene (322 nm) + Cd (5 mg/L)
Absorbance
0.35
0.3
0.25
0.2
0.15
0.1
0.05
0
0
2
4
6
8
Concentration mg/L
y = 0.0442x + 0.0275
R² = 0.999

Fig. B.8: Standard calibration curves for phenanthrene

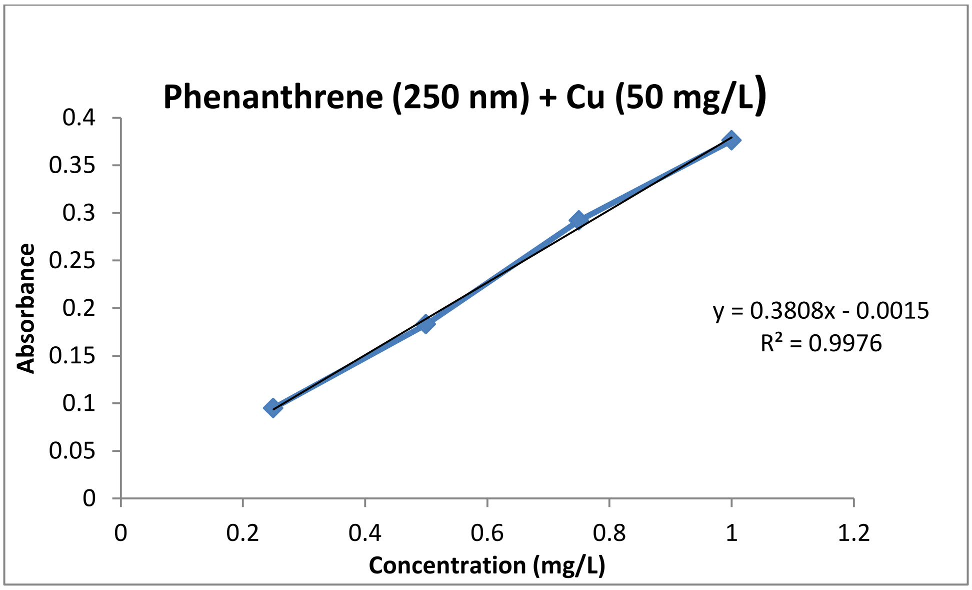

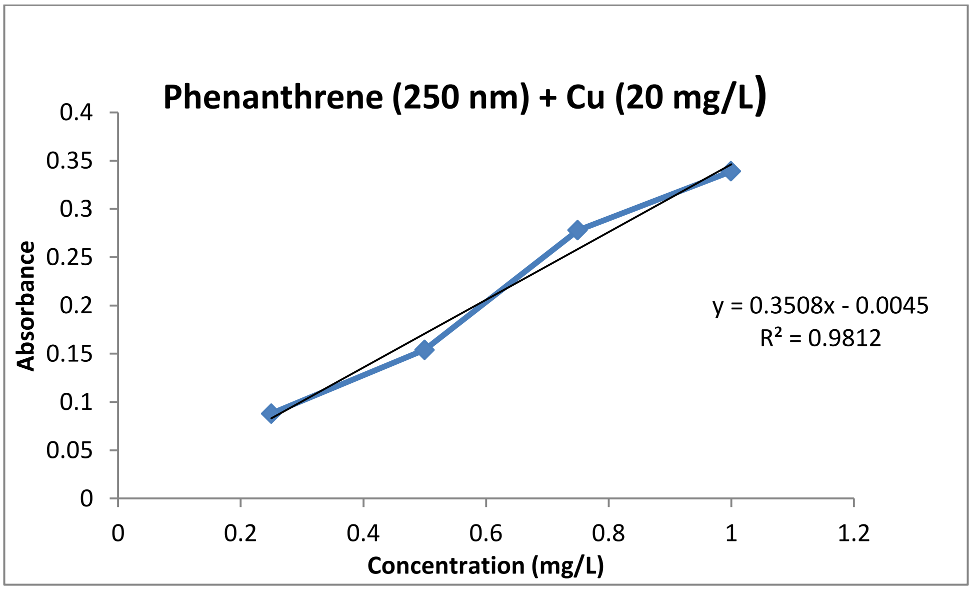

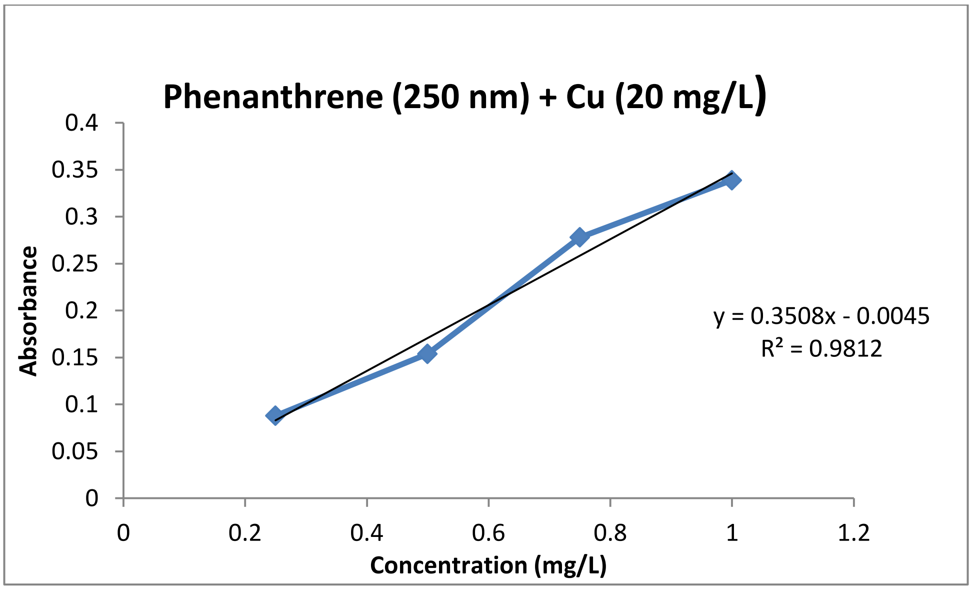
Phenanthrene (250 nm) + Cu (20 mg/L)
Absorbance
0.4
0.35
0.3
0.25
0.2
0.15
0.1
0.05
0
0
0.2
0.4
0.6
0.8
1
1.2
Concentration (mg/L)
y = 0.3508x - 0.0045
R² = 0.9812

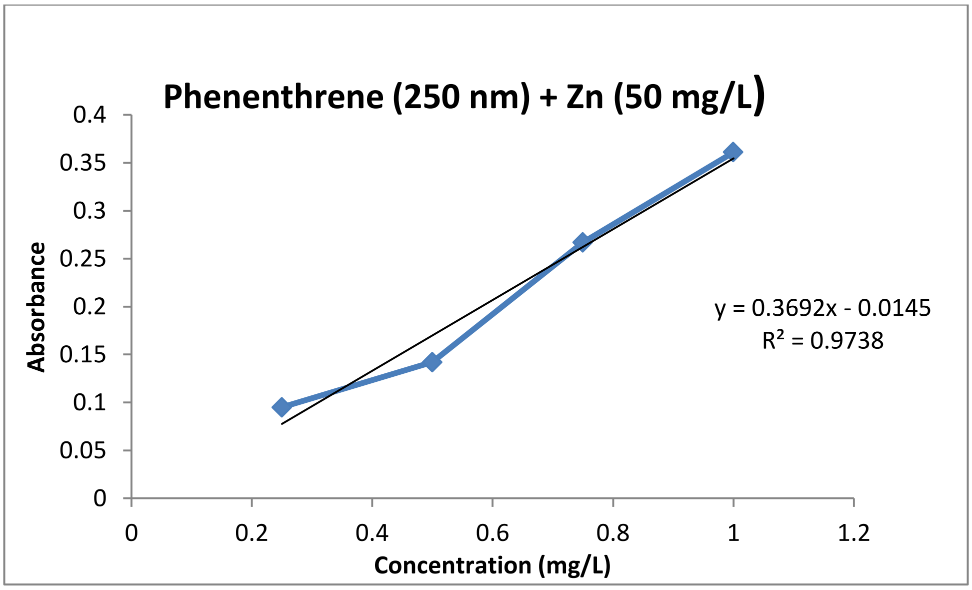
Phenenthrene (250 nm) + Zn (50 mg/L)
Absorbance
0.4
0.35
0.3
0.25
0.2
0.15
0.1
0.05
0
0
0.2
0.4
0.6
0.8
1
1.2
Concentration (mg/L)
y = 0.3692x - 0.0145
R² = 0.9738

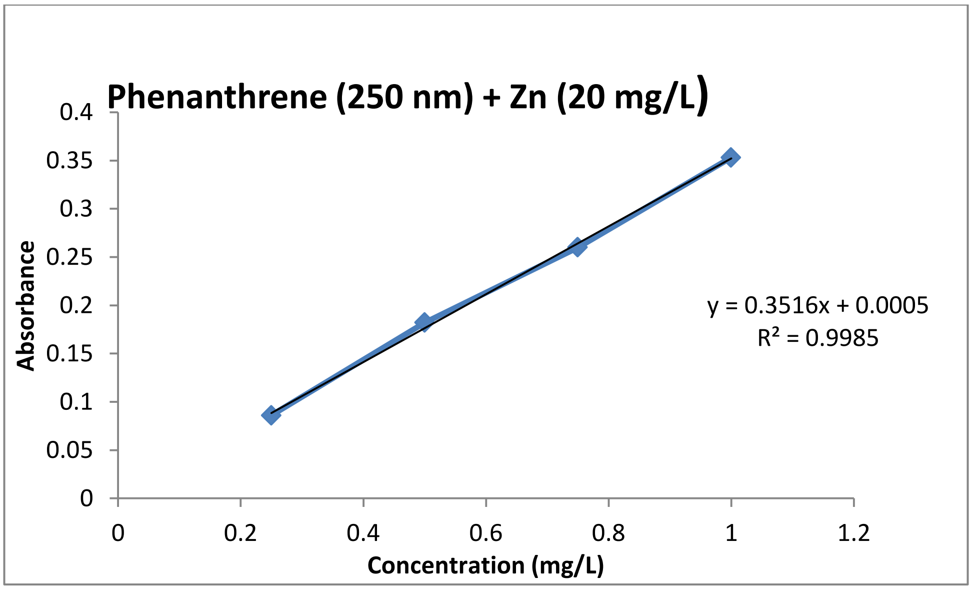
Phenanthrene (250 nm) + Zn (20 mg/L)
Absorbance
0.4
0.35
0.3
0.25
0.2
0.15
0.1
0.05
0
0
0.2
0.4
0.6
0.8
1
1.2
Concentration (mg/L)
y = 0.3516x + 0.0005
R² = 0.9985

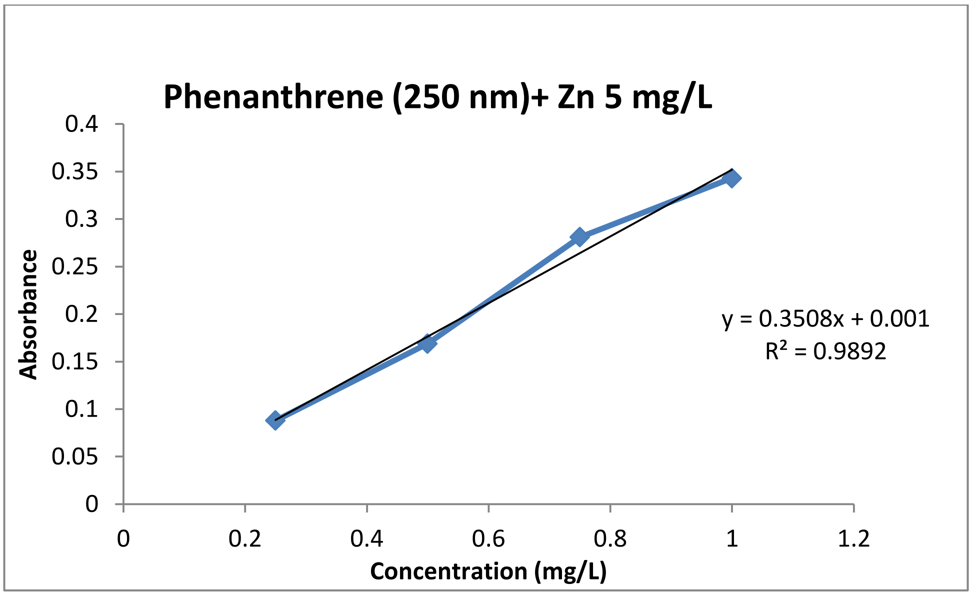
Phenanthrene (250 nm)+ Zn 5 mg/L
Absorbance
0.4
0.35
0.3
0.25
0.2
0.15
0.1
0.05
0
0
0.2
0.4
0.6
0.8
1
1.2
Concentration (mg/L)
y = 0.3508x + 0.001
R² = 0.9892

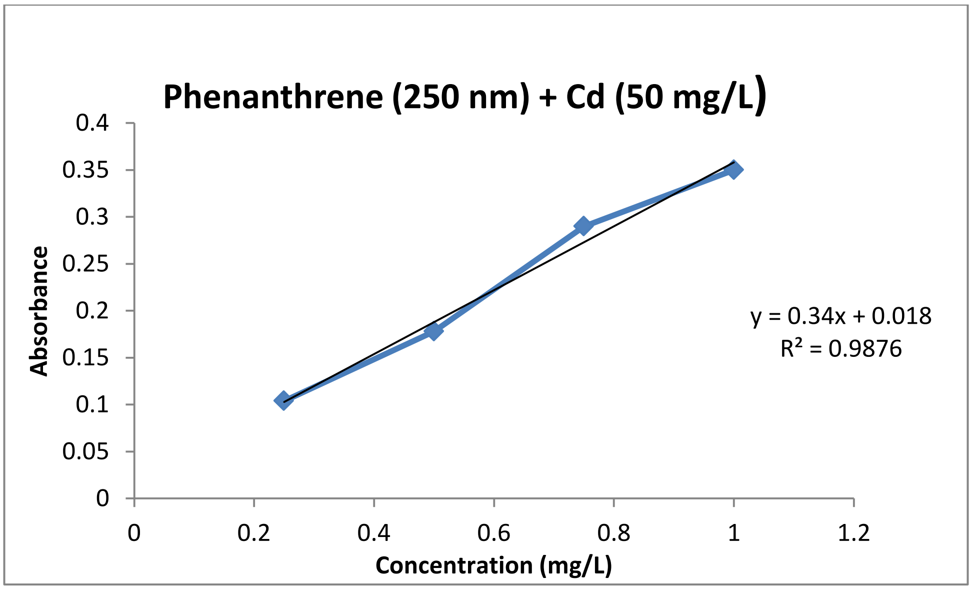
Phenanthrene (250 nm) + Cd (50 mg/L)
Absorbance
0.4
0.35
0.3
0.25
0.2
0.15
0.1
0.05
0
0
0.2
0.4
0.6
0.8
1
1.2
Concentration (mg/L)
y = 0.34x + 0.018
R² = 0.9876

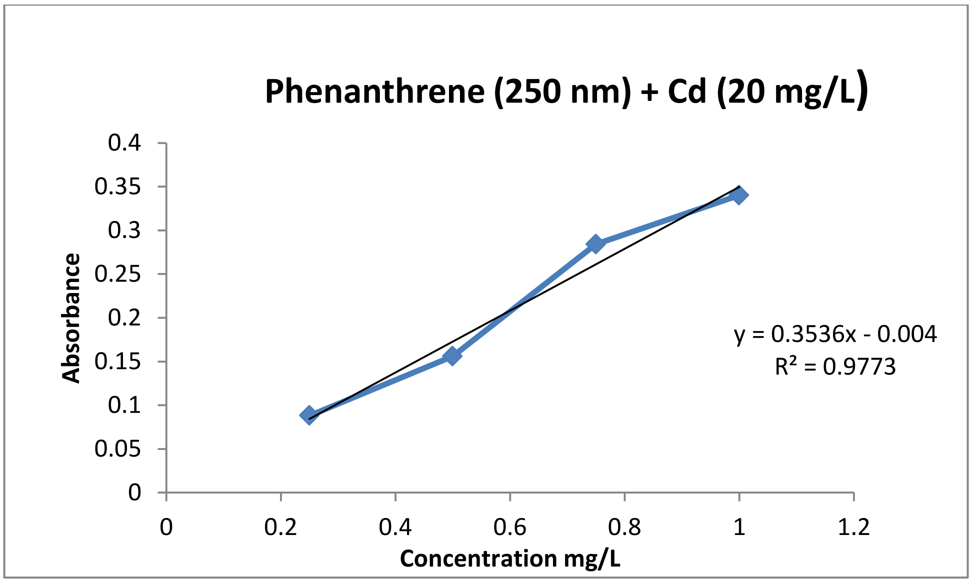
Phenanthrene (250 nm) + Cd (20 mg/L)
Absorbance
0.4
0.35
0.3
0.25
0.2
0.15
0.1
0.05
0
0
0.2
0.4
0.6
0.8
1
1.2
Concentration mg/L
y = 0.3536x - 0.004
R² = 0.9773

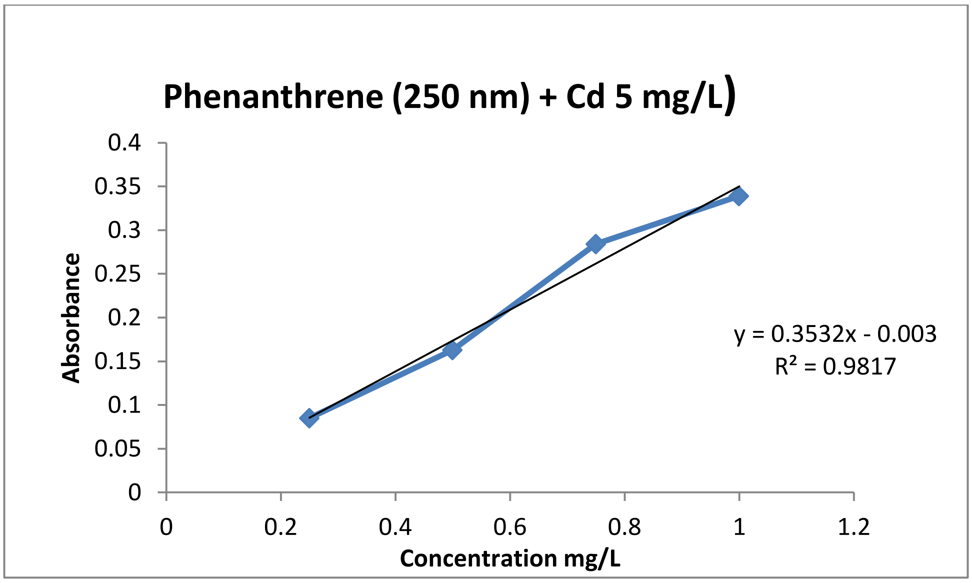

Fig. B.9: Percentage removal of PAHs (initial concentration 1 mg/L) and metals (initial concentration 5 mg/L)

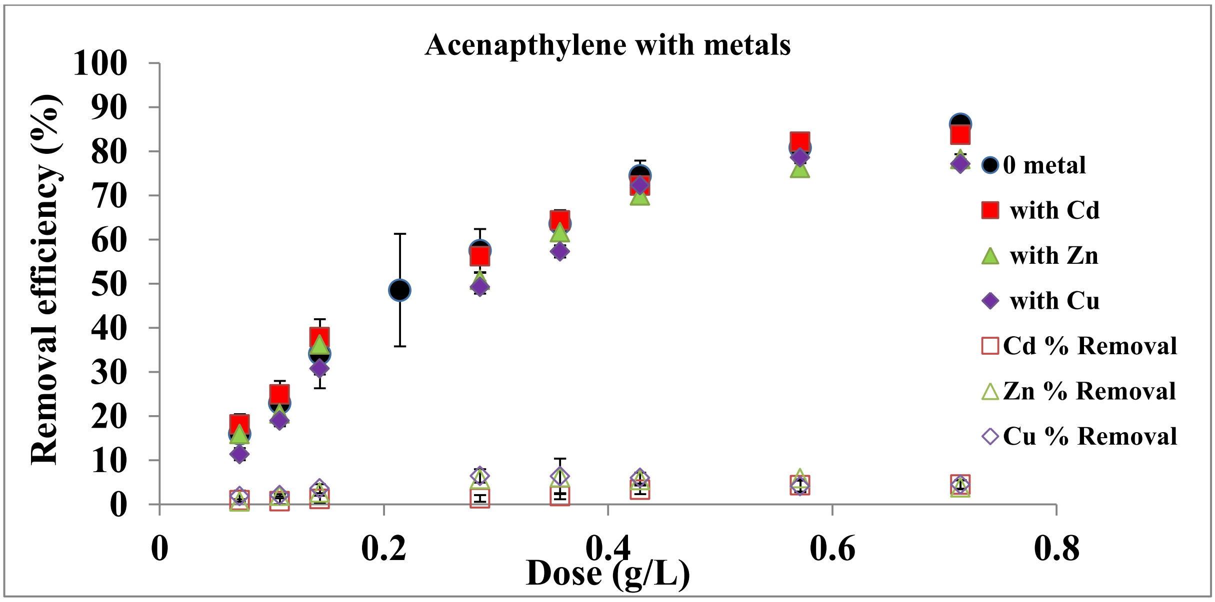

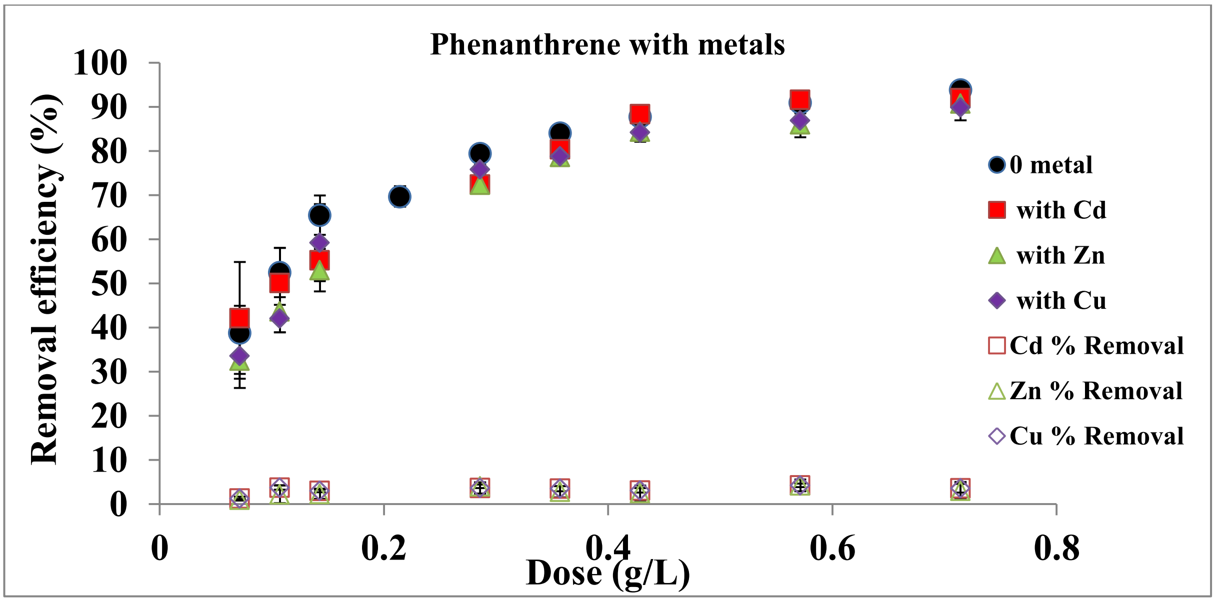

Fig. B.10: Amounts of PAHs (initial concentration 1 mg/L) adsorbed in the presence of metals (5 mg/L)

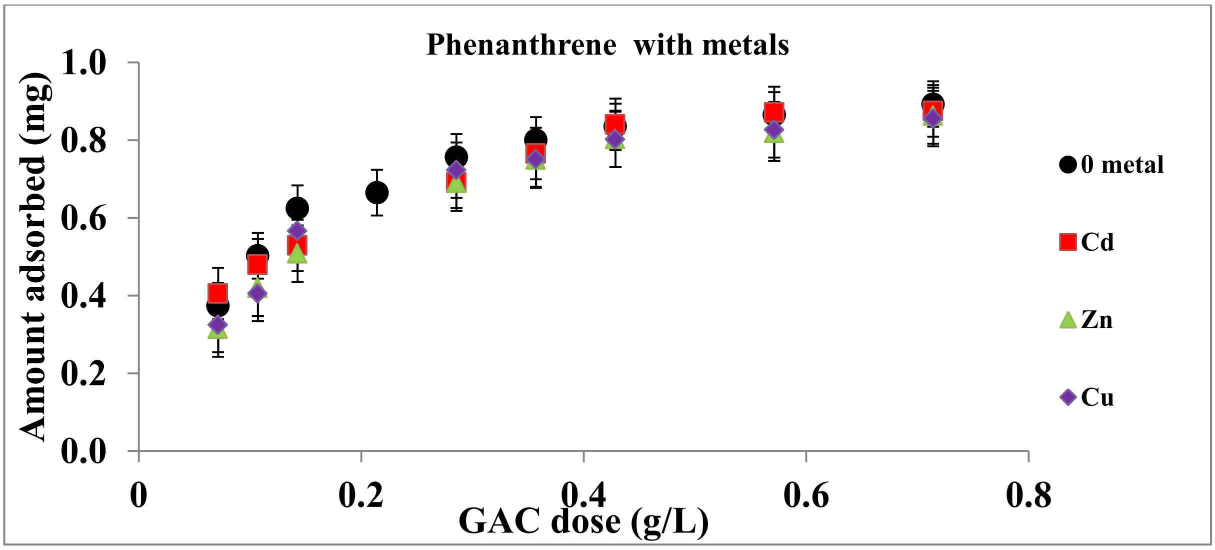

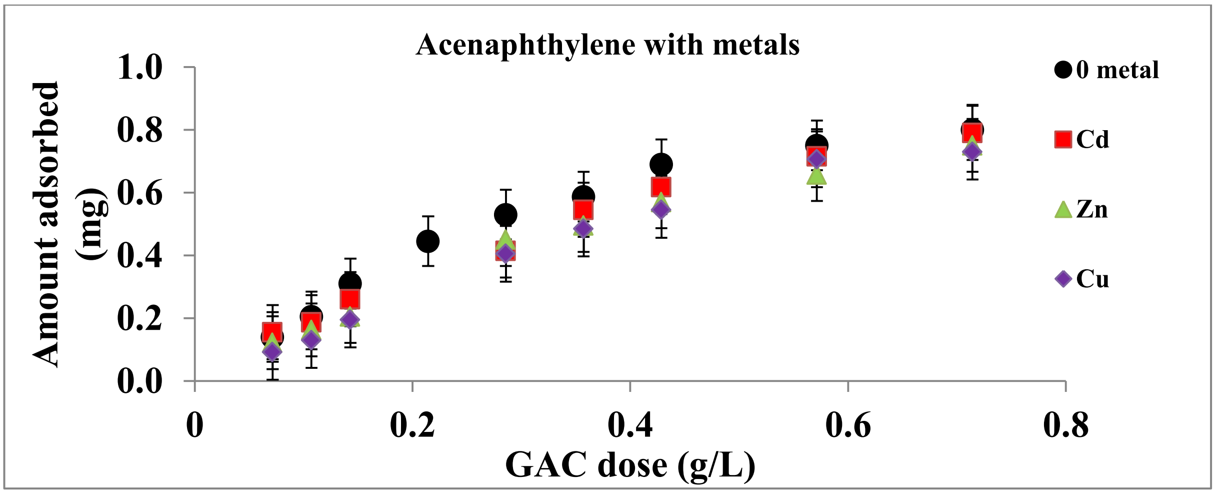

Fig. B.11: Amounts of metals (initial concentration 5 mg/L) adsorbed in the presence of PAHs (initial concentration 1 mg/L)

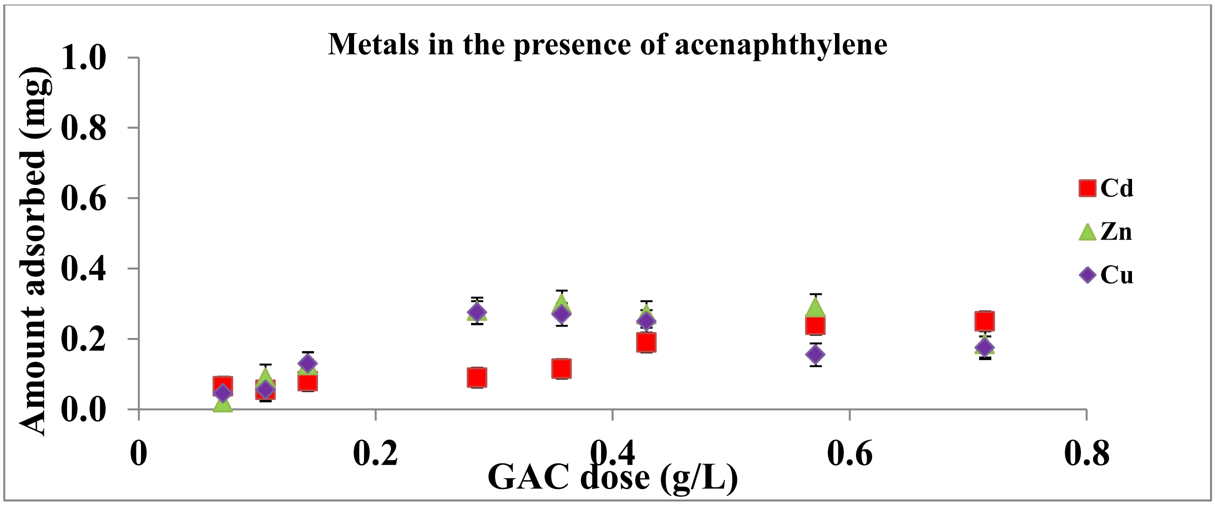

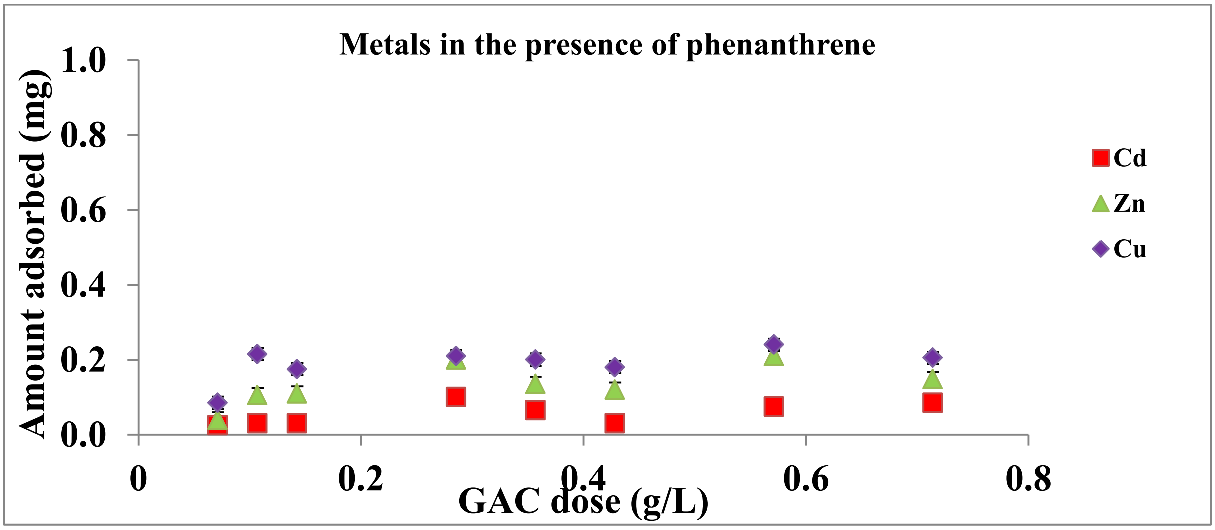

Appendix C

Table C.1 T-N removal (100mm/hr)

Number of hours	R165			R165+ 10% Zeolite		
	T-N	NO3-N	TKN	T-N	NO3-N	TKN
1	3.85	2.76	0.59	3.76	2.71	0.59
2	3.41	2.76	0.44	3.73	2.76	0.53
3	3.86	2.91	0.45	3.86	2.88	0.56
4	3.85	2.96	0.49	3.48	2.76	0.42
6	3.96	2.88	0.51	3.68	2.83	0.51
8	3.93	2.75	0.48	3.94	2.64	0.84
12	3.98	2.76	0.72	3.62	2.74	0.48
16	3.71	2.84	0.57	3.65	2.82	0.54

DOC Removal

Table C.2: DOC removal (Feed DOC = 8.5-8.8 mg/L) at 100mm/hr

Number of hours	R165	R165+5% Zeolite + 0.3 % GAC	R165+10% Zeolite + 0.3 % GAC	R165+20% Zeolite+ 0.3 % GAC
1	8.12	7.32	7.16	7.14
2	8.55	7.98	7.35	7.89
3	8.55	7.72	7.48	7.47
4	8.31	8.61	8.34	8.03
8	8.71	8.63	8.42	8.08
12	8.61	8.42	8.52	8.19
16	8.68	8.78	8.74	8.11
20	8.64	7.87	8.25	8.15
24			8.43	8.24
28			8.65	8.11

Table C.3: Conductivity and pH removal at flow velocity 100 mm/hr

Number of hours	**R165**		**R165 +10% Zeolite**	
	pH	Conductivity (µS/ cm)	Conductivity (µS/ cm)	pH
Feed	6.88+/-2	685+/-2	685+/-2	6.88+/-2
1	6.88	618	428	6.92
2	6.83	645	586	6.94
3	6.84	654	645	6.97
4	6.89	669	665	6.94
5	6.84	681	682	6.97
6	6.88	684	683	6.94
7	6.82	682	684	6.94
9	6.88	683	680	6.94
10	6.71	687	689	6.95
11	6.51	690	687	6.88
12	6.45	694	689	6.9
13	6.54	682	685	6.85
14	6.48	687	689	6.95
15	6.49	687	683	6.99
16	6.56	688	679	6.94
17	6.63	685	684	6.92

18	6.62	680	689	6.9
19	6.64	689	688	6.87
20	6.74	684	687	6.89
21	6.78	684	689	6.88
22	6.79	685	684	6.92
23	6.8	686	678	6.93
24	6.76	685	687	6.94

Table C.4 Conductivity and pH removal at flow velocity of 300 mm/hr

Number of hours	**pH**	**Conductivity (µS/ cm)**
Feed	6.80+/- 2	677+/-2
0.25	6.95	576
0.5	6.91	636
0.75	6.98	655
1	6.94	668
1.15	6.96	667
1.3	6.94	677
2	6.97	673
2.3	7.01	670
3	6.94	678
3.3	6.97	678

4	7.02	677
4.3	6.94	679
5	7.10	678